

**SONO, PHOTO AND SONOPHOTO CATALYTIC
REMOVAL OF CHEMICAL AND BACTERIAL
POLLUTANTS FROM WASTEWATER**

Thesis submitted to

Cochin University of Science and Technology

In partial fulfillment of the requirements for the award of the degree of

Doctor of Philosophy

in

Environmental Technology

Under the faculty of Environmental Studies

By

S. G. Anju

(Reg. No. 3878)



**SCHOOL OF ENVIRONMENTAL STUDIES
COCHIN UNIVERSITY OF SCIENCE AND TECHNOLOGY**

KOCHI - 682 022

November 2015

Sono, Photo and Sonophoto Catalytic Removal of Chemical and Bacterial Pollutants from Wastewater

Ph.D. Thesis under the Faculty of Environmental Studies

Author

S.G. Anju
Research Scholar
School of Environmental Studies
Cochin University of Science and Technology
Kochi – 682 022
Kerala, India

Supervising Guide

Dr. Suguna Yesodharan
Professor
School of Environmental Studies,
Cochin University of Science and Technology
Kochi – 682 022
Kerala, India

School of Environmental Studies
Cochin University of Science and Technology
Kochi, Kerala, India 682 022

November 2015



SCHOOL OF ENVIRONMENTAL STUDIES
COCHIN UNIVERSITY OF SCIENCE AND TECHNOLOGY

KOCHI - 682 022

Dr. Suguna Yesodharan
Professor

Certificate

This is to certify that this thesis entitled "**Sono, Photo and Sonophoto Catalytic Removal of Chemical and Bacterial Pollutants from Wastewater**" is an authentic record of the research work carried out by **Smt. S. G. Anju**, full-time Research Scholar (Reg. No. 3878) under my guidance at the School of Environmental Studies, Cochin University of Science and Technology in partial fulfillment of the requirements for the award of the degree of Doctor of Philosophy in Environmental Technology and no part of this work has previously formed the basis for the award of any other degree, diploma, associateship, fellowship or any other similar title or recognition. All the relevant corrections and modifications suggested by the audience during the pre-synopsis seminar and recommended by the Doctoral committee have been incorporated in the thesis.

Kochi - 22
Date: /11/2015

Dr. Suguna Yesodharan
(Supervising Guide)

Declaration

I do hereby declare that the work presented in the thesis entitled "**Sono, Photo and Sonophoto Catalytic Removal of Chemical and Bacterial Pollutants from Wastewater**" is based on the authentic record of the original work done by me, for my Doctoral Degree under the guidance of **Dr. Suguna Yesodharan**, Professor, School of Environmental Studies, Cochin University of Science and Technology in partial fulfillment of the requirements for the award of the degree of Doctor of Philosophy in Environmental Technology and no part of this work has previously formed the basis for the award of any other degree, diploma, associateship, fellowship or any other similar title or recognition.

Kochi - 22

Date: /11/2015

S. G. Anju

Acknowledgements

It gives me immense pleasure to acknowledge all those people who have helped me in one way or other in accomplishing this piece of work successfully. I humbly dedicate this work to all those who have helped me in exploring the expanses of knowledge.

I take immense pleasure to express my sincere thanks and deep sense of gratitude to my supervising guide, Dr. Suguna Yesodharan, Professor, School of Environmental Studies (SES), Cochin University of Science and Technology (CUSAT) for her inspiring guidance, heartfelt support, motherly affection and unstinted co-operation in this research work,

I find no words to express my intense gratitude and respect to Dr. E.P. Yesodharan, Professor (Emeritus) SES, CUSAT who was my motivation to venture into the world of Advanced Oxidation Processes. I feel myself honoured and fortunate to enjoy a wonderful research atmosphere in his presence. I am really short of words to express my sincere appreciation for his patience and tolerance to me throughout this period. His understanding, encouragement and personal guidance have provided me with a good base for the present thesis.

I offer my gratitude to the present Director, SES, Dr. S. Rajathy as well as previous Directors Prof. I. S. Bright Singh, Prof. Suguna Yesodharan, Prof. Ammini Joseph and Dr. Harindranathan Nair for providing all the facilities of the school for the smooth conduct of the study. I also wish to place on record my thanks to Dr. Sivanandan Achari and Mr. M. Anand, teachers of the school, for all their suggestions, help, support and encouragement throughout the period of research. I also thank the non-teaching staff of the school for their help and assistance.

I would like to express my sincere and heartfelt gratitude to all the research scholars of our laboratory, Dr. Suja, Ms. Jyothi, Ms. Sindhu, Ms. Phonsy,

Mr. Sabin, Mr. Rajeev, Mr. Hariprasad, Ms. Veena, Ms. Gayathri, Ms. Vidya and Ms. Deepthi for their timely advice, help and affection, which made my stay in the laboratory a pleasant one.

I recall with love and gratitude the sincere cooperation and encouragement, received from my friends Dr. Abesh, Mr. Haneesh, Dr. Dipson (late), Ms. Bindiya, Ms. Chithra, Ms. Teena, Mr. Rojith, Mr. Rakesh, Ms. Asha and Ms. Dhanya. I thank all the research scholars and other friends at CUSAT for their support throughout the program.

I would like to extend my gratitude to CUSAT for providing me with the facility to conduct research as well as awarding me the University Research Fellowship, UGC-BSR and DST-PURSE.

It's impossible to literally express my gratitude to my beloved parents, in-laws, sister (Sreelakshmi), brothers (Kannan, Amarnath and Aarav) and my Husband (Sreeraj) for the affection, support and hope they provided.

Above all, this piece of work is accomplished with the blessings and powers that work within me and also the people behind my life. I bow before GOD for all with a sense of humanity and gratitude.....

S. G. Anju

||| Preface |||

The term 'water pollution' broadly refers to the contamination of water and water bodies (e.g. lakes, rivers, oceans, groundwater etc). Water pollution occurs when pollutants are discharged directly or indirectly into water bodies without adequate treatment to remove the harmful contaminants. This affects not only the plants and organisms living in these bodies of water but also the entire natural biological communities and the biodiversity.

Advanced Oxidation Processes (AOPs) have been tested as environment-friendly techniques for the treatment of contaminated water, in view of their ability to convert pollutants into harmless end products. These techniques refer to a set of treatment procedures designed to remove organic or inorganic contaminants in wastewater by oxidation. The contaminants are oxidized by different reagents such as air, oxygen, ozone, and hydrogen peroxide which are introduced in precise, pre-programmed dosages, sequences and combinations under appropriate conditions. The procedure when combined with light in presence of catalyst is known as photocatalysis. When ultrasound (US) is used as the energy source, the process is referred as sonication. Sonication in presence of catalyst is referred as sonocatalysis. Of late, combination of light and sound as energy sources has been tested for the decontamination of wastewater in the presence of suitable catalyst. In this case, the process is referred as sonophotocatalysis. These AOPs are specially advantageous in pollution control and waste water treatment because unlike many other technologies, they do not just transfer the pollutant from one phase to

another but completely degrade them into innocuous substances such as CO₂ and H₂O.

In the present study, the application of three Advanced Oxidation Process (AOP) i.e., sonocatalysis, photocatalysis and sonophotocatalysis for the destruction of very small amounts of chemical and microbial pollutants in water is examined using ZnO and TiO₂ as catalysts. The investigations are mainly focused on:

- i) Evaluation of ZnO, TiO₂ and their combination as sono, photo and sonophotocatalysts for the degradation of water pollutants.
- ii) Optimizing the dosage, particle size, composition etc., of the catalysts under each of the above AOPs for the degradation of selected pollutants.
- iii) Optimizing reaction parameters such as reaction time, pH, pollutant load, concentration of O₂, etc., for the degradation of pollutant under each of the three AOPs.
- iv) Evaluating the effect of contaminants such as salts likely to be present in water on the efficiency of AOPs for the mineralization of chemical pollutants.
- v) Understanding the kinetics and mechanism of the sono, photo and sonophoto catalytic removal of chemical pollutants in water.
- vi) Investigating the possibility of using the least investigated AOP i.e., sonocatalysis, for the removal of few typical bacterial contaminants in water.

The thesis reports the results of our in-depth investigation on the application of sono, photo and sonophotocatalysis mediated by semiconductor oxides, ZnO, TiO₂ and their combination for the removal of chemical and bacterial pollutants in trace amounts from water. The thesis is presented in seven chapters as follows:

Chapter 1- Introduction: Background literature.

Chapter 2- Objectives of the study, Materials used and Plan of the thesis.

Chapter 3- Semiconductor Oxide Mediated Photocatalytic Degradation of Phenol in Water.

Chapter 4- Semiconductor Oxide Mediated Sonocatalytic Degradation of Phenol in Water.

Chapter 5- Semiconductor Oxide Mediated Sonophotocatalytic Degradation of Phenol in Water.

Chapter 6- Zinc Oxide Mediated Sonocatalytic Removal of Bacterial Contaminants from Water.

Chapter 7- Summary and Conclusions.

The lists of research publications/ books referred in various chapters are given under the title 'References'.

List of papers published in journals /presented in conferences based on the current study is given as Annexure II.

Annexure III consists of reprints of the research paper, based on the current study published in various journals.

Contents

Chapter 1

INTRODUCTION: BACKGROUND LITERATURE.....	01 - 44
1.1 General.....	01
1.2 Advanced Oxidation Processes (AOPs)	04
1.2.1 Theory of Advanced Oxidation Processes	08
1.3 Photocatalysis as an AOP	10
1.3.1 Homogeneous Photocatalysis	11
1.3.1.1 UV/Hydrogen peroxide (UV/ H ₂ O ₂)	11
1.3.1.2 UV/Ozone (UV /O ₃).....	13
1.3.1.3 UV/ Ozone and Hydrogen peroxide (UV /O ₃ /H ₂ O ₂)	15
1.3.1.4 Photo-Fenton system (UV/Fe ²⁺ /H ₂ O ₂)	16
1.3.2 Heterogeneous Photocatalysis.....	18
1.3.2.1 General Mechanism	19
1.3.2.2 Importance of Semiconductors as photocatalysts	22
1.3.2.3 Some typical photocatalytic degradation studies	26
1.4 Ultrasonic Cavitation / Sonication	29
1.4.1 Sonolysis/Sonocatalysis in water treatment: Case Studies	35
1.4.2 Sonocatalytic inactivation of bacterial pollutants.....	36
1.5 Sonophotocatalytic processes	39

Chapter 2

OBJECTIVES OF THE STUDY, MATERIALS USED AND PLAN OF THE THESIS	45 - 58
2.1 Objectives	45
2.2 Materials	47
2.2.1 Zinc oxide (ZnO).....	47
2.2.2 Titanium dioxide (TiO ₂)	50
2.2.3 Phenol	53
2.2.4 Hydrogen peroxide (H ₂ O ₂).....	54
2.2.5 Miscellaneous materials.....	55
2.3 Plan of the thesis	55

Chapter 3

SEMICONDUCTOR OXIDES MEDIATED PHOTOCATALYTIC DEGRADATION OF PHENOL IN WATER.....	59 - 107
3.1 Introduction.....	59
3.2 Experimental Details	60
3.2.1 Materials	60

3.2.2	Analytical Procedures	61
3.2.3	Adsorption	62
3.2.4	Photocatalytic Experimental set up	63
3.3	Results and Discussion	65
3.3.1	Catalyst characterization and Preliminary experiments.....	65
3.3.2	Effect of catalyst dosage	73
3.3.3	Effect of irradiation time	75
3.3.4	Effect of concentration	76
3.3.5	Effect of pH	82
3.3.6	Effect of reaction volume	87
3.3.7	Effect of particle size.....	89
3.3.8	Effect of aeration/deaeration.....	90
3.4	Probable mechanism of the photocatalytic degradation of phenol in presence of semiconductor	92
3.5	Formation and decomposition of H ₂ O ₂	97
3.6	Effect of anions	101
3.7	Conclusions.....	107

Chapter 4

SEMICONDUCTOR OXIDES MEDIATED

SONOCATALYTIC DEGRADATION OF PHENOL

IN WATER..... 109 - 151

4.1	Introduction.....	109
4.2	Experimental Details	112
4.2.1	Materials	112
4.2.2	Equipment Used	112
4.2.3	Experimental set up	112
4.2.4	Analytical Methods used	113
4.3	Results and Discussion	113
4.3.1	Effect of irradiation time	116
4.3.2	Effect of catalyst dosage	117
4.3.3	Effect of concentration	121
4.3.4	Effect of pH	126
4.3.5	Formation and decomposition of H ₂ O ₂	129
4.3.6	Effect of reaction volume	133
4.3.7	Effect of particle size.....	135
4.3.8	Effect of ultrasonic frequency.....	137
4.3.9	Effect of aeration/deaeration.....	138
4.4	General Mechanism of sonocatalysis	140
4.5	Effect of anions	143
4.6	Conclusions.....	150

Chapter 5

SEMICONDUCTOR OXIDES MEDIATED SONOPHOTOCATALYTIC DEGRADATION OF

PHENOL IN WATER 153 - 195

5.1	Introduction.....	153
5.2	Experimental Details	155
5.2.1	Materials	155
5.2.2	Equipment Used.....	155
5.2.3	Experiments and Analytical Methods.....	155
5.3	Results and Discussion	156
5.3.1	Effect of catalyst loading.....	160
5.3.2	Effect of concentration	163
5.3.3	Effect of pH	167
5.3.4	Effect of reaction volume	170
5.3.5	Effect of particle size.....	173
5.3.6	Effect of aeration/deaeration.....	174
5.4	Mechanism of the Sonophotocatalytic degradation	175
5.5	Effect of anions	180
5.6	Conclusions.....	195

Chapter 6

ZINC OXIDE MEDIATED SONOCATALYTIC REMOVAL

OF BACTERIAL CONTAMINANTS FROM WATER 197 - 239

6.1	Introduction.....	197
6.2	Experimental Details	199
6.2.1	Materials	199
6.2.2	Analytical Methods Used.....	199
6.2.3	Microorganisms chosen for the study.....	199
6.2.4	Culture conditions	202
6.3	Results and Discussion	204
6.3.1	Effect of catalyst loading	207
6.3.2	Effect of concentration	220
6.3.3	Effect of pH	223
6.3.4	Effect of H ₂ O ₂	228
6.4	Re-emergence	232
6.5	Mechanism of disinfection	234
6.6	Conclusions.....	238

Chapter 7

SUMMARY AND CONCLUSIONS 241 - 245

REFERENCES.....	247 - 271
Annexure I : List of Abbreviations and Symbols.....	273 - 274
Annexure II: Research Papers based on the current investigation.	275 - 278
Annexure III: Reprints of Paper published	279 - 331

.....❧.....

INTRODUCTION: BACKGROUND LITERATURE

- 1.1 *General*
- 1.2 *Advanced Oxidation Processes (AOPs)*
- 1.3 *Photocatalysis as an AOP*
- 1.4 *Ultrasonic Cavitation / Sonication*
- 1.5 *Sonophotocatalytic processes*

1.1 General

Earth is known as water planet, with over 97 % of its water in the oceans, ~ 2 % locked up in glaciers and the remaining ~ 1% as fresh water. Water is one of the most essential ingredients to generate and sustain all forms of life. Unfortunately, many of the water resources are heavily polluted today due to reckless and unchecked human activity. If the deterioration in the quality and quantity of water continues at today's rate, a stage will be reached when "water is everywhere but not a drop to drink".

Water is a basic requirement for all industrial, domestic and commercial activities. The wastewater generated from different activities contains various contaminants that are harmful to all kinds of flora and fauna on the planet. Common water pollutants found in ground and surface waters include textile dyes, hydrocarbons, haloalkanes, alcohols, carboxylic acids, aromatic compounds, detergents, agrochemicals like insecticides and herbicides, inorganic compounds like heavy metals such

as mercury, cadmium and lead, noxious gases and pathogens like bacteria, fungi and viruses [1-4]. It is estimated that there are about 5 million registered man-made substances today, of which ~ 70,000 are widely used worldwide. Approximately, 1000 new chemical substances are added to the list each year. Water pollution has become a global concern and is one of the major threats that humanity is facing today.

According to UNESCO study, over two million tons of wastewater is dumped into the world's rivers and lakes every day. Severe overuse and clearance of ecologically important forests, intensive agriculture, expansion of urban infrastructures and increase in tourism are having enormous impact on the natural water balance and existing water resources. Today, water shortage is recognized as one of the most serious political and social issues in many developing countries. It is estimated that around 4 billion people worldwide have no or little access to clean and sanitized water supply. Millions of people die from severe water-borne diseases like typhoid, hepatitis and cholera annually [5]. The situation is expected to be worse in near future due to increase in the discharge of micro and macro pollutants and contaminants into the natural water cycle [6-8]. The United Nations has predicted that two-third of the world's population will experience severe water-scarcity by 2025.

Providing fresh and safe water for drinking and sanitation to every individual has become a key challenge today. This demands persistent efforts not only by the government, the industry or civic bodies but also by every citizen, to economise and conserve water resources. More stringent environmental regulations and emission limits are introduced

with this objective. Industries are mandated to improve or develop new technologies capable of effective removal of pollution loads, reduction of wastewater volume recycling and reuse of wastewater.

Traditional waste water treatment systems involving the use of various mechanical, biological, physical and chemical processes such as coagulation/flocculation, chlorination, membrane separation etc., do not lead to complete mineralization of the pollutants and generally transfer them from one phase to another. This causes secondary loading of the environment and more waste disposal problems. Conventional methods are also clearly not suitable for treating toxic, non-biodegradable organic pollutants. Hence, new improved technologies have to be developed and used for the treatment of water.

Conventional wastewater treatment consists in the following three steps:

- 1. Primary treatment:** This involves the removal of solids from water by physical methods. These include simple techniques such as sieving of larger particles and debris, sedimentation or settling of particulate matter etc. This brings about a significant reduction in the pollutant load as many types of pollution are associated with particulate matter.
- 2. Secondary treatment:** This is meant for the removal of organic contaminants from water using biological methods. Aerobic and anaerobic treatment processes are used. These mainly include the activated sludge process, treatment ponds and lagoons.

- 3. Tertiary treatment:** Even after the completion of primary and secondary treatment, the wastewater is not of sufficient quality to be used as drinking water or to be discharged directly. So a number of processes are used for the tertiary treatment depending on the nature of the contaminant and the extent of the separation required. Some of these are ion-exchange and membrane processes.

These are also termed as physical, biological and chemical treatments. The procedure remains the same as above.

Many of these methods are grossly inadequate and unacceptable to remove the wide variety of toxic contaminants present in traces in water [9]. This can be overcome to a great extent by using the recently emerged Advanced Oxidation Processes (AOPs).

1.2 Advanced Oxidation Processes (AOPs)

AOPs have been proven successful for the safe removal of various potentially harmful compounds that could not be effectively removed by the conventional treatment [10-25]. They are cheaper, more efficient, and ecofriendly and are based on the physicochemical processes that produce profound changes in the structure of chemical and biological species.

They offer many advantages over the traditional wastewater treatment techniques such as activated carbon adsorption, chemical oxidation, biological treatment etc. For instance, activated carbon adsorption involves phase transfer of pollutants without decomposition and thus

creates another pollution problem. Chemical oxidation is unable to mineralize all organic substances and is only economically suitable for the removal of pollutants at high concentrations. In biological treatment, the main drawbacks are slow reaction rates, disposal of sludge and the need for strict control of pH and temperature.

The concept of AOP was initially proposed by Glaze *et al.*, in 1987 [12]. They defined AOPs as "processes at near ambient temperature and pressure which involve the generation of highly reactive hydroxyl radicals (HO[•]) in sufficient quantity to effect water purification". The kinetics of the reaction is generally first order with respect to the concentration of the species to be oxidized. These technologies can be applied successfully to remove the last traces of pollutants that are partially removed by conventional methods. They can also be used for the purification and disinfection of drinking water. The ultimate goal of these processes is to mineralize the organic contaminants present in water to carbon dioxide, water and harmless inorganic salts through degradation reactions.

AOPs can often achieve oxidative destruction of difficult to degrade contaminants such as halogenated hydrocarbons (trichloroethane, trichloroethylene), aromatic compounds (benzene, toluene, ethylbenzene, xylene, pentachlorophenol and nitrophenols), detergents, pesticides, etc. They can also be used to oxidize inorganic contaminants such as cyanide, sulphide, and nitrite. When applied appropriately, AOPs reduce the contaminant concentration from several hundred ppm to less than 5 ppb. That is why they are called "The treatment processes of the 21st century".

AOPs are also called Advanced Oxidation Technologies (AOTs) or sometimes Enhanced Oxidation Processes (EOPs) [13-15].

AOPs can be classified according to the reaction phase (homogeneous or heterogeneous) or the methods used to generate the HO[•] radicals (chemical, electrochemical, sonochemical photochemical etc). Some of the commonly used Advanced Oxidation Processes are listed in Fig. 1.1.

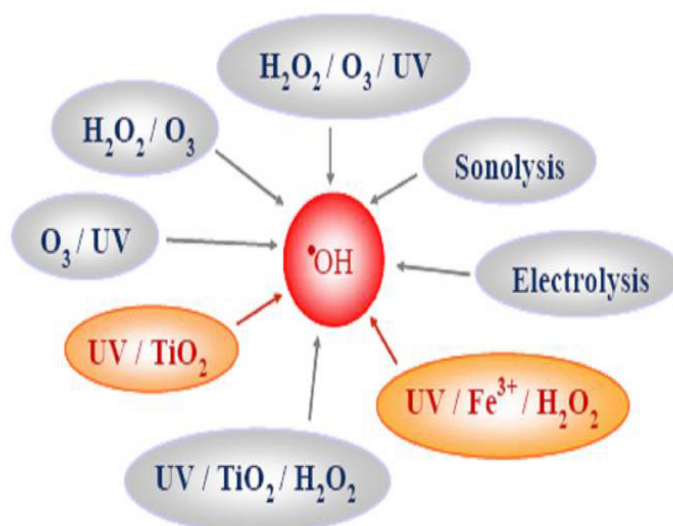


Fig.1.1: Commonly used Advanced Oxidation Processes (UV: Ultraviolet light) [16].

As most of the widely investigated AOPs use light as the energy source, they are also classified as photochemical and nonphotochemical processes (Table 1.1).

Table 1.1: Photochemical and Non-photochemical AOPs.

Photochemical AOPs	Non-photochemical AOPs
H ₂ O ₂ /UV	O ₃ / HO [•]
O ₃ /UV	O ₃ /H ₂ O ₂
O ₃ / H ₂ O ₂ /UV	O ₃ /US
Fe ²⁺ / H ₂ O ₂ /UV (Photo Fenton)	O ₃ /GAC*
TiO ₂ /UV, ZnO/UV	Fe ²⁺ /H ₂ O ₂ (Fenton system)
H ₂ O ₂ /TiO ₂ /UV	Electro-Fenton
O ₂ / TiO ₂ /UV	Electron beam irradiation
UV/US	Ultrasound (US)
	H ₂ O ₂ /US

*GAC- Granulated Activated Carbon

Most of the photochemical AOPs use a combination of strong oxidizing agents (e.g. H₂O₂, O₃) with catalysts (e.g. transition metal ions) and irradiation (e.g. ultraviolet, visible). These treatment processes are considered as very promising for the remediation of contaminated ground, surface and wastewaters containing non-biodegradable organic pollutants. The main advantages are high rates of pollutant oxidation, flexibility concerning water quality variations, and small dimensions of the equipment. AOPs degrade pollutants rather than concentrating or transferring them to a different phase and they do not generate secondary waste materials that need be disposed of [17, 18]. The main disadvantages are relatively high treatment costs and special safety requirements because of the use of very reactive chemicals like ozone, hydrogen peroxide etc., and high-energy sources like UV lamps, electron beams and radioactive sources.

Extensive research is in progress around the world on the development and improvement of AOPs [3, 20-27]. Irrespective of the reaction system,

all these processes involve the production of hydroxyl radicals ($\cdot\text{OH}$) which are extremely powerful and non-selective oxidants capable of oxidizing majority of organic compounds [19, 22, 26, 27].

1.2.1 Theory of Advanced Oxidation Processes

The general mechanism of AOP involves the generation of highly reactive free radicals ($\text{HO}\cdot$) which are effective in destroying organic chemicals due to their electrophilic and non-selective nature. The characteristics of $\text{HO}\cdot$ are shown in Fig. 1.2.

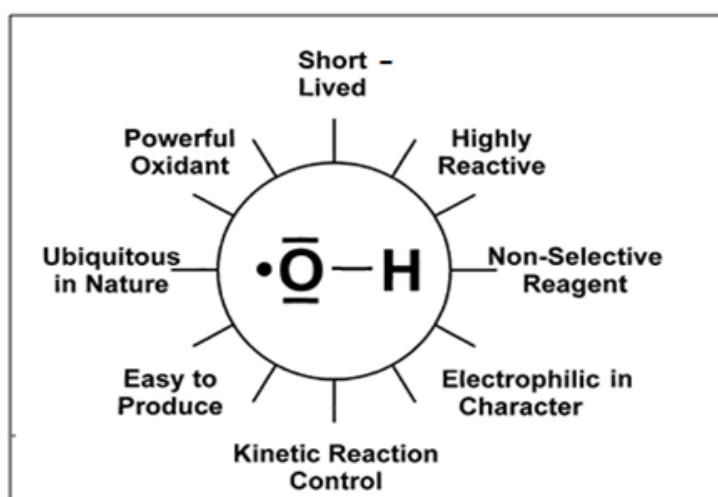


Fig.1.2: Characteristic features of the hydroxyl radical [16].

Because of their high reactivity, $\text{HO}\cdot$ radicals must be generated continuously “in-situ” through chemical or photochemical reactions. They attack most part of organic molecules with rate constants usually of the order of $10^6\text{-}10^9\text{M}^{-1}\text{s}^{-1}$. Hydroxyl radicals are known to be the second strongest oxidants after fluorine as shown in Table 1.2.

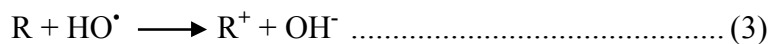
Table 1.2: Oxidation potential of common oxidizing agents.

Sr. no.	Oxidation species	Oxidation potential, eV
1	Fluorine	3.06
2	Hydroxyl radical	2.80
3	Sulphate radical	2.60
4	Atomic oxygen	2.42
5	Nascent oxygen	2.42
6	Ozone	2.07
7	Persulphate	2.01
8	Hydrogen peroxide	1.77
9	Perhydroxyl radical	1.70
10	Permanganate	1.68
11	Hypobromous acid	1.59
12	Hypochlorous Acid	1.49
13	Hypochlorite	1.49
14	Hypoiodous acid	1.45
15	Chlorine	1.36
16	Chlorine dioxide	1.27
17	Oxygen(molecular)	1.23
18	Bromine	1.09
19	Iodine	0.54

Hydroxyl radicals can be generated by different oxidation processes shown in Fig. 1.1. Heterogeneous photocatalysis using semiconductors such as zinc oxide (ZnO/UV) and titanium dioxide (TiO₂/UV), sonolysis, sonocatalysis, microwave catalysis as well as combination of these also proceed through HO[•]. In AOPs, once the hydroxyl radicals are generated, they react with most of the pollutants, yielding peroxy radicals which

further initiate chain reactions, leading finally to the formation of CO₂, H₂O and inorganic salts.

The hydroxyl radical (HO[•]) attacks the organic chemicals by radical addition (Eq.1), hydrogen abstraction (Eq.2) and/ or electron transfer (Eq.3) [5].



R is a typical organic chemical.

The efficiency of production and the reactivity of the radicals and of the degradation process depends on: (1) the energy needed to homolyze a given chemical bond, (2) the concentration of dissolved molecular oxygen, (3) the concentration of the target pollutant and (4) the concentration of the OH radical. Other factors influencing the efficiency include temperature, pH, presence of ions in the solution, presence and the concentration of radical scavengers etc.

1.3 Photocatalysis as an AOP

Photocatalysis, which uses light as the energy source for activation, can be either homogeneous or heterogeneous. The process, in general consists of (i) photochemical irradiation with ultraviolet/ visible light coupled with powerful oxidizing agents like ozone, hydrogen peroxide and /or a catalyst, (ii) Fenton and Photo-Fenton catalytic processes

(iii) Electron Beam Irradiation based processes and (iv) Sonolysis generated photocatalysis [20, 28-30].

1.3.1 Homogeneous Photocatalysis

Homogeneous photocatalysis (single phase system) has been used to treat contaminated water since 1970s. The method involves the usage of an oxidant to generate radicals, which attack the organic pollutants to initiate oxidation. In the homogeneous aqueous systems that employ simple solar irradiation, only primary structural changes take place in the original molecule and no complete mineralization can be achieved. The early encouraging results were obtained with UV/Ozone and UV/ H₂O₂. The use of UV light for homogeneous photocatalysis of pollutants can result in either (i) direct photo degradation, which proceeds following direct excitation of the pollutant by UV light or (ii) photo-oxidation, where light, drives oxidation processes principally initiated by hydroxyl radicals. The oxidizing strength of hydrogen peroxide alone is relatively weak, but irradiation by UV light enhances the rate and the strength of oxidation through the production of increased amounts of reactive hydroxyl radicals.

1.3.1.1 UV/Hydrogen peroxide (UV/ H₂O₂)

This homogeneous system involves the formation of HO[•] radicals from hydrogen peroxide and subsequent propagation reactions. Photolysis of H₂O₂ results in the cleavage of the molecule into hydroxyl radicals which interact with the pollutants and degrade them. The general mechanism of the process is shown in Fig. 1.3.

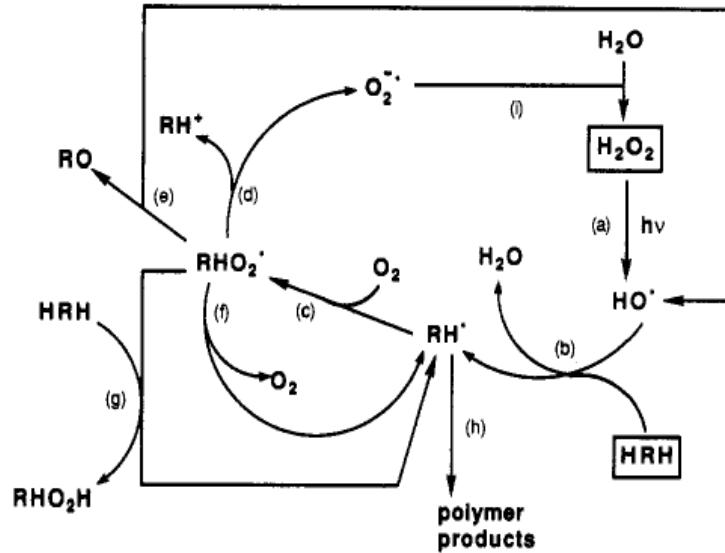
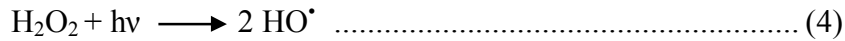
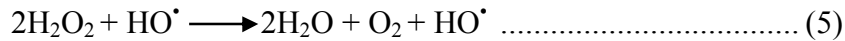


Fig.1.3: Reaction sequence for the UV/H₂O₂ process [31].



H₂O₂ is relatively harmless because it is found among the natural metabolites of many organisms. H₂O₂ is a weak acid, a powerful oxidant and an unstable compound. The rate of photolysis of aqueous H₂O₂ has been found to be pH dependent and increases under alkaline conditions. On the other hand, hydrogen peroxide is known to decompose by a dismutation reaction (Eq. 5) with a maximum rate when the pH becomes equal to its pK_a value [3].



H₂O₂ when used alone is not as effective as its combination with different oxidants to mineralize, degrade and/or decolorize the effluents [1, 2]. The use of hydrogen peroxide is now very common for the treatment of contaminated water due to the following practical advantages:

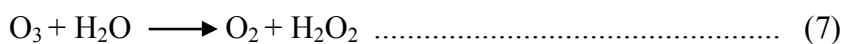
- 1) H_2O_2 is readily available in the solution form that can be diluted to give desired concentrations.
- 2) It does not lead to air emissions.
- 3) It has high quantum yield for hydroxyl radical formation.
- 4) H_2O_2 can be stored safely onsite and
- 5) It has infinite solubility in water.

The drawbacks include low molar extinction coefficient in the near UV-region and small absorption cross section at 254 nm.

UV/ H_2O_2 process is efficient in mineralizing organic pollutants and the process has been widely used for removal of dyes [5-7]. The combined use of UV/ H_2O_2 with ultrasonic waves (US) for the waste water treatment has been found to be very effective [8-10]. It has also been widely studied for the degradation of phenolic compounds and other such contaminants from waste water [5, 14, 28-32].

1.3.1.2 UV/Ozone (UV/ O_3)

Ozonisation is a well-known treatment process in water purification. The Ozone/UV process is frequently applied for the degradation of a wide range of compounds. In an ozonation process, oxidation occurs in two ways. One is the direct reaction between the ozone and the dissolved compounds (Eq. 6) and the other is the radical route in which the HO^\bullet radicals produced during the ozone decomposition (Eqs. 7 and 8) react with the dissolved compounds.



Ozone readily absorbs UV radiation at 254 nm and reacts with H₂O producing H₂O₂ as an intermediate, which then decomposes to give ·OH. In addition to the above, OH radicals are produced by the following step [3, 12]:



The reactive free radicals interact with the pollutant molecule, leading to its degradation and in many cases eventually mineralization.

Several studies have been reported on the application of the process for the removal of different aromatic compounds [14-19]. It has also been reported that the UV/ O₃ process is more efficient than the UV/H₂O₂ system [17, 18]. Kinetic models for the reaction of ozone with different organic and inorganic compounds have also been reported [21, 22, 25].

Advantages of this process are:

- 1) O₃/UV process is more efficient in generating hydroxyl radicals, because of its high molar extinction coefficient at 254nm.
- 2) Destruction of toxic refractory organics and microbial populations.
- 3) Higher rates of degradation compared to using UV or Ozone alone.

Drawbacks of this process are:

- 1) O_3 does not absorb at wavelengths > 300 nm.
- 2) Low- pressure mercury lamps emitting short UV radiation (UV-C) required.
- 3) Low solubility of ozone in water.
- 4) Potential secondary reactions of the oxidative intermediates.

1.3.1.3 UV/ Ozone and Hydrogen peroxide (UV/ O_3/H_2O_2)

Addition of hydrogen peroxide results in enhancement of the UV/ O_3 process efficiency [24-26] due to the dominant production of $\cdot OH$ radicals. Consequently, this is a very powerful method for the fast and complete mineralization of pollutants, as evidenced by the rate of TOC removal [3, 17, 24]. Fig.1.4. shows the reaction pathways in the UV/ ozone and ozone/ H_2O_2 systems.

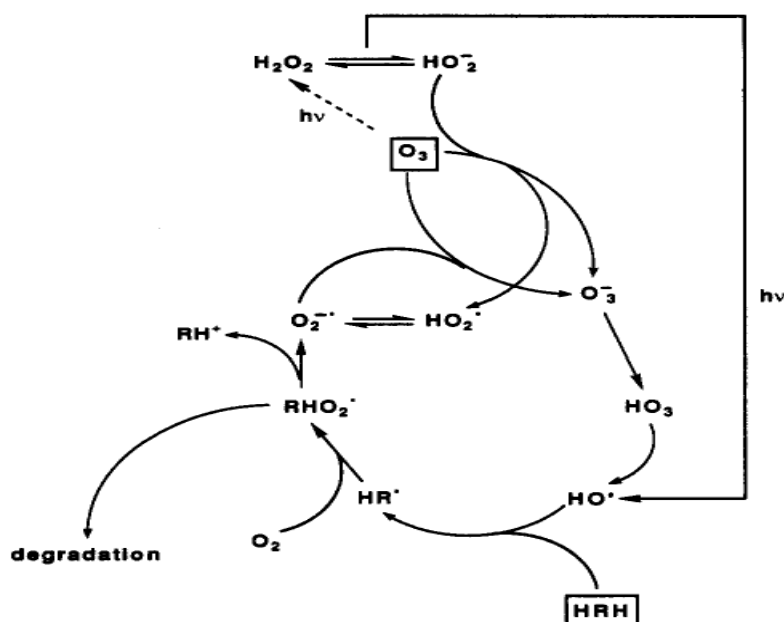


Fig.1.4: Reaction pathways in the UV/ozone and ozone/ H_2O_2 systems [3, 31].

The mechanism also illustrates the role played by H_2O_2 formed in-situ during the ozone decomposition in aqueous solution, as shown earlier.

1.3.1.4 Photo-Fenton system ($\text{UV}/\text{Fe}^{2+}/\text{H}_2\text{O}_2$)

The Photo-Fenton process is known for its ability to oxidize refractory compounds present in water and wastewater through the addition of UV radiation (sunlight or artificial sources of UV radiation) to the classical Fenton reagent, $\text{Fe}^{2+}/\text{H}_2\text{O}_2$. Fenton reaction rates are considerably increased by irradiation with UV/Visible light. Typical photo-Fenton-type system is shown in Fig.1.5. Fenton's reagent is able to destroy toxic compounds such as phenols, herbicides etc present in waste waters. In Photo-Fenton processes more number of HO^\bullet radicals is produced through both direct H_2O_2 photolysis and interaction of UV radiation with the iron species in aqueous solution. This leads to increased reaction rates and higher degrees of mineralization [2, 23, 24, 29].

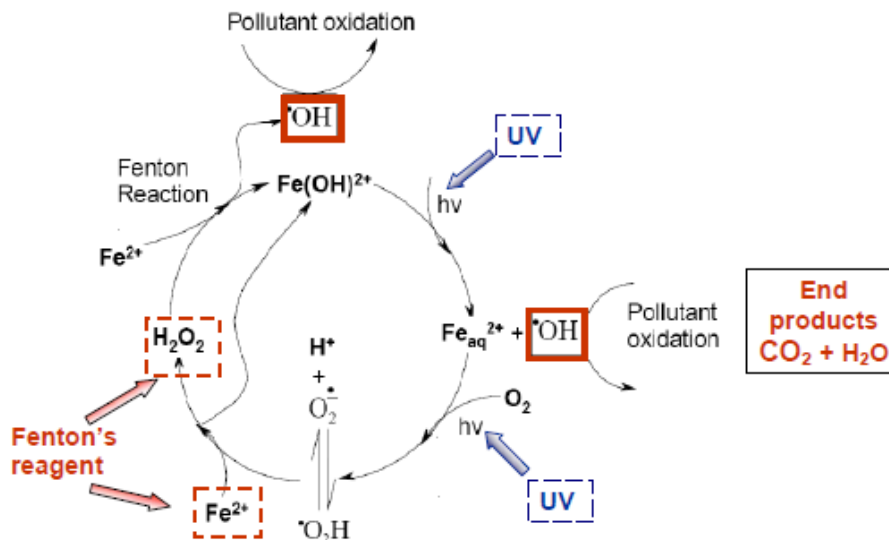
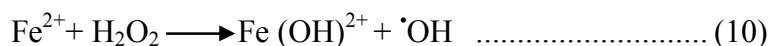


Fig.1.5: Reaction processes in $\text{UV}/\text{H}_2\text{O}_2$ and UV/Fenton systems [33].

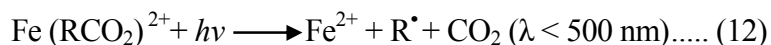
In Fenton reaction, the rate constant for the reaction of ferrous ion with hydrogen peroxide is very high and Fe (II) gets oxidised to Fe (III) in a few seconds to minutes in presence of excess amounts of hydrogen peroxide.



The ferric ions, represented by the complex $\text{Fe}(\text{OH})^{2+}$, is reduced back to Fe^{2+} by UV-visible irradiation according to Eq.11.



The ferric species can also form complexes with the initial organic compounds and/or degradation products, leading to photo-reduction back to Fe^{2+} according to Eq. 12:



The $\cdot\text{HO}$ radical formed will attack the organic substrates present in the wastewater. Since this reaction can be driven by low energy photons, solar irradiation [30] can be used as light source and this significantly reduces the operational cost of the treatment. Photo-Fenton process has been proven efficient in removing hydrocarbons even from saline wastewater. Heterogeneous Photo-Fenton process has been used for the pretreatment of winery wastewater [34-38]. The advantages of fenton/photofenton process for wastewater treatment include: (1) iron is a highly abundant and non-toxic element, and (2) hydrogen peroxide is easy to handle and environmentally benign [39]. However, it involves consumption of one Fe^{2+} ion for each $\cdot\text{OH}$ radical produced, demanding a high concentration of Fe (II).

1.3.2 Heterogeneous Photocatalysis

Heterogeneous photocatalysis involves the utilization of light source to photo-excite a semiconductor catalyst in presence of oxygen to produce an electron/hole pair. This leads to the formation of bound hydroxyl radicals or free holes. The organic pollutants can be completely mineralized by reaction with these oxidizers to form CO₂, water and salts. It is an efficient method for the degradation of a variety of pollutants in aqueous systems especially while using inexpensive solar irradiation [1-2, 14, 18, 28-30, 34-38]. The main advantages of this process are:

- i) It is inherently destructive in nature;
- ii) It involves mass transfer;
- iii) It can be carried out under ambient conditions using atmospheric oxygen as the oxidant and
- iv) It leads to complete mineralization of organic carbon into CO₂.

However, distribution and utilization of light energy in presence of solid catalyst material in liquid or gaseous mixtures make this process more complex compared to homogeneous process. Three components required for the heterogeneous photocatalytic reaction are: an emitted photon of appropriate wavelength, a catalyst surface (usually a semiconductor material) and a strong oxidizing agent (in most cases oxygen).

This process can also be carried out utilizing the near part of solar spectrum ($\lambda < 380\text{nm}$). Heterogeneous photocatalysis is utilized in a variety of reactions like organic synthesis, water splitting, photoreduction, hydrogen transfer, metal deposition, disinfection, anti-cancer therapy,

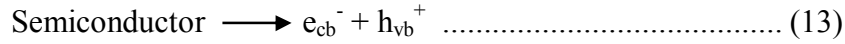
water detoxification and gaseous pollutant removal. In this context, semiconductor photocatalysis using semiconductor oxides as catalyst has received more attention, compared to other catalysts.

Advantages of using semiconductors in Photocatalysis are:

- i) They are inexpensive.
- ii) They are non-toxic.
- iii) They have high surface area.
- iv) They exhibit broad absorption spectra with high absorption coefficients.
- v) They have tunable properties which can be modified by size reduction, doping, sensitization, etc.
- vi) They are capable of participating in multielectron transfer process.
- vii) Their extended use is possible without substantial loss in photocatalytic activity.
- viii) When recovered by filtration or centrifugation or when immobilized, semiconductor particles retain much of their native activity after repeated catalytic cycles [36-38].

1.3.2.1 General Mechanism

When a semiconductor is illuminated by light with energy equal to or greater than band-gap energy, the valence band electrons are excited to the conduction band, leaving positive holes in the valence band:



The excited electron-hole pairs generated can recombine, either in the bulk or at the surface releasing the input energy as heat, with no chemical effect. However, if the electrons (and holes) migrate to the surface of the semiconductor without recombination, they can participate in various oxidation and reduction reactions with adsorbed species such as water, oxygen, and other organic or inorganic species. These processes, i.e., oxidation of a suitable electron donor adsorbed on the surface by photogenerated hole and reduction of electron acceptor adsorbed on the surface by photogenerated electron, constitute the basic mechanisms of photocatalytic water/air remediation and photocatalytic hydrogen production, respectively. A simple mechanism for photocatalytic process on a semiconductor is presented in Fig. 1.6.

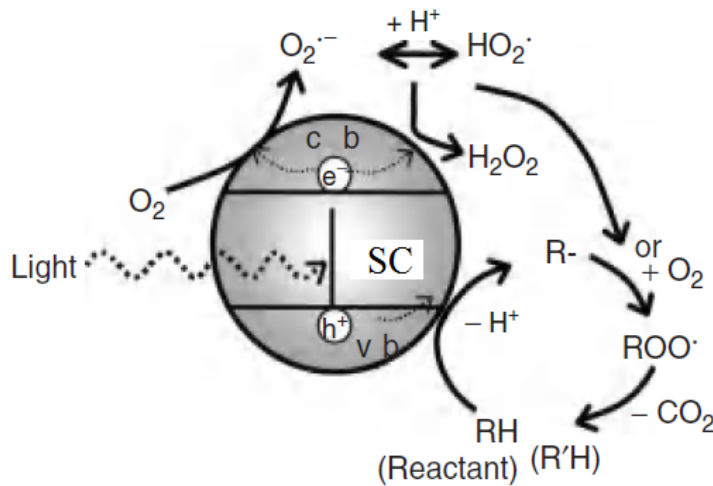
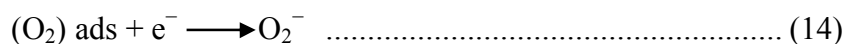


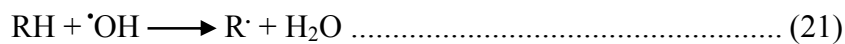
Fig.1.6: A simplified mechanism for the photocatalytic process on a semiconductor [34].

The reaction steps involved in the process after the photoexcitation as in reaction (13) are summarized as follows.



The positive hole can oxidize pollutants directly. However, in most cases it reacts with water (i.e., hydroxide ion, OH⁻) to produce the hydroxyl radical (•OH), which is a very powerful oxidant with an oxidation potential of 2.8 V vs NHE. •OH rapidly attacks pollutants at the surface as well as in solution and mineralizes them into CO₂, H₂O etc [40, 41].

Hydroxyl radical (•OH) and superoxide radical anion (O₂⁻) are the primary oxidizing species in the photocatalytic oxidation processes. They cause the degradation of the organic (RH) pollutants by oxidation via successive attack by OH radicals.



Photocatalytic degradation of environmental contaminants using semiconductor photocatalysts has been investigated widely ever since the pioneering work of Fujishima and Honda in early 1972 [42]. Many review papers on semiconductor photocatalysis can be found in literature [43-46]. Many of these investigations have utilized aqueous suspensions of semiconductors illuminated by UV light to photodegrade the pollutants.

1.3.2.2 Importance of Semiconductors as photocatalysts

Semiconductor photocatalysis offers many advantages for the removal of pollutants at low concentration from water. These include:

- i) Complete oxidation of organic pollutants within few hours
- ii) No formation of polycyclic products
- iii) Availability of highly active and cheap catalysts capable of adapting to specially designed reactor systems.
- iv) Oxidation of pollutants in the ppb range etc.

Several semiconductors have been studied as potential photocatalysts for this purpose. These include: CdS, ZnS, ZnO, TiO₂, WO₃, NbO₂, ZnO/TiO₂, TiO₂/SiO₂ and TiO₂/Al₂O₃. Among these, TiO₂ is one of the most popular and promising materials, because of its stability under harsh conditions, commercial availability, existence in different allotropic forms with high photo-activity, possibility of its coating as a thin film on solid support, ease of preparation in the laboratory etc. Its absorption spectrum overlaps with the solar spectrum in UV region and hence opens up the possibility of using solar energy at least partially as the source of irradiation.

Semiconductors have electric resistivity values generally in the range of 10^{-2} to 10^9 ohm-cm at room temperature, i.e., intermediate between that of conductors ($< 10^{-6}$ ohms-cm) and insulators (10^{14} to 10^{22} ohm-cm) [46]. In the semiconductor, the highest occupied energy band is called the valence band (VB) and lowest empty energy band is called the conduction band (CB). These two bands are separated by an energy band called band gap, (E_g). Fig.1.7 shows the band structure and band filling in metals, insulators and semiconductors [47].

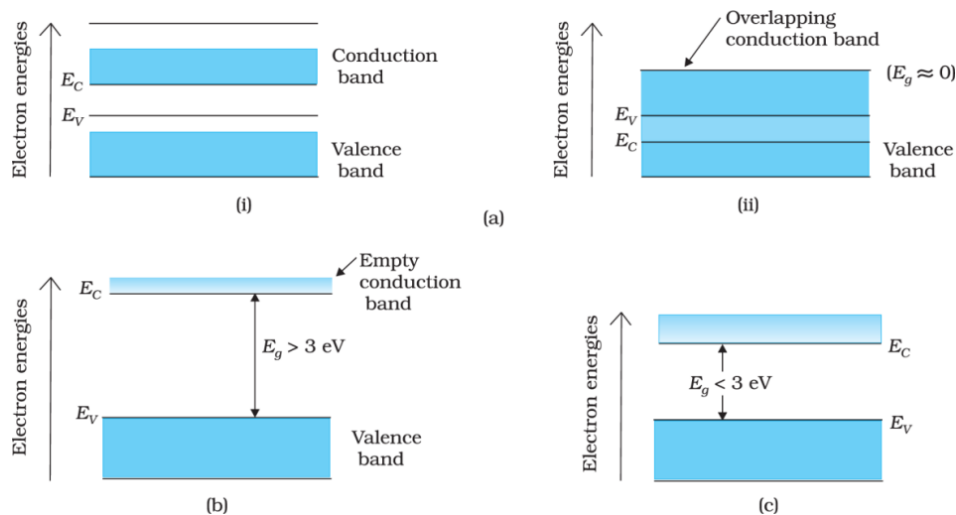


Fig.1.7: Difference between energy bands in (a) metals, (b) insulators and (c) Semiconductors [47].

Electrons which are in the valence band cannot move easily, but electrons in the conduction band can move freely.

Semiconductors can be classified into intrinsic and extrinsic semiconductors. In intrinsic semiconductors, electrons can be excited to the conduction band leaving the same number of holes in the valence band. In order to promote conductivity of extrinsic semiconductors, they must be doped with adequate number of impurities, such as metal oxides or sulfur

compounds. Depending on the nature of impurities introduced, the extrinsic semiconductors can be divided into n-type (in which majority charge carriers are electrons) and p-type (in which majority charge carriers are holes).

In semiconductors, mobile charge carriers can be generated by three different mechanisms:

- 1) Thermal excitation: If the band gap energy is sufficiently small ($< \frac{1}{2}$ eV) thermal excitation can promote electrons from valence band to the conduction band.
- 2) Photoexcitation: In this case, an electron can be promoted from the valence band to the conduction band upon absorption of a photon of light, provided that the photon energy is greater or equal to the band gap energy and
- 3) Doping: In this process new levels are introduced into the band gap. Two types of doping can be distinguished. In n-type doping with group III elements like B, Al, Ga and In, occupied donor levels are created near the conduction band edge where current is carried mainly by negative charge carriers. Likewise, p-type doping with group V elements like P, As, Sb and Bi results in the formation of empty acceptor levels near the valence band, creates positive charge carriers where current is carried mainly by positive charges. The surface defects and impurities in n-type or p-type semiconductors are responsible for the change in band gap of the semiconductor. Table 1.3 lists some selected semiconductor materials, which have been investigated for photocatalytic reactions. Respective VB and CB potentials and band gap energy are also provided.

Table 1.3: Band Position of Common Semiconductor Photocatalysts at pH=1.

Semiconductor	Valence Band Potential (eV vs.NHE)	Conduction Band Potential (eV vs. NHE)	Band gap Energy, E_g (eV)	Band gap Wavelength (nm)
TiO ₂	+3.1	-0.1	3.2	388
SnO ₂	+4.1	+0.3	3.9	318
ZnO	+3.0	-0.2	3.2	388
ZnS	+1.4	-2.4	3.7	335
WO ₃	+3.0	+0.2	2.8	443
CdS	+2.1	-0.4	1.4	496
CdSe	+1.6	-0.1	1.7	729
GaAs	+1.0	-0.4	1.4	886
GaP	+1.3	-1.0	2.3	539

TiO₂ is proven to be the most suitable photocatalyst for environmental applications [12, 13, 18, 27]. In spite of vigorous search for the ideal photocatalyst for more than two decades, titania still remains as a benchmark against which any emerging candidate material will be measured. Furthermore, TiO₂ is of special interest since it can use natural (solar) UV radiation. It has an appropriate E_g i.e., 3.2 eV Vs NHE, which can be surpassed by the energy of a solar photon. So it absorbs the near UV light ($\lambda < 388\text{nm}$). Due to faster electron transfer to molecular oxygen, TiO₂ is found to be very efficient for photocatalytic degradation of pollutants [48-50].

Another semiconductor with characteristics similar to TiO₂ and tested as a suitable alternative is ZnO. However, ZnO dissolves in acidic solutions, is susceptible to photocorrosion and therefore cannot be used

for commercial applications. Other semiconductor materials such as CdS or GaP can absorb larger fractions of the solar spectrum compared to TiO₂ or ZnO and form chemically activated surface-bound intermediates. But unfortunately, such catalysts get degraded during repeated catalytic cycles which is usually required for the commercial application of heterogeneous photocatalysis [49-54].

1.3.2.3 Some typical photocatalytic degradation studies

Many photocatalytic degradation studies [42, 53-55] show that the catalytic activities are strongly influenced by the crystal structure and chemical composition of the catalyst. Photocatalysis for the purification of contaminated water especially for the removal of toxic organic pollutants has been attracting attention in recent years [56, 57]. Various investigators have demonstrated that sun is a useful energy source for driving photocatalytic processes. A number of reviews have been published in recent years on various aspects of photocatalysis, including developments in the areas of catalysts, energy sources, types of organic and inorganic pollutants etc [56-66]. Some important studies relevant in the present context are discussed below. This is not a complete list of publications in the field since the exhaustive literature on the photocatalytic degradation of various pollutants cannot be included within the limits of the current context.

Phenols have always been the subject of many photocatalytic studies [58, 59]. Han *et al.*, [48] reported that the rate of degradation of phenols depends on the structure of the substrate. The degradation was shown to follow a pseudo first order kinetics. Addition of small quantities of Pt and Ag is reported to enhance the efficiency of TiO₂ catalysts. Ag/ TiO₂ catalyst,

prepared by deposition of small amounts of metallic silver by in situ metal ion photoreduction, is found to be very efficient for the mineralization of trace amounts of phenol in water [54]. The availability of dissolved oxygen is another key factor that determines the efficiency of degradation [55]. Pandiyan *et al.*, [67] have investigated the dehalogenation and destruction of halogenated phenols using photochemical methods. Dehalogenation was faster for mono halogenated phenols than for poly-substituted phenols.

Wu and Zhang [68] reported that a thin film of TiO₂ (anatase) prepared by the direct oxidation of metallic titanium using H₂O₂ is highly efficient for the photodegradation of Rhodamine B in water. The dye decayed directly to colourless end products i.e. water, CO₂ and mineral acids. Another interesting catalyst that enhanced the photodegradation of Rhodamine B is ZnFe₂O₄ doped TiO₂ [69].

Chen *et al.*, [70] investigated the role of semiconductors on the photodegradation of an azo dye, Acid Orange 7 (AO7) in UV-illuminated TiO₂ suspension. TiO₂ deposited on activated carbon (TiO₂/AC), showed higher photo activity for the photo oxidation of methyl orange. TiO₂/AC had higher efficiency than either pure TiO₂ particles, or simple mixture of TiO₂ powder with activated carbon [71]. Ethyl Violet (EV) was shown to be degrading completely in aqueous TiO₂ dispersions by visible light irradiation. During visible light irradiation, the characteristic absorption band of the dye decreased rapidly and shifted to lower wavelength. However, no new absorption bands appeared even in the ultraviolet range [72].

The photocatalytic degradation of Dimethoate, an organophosphorous pesticide has also been investigated [73]. Minero *et al.*, [74] studied the

photocatalytic degradation of Nitrobenzene (NB) on TiO₂ and ZnO. Complete mineralization was achieved with TiO₂. Mathews [75] also reported that more than 90% of NB mineralization was achieved with TiO₂ and sunlight.

Muneer *et al.*, [66] investigated the photodegradation of two selected pesticides 3-tert-butyl-5-chloro-6-methyluracil (Terbacil) and 2,4,5-tribromoimidazole (Imidazole) in aqueous suspensions of TiO₂ under a variety of conditions. Shankar *et al.*, [76] used a thin-film reactor with immobilized TiO₂ for photocatalytic mineralization of common pesticides, 2,4-dichlorophenoxyacetic acid (DPA) and monocrotophos (MCP). The results clearly demonstrated that the good adsorption capacity of the support and the effective utilization of light by TiO₂, improved the photocatalytic activity of supported TiO₂.

Oyama *et al.*, [77] investigated the photodegradation of a commercial detergent containing an anionic surfactant and a fluorescent whitening agent in aqueous TiO₂ dispersion under solar irradiation. The degradation process followed apparent first-order kinetics. Horvath *et al.*, [78] investigated the Fe (III)-photo-induced oxidation of anionic lauryl sulfate (LS⁻) and cationic cetyltrimethylammonium (CTA⁺) surfactants in aqueous solution. A mechanism suggesting a major role for OH radicals in degradation of the surfactants is also proposed.

Djebbar *et al.*, [79] reported the photocatalytic degradation of many chlorinated organic compounds by semiconductor particles. Hariharan [80] investigated the photodegradation of chlorinated aromatic compounds using ZnO nanoparticles (ZnO-nano) in aqueous solutions. ZnO

nanoparticles served as a better catalyst compared to bulk ZnO and commercially available Degussa TiO₂ in achieving degradation of the contaminants.

Photocatalytic degradation of various azo dyes in water in the presence of ZnO as a photocatalyst under UV light irradiation has been studied using a slurry reactor [40, 41]. Similar studies have been made under sunlight as well. But the application of ZnO as a photocatalyst remains limited by pH [42].

Combination of semiconductors has yielded significant enhancement in photoactivity compared to individual components [42, 43]. This enhancement is attributed to an efficient charge-separation process and a subsequent higher availability of the reactive electron-hole pairs. However, the process may not be that simple. The chemistry of the substrate as well as the reaction intermediates and their interaction may also have an important role in determining the ultimate photoactivity of a catalyst. More studies are needed to understand the precise role of the catalysts, especially in the processes taking place at the interface.

1.4 Ultrasonic Cavitation/Sonication

Ultrasonic technology has been receiving attention in recent years as an AOP for wastewater treatment. Ultrasound refers to sound energy at frequencies above the range that is normally audible to human beings (i.e. >16 kHz). The upper limit of ultrasonic frequency is not well defined but it is generally considered as 5MHz in gases and 500MHz in liquids and solids. The range 20 to 100 kHz is designated as power ultrasound,

while frequencies up to 1 MHz are known as high frequencies or diagnostic frequencies.

Environmental Sonochemistry is a rapidly growing area. The effects of ultrasonic waves on materials were first observed by British nautical engineers in 1894. These are longitudinal waves comprising of rarefactions (negative pressures) and compressions (positive pressures) generated by spinning propellers. The alternating cycles of compression and rarefaction can produce the phenomenon of “cavitation” which is also known as hydrodynamic cavitation.

Cavitation is the formation, growth and collapse of bubbles in the liquid. This occurs whenever a new surface or cavity is created within a liquid. A cavity is any bounded volume, whether empty or containing gas or vapor, with at least part of the boundary being liquid. The collapse of the bubbles induces localized supercritical conditions like high temperature, high pressure, electrical discharges, and plasma effects. It has been reported that the gaseous contents of a collapsing cavity reach temperatures as high as 5500 °C. The liquid immediately surrounding the cavity reaches upto 2100 °C. The pressure is estimated to be 500 atmospheres. These conditions create transient supercritical water. Fig.1.8. shows the production of bubbles by liquids irradiated with ultrasound. These bubbles oscillate, grow a little more during the expansion phase of the sound wave and then shrink during the compression phase. Under proper conditions, these bubbles can undergo violent collapse, generating very high pressures and temperatures. When the bubbles implode in irradiated liquids the resulting compression is so rapid that little heat can escape from the bubble

during the process. However, the surrounding liquid, which, is still cold will quickly quench the heated cavity.

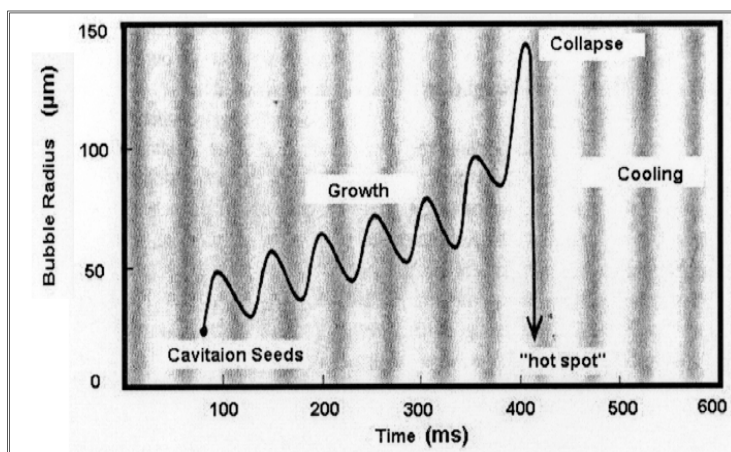


Fig. 1.8: Cavitation and Implosion phenomena [81].

Thus, ultrasound produces mechanical energy that can result in permanent physical change to the materials subjected to it through the unique cavitation phenomenon. Volume ratios of the solvents and solutes play an important role in the shape of the crystals. The exposure of supersaturated solution to ultrasonic field speeds up crystallization resulting in smaller crystals. Lower ultrasonic frequencies in the 20-30 kHz range are more effective in breaking up large crystals by cavitation. Thus, cavitation serves as a means of producing multitude of micro reactors. In spite of the extreme local temperature and pressure conditions created by the cavity implosion, it is possible to have good control over the sonochemical reactions. The intensity of cavity implosion and hence, the nature of the reaction is controlled by factors such as acoustic frequency, acoustic intensity, bulk temperature, static pressure and the choice of liquid or dissolved gas. Under these extreme conditions dissolved oxygen

molecules and water molecules are cleaved producing $\cdot\text{H}$, $\cdot\text{O}$ and $\text{OH}\cdot$. These entities react with each other and with H_2O and O_2 during the quick cooling phase, producing HO_2 radicals and H_2O_2 . In this molecular environment, organic compounds are decomposed and inorganic compounds are oxidized or reduced.

This property of US inducing radical formation has found application in sonolysis of water, sonolytic degradation of aqueous organic pollutants and sonochemical synthesis of chemicals. The underlying phenomena include cavitation, microstreaming, and localized supercritical conditions, which can lead to sonolytic splitting of water as well as pyrolysis of a vaporized molecule. The creation and collapse of transient and stable cavitation bubbles is schematically presented in Fig. 1.9.

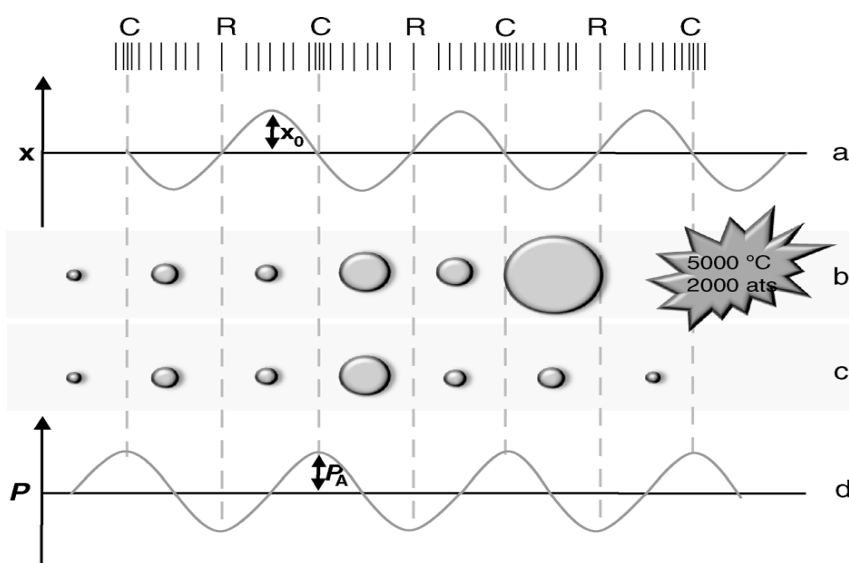


Fig.1.9: Creation and collapse of transient and stable cavitation bubbles: (a) Displacement graph; (b) Transient cavitation; (c) Stable cavitation; (d) Pressure graph [81].

In aqueous phase sonolysis, there are three potential sites for sonochemical activity, as shown in Fig. 1.10.

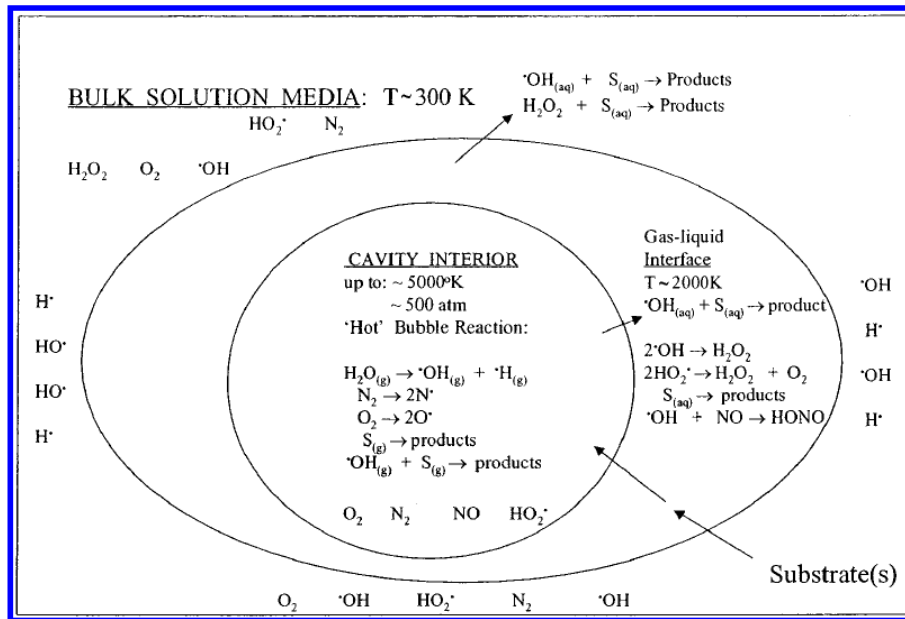
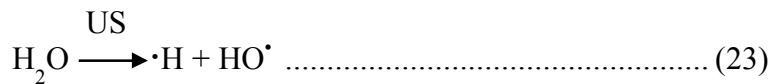


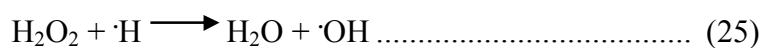
Fig.1.10: The three reaction zones of cavitation [82].

- (1) The gaseous region of the cavitation bubble where volatile and hydrophobic species are easily degraded through pyrolytic reaction. Hydroxyl radicals are formed here through sonolysis of water as shown below:



- (2) The bubble–liquid interface where hydroxyl radicals are localized. Radical reactions predominate here although pyrolytic reactions may also occur to a lesser extent.

- (3) The liquid bulk where secondary sonochemical activity may take place mainly due to free radicals that have escaped from the interface and migrated to the liquid bulk. Hydroxyl radicals can also recombine yielding hydrogen peroxide which in turn, reacts with hydrogen radical to regenerate hydroxyl radicals again.



The formation of free radicals during sonolysis of water has been explored in many studies for the sonolytic degradation of aqueous organic pollutants and sonochemical synthesis of chemicals. These phenomena can also lead to sonolytic splitting of water as well as pyrolysis of the vaporized molecules [81-86]

The advantages of sonication in waste treatment are:

- 1) Toxic wastes can be treated
- 2) Environmental friendly technology using only electricity as the input.
- 3) The energy consumption is flexible and depends on the Chemical Oxygen Demand (COD).
- 4) The treatment can be stopped by simply switching the power off.
- 5) Cost-effective and safe.
- 6) Even effluents with low conductivity can be treated [84].

Gogate and Pandit [4] have summarized the current status of the hydrodynamic cavitation reactors in an excellent review. The bubble dynamics analysis and optimum design considerations are also well illustrated.

1.4.1 Sonolysis/Sonocatalysis in water treatment: Case Studies

The sonolysis of Diclofenac in water was investigated at ultrasound frequencies of 24, 216, 617, and 850 kHz in presence of various catalysts like TiO₂, SiO₂, SnO₂, and titanosilicate. The highest rate of degradation is achieved at 617 kHz. The relative concentration of Diclofenac decreased from 100% to 16% in 30 minutes in presence of titanium dioxide (P25) [87].

The sonolysis of 4-chlorophenol (4-CP) was investigated in oxygen saturated aqueous solutions under different operating conditions. Degradation takes place in the solution bulk at low reactant concentrations and follows pseudo first order kinetics [88].

Investigation on the sonochemical degradation of Dichlorvos in a batch reactor showed that acoustic power and nature of sparge gas greatly affect the degradation efficiency [89]. Studies on the effect of ultrasound power, H₂O₂, NaCl and external gases on the degradation of oxalic acid showed that H₂O₂ had negative contribution to the degradation [90]. Upto an optimum concentration, NaCl enhances the degree of degradation.

Okitsu *et al.*, [91] studied the sonochemical decolorization and degradation of the Azo dyes Reactive Red 22 and Methyl Orange. It was reported that Azo dye molecules were mainly decomposed by OH radicals

formed from the water sonolysis. Mahamuni and Pandit [92] employed a hybrid technique of ozonation coupled with cavitation for the degradation of phenol. The hybrid technology is more efficient and leads to the formation of intermediates that can further be subjected to biodegradation.

Guo *et al.*, [93] studied the influence of ultrasonic output intensity, solution pH, H₂O₂ concentration and addition of Fenton reagent on the degradation of 2, 4-Dinitrophenol (DNP) under ultrasonic irradiation. It was observed that sono-oxidation in combination with FeSO₄/H₂O₂ exhibited a synergistic effect for DNP degradation. The hybrid effect of light and ultrasonic waves was first confirmed by Yano *et al.*, [94] for the complete mineralization of propyzamide with TiO₂ and H₂O₂.

1.4.2 Sonocatalytic inactivation of bacterial pollutants

Several methods, such as pasteurization, chlorination, ozonation, UV and ultrasound (US) irradiation have been utilized over the years for the inactivation of microorganisms. Ultrasound irradiation is one of the most attractive treatment techniques since the inactivation can be achieved under ambient conditions of pressure and temperature without any chemical treatment [95-98]. The damaging effect of ultrasound on microorganisms was recognized as early as in early 1929, when Harvey and Loomis studied the destruction of luminous bacteria using high frequency sound waves at 375 kHz [99]. In recent years, extensive research is focused on the effect of ultrasound on microorganisms, in particular, the mechanism of US interaction with the microbial cell and materials. Microstreaming cavitation phenomenon (as discussed earlier)

produces shock wave and associated shear disruption. Localized heating and free radical formation were identified as the primary causes for the destruction of cell membrane and consequent inactivation of microorganisms in water. Ultrasound is able to inactivate bacteria and deagglomerate bacterial clusters or flocs through a number of physical, chemical and mechanical effects arising from cavitation. Microorganisms which are mostly hydrophobic, may act as nuclei to induce cavitation in ultrasonic field. This effect may enhance disinfection efficiency.

The inactivation rate depends on the duration of sonication, ultrasonic power level, its frequency, the nature of dissolved gas and properties of microorganisms including the size and shape of the cell. The inactivation is explained in terms of physical effects and/or chemical effects generated during the ultrasonic irradiation. The chemical effects in liquid include cavitation and resultant localized supercritical conditions as explained earlier [100-104]. The ROS formed during the sonication can disrupt or damage various cellular functions or structures of microorganisms and thus play a significant role in the cell killing process through DNA damage. Furuta *et al.*, [100] have suggested that the physical effects due to the shock waves might be more important than the chemical effects for the inactivation of *E.coli*.

Piyasena *et al.*, [101] suggested that the mechanism of microbial inactivation by ultrasound is dependent on the microbial species. Gram-negative bacteria usually have a thinner cell wall with an outer membrane, while the Gram-positive bacteria possess a thicker cell wall and lack the outer membrane. Ananta *et al.*, [102] proposed that ultrasonic biological

effects on different types of Gram-negative and Gram-positive bacteria are due to the differentiating feature in the cell morphology. Similar suggestions about the inactivation mechanism were given by Alvarez *et al.*, [103] who investigated bacterial species with different cell structures using the underwater shock waves.

Unfortunately, US technique is too expensive to be used as a general microbiological decontamination tool. However, over the last two decades, it has been reported that microorganisms are becoming resistant to the disinfection techniques involving chemicals, UV and heat treatment. This has revived the interest in US as an adjunct to other techniques. High power ultrasound radiation in conjunction with conventional disinfectants such as chlorine and hydrogen peroxide has been successfully applied in the destruction of fecal coliforms and protozoa. The inactivation of *E.coli* and *Hansenula polymorpha* has been achieved through the US irradiation of TiO₂ suspension in water [101-103].

Ince and Belen [104] observed that the concentration of *E. coli* in deionized water decreased with treatment time at 20 kHz of sonication. Added solids (ceramic granules, metallic zinc particles, and activated carbon) improved the inactivation of *E. coli*. All bacteria were affected by the ultrasound with the bactericidal effect increasing with time and intensity of irradiation.

Koda *et al.*, [105] reported that the OH radicals play an important role in the *E.coli* inactivation by ultrasound.

1.5 Sonophotocatalytic processes

Although both photocatalytic and sonolytic degradation of organic pollutants have been found to be useful in the remediation of environmental contaminants, there is an optimum limit for these individual processes. In this context, sonophotocatalysis (SPC) which refers to the simultaneous application of ultrasound and photocatalysis to a system has gained importance. The degradation rate could be higher than, or equal to the sum of the individual degradation rates for photocatalysis and sonolysis. Synergy in sonophotocatalysis in which the combined efficiency is more than the sum of the efficiencies for the individual processes is reported in few cases [106]. The synergistic effect of sonophotocatalysis is schematically presented in Fig.1.11.

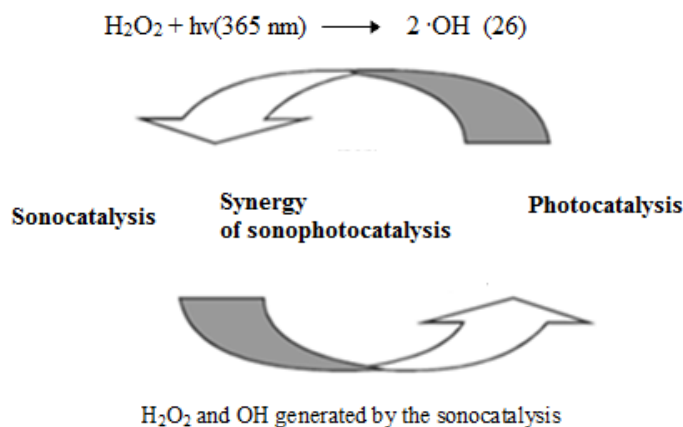


Fig.1.11: Synergistic effect of sonophotocatalysis [106].

The basic reaction mechanism for ultrasound initiated degradation as well as photocatalytic oxidation involves the generation of free radicals and their subsequent attack on the organic pollutant. If the two modes of

irradiation (UV and ultrasound) are operated in combination, more number of free radicals will be available for the reaction thereby increasing the rate of reaction.

Ultrasound may also modify the rate of photocatalytic degradation by promoting the deaggregation of the catalyst. This will increase its active surface area, and thereby the amount of reactive radical species through cavitations and ultimately enhanced degradation/mineralization of the pollutant.

The effectiveness of SPC in the degradation/ mineralization of pollutants can be attributed to the following: (i) Ultrasound provides an extra source of $\cdot\text{OH}$ radicals through cavitation; (ii) acoustic cavitation can remove intermediates from the photocatalytic active sites and make the sites available for fresh adsorption and activation. (iii) Acoustic cavitation generates a number of physical effects, such as shear forces, turbulence and micro-streaming that help to regenerate the active catalytic surface. (iv) Acoustic cavitation increases the uniformity of the dispersion, when the catalyst or the pollutant is in the form of a powder or an agglomerate, thereby increasing the available surface area; (v) Acoustic cavitation is able to enhance mass transfer towards the liquid–solid interface; (vi) Acoustic cavitation is capable of accelerating the rate of adsorption of reactant on the photocatalyst and (vii) sonolysis is likely to decompose the hydrophobic part of the pollutant compound, which is unlikely to occur on the surface of the photocatalyst.

From the above effects of acoustic cavitation, it is clear that the simultaneous use of the two techniques will be more effective, possibly

leading to synergy. However, their sequential combination may result only in simple additive effects. The efficiency as well as the synergy will depend on the frequency of sonolysis. Photocatalysis combined with high frequency sonolysis results in an overall pollutant degradation rate that is equal to the sum of the individual rates. However, low frequency sonolysis in combination with photocatalysis results in stronger synergistic effect. In this case the synergistic effect depends on the level of US power.

Sonophotocatalysis has been studied as a possible technique for the degradation of various organics such as salicylic acid, propylamide, 1,4-dioxane, 2-(butylamino) ethanethiol, 2-chlorophenol, dyes and MTBE (Methyl tertiary butyl ether). Adewuyi *et al.*, [82, 83] have made an extensive overview of different studies on the use of sonophotocatalysis for treatment of wastewaters. Berberidou. *et al.*, [107] observed that the degradation of Malachite Green (MG) in water by TiO₂ sonophotocatalysis was faster than the respective individual processes which was attributed to the enhancement of formation of reactive radicals as well as the increase in the active surface area of the catalyst. The hybrid effect of the irradiation by light and ultrasonic waves in conjunction with H₂O₂ was first confirmed by Yano *et al.*, [94]. They investigated the mineralization of propylamide and reported that the reaction carried out in batch operation system followed a pseudo-first-order kinetic model at different pH and peroxide dosages. Harada *et al.*, [108] reported enhanced efficiency of sonophotocatalytic reaction in water splitting using TiO₂ photocatalyst.

Selli [109] have reported the synergistic effect of sonophotocatalysis in the degradation of Acid Orange 8 in aqueous suspensions, when low ultrasound frequency is used. Pe´rez *et al.*, [110] also reported similar results from a comparative study of the sonolytic, photocatalytic and sonophotocatalytic degradation of Malachite Green in water. Kulkarni *et al.*, [111] reported that photocatalysis combined with ultrasound yields higher degradation rates of the contaminants. This is explained based on the standard effects of ultrasound on photocatalyst: i.e., the mechanical effects of cavitations involving photocatalyst surface cleaning and increased mass transfer of the polluting species to the powdered catalyst surface. The sonophotocatalytic degradation of Basic Blue 9, an industrial textile dye was studied in presence of ultrasound (20 kHz) and TiO₂ slurry catalyst employing a UV lamp (15W, 352 nm) by Martinez and Gonzatez [112]. The color removal efficiency was ~ 43% under sonolysis, 85% under photocatalysis and 97% under sonophotocatalysis after 50 min of irradiation time. Davydov *et al.*, [113] studied the effect of ultrasound on the photodegradation of salicylic acid on four commercial titania powders. Synergistic effects were noticed only for catalysts with smaller particle size (such as Hombikat), while no enhancement was observed for the largest particle size photocatalyst TiO₂ (Aldrich anatase). Degussa P25 exhibited the highest overall activity. The presence of stable intermediates in the bulk solution was observed during the photocatalytic degradation of phenol. The presence of ultrasound, however, eliminates the toxic intermediates and leads to complete mineralization.

The sonophotocatalytic degradation of phenolic compounds in presence of H₂O₂ in agro-industrial effluents was investigated by

Silva *et al.*, [114]. They also observed the synergy compared to the respective individual treatments or their serial combination, i.e. sonolysis and photocatalysis. H₂O₂ enhanced the process efficiency which is attributed to an increase in the production of hydroxyl radicals via water sonolysis and H₂O₂ cleavage. Acceleration of mass transfer of reagents onto the TiO₂ surface as well as removal of any impurities from its surface also contributes to the enhanced efficiency [115].

Extensive research is being done on this technology in recent years for the degradation of pollutants like dyes, phenols, substituted phenols, alkyl halides, aromatic halides, substituted halides, herbicides, pesticides, inorganic chemicals etc. Almost all the studies are made using TiO₂ as the catalyst. Not much work has been done with ZnO even though its characteristics as a semiconductor are comparable to those of TiO₂. Hence, in the current study, a detailed investigation is undertaken on the removal of trace amounts of phenol contaminants and microorganisms in water under US, UV and US+UV irradiation in presence of ZnO.

Many of the AOPs using catalyst aimed at water purification are carried out with the catalyst suspended as fine particles in the contaminated water, employing a low solid concentration and a slurry reactor. The reactor configurations tested include fixed bed, fluidized bed, immobilized membrane fixed on the reactor walls, a reactive wall reactor and an immobilized film coated on a bundle of optical fibers. It had been generally accepted but not conclusively established that the highest efficiency is obtained with the suspended solid approach. However, the cost of separating the catalyst from the treated water for recycling may

partially offset this advantage. The scaling up of slurry type reactors for large-scale applications poses challenges, especially in the case of parameters for optimum energy (light, sound, MW etc) absorption. In any case, the suspended catalyst system still remains the most promising in terms of efficiency. Present study is also using a similar system with the objective of enhancing the efficiency and understanding the process better in the case of AOPs involving sono, photo and sonophoto catalysis and their modifications.



Chapter 2

OBJECTIVES OF THE STUDY, MATERIALS USED AND PLAN OF THE THESIS

- 2.1 *Objectives*
- 2.2 *Materials*
- 2.3 *Plan of the thesis*

2.1 Objectives

As brought out in Chapter 1, semiconductor photocatalysis, sonocatalysis, sonolysis and sonophotocatalysis have been widely investigated in recent years as viable candidates for the removal of toxic pollutants in traces from water. These studies were mainly focusing on the disappearance of the pollutant with little attention given to the fate of intermediates, in particular the co-product H_2O_2 . Not many studies are available on the comparative assessment of sono, photo and sonophotocatalysis with the objective of identifying appropriate technology for the removal of water pollutants and exploiting the synergy in sonophotocatalysis. The potential of ZnO as a semiconductor photocatalyst also has not been fully exploited since most of the attention was focussed on another semiconductor oxide i.e., TiO_2 .

Against this background, the main objective of the current study is to evaluate the effectiveness of sono, photo and sonophoto catalytic processes

mediated by semiconductor oxides ZnO and TiO₂ and their combination, for the removal of trace amounts of the recalcitrant organic pollutant phenol and bacterial contaminants from water. Assessment of the fate of H₂O₂ formed concurrently in the process is another major objective.

Specific aims under the above broad objectives and the relevant activities undertaken to accomplish them are as follows:

- 1) Comparative assessment of ZnO, TiO₂ and their combination as sono, photo and sonophotocatalysts for the degradation of water pollutants.
- 2) Optimizing the dosage, particle size, composition etc., of the catalysts under each of the above Advanced Oxidation Processes for the degradation of the selected pollutant.
- 3) Optimizing reaction parameters such as reaction time, pH, pollutant load, concentration of O₂, etc., for the degradation of the pollutant under each of the three AOPs.
- 4) Evaluating the effect of natural contaminants such as salts in water on the efficiency of AOPs for the mineralization of the chemical pollutants.
- 5) Understanding the kinetics and mechanism of the sono, photo and sonophoto catalytic removal of chemical pollutants from water.
- 6) Investigating the possibility of using the least investigated AOP i.e., sonocatalysis, for the removal of few typical bacterial contaminants from water.

2.2 Materials

The catalysts chosen for the study are TiO_2 , ZnO and their combination. Of these, TiO_2 is the most widely used and best understood photocatalyst. ZnO was generally neglected by many, probably due to its vulnerability to corrosion and photo dissolution at acidic pH. The real potential of ZnO as a better absorber of light has not been properly exploited in photocatalysis. The present study aims at, among other things, evaluating ZnO as a viable catalyst in Advanced Oxidation Processes for waste water treatment.

2.2.1 Zinc Oxide (ZnO):

Zinc oxide is an inorganic compound with the formula ZnO . It usually appears as a white powder, nearly insoluble in water. It crystallizes in three forms: hexagonal wurtzite, cubic zinc blende and the rarely observed cubic rock salt. The wurtzite structure is the most stable at ambient pressure and temperature and thus the most common. Zinc blende form can be stabilized by growing ZnO on substances with cubic lattice structure. In both cases, the zinc and oxide centers are tetrahedral; each Zn ion is surrounded by a tetrahedron of O ions and vice-versa. This tetrahedral coordination gives rise to polar symmetry along the hexagonal axis. This polarity is responsible for a number of properties of ZnO . The wurtzite structure is shown in Fig. 2.1. The black spheres represent Zn atoms and grey spheres represent O atoms.

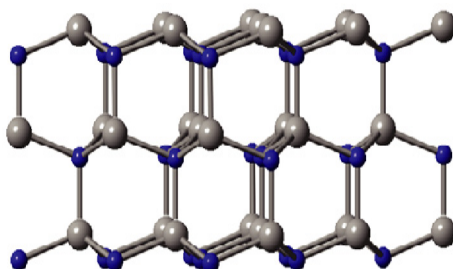


Fig.2.1: Structure of ZnO wurtzite [116].

ZnO is an inexpensive, moisture stable, reusable and commercially available catalyst [116-120]. The powder is widely used as an additive for numerous materials and products including plastics, ceramics, glass, cement, rubber (e.g. car tyres), lubricants, paints, ointments, adhesives, sealants, pigments, foods (sources of Zn nutrient), batteries, ferrites, fire retardants, first-aid tapes etc. ZnO is present in the earth crust as zincite. However, commercial ZnO is produced synthetically.

ZnO is often called II-VI semiconductor because zinc and oxygen belong to the 2nd and 6th groups of the periodic table, respectively. It has several favorable properties like good transparency, high electron mobility, wide band gap, strong room-temperature luminescence, etc., which are important in photocatalysis. The biggest advantage of ZnO is that it can absorb a relatively larger fraction of UV spectrum compared to TiO₂. Other favorable factors include; stability, non-toxicity, high catalytic efficiency, low cost and abundance in nature [121-126].

ZnO has a band gap of $E_g = 3.4$ eV at low temperature and 3.37 eV at room temperature and a large free-exciton binding energy (60 mV at room temperature). Hence, excitonic emission processes can persist at or even above room temperature. Advantages associated with large band gap include higher breakdown voltages, ability to sustain large electric fields, lower electronic noise, high-temperature and high-power operations. The band gap of ZnO can further be tuned from ~3–4 eV by its alloying with magnesium oxide or cadmium oxide. Mostly ZnO has n-type character, even in the absence of intentional doping. Controllable n-type doping is easily achieved by substituting Zn with group-III elements such as Al, Ga,

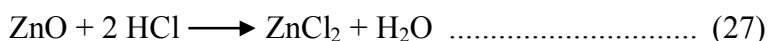
In or by substituting oxygen with group-VII elements like chlorine or iodine. These facts combined with the advantage of lower cost when compared with TiO₂, imply that ZnO is a promising alternative to TiO₂ in photocatalysis. In many cases photodegradation mechanism is also similar in the case of ZnO and TiO₂, though, at acidic pH range ZnO is considered to be less efficient due to its corrosion. The photocatalytic activity also depends upon the crystallinity, surface area and particle morphology, which in turn depend on the method of preparation. Some of the physical, chemical and electronic properties of ZnO are listed in Table 2.1.

Table 2.1: Properties of Zinc oxide.

Crystal structure	Quartzite
Lattice parameters at 300K	
a ₀	0.32495 nm
c ₀	0.52069 nm
Density	5.606 g/cm ³
Melting point	1975 ⁰ C
Boiling point	2360 ⁰ C
Refractive index	2.0041
Energy gap	3.4 eV, direct
Photoluminescence	375 nm
High electron mobility	>100cm ² /Vs
Exciton binding energy	60meV
Electron effective mass	0.24
Solubility in water	0.16 mg/100mL(20 ⁰ C)
Hole effective mass	0.59

Crystalline zinc oxide is thermochromic, changing from white to yellow when heated and reverting to white on cooling in air. This color

change is caused by a very small loss of oxygen at high temperatures to form the non-stoichiometric, $Zn_{1+x}O$, where, $x= 0.00007$ at $800\text{ }^{\circ}C$. Zinc oxide is an amphoteric oxide. It is nearly insoluble in water and alcohol, but is soluble in most acids, such as hydrochloric acid:



Bases also degrade ZnO to give soluble zincates:



It reacts with hydrogen sulfide to give the Zinc sulfide.



This reaction is used commercially for removing H_2S using ZnO powder as a deodorant.

2.2.2 Titanium dioxide (TiO_2)

TiO_2 is the most investigated photocatalyst for the removal of organic pollutants from water. It is white in colour, inexpensive, chemically stable and harmless, and has no absorption in the visible region. In photocatalysis, the activity of TiO_2 in suspension depends on the physical properties of the catalyst (e.g. crystal structure, surface area, surface hydroxyls, particle size) and operating condition (e.g light intensity, oxygen, initial concentration of chemical, amount of TiO_2 and pH value). Titanium dioxide can crystallize in three structures, i.e. rutile (tetragonal), anatase (tetragonal) and brookite (orthorhombic). Among these, rutile is thermodynamically the most stable, whereas anatase and

brookite are metastable and transform to rutile on heating. In spite of the similarity between anatase and brookite, the latter occurs rarely compared to the anatase form and exhibits no significant photocatalytic activity under daylight irradiation. Rutile and anatase have more industrial applications. Rutile has the smallest band gap, being 3.0 eV (corresponding to a cut-off wavelength 413 nm, while anatase has a slightly higher band gap of 3.2 eV (cut of wavelength 388 nm). Both band gaps are close to the limiting wavelength between UV-A light (320–400 nm) and visible light (400–700 nm). Doping TiO₂ with metals like iron and tungsten and non-metal species like carbon, nitrogen and sulphur are attempted in order to reduce the band gap energy and extend applicable wavelength range.

There are four polymorphs of TiO₂ found in nature; rutile (tetragonal), anatase (tetragonal), brookite (orthorhombic) and TiO₂ B (monoclinic). Other structures exist as well. For example, cotunnite TiO₂ has been synthesized at high pressures and is one of the hardest polycrystalline materials. Particle size experiments suggested that, in TiO₂ crystals less than a few tens of nanometers in diameter, anatase is more stable than rutile due to surface energy effects.

Only anatase and rutile forms find application in most cases. Fig. 2.2. shows the bulk structures of rutile and anatase TiO₂. Anatase has been found, to be photocatalytically more active than rutile in most of the cases.

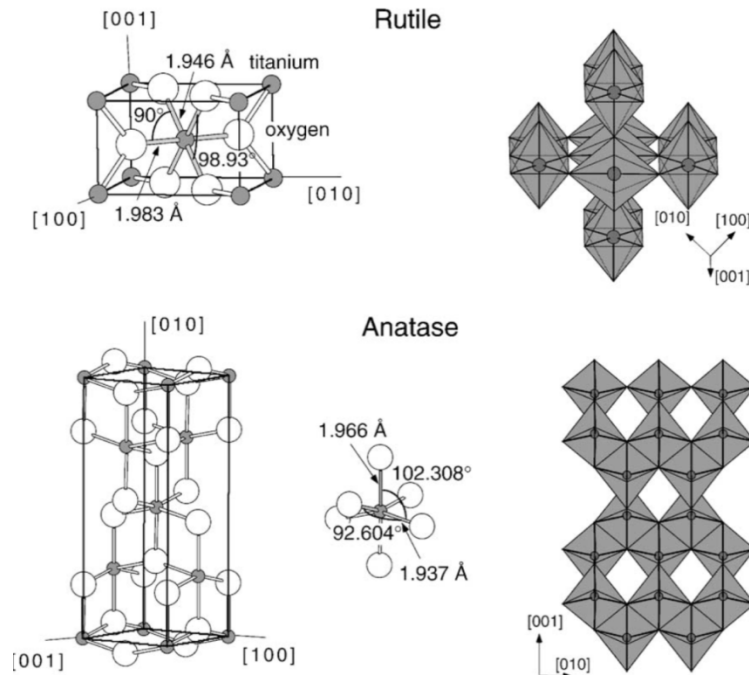


Fig. 2.2: Bulk structure of Rutile and Anatase TiO₂ [127]

Fig.2.3. shows the unit cell structure of the rutile and anatase crystal where the grey spheres are oxygen atoms and black spheres are Ti.

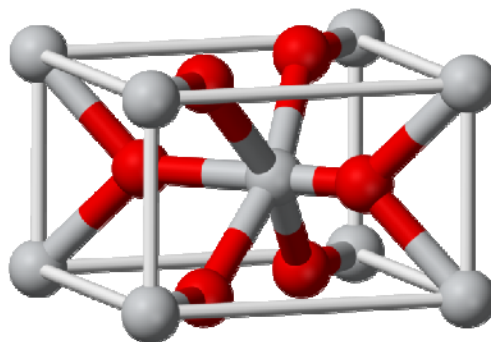


Fig. 2.3: Unit cell of rutile TiO₂ [127]

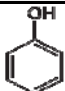
The structure of rutile and anatase can be described in terms of chain of TiO₆ octahedra. The crystal structures of the two differ by the distortion of each octahedron and by the assembly pattern of the octahedral chain. Each

Ti⁴⁺ ion is surrounded by an octahedron of six O²⁻ ions. The octahedron in rutile is not regular, showing a slight orthorhombic distortion. The octahedron in anatase is significantly distorted so that its symmetry is lower than orthorhombic. In rutile structure each octahedron is in contact with 10 neighbor octahedron each (two sharing edge oxygen pairs and eight sharing corner oxygen atoms) while in the anatase structure, each octahedron is in contact with eight neighbours (four sharing an edge and four sharing a corner). Of the two crystalline phases, anatase is believed to possess better photocatalytic and photoelectrochemical conversion performances probably because of its open structure compared to rutile [127-129].

2.2.3 Phenol

Large amount of phenol is produced and used annually worldwide in industries such as wood preservative, detergents, disinfectants, pharmaceuticals, polymers, other bulk chemicals etc. The annual global production of phenol is over 3 million tons. Table 2.2. shows some of the physical characteristics of phenol.

Table 2.2: Characteristics of Phenol.

Molecular formula	C ₆ H ₆ O
Structure	
Molar mass	94.11 g mol ⁻¹
Appearance	White Crystalline
Stability	Stable, Flammable
Density	1.07 g/cm ³
Specific Gravity	1.07
Melting point	40.5 °C, 314 K, 105 °F
Boiling point	181.7 °C, 455 K, 359 °F
Solubility in water	8.3 g/100 ml (20 °C)
Acidity (pK _a)	9.95
Dipole moment	1.7 D

Phenol and its derivatives are well known for their acute toxicity and bio-recalcitrant nature. The EPA (USA) has included them in the priority control list of 129 toxic pollutants. According to Environment Protection Rules of Central Pollution Control Board, India (1992), the discharge limit of phenols in inland water is 1 mg/L. The adverse effects of phenol include respiratory irritation, headache and burning eyes. Exposure to high amounts of phenol causes skin burns, liver damage, irregular heartbeat and even death. Phenol can have beneficial effects when used medically as an antiseptic. The phenol used in the current study is of AnalaR Grade supplied by Qualigens (India) and its purity is 99.5%.

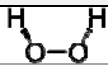
2.2.4 Hydrogen peroxide (H₂O₂)

Hydrogen peroxide is a chemical compound with the formula H₂O₂. It is normally used as a powerful oxidizing agent. In its pure form it is a colorless liquid, slightly more viscous than water. It can however act as a reducing agent for strong oxidants. When it decomposes, it forms water and releases oxygen which makes it an attractive environment-friendly product. It is a clean oxidant.



The characteristics of H₂O₂ are summarized in Table 2.3

Table 2.3: Characteristics of Hydrogen peroxide.

Molecular formula	H ₂ O ₂
Structure	
Molar mass	34.0147 g/mol
Appearance	Colorless in solution
Density	1.135g/cm ³ (20°C) (30%) 1.450 g/cm ³ (20°C, pure)
Melting point	-0.43 ⁰ C (31.23 ⁰ F; 272.72 K)
Boiling point	150.2°C (302.4°F; 423.3 K) (decomposes)
Solubility in water	Miscible

2.2.5 Miscellaneous materials

Details of various other materials used in the study and their characteristics are provided in the respective chapters.

2.3 Plan of the thesis

The current thesis is divided into seven chapters. Each chapter has its own specific objectives, experimental procedures, results, discussion and conclusions as is relevant.

Chapter 1 entitled, “**General Introduction: Background Literature**”, gives an overview of recent relevant literature and discussion on various types of AOPs with special focus on the application of sonocatalysis, photocatalysis and sonophotocatalysis in pollution control and water treatment.

Chapter 2 entitled, “**Objectives of the study, Materials used and Plan of the thesis**”, describes the main objective of the study, specific activities undertaken to accomplish the objective and plan of the thesis. Characteristics of the main materials used in the study; ZnO, TiO₂ and phenol are also briefly discussed.

Chapter 3 entitled, “**Semiconductor Oxides Mediated Photocatalytic Degradation of Phenol in Water**”, deals with photocatalytic degradation of phenol in presence of semiconductor oxides (ZnO, TiO₂ and coupled ZnO-TiO₂) under different experimental conditions. Detailed experimental procedure followed, reactor details, analytical procedures etc., are also provided. This chapter clearly illustrates that photocatalysis is an efficient tool for the removal of phenol from water. Major findings reported in

the chapter were presented as an original research paper entitled, “Augmentation of the photocatalytic activity of semiconductor oxides: investigations on the coupling of ZnO and TiO₂”, in the **26th Kerala Science Congress**, Wayanad held in Jan. 2014, (p. 210 of the proceedings). Some of the results are published as an original research paper entitled “Semiconductor Mediated Photocatalytic Degradation of Plastics and Recalcitrant Organic Pollutants in Water: Effect of Additives and Fate of Insitu Formed H₂O₂” in **Journal of Advanced Oxidation Technologies**, 18 (2015) 85-97.

Chapter 4 entitled, “**Semiconductor Oxides Mediated Sonocatalytic Degradation of Phenol in Water**”, deals with the sonocatalytic degradation of phenol in presence of semiconductors (ZnO, TiO₂ and coupled ZnO-TiO₂) under different experimental conditions. Relevant experimental procedures and analytical techniques are also described. Some of the results which are presented in this chapter are published as original research paper entitled, “Ultrasound assisted semiconductor mediated catalytic degradation of organic pollutants in water: Comparative efficacy of ZnO, TiO₂ and ZnO-TiO₂”, in **Research Journal of Recent Sciences**, 1(2012) 191-201.

Chapter 5 entitled, “**Semiconductor Oxides Mediated Sonophotocatalytic Degradation of Phenol in Water**”, deals with the hybrid technique of sonophotocatalysis and its application for the degradation phenol in presence of semiconductor oxides ZnO, TiO₂ and coupled ZnO-TiO₂ under different experimental conditions. The chapter reveals the synergy of sonophotocatalysis in which the efficiency of the process is more than

the individual sono or photocatalysis or their additive effect. Some of the results from this chapter were published in the original research paper entitled, “Zinc oxide mediated sonophotocatalytic degradation of phenol in water”, in *Chemical Engineering Journal*, 84–93 (2012) 189–190. Another research paper entitled, “Semiconductor Mediated Sonophotocatalytic Degradation of Organic Pollutants in Water” is presented in *23rd Kerala Science congress*, Jan. 2011 (p.156 of the proceedings)

Chapter 6 entitled, “**Zinc Oxide Mediated Sonocatalytic Removal of Bacterial contaminants in water**”, deals with the application of ZnO sonocatalysis for the removal of bacterial pollutants in water. The chapter illustrates that both gram –ve and gram +ve bacteria are irreversibly destroyed by sonocatalysis. The influence of various parameters on the destruction and re-emergence of the bacteria is investigated and presented. Some of the results from this chapter were published as an original research paper entitled, “Investigations on semiconductor sonocatalysis for the removal of pathological micro-organisms in water”, in the journal, *Desalination and Water Treatment*, (2014) pp.1-8. Part of the findings were also presented as an original research paper entitled, “Advanced Oxidation Processes for the chemical and bacterial decontamination of water: Inactivation of *Bacillus subtilis* by sonocatalysis”, in the **3rd International Science Congress**, held at Coimbatore in Dec. 2013 (p.83, of the proceedings). Another research paper entitled “Irreversible Sonocatalytic Deactivation of *Bacillus subtilis* in water” was presented in *2nd Asia-Oceania Sonochemical Society Conference(AOSS-2)*, held at Kuala Lumpur, Malaysia in July 2015 (p.71, of the proceedings).

Chapters 7 entitled, “**Summary and Conclusions**”, summarizes the findings of the study and highlight the conclusions.

Annexure I lists the abbreviations used in the thesis. Expansions of respective abbreviations are also shown in the first place where they appear in the thesis.

Annexure II gives the list of research papers published/presented in conferences, based on the work.

Annexure III provides reprints of five (5) research papers based on the investigation, published in various referred journals.

.....❧.....

SEMICONDUCTOR OXIDES MEDIATED PHOTOCATALYTIC DEGRADATION OF PHENOL IN WATER

- 3.1 *Introduction*
- 3.2 *Experimental Details*
- 3.3 *Results and Discussion*
- 3.4 *Probable mechanism of the photocatalytic degradation of phenol in presence of semiconductor*
- 3.5 *Formation and decomposition of H_2O_2*
- 3.6 *Effect of anions*
- 3.7 *Conclusions*

3.1 Introduction

Phenol, as stated in chapters 1 and 2, is a major pollutant found in effluent streams from various chemical industries producing resins, plastics, textiles, pulp paper, etc., and is often used as a model pollutant in wastewater remediation studies. Even at low concentration, it is considered to be toxic and is not allowed to be discharged directly into surface waters or to the normal sewage system. Semiconductor photocatalysis has emerged as an important destruction technology for the mineralization of organic pollutants in water resulting in CO_2 , H_2O and mineral acids or their salts as end products.

In this chapter, the photocatalytic activity of ZnO, TiO₂ and ZnO-TiO₂ for the degradation of trace amounts of phenol in water is evaluated under various reaction conditions and in presence of various additives. Over the years, a large number of semiconductors have been reported as potential photocatalysts. The most widely studied among them are TiO₂, ZnO and CdS. In fact, TiO₂ has been one of the most active photocatalysts reported so far and has become the bench mark against which photocatalytic activity of other semiconductors is measured. ZnO is a suitable alternative to TiO₂ and is in fact more efficient than TiO₂ for several applications. Similarly, coupled semiconductor systems such as CdS/TiO₂, ZnO/Fe₂O₃ and ZnO/TiO₂ have also been reported to modify the photocatalytic activity of their constituents. [56, 57, 87,130,131]. In this chapter, the photocatalytic degradation of phenol and its mineralization on ZnO, TiO₂ and ZnO/TiO₂ are investigated in detail. The fate of H₂O₂ formed concurrently is also monitored which provided fresh insight for the first time into the inconsistency reported with respect to the amount of H₂O₂ formed in photocatalytic systems.

3.2 Experimental Details

3.2.1 Materials

Phenol AnalaR Grade (99.5% purity) from Qualigens (India) was used as such without further purification. ZnO and TiO₂ used in the study were supplied by Merck (India) Limited. In both cases, the particles were approximately spherical and non-porous with a purity of over 99%. H₂O₂ (30% W/V) used was from Ramkem Limited (India). The water used for all experiments was purified by double distillation. Other chemicals used

such as NaCl, NaI, Na₂SO₄, Al₂O₃, Fe₂O₃, NaF, Na₂CO₃, NaNO₃, NaBr and Na₃PO₄.12H₂O were of Reagent grade and used as such without further purification. ZnO/TiO₂ composites were prepared by thorough physical mixing of required amounts of ZnO and TiO₂ catalysts for 30 minutes.

3.2.2 Analytical Procedures

The concentration of phenol in routine experiments was followed by spectrophotometry. At periodic intervals, samples were drawn from the reactor, centrifuged and the centrifugate was analysed for the concentration of phenol left behind. The analysis is based on the reaction of phenolic compounds with 4-amino antipyrine at pH 7.9 ± 0.1 in presence of potassium ferricyanide to form a coloured antipyrine dye. The absorbance of this dye solution is measured at 500 nm using a spectrophotometer (Varian UV-VIS spectrophotometer). A similar reaction system kept in the dark under exactly identical conditions but without UV irradiation was used as the reference. The major intermediates of phenol degradation before ultimate mineralization were verified by high performance liquid chromatography (Microbondapack C18 column of 36 cm length. Eluting solvent was water-acetonitrile in the ratio 80:20, UV detector). The identified intermediates such as catechol, hydroquinone and benzoquinone are not consistently detected or detected only in negligible quantities by HPLC analysis, indicating that they undergo faster/ comparable degradation in relation to the parent compound. Hence, they are not expected to interfere in the spectrophotometric analysis of phenol.

Surface area of the catalysts was measured using BET method using TriStar 3000.V6.07A. The X-ray diffraction (XRD) measurements were made using Rigaku X-ray diffractometer with Cu-K α radiation. Scanning Electron Microscopy (SEM) measurements were performed using JEOL Model JSM-6390 LV. Total organic carbon content of reaction solution was recorded using the TOC Analyzer Vario TOC CUBE (Elementer Analysen systeme make).

H₂O₂ was analyzed by iodometry. The oxidation of iodide ions by H₂O₂ generated insitu was carried out in 1N sulphuric acid in presence of a few drops of saturated ammonium molybdate solution, which acts as a catalyst. The reaction was allowed to go to completion (5 minutes) in the dark. The liberated iodine was then titrated against a standard solution of sodium thiosulphate of concentration 2×10^{-3} N prepared freshly from 10^{-1} N stock solution. Freshly prepared starch was used as the indicator. Mineralization was identified from the evolution of CO₂ after prolonged US irradiation. CO₂ was detected by the precipitation of BaCO₃ when the gas phase above the reaction suspension flushed with O₂ was passed through Ba(OH)₂ solution. In addition, TOC in the mixture was determined using the TOC analyzer to confirm the complete mineralization.

3.2.3 Adsorption

A fixed amount (0.1 g) of the catalyst was introduced into 50ml of phenol solution of required concentration in a 100 mL beaker and the pH was adjusted as required. The suspension was agitated continuously at a constant temperature of $29 \pm 1^{\circ}\text{C}$ for 2 hrs to achieve equilibrium. This was then centrifuged at 3000 rpm for 10 min. After centrifugation, the concentration

of phenol in the centrifugate was determined spectrophotometrically. The adsorbate uptake was calculated from the relation:

$$q_e = (C_0 - C_e) V / W \dots\dots\dots (31)$$

where C_0 is the initial adsorbate concentration (mg/L), C_e is the equilibrium adsorbate concentration in solution (mg/L), V is the volume of the solution in litre, W is the mass of the adsorbent in gram and q_e is the amount adsorbed in mg per gram of the adsorbent at equilibrium.

3.2.4 Photocatalytic Experimental set up

In a typical experiment, required amount of the catalyst is suspended in an aqueous solution of phenol of desired concentration in the reactor. Simple glass beakers (250 ml) were used as reactors in routine experiments. The beakers were placed in a water bath through which water at the required temperature was circulated. The catalyst substrate suspension was continuously mixed using a magnetic stirrer. The suspension was illuminated with a 400W super high-pressure mercury lamp mounted above the system [Fig. 3.1(a)]. For specific experiments specially designed jacketed reactor [Fig. 3.1(b)] was used. This reactor has provision for circulation of water in the jacket and bubbling gas through the suspension. At periodic intervals, samples were drawn, the suspended catalyst particles were removed by centrifugation and the concentration of phenol left behind was analyzed as explained under analytical procedure. In this case also, a similar reaction system kept in the dark under exactly identical conditions but without UV irradiation was used as the reference. The samples were also analysed for the presence of H_2O_2 and quantified the same as and when required. For the identification

of intermediates, higher concentration of phenol [1000 ppm] and higher loading of catalyst were used in the experiments. The irradiation is done upto ~ 50% degradation of phenol and the solution was analysed by HPLC for the intermediates. Similarly, for confirming the mineralization, evolution of CO₂, at higher concentration of phenol and higher loadings of catalyst was measured.

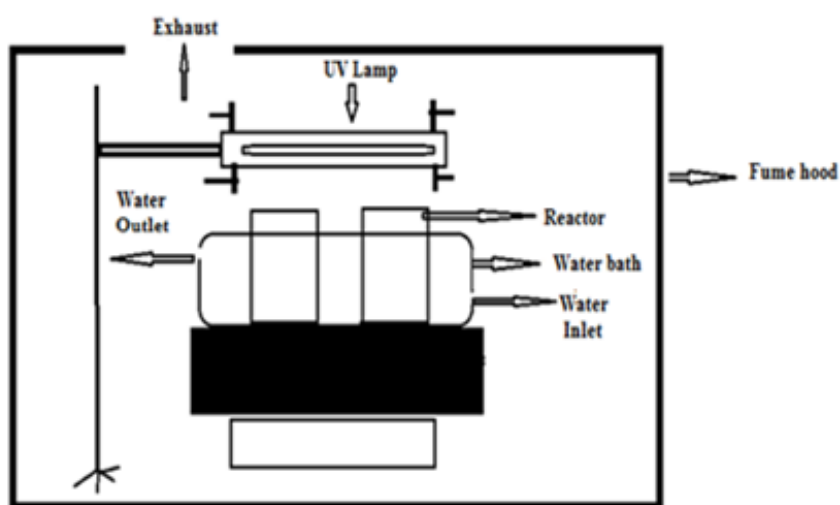


Fig.3.1(a): A schematic diagram of the photocatalytic experimental set up.

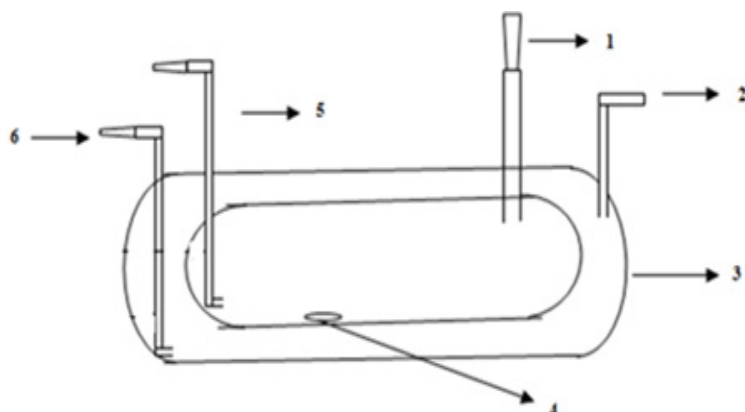


Fig.3.1(b): Typical photoreactor used in the study: 1. Sample inlet, 2. Water outlet, 3. Outer jacket, 4. Magnetic pellet, 5. Gas purging tube, 6. Water inlet.

3.3 Results and Discussion

3.3.1 Catalyst characterization and Preliminary experiments

The catalysts ZnO and TiO₂ used in the study were characterized by surface area, particle size analysis, pore size distribution, adsorption, X-Ray Diffraction (XRD) and Scanning Electron Microscopy (SEM). The pore size distribution is shown in Fig. 3.2 (a & b).

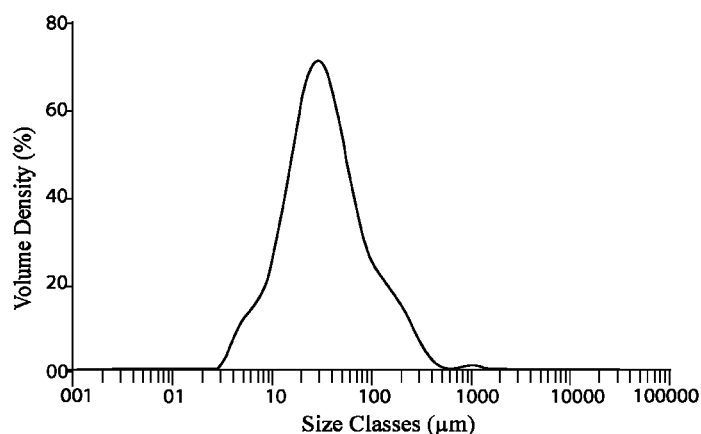


Fig. 3.2(a): Pore size distribution of ZnO.

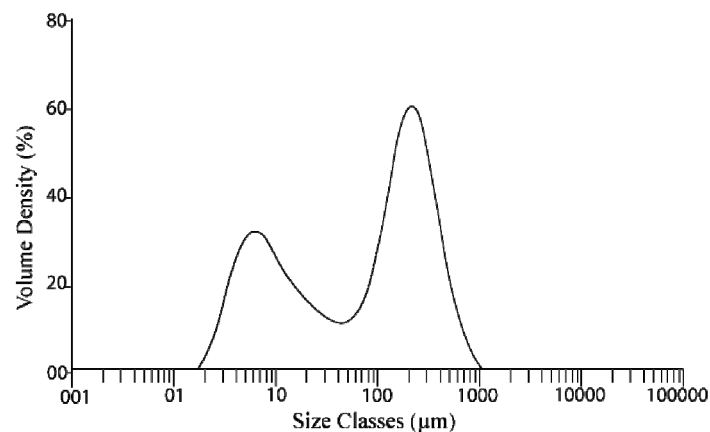


Fig. 3.2(b): Pore size distribution of TiO₂.

The XRD patterns of TiO₂ (anatase), TiO₂ (rutile), TiO₂ (commercial) containing anatase and rutile form, ZnO and composite ZnO-TiO₂ with a

molar proportion of 4:6 are shown in Fig. 3.3 (a, b, c, d & e) respectively. The characteristic diffraction peaks of rutile, anatase as well as the commercial sample showed that the TiO_2 contains approximately 75% anatase and 25% rutile. In the case of ZnO, three sharp peaks are found from 30 to 40° with very high intensity. These diffraction peaks are also found in the XRD pattern of composite ZnO- TiO_2 powder [3.3 (e)]. The composite powder contains the two crystalline phases belonging to anatase TiO_2 and ZnO. The surface areas of TiO_2 and ZnO, as determined by the BET technique, were approximately $15\text{m}^2/\text{g}$ and $12\text{m}^2/\text{g}$ respectively. Fig. 3.3 (f, g & h) gives the SEM images of the samples mentioned above. The average particle size of both TiO_2 and ZnO was approximately in the range 0.1 to $4.0\ \mu\text{m}$. Average dynamic particle size as determined by Malvern mastersizer is $3.2\ \mu\text{m}$.

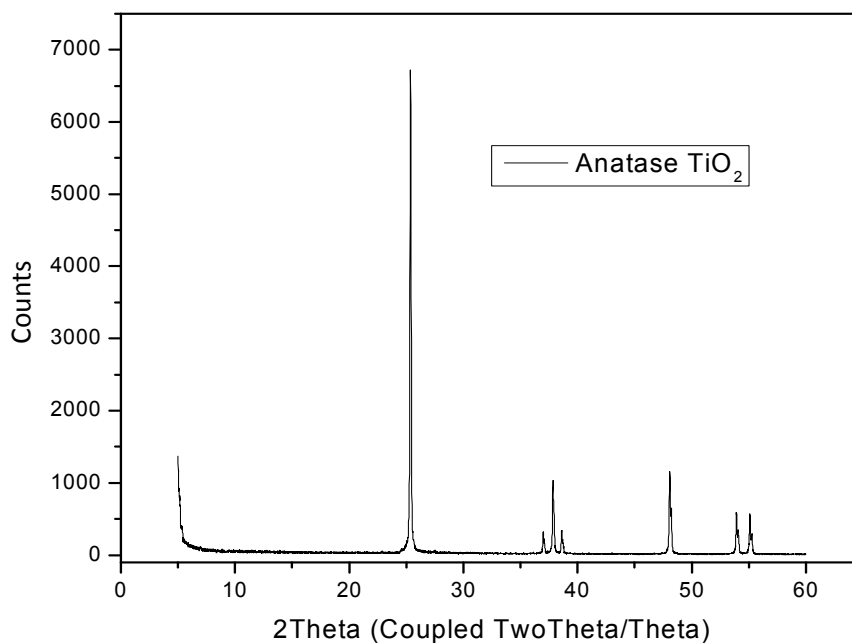


Fig.3.3(a): XRD pattern of TiO_2 (Anatase).

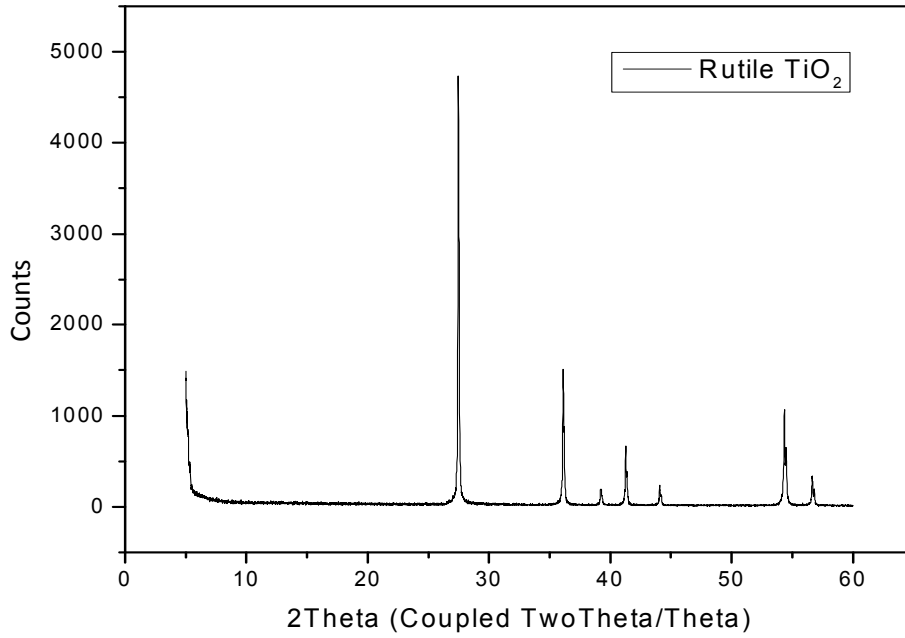


Fig.3.3(b): XRD pattern of TiO₂ (Rutile).

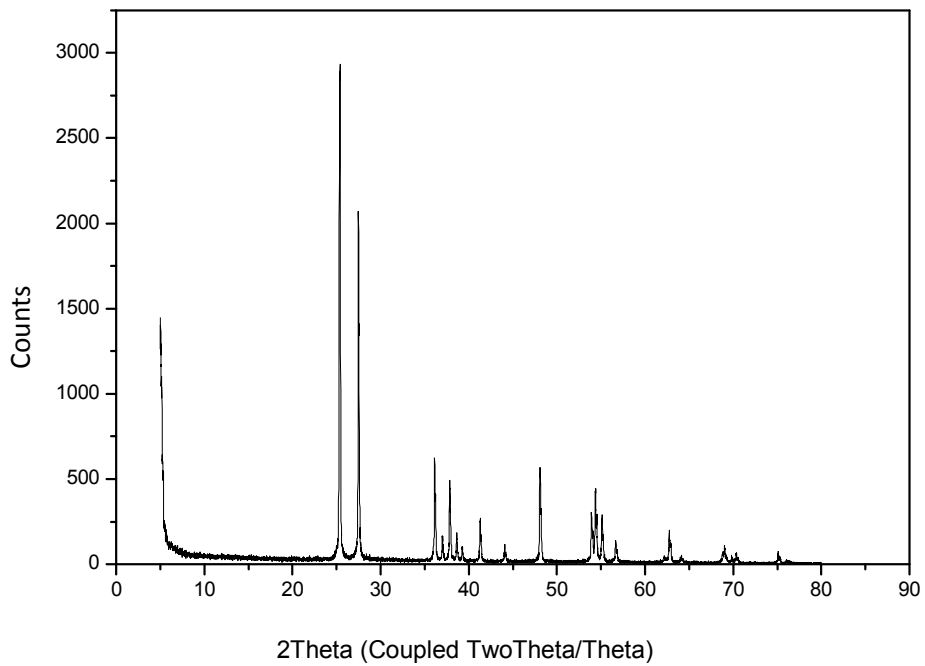


Fig.3.3(c): XRD pattern Commercial TiO₂ (Anatase and Rutile).

ZnO commercial merck sample 2 (Coupled TwoTheta/Theta)

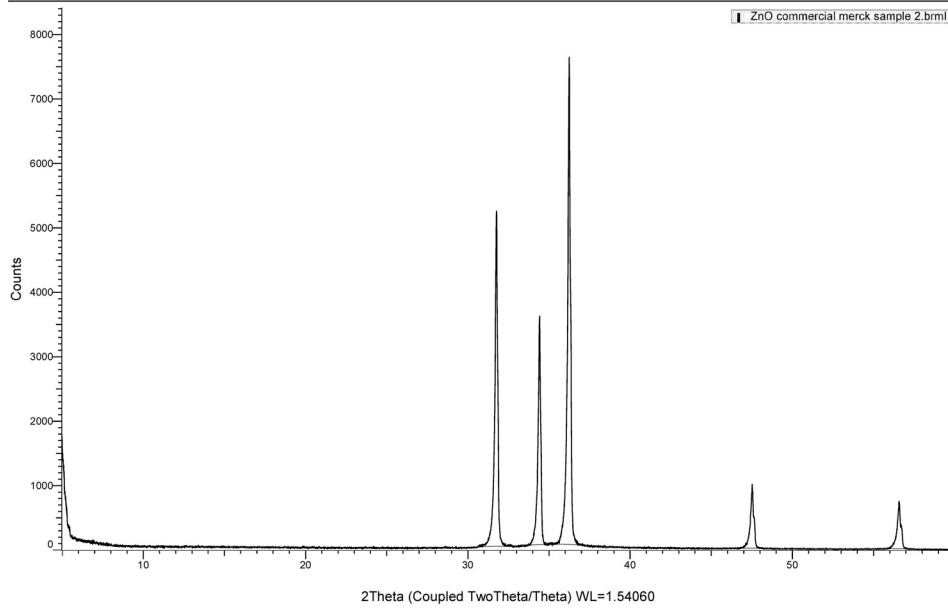


Fig.3.3(d): XRD pattern of ZnO.

TiO2 ZnO Mixed oxide 29102013 (Coupled TwoTheta/Theta)

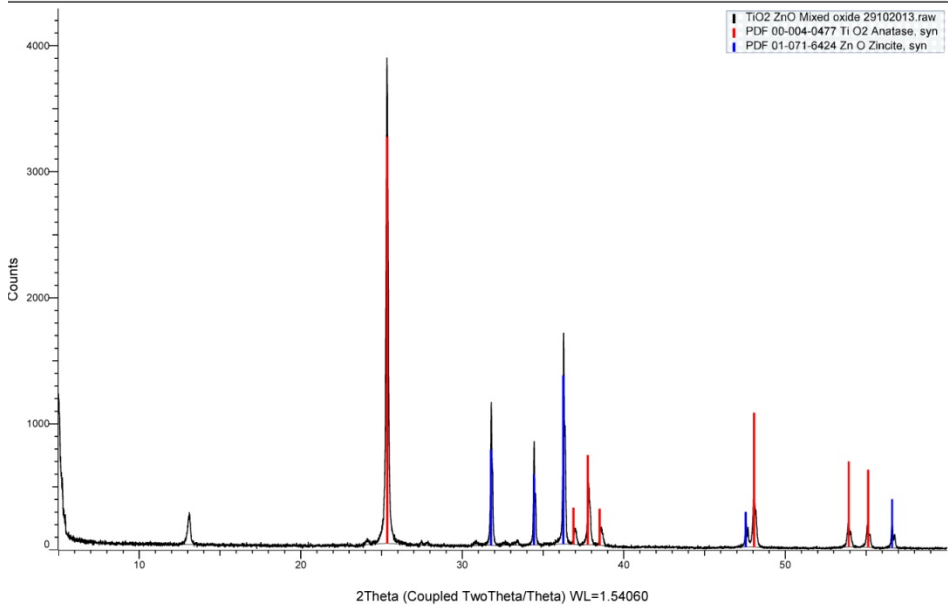


Fig.3.3(e): XRD pattern of ZnO-TiO₂.

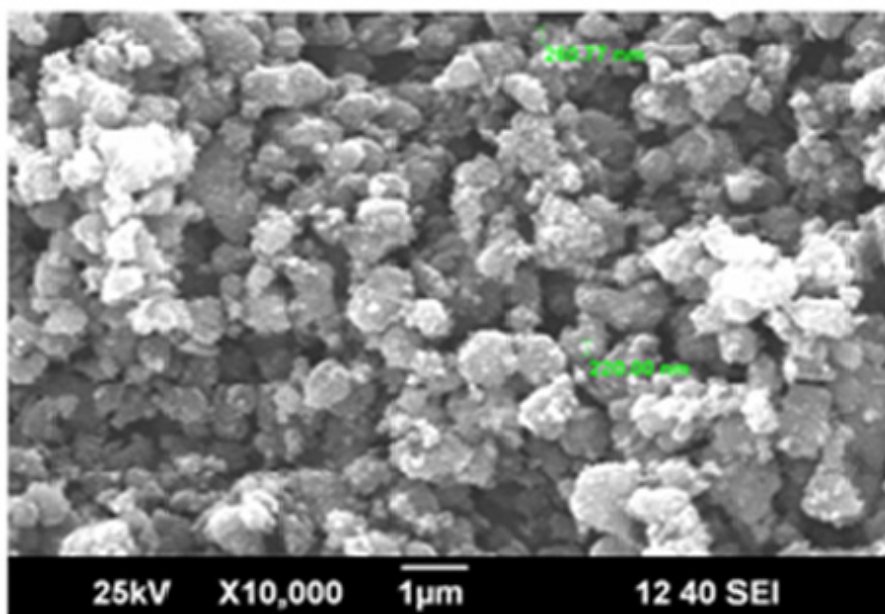


Fig.3.3(f): SEM image of TiO₂.

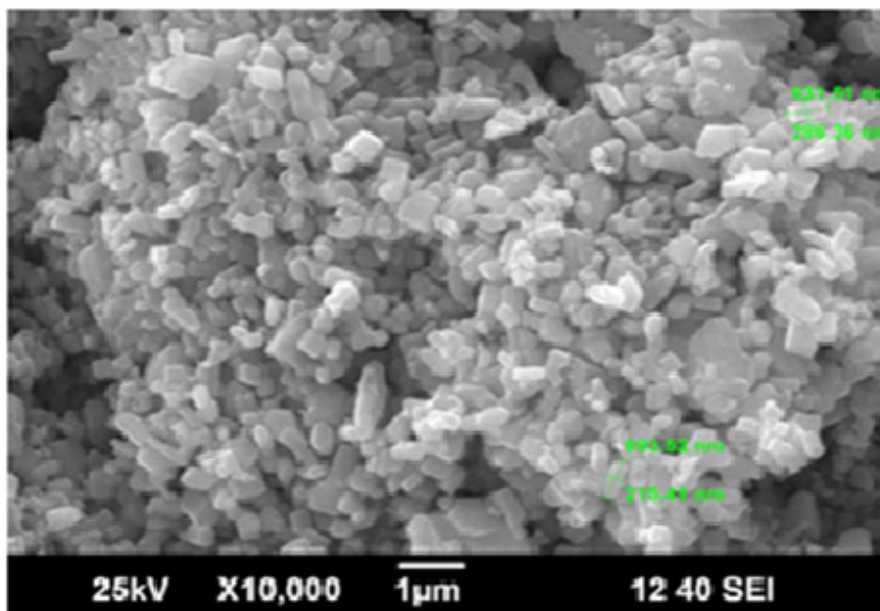


Fig.3.3 (g): SEM image of ZnO.

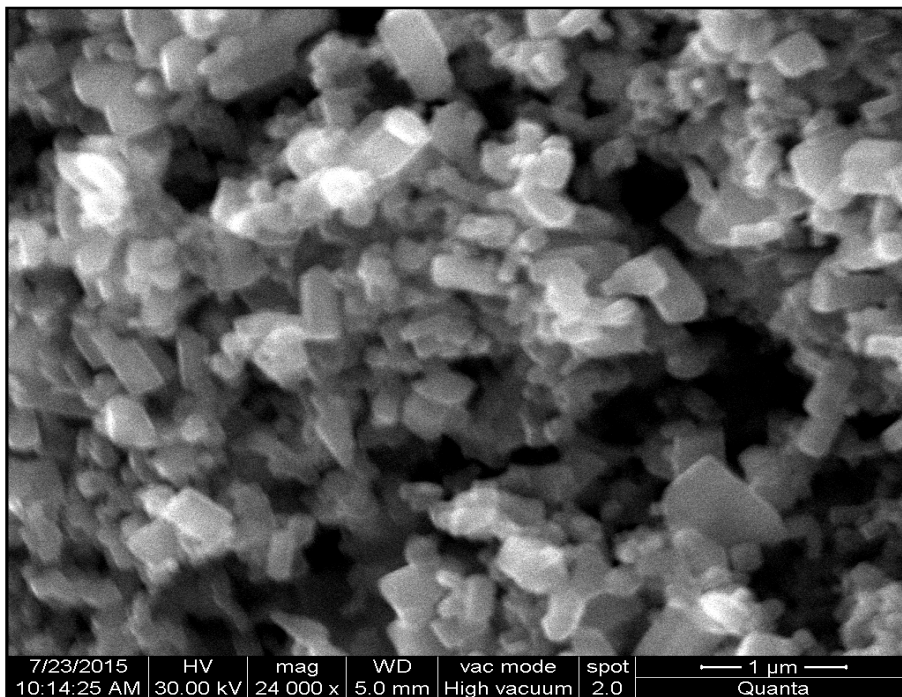


Fig.3.3 (h): SEM image of ZnO-TiO₂

Preliminary investigations on the photocatalytic degradation of phenol were made using ZnO, TiO₂, and ZnO-TiO₂ catalysts under identical conditions. The results are shown in Fig. 3.4. ZnO, TiO₂ and ZnO-TiO₂ (1:1 w/w) yielded 55%, 63% and 67% degradation of phenol respectively in 2 hr irradiation time.

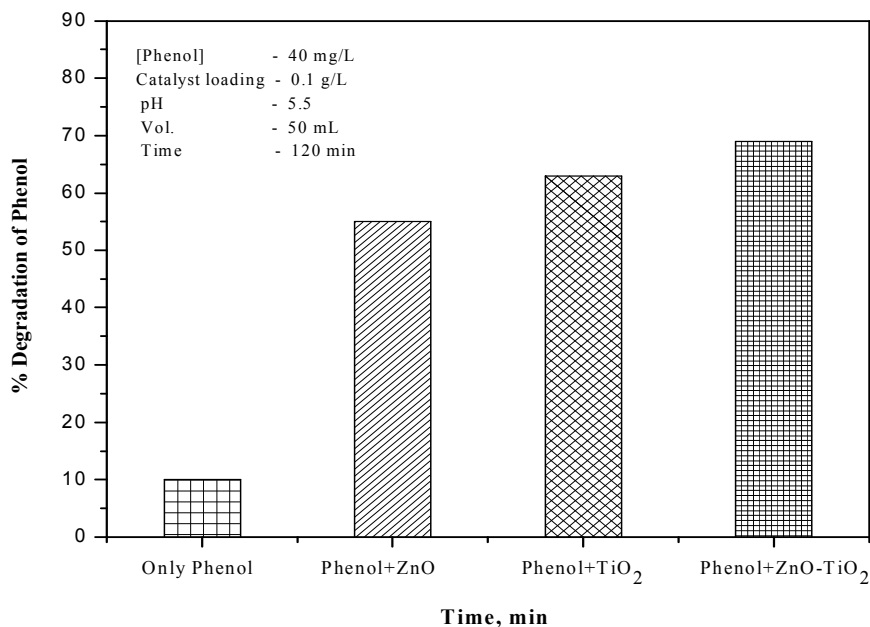


Fig. 3.4: Comparison of photocatalytic activities of ZnO, TiO₂ and ZnO-TiO₂.

Experiments conducted in the absence of either catalyst or light showed no significant degradation of phenol suggesting that both catalyst and light are essential for the degradation. This is expected on the basis of the general mechanism of photocatalysis. Photoexcitation of the semiconductor, results in the formation of an electron-hole pair on the surface of catalyst. These electrons and holes are responsible for the production of hydroxyl radical species that interact with the pollutants, degrade and eventually mineralize them. Both ZnO and TiO₂ have comparable photocatalytic efficiency (55% and 63%), though TiO₂ is slightly more active. Combining them does not modify the efficiency significantly as seen in Fig. 3.4. The adsorption study at the respective optimum dosage of catalyst (Section 3.3.2) shows that TiO₂ is a better

adsorbent compared to the other two catalysts i.e. 3.6, 8.8 and 4.4 mg/g for ZnO, TiO₂ and ZnO-TiO₂ respectively.

Fig. 3.5 shows the efficacy of ZnO/TiO₂ at various weight ratios for the photodegradation of phenol under identical conditions. The percentage degradation varied slightly with the composition of ZnO-TiO₂. Maximum degradation of 67% is observed at the ratio 4:6 (ZnO-TiO₂).

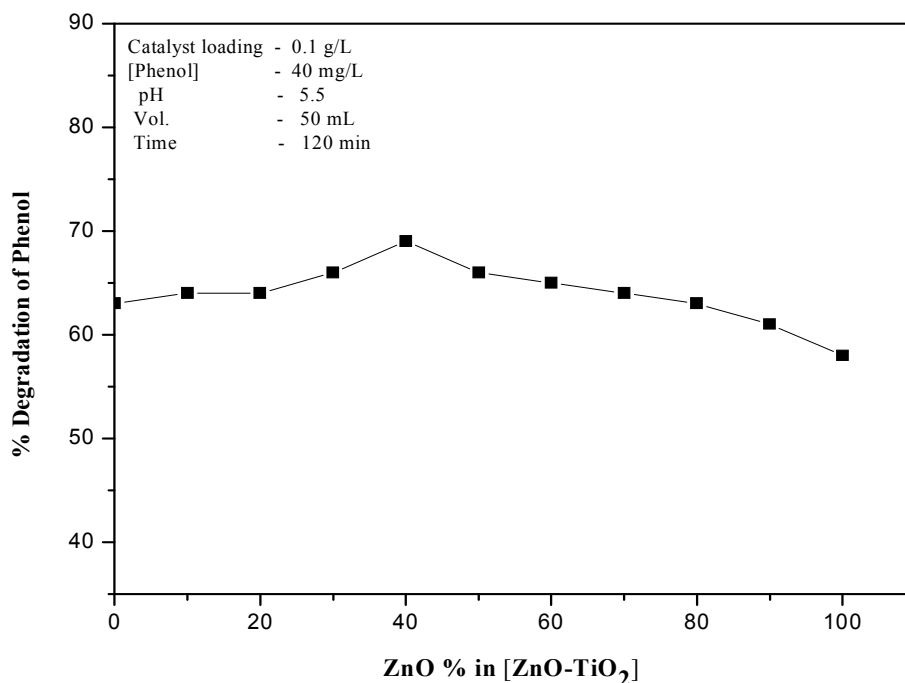


Fig.3.5: Effect of variation of ZnO in ZnO-TiO₂ on its photocatalytic activity.

Pure TiO₂ powder (Zn/Ti = 0:1) gives ~ 63% degradation of phenol under UV irradiation and the corresponding adsorption (8.8 mg/g) of phenol is also the highest. The degradation of phenol in presence of TiO₂ is not affected by addition of ZnO upto 20%. Thereafter it slowly increases with increase ZnO concentration, reaches an optimum at the ratio 4:6 (ZnO-TiO₂)

and slowly decreases or stabilizes. The inter-particle electron transfer (IPET) in coupled ZnO-TiO₂ [132] which is reported to be responsible for the higher photocatalytic activity of coupled ZnO-TiO₂ is not fully seen here though its contribution cannot be completely ruled out. Since TiO₂ is slightly more active compared to ZnO, the modest improvement in efficiency in presence of the latter can be attributed to the IPET and better absorption of light.

3.3.2 Effect of catalyst dosage

Optimizing catalyst concentration is important in order to avoid the uneconomical use of catalyst and to ensure maximum absorption of photons. Hence, the effect of catalyst dosage on the photocatalytic degradation of phenol is studied at different loadings of ZnO, TiO₂ and ZnO-TiO₂ (4:6) keeping all other parameters constant. The results are shown in Fig. 3.6.

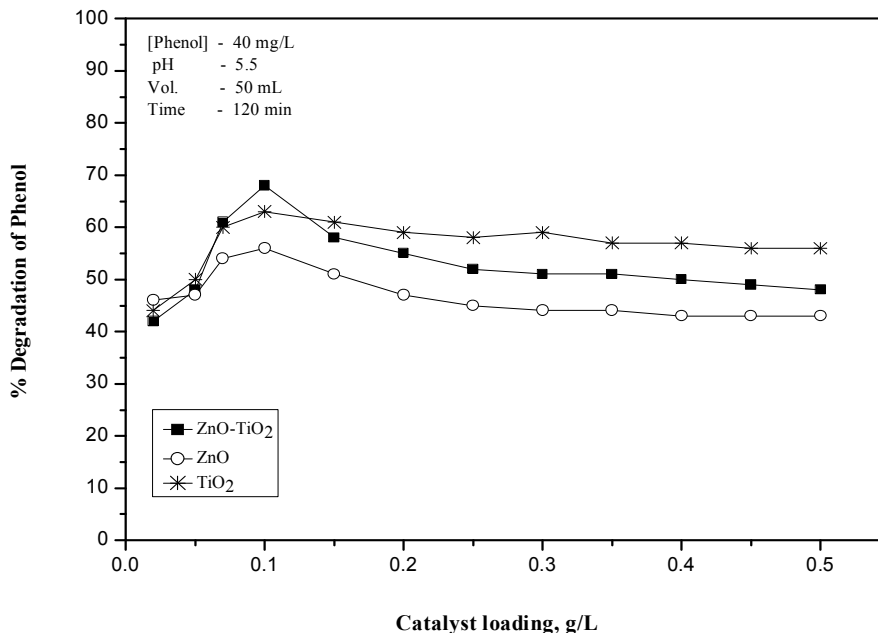


Fig.3.6: Effect of catalyst loading on the photocatalytic degradation of phenol over ZnO, TiO₂ and ZnO-TiO₂.

It is seen that in all three cases, increase in the catalyst loading from 0.02 to 0.10 g/L increases the phenol degradation fairly sharply followed by a slow and steady decrease and eventual stabilization at higher loadings. This is characteristic of many such reactions in heterogeneous photocatalysis [57,130,133-141].

The degradation efficiency is higher at the higher catalyst loading, due to the efficient absorption of light and increased number of adsorption sites available which lead to the formation of higher number of reactive hydroxyl radicals and their interaction. Higher amount of catalyst loading may lead to more efficient utilization of incident photons striking the catalyst surface. Also there will be more number of active sites for adsorption of phenol as well as generation of Reactive Oxygen Species (ROS) at the surface. However, increase in the catalyst concentration beyond the optimum will result in the scattering and reduced passage of light through the sample. Another reason may be the aggregation of catalyst particles causing a decrease in the number of available active surface sites. The particles cannot be fully and effectively suspended beyond a particular loading in a particular reactor which also leads to suboptimal penetration of light and reduced adsorption of the substrate on the surface. At higher loading, the catalyst has a tendency to settle at the bottom of the reactor. It is also possible that at higher loading, part of the originally activated semiconductor is deactivated through collision with ground state catalyst according to the equation [56, 57, 59, 130, 131,142].



Where, MO is semiconductor oxide such as ZnO, TiO₂ and ZnO-TiO₂. MO* and MO[#] are its activated and deactivated forms respectively. All those factors together contribute to a decrease in the efficiency of the catalyst beyond the optimum level.

All further studies were done using the optimum loading of 0.1 g/L for all three catalysts, i.e, ZnO, TiO₂ and ZnO-TiO₂.

3.3.3 Effect of irradiation time

The effect of irradiation time on the photocatalytic degradation of phenol is shown in Fig.3.7. The percentage degradation of phenol increases as the irradiation time increases. The mixed catalyst, ZnO-TiO₂, has better degradation efficiency than the individual components i.e. ZnO and TiO₂ throughout the irradiation period. The percentage removal reaches an optimum and levels off with time. As the time increases, the concentration of phenol available for interaction with the surface decreases. Also some of the active sites on the catalyst surface will be covered by the reaction intermediates. The availability of oxygen also is affected due to depletion of adsorbed as well as dissolved oxygen. The composition of the system also becomes complicated with too many products which reduces the effectiveness of penetration of light. Hence, the degradation reaches a plateau which can be broken only by modifying the reaction conditions.

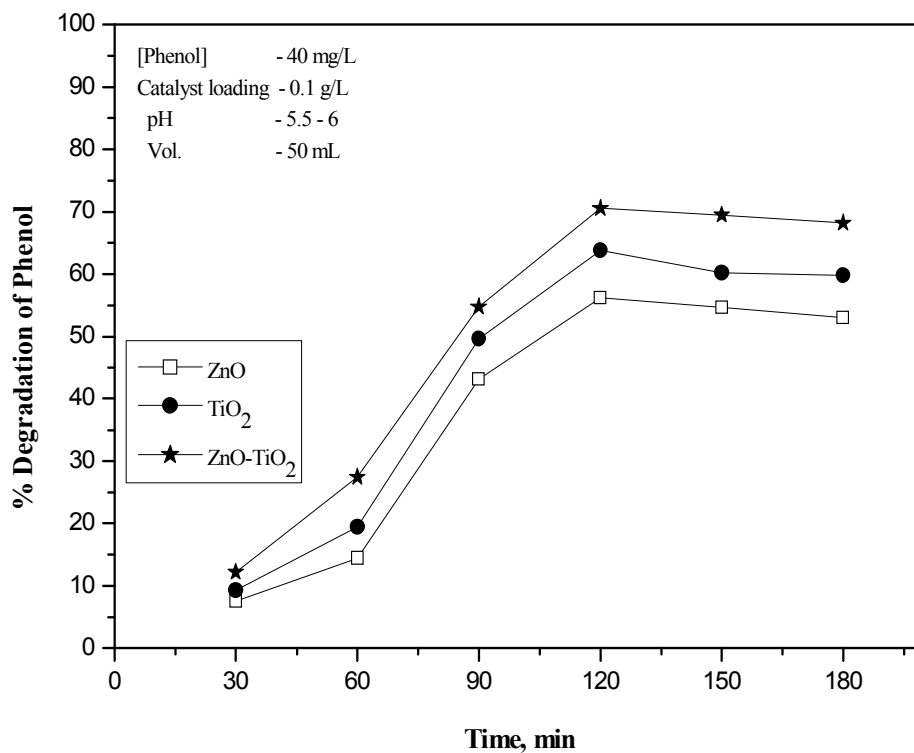


Fig.3.7: Effect of irradiation time on the photocatalytic degradation of phenol over ZnO, TiO₂ and ZnO-TiO₂.

3.3.4 Effect of concentration

The effect of initial concentration of phenol on the rate of its photocatalytic degradation in presence of ZnO, TiO₂ and ZnO-TiO₂ catalysts was studied, by varying the concentration over the range of 10–60 mg/L in presence of 0.1g L⁻¹ catalyst under UV light. The results are shown in Fig. 3.8(a).

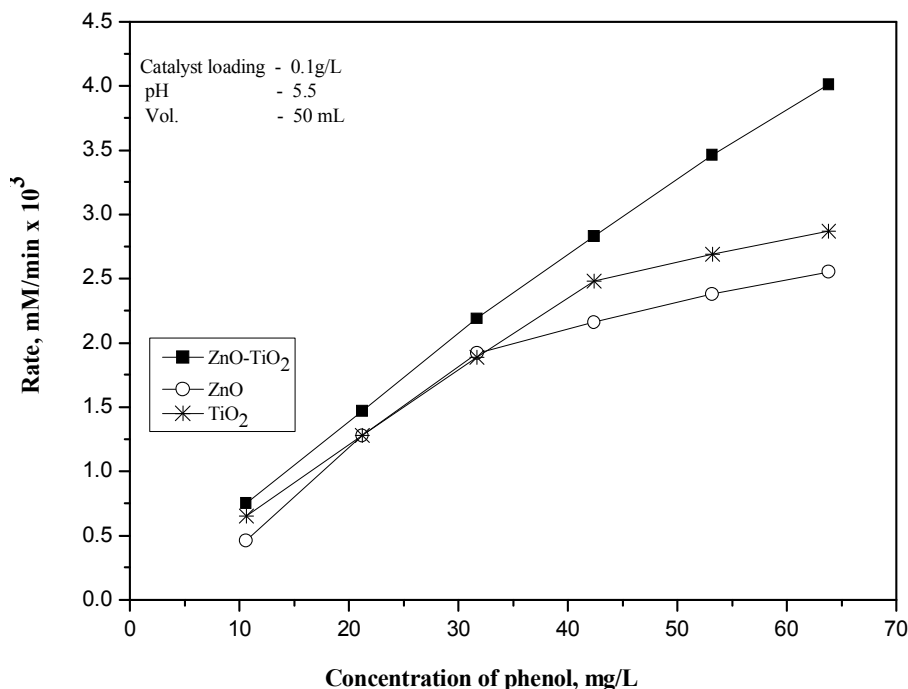


Fig.3.8 (a): Effect of concentration of phenol on its photocatalytic degradation over ZnO, TiO₂ and ZnO-TiO₂.

The rate degradation of phenol increases with increase in concentration in all cases. The rate slows down and eventually stabilizes in the case of pure ZnO and TiO₂ at 30 and 40 mg/L respectively. However, the rate continues to increase even at higher concentration of phenol in the case of ZnO-TiO₂ combination.

At higher concentration of substrate beyond the optimum, it may be presumed that active sites are fully covered by the phenol molecule and its degradation intermediates. Hence the ability of the surface to absorb light and to generate more electron-hole pairs is reduced. This reduces the photodegradation efficiency of this catalyst. As the phenol concentration is increased, there is a decrease in the path length of photon entering into

the phenol solution because, at high concentration, a significant amount of UV light may be absorbed by the phenol molecules themselves rather than the catalyst. This also will reduce the catalyst efficiency. In the case of ZnO-TiO₂, continuing increase in degradation rate even beyond the optimum phenol concentration for ZnO or TiO₂, indicates the availability of more reaction sites. Hence the formation/availability of electrons and hole may be more which can react with even more molecules of the substrate in this case. This is possible due to the Interparticle Electron Transfer in the case of ZnO-TiO₂ which increases the availability of electrons and holes, as discussed earlier.

The photo catalytic degradation of organic contaminants over semiconductor oxides generally follows Langmuir- Hinshelwood Kinetic model [130]:

$$-dC/dt = r_0 = k_r K C_0 / (1 + K C_0) \dots\dots\dots (33)$$

where r_0 is the initial rate of disappearance ($\text{mgL}^{-1}\text{min}^{-1}$) of the pollutant, C_0 (mgL^{-1}) its initial concentration, t is the illumination time, k_r is the reaction rate constant at maximum surface concentration and K the equilibrium adsorption constant. Eq.33 can be rewritten as

$$1/r_0 = 1/k_r + 1/k_r K \cdot 1/C_0 \dots\dots\dots (34)$$

Plot of $1/r_0$ vs $1/C_0$ yields a straight line in the case of first order kinetics and L-H mechanism. Another more accepted mode of verifying the kinetics is by integrating equation 33, which yields the relation,

$$\ln(C_0/C) + K(C_0-C) = k_r K t \dots\dots\dots (35)$$

When C_0 is very small, the above equation becomes

$$\ln [C_0/C] = -\ln [C/C_0]= k_r Kt = k_{app}t \text{ where } \dots\dots\dots (36)$$

k_{app} is the apparent rate constant

Plotting of $-\ln [C/C_0]$ vs time in the concentration range of 10–40 mg/L (Fig. 3.8(b) shows linear dependence indicating first order kinetics, in the case of ZnO. Beyond this concentration, the rates become independent of the concentration indicating decrease in the order and eventually zero order kinetics.

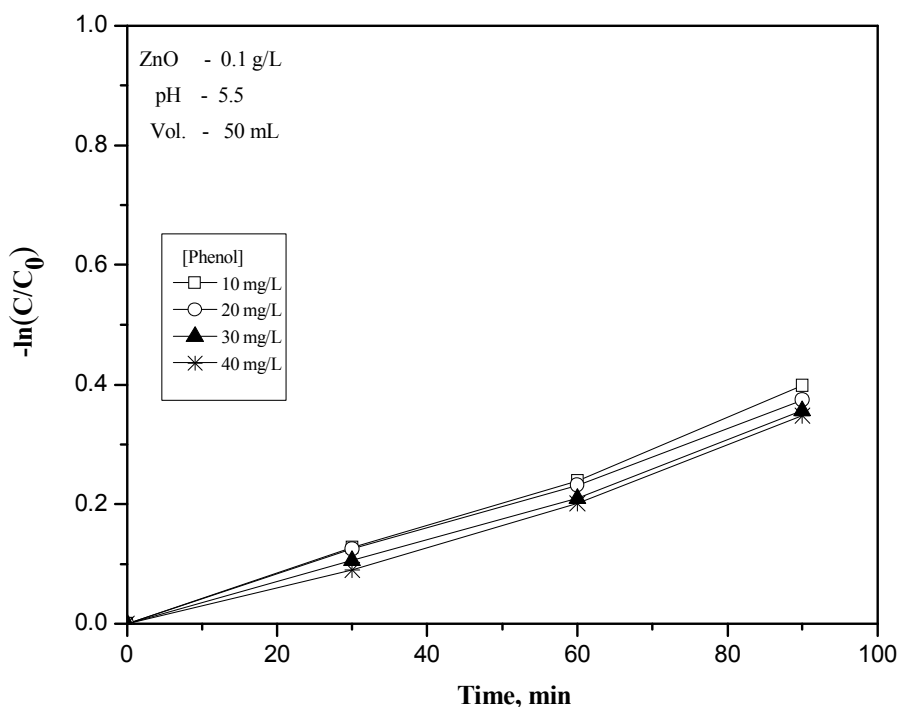


Fig.3.8 (b): Kinetics of ZnO mediated photocatalytic degradation of phenol

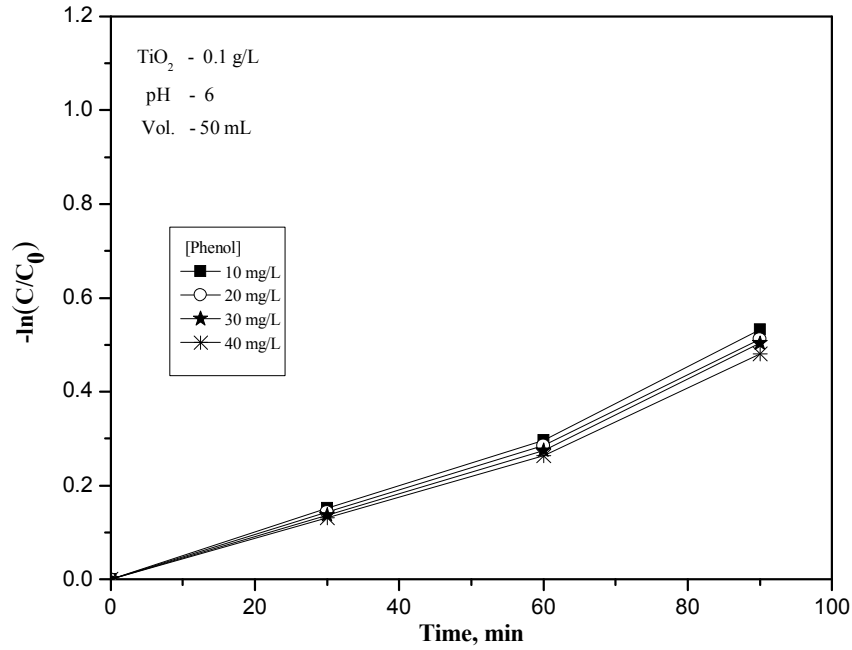


Fig.3.8 (c): Kinetics of TiO_2 mediated photocatalytic degradation of phenol.

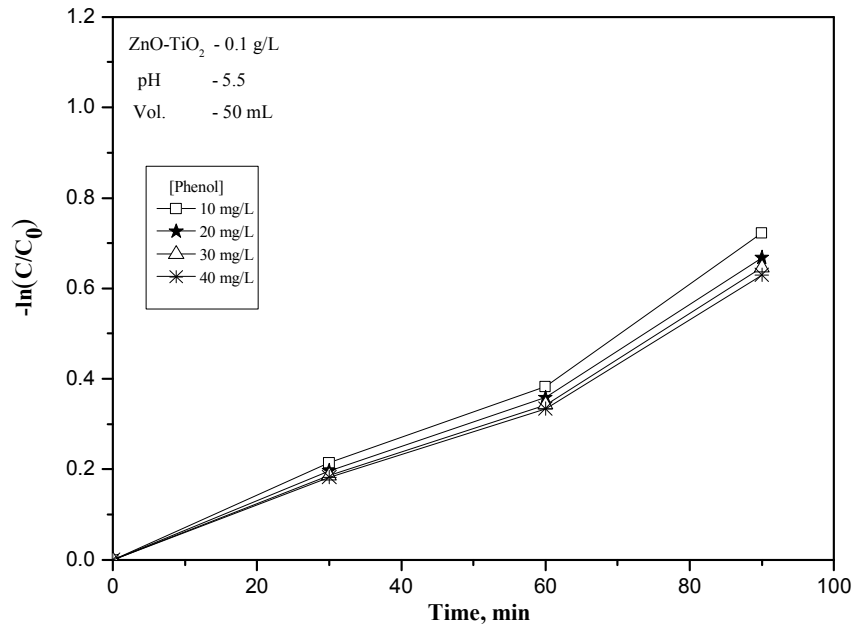


Fig.3.8 (d): Kinetics of ZnO-TiO_2 mediated photocatalytic degradation of phenol.

In the case of TiO_2 and ZnO-TiO_2 , the plot is not strictly linear in the concentration range (10-40 mg/L) as seen in Fig. 3.8 (c & d). Hence the kinetics may be different from that in the case of ZnO . This needs more detailed investigation especially due to the IPET and other combination effects of ZnO or TiO_2 .

It is clear that, in the case of all three catalysts, the rate increases with increase in initial concentration of the substrate at lower concentration range. The results are consistent with first order kinetics. However, at higher concentrations, in the case of ZnO and TiO_2 the increase in rate slows down, suggesting a reduction in the order of the reaction. In the case of ZnO-TiO_2 , the rate continues to increase with concentration at least in the range of our study and hence the variable kinetics is not manifested here. At high substrate concentrations, all the catalytic sites of the semiconductor surface are occupied and concentration is not a constraint for the reaction to proceed. At low concentrations, the number of catalytic sites is not the limiting factor for the degradation rate, which is then proportional to the substrate concentration in accordance with apparent first order kinetics. The generation and migration of photogenerated electron-hole pairs in the semiconductor oxide catalysts and the reaction between photogenerated hole (hydroxyl radical) and organic compounds are the two processes that occur in series. Therefore, each step may become rate determining for the overall process. At lower concentrations, the latter process dominates and therefore the degradation rate increases linearly with the concentration of the organic compound. On the contrary, at higher concentrations, the former will become the governing step and the degradation rate increases

slowly with concentration and even a constant degradation rate may be reached at higher concentration for a given illumination intensity. The effective number of active sites available for phenol adsorption is drastically reduced, once the surface is almost fully occupied and this also contributes to the reduction in rate of degradation at higher substrate concentrations. However, in the case ZnO/TiO₂, the availability of electron and hole will be more compared to ZnO or TiO₂ individually due to IPET and this leads to an increase in the rate of degradation even at relatively higher concentration of the substrate. Decrease in the rate of photocatalytic degradation and hence, in the order of the reaction at higher concentrations of the reactant has been reported earlier also [133,143-150]. With increase in concentration of substrate, more reactant molecules get adsorbed onto the catalyst site, get activated and interact with correspondingly more Reactive Oxygen Species. This will continue until all the surface sites are occupied by the substrate. Thereafter, increase in concentration cannot result in increased surface occupation and the phenol removal becomes independent of its concentration. Complete domination of the surface by the reactant/ intermediates/ products can result in suppression of the generation of surface initiated reactive free radicals which also results in decreased rate.

3.3.5 Effect of pH

Photocatalytic reaction of organic compounds in solution takes place on the particulate surface of the semiconductor. The pH of the reaction medium is known to have a strong influence on UV-induced degradation of organic pollutants. In photolysis, the possibility of bond breakage and its site might be different at different pH due to the

difference in the distribution of molecular charges. The surface charge of semiconductors, the interfacial electron transfer and the photoredox processes occurring in their presence are also affected by pH. Hence, the effect of pH on the photocatalytic degradation of phenol was investigated in the range 3-11, in presence of ZnO, TiO₂ and ZnO-TiO₂. The pH of the suspension was adjusted initially and was not controlled during irradiation. The results are shown in Fig. 3.9(a).

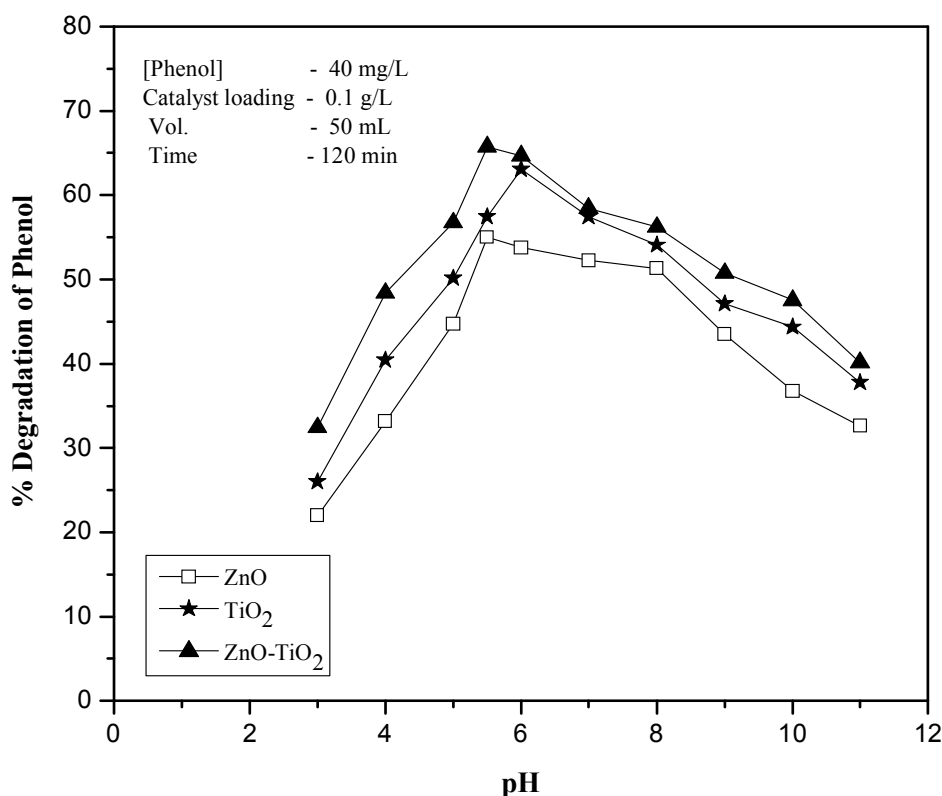


Fig.3.9(a): Effect of pH on the photocatalytic degradation of phenol over ZnO, TiO₂ and ZnO-TiO₂.

The degradation rate of the pollutant was found to increase with increase in pH initially in presence of all three catalysts. However, the

degradation decreases above pH 5, in the case of ZnO and ZnO-TiO₂ and above pH \approx 6 in the case of TiO₂. The point of zero charge (PZC) of ZnO and TiO₂ are about 9.3 and 6.5 respectively. Depending on the pH, the catalyst surface will be either positively charged (for pH < PZC) or negatively charged (for pH > PZC), or remain neutral (for pH = PZC). This characteristic significantly affects the adsorption and desorption properties of the semiconductor. In addition, the chemical characteristic of the pollutants are also influenced by pH.

The optimum pH for efficient degradation of phenol is 5.5-6.0 in all cases. The degradation is less in extreme acidic and alkaline region. With increase in pH from 3 to 6, the degradation of phenol increases. For ZnO-TiO₂, the pH effect is quite similar to that of ZnO. Higher degradation efficiency in the acidic range has been reported for phenol using TiO₂ as the catalyst [133,151]. At pH < PZC when catalyst surface is positively charged, phenol in its neutral form can get closer to the surface or weakly adsorbed. At pH > PZC, when the ZnO/TiO₂/ZnO-TiO₂ surface is negatively charged, phenol in its neutral or ionized form will keep away from the surface thereby resulting in reduced degradation. In extremely acidic solutions, photodegradation efficiency is less. In the case of ZnO, it is also because of photocorrosion which is significant at pH less than 4. As expected, the pH effect on ZnO-TiO₂ is a combination of the individual effects of ZnO and TiO₂. In order to verify the correlation between the extent of adsorption and degradation of phenol on the catalysts at different pH, the effect of pH on the adsorption on respective catalysts is measured. Results are shown in Fig. 3.9(b).

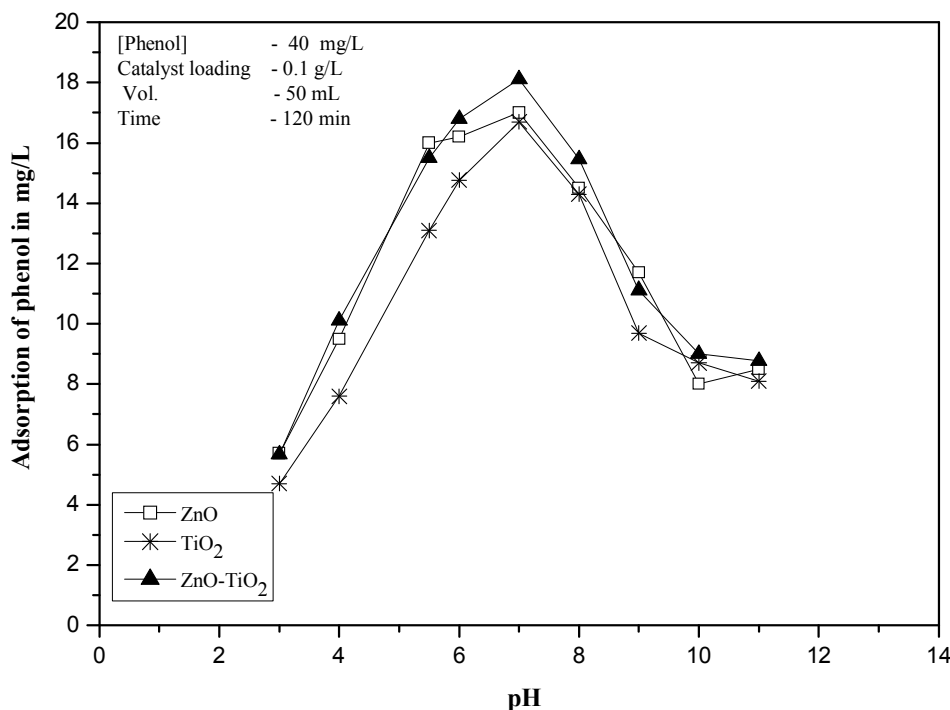
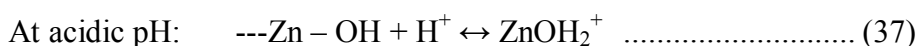


Fig.3.9 (b): Effect of pH on the adsorption of phenol from water on ZnO, TiO₂ and ZnO-TiO₂.

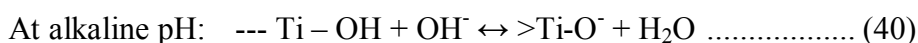
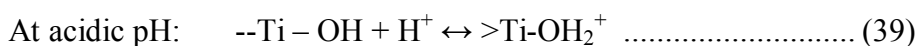
As seen, maximum adsorption is observed in the range 5.5–7.0 and it decreases thereafter in the alkaline range. The results further indicate that the pH dependence of photocatalytic degradation of phenol cannot be fully correlated to the adsorption characteristics even though the trend shows some similarities. In addition to affecting the surface properties of the catalyst, pH also influences direct photolysis of phenol and the reactive $\bullet\text{OH}$ radical formation [152]. Alkaline range is expected to favour the formation of more OH radicals from the large quantity of OH ions present which could enhance the degradation significantly. However, this is not reflected in the actual degradation rate possibly due to the poor adsorption.

The effect of pH can be explained at least partially based on the amphoteric behaviour and surface charge of catalyst. The acid-base property of metal oxides can influence their photocatalytic activity significantly. Solution pH influences the ionization state of ZnO surface according to the reactions:



pKa value of phenol is 9.98. In the alkaline pH range, where phenol is expected to be in the ionized form, the adsorption on ZnO will be weaker. Hence, the surface mediated degradation will be less. However, under acidic conditions, phenol which remains mainly in the neutral form can get adsorbed or come closer to the catalyst surface as explained earlier, resulting in its degradation via interaction with bulk hydroxyl radicals produced in the aqueous media. However, the concentration of $\cdot\text{OH}$ radicals will be relatively less. In the optimum pH range of 5.5-7, there will be reasonably good proximity of phenol to the surface adsorption and adequate population of $\cdot\text{OH}$ radicals which will explain the optimum degradation of phenol.

In the case of TiO_2 , solution pH influences the ionization state of TiO_2 surface according to the reactions:



At $\text{pH} < \sim 7$, when the TiO_2 surface is positively charged, phenol which is in neutral form can get closer to the surface or weakly adsorbed. At $\text{pH} > 7$, when the surface is negatively charged, phenol in neutral or ionized form will keep away from the surface. The mechanism of pH effect is same as in the case of ZnO and hence the similarity in the trend. As expected, the pH effect on the ZnO- TiO_2 is more or less similar to that on ZnO. The results clearly indicate that there is no well-defined direct correlation between PZC of the semiconductor oxide catalyst, adsorption and the photocatalytic degradation rate. This is in line with the observation reported by many other workers also [153-158].

3.3.6 Effect of reaction volume

Optimization of reaction volume and hence reactor size is important from the commercial application angle for any process. Hence the effect of reaction volume on the rate of photocatalytic degradation of phenol is investigated and the results are shown in Fig. 3.10(a). It is seen that the % degradation decreased with increasing reaction volume. However, the actual rate of degradation in terms of the number of molecules of phenol degrading increases with volume. The rate of degradation even slows down at higher volume and stabilizes. The rate of degradation with volume of the reaction system is plotted in Fig. 3.10(b). The increasing rate with increase in volume may be attributed to the higher number of phenol molecules in the system which leads to more frequent interaction with surface and the reactive free radicals generated from it. However when the volume exceeds the critical limit, penetration of the light becomes less, light gets scattered and photons reaching the surface of the catalyst will be less. Further the surface also will get saturated with the phenol molecules.

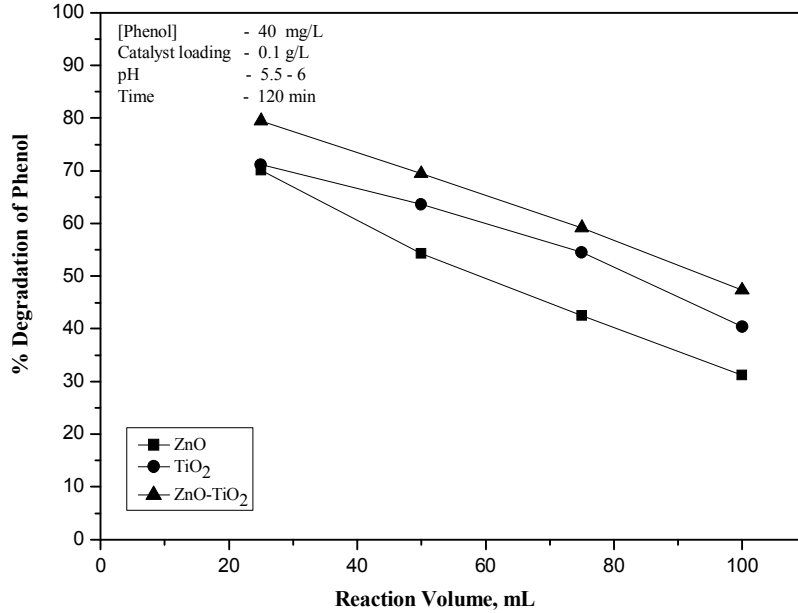


Fig.3.10 (a): Effect of reaction volume on the photocatalytic degradation of phenol over ZnO, TiO₂ and ZnO-TiO₂.

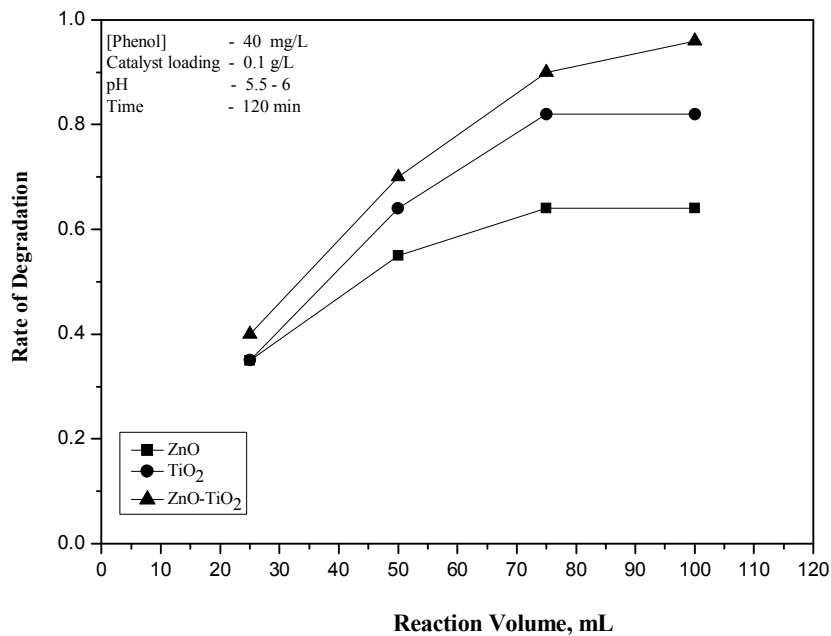


Fig.3.10 (b): Effect of reaction volume on the rate of degradation of phenol.

This results in stabilized or decreased rate of the semiconductor activation and phenol degradation. Hence reaction volume vs reactor geometry and size are important in the design of a photocatalytic system.

3.3.7 Effect of particle size

Particle size is one of the important parameters that influences the photocatalytic efficiency of semiconductors. The inverse relation between particle size of the catalyst and the rate of photocatalytic reactions has been reported in many instances. Decrease in particle size leads to increase in surface area, more surface sites for adsorption of the pollutant and better surface promoted interaction between the reactants resulting in higher conversion in photocatalysis. The effect of particle size in the range 4.5 to 18 μm on the degradation of phenol is investigated and the results are shown in Fig. 3.11. The influence of particle size in this limited range is minimal for ZnO, TiO₂ and ZnO-TiO₂. However, particles in the nano ranges at one end and higher size at the other end can influence the rate of photocatalytic degradation significantly. The effect of particle size, shape, distribution etc of the catalyst on the photocatalytic degradation of trace pollutants in a major field of investigation, especially in identifying optimum characteristic for catalyst particle. That is beyond the scope of the current study and hence not pursued.

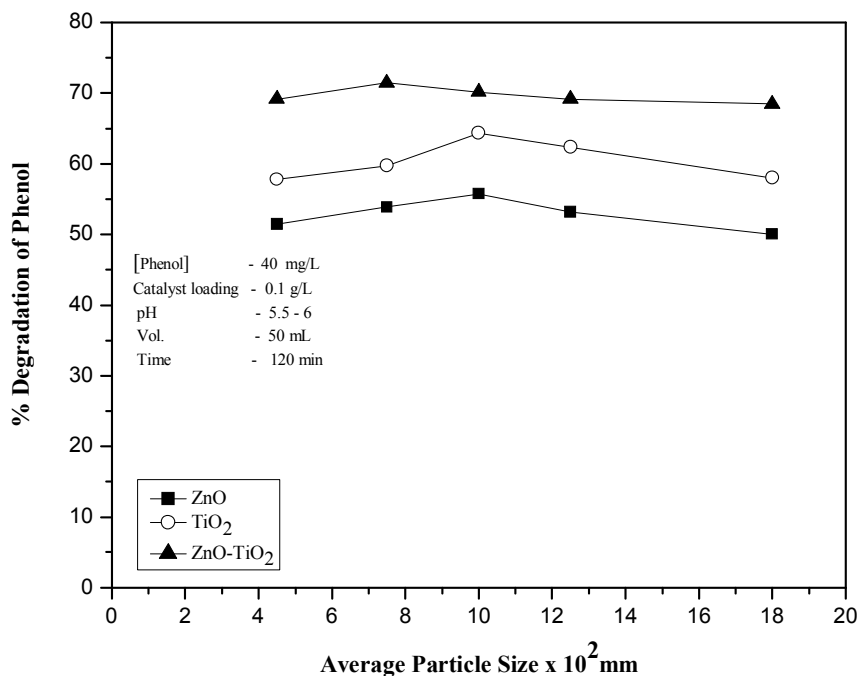


Fig.3.11: Effect of particle size on the photocatalytic degradation of phenol over ZnO, TiO₂ and ZnO-TiO₂.

3.3.8 Effect of aeration/deaeration

O₂ dissolved in the system/ remaining adsorbed on the catalyst is known to play an important role in the photocatalytic degradation reaction. The O₂ serves as an electron scavenger by trapping electron from the conduction band and preventing recombination [95]. The reduction of O₂ and the adsorption of substrate take place at different locations on the catalyst surface and hence presence of O₂ is not detrimental to the adsorption efficiency. O₂ also contributes to the formation of ROS, stabilization of reactive free radicals, intermediates, mineralization and direct photocatalytic reaction.

The effect of dissolved air/oxygen on the photocatalytic degradation of phenol was tested by purging the system with N₂ for 1 hr in the presence of each of the three catalysts. The results are as shown in Table 3.1. The degradation rate is inhibited in the system purged with N₂. Introduction of air into the system enhances the degradation because of increased supply of O₂ including the replacement. This shows that dissolved oxygen has a significant role in the photocatalytic degradation of phenol. The main role of O₂ is inhibition of the electron-hole recombination and thus enhancing the formation of ROS. O₂ also enhances the amount of H₂O₂ and in turn OH radicals which enhances the efficiency of photocatalysis.



Table 3.1: Effect of aeration/deaeration of the reaction system on the photocatalytic degradation of phenol.

[Catalyst]: [0.1g/L]; [phenol]: 40 mg/L; pH: 5.5-6; Reaction Volume: 50 ml; Irradiation Time: 120 min.

Purging gas	Percentage Degradation of phenol on		
	ZnO	TiO ₂	ZnO-TiO ₂
None	55	62	67
N ₂	23	30	37
Air	65	79	83

3.4 Probable mechanism of the photocatalytic degradation of phenol in presence of semiconductor

The primary step in heterogeneous photocatalytic process is the adsorption of the organic substrate on the surface sites. Activation of semiconductor is achieved through the absorption of a photon ($h\nu$) from UV irradiation source. When the energy is sufficient, depending on the band gap of the semiconductor, promotion of an electron from the valence band to the conduction band takes place. Thus electron hole pairs are created. The electrons are taken up by adsorbed O_2 resulting in the formation of superoxide radical anion and ultimately OH radicals through a series of reactions. The radicals and other reactive oxygen species initiated by the activated catalyst surface interact with the substrate (phenol). The basic mechanism of the photocatalytic degradation can be schematically represented in different forms. One of the simplest schematic presentations is given in Fig. 3.12.

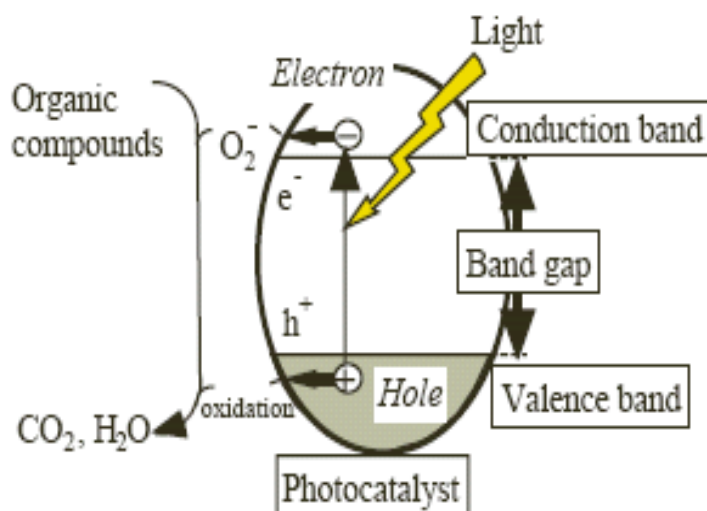
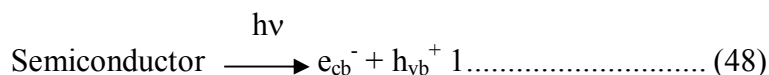


Fig.3.12: A simplified mechanism for photocatalytic process on a semiconductor [34].

Various steps involved in the process are as follows.

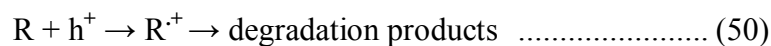
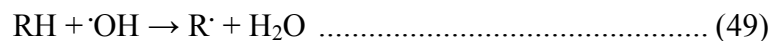


The excited electron-hole pairs generated can recombine, either in the bulk or at the surface releasing the input energy as heat, with no chemical effect. However, if the electrons and holes migrate to the surface of the semiconductor without recombination, they can participate in various oxidation and reduction reactions with adsorbed species such as water, oxygen, and other organic or inorganic species. These processes, i.e., oxidation of a suitable electron donor adsorbed on the surface by photogenerated hole and reduction of electron acceptor adsorbed on the surface by photogenerated electron, constitute the basic mechanisms of photocatalytic water/air remediation and photocatalytic hydrogen production, respectively.

The reaction steps involved in the process after the photoexcitation as in reaction (48) as given in reaction (41 - 47).

The positive hole can oxidize pollutants directly. However, in most cases it reacts with water (i.e., hydroxide ion, OH⁻) to produce the hydroxyl radical ([•]OH), which is a very powerful oxidant with oxidation potential of 2.8 V vs NHE. [•]OH rapidly attacks pollutants at the surface as well as in solution and mineralizes them into CO₂, H₂O etc [40, 41].

Hydroxyl radical ([•]OH) and superoxide radical anion (O₂^{•-}) are the primary oxidizing species in the photocatalytic oxidation processes. They cause the degradation of the organic (RH) pollutants by oxidation via successive attack by OH radicals:



Various intermediates have been reported during the photocatalytic degradation of phenol [159]. These include catechol (CC), hydroquinone (HQ) and p-benzoquinone (BQ), pyrogallol (PG), Hydroxy benzoquinone (HBQ) etc. (see Fig. 3.13) However, in the present case, only three intermediates could be identified. They are CC, HQ and BQ. Preliminary studies showed that intermediates also get degraded faster. Hence they go undetected.

Various reactive oxygen species formed as above will interact with phenol as shown in Fig. 3.13. Ultimately all these intermediates also get degraded and eventually mineralize into CO_2 and H_2O as shown below:

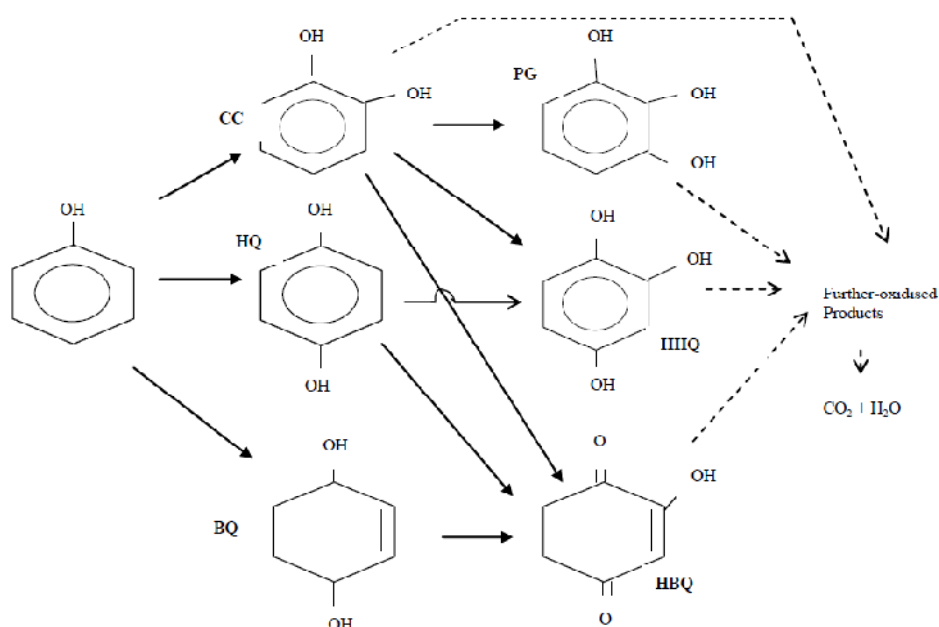
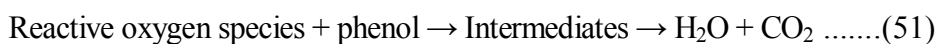


Fig.3.13: Various reactive oxygen species formed in the reaction system.

The moderately enhanced activity of ZnO-TiO₂ compared to individual ZnO and TiO₂ may be explained partially based on the improved adsorption and the concept of interparticulate electron transfer [153]. In ZnO/TiO₂ composites, the electron is transferred from the conduction band of ZnO to the conduction band of TiO₂ under illumination and, conversely, the hole is transferred from the valence band of TiO₂ to the valence band of ZnO, decreasing the pairs' recombination rate. This charge separation effectively increases the lifetime of the charge carriers and enhances the efficiency of the interfacial charge transfer to adsorbed substrates. When both semiconductors in coupled system are illuminated simultaneously and their valence and conduction bands are suitably disposed, both electron and hole transfer can occur. This will influence the efficacy of degradation mediated by the oxides. The concept of IPET is illustrated with the help of various semiconductor pairs in Fig. 3.14 [160-165].

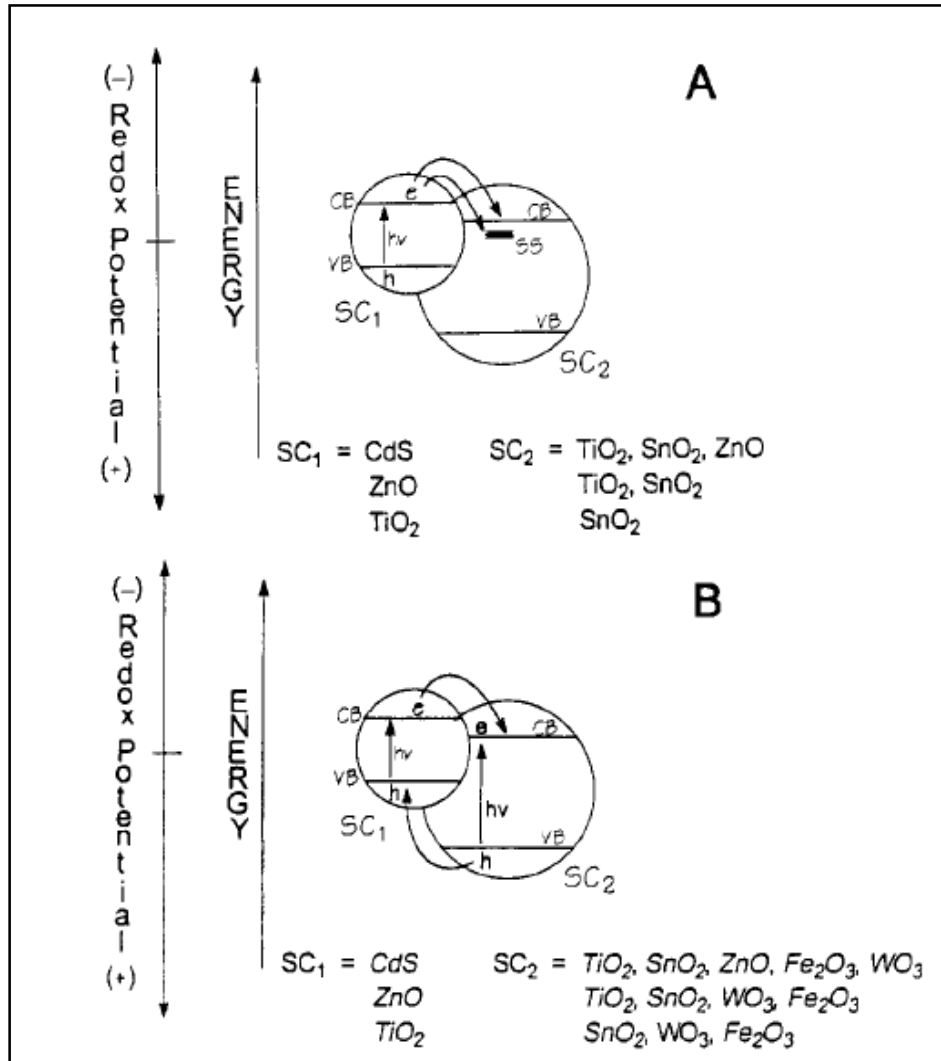


Fig.3.14: (A). Energy diagram illustrating the coupling of various semiconductors (SCs) in which vectorial electron transfer occurs from light - activated SC to the non-activated SC.
 (B): Diagram depicting the coupling of various SCs in which vectorial displacement of electrons and holes is possible.

3.5 Formation and decomposition of H₂O₂

H₂O₂ is detected as a by-product during the photocatalytic degradation of phenol in presence of ZnO, TiO₂ as well as ZnO-TiO₂. However, its concentration does not increase with time or with the degradation of phenol. In fact, the concentration of H₂O₂ is increasing and decreasing periodically indicating concurrent formation and decomposition. The variation in the concentration of H₂O₂ with time in presence of ZnO, TiO₂ and ZnO-TiO₂ is given in Fig.3.15.

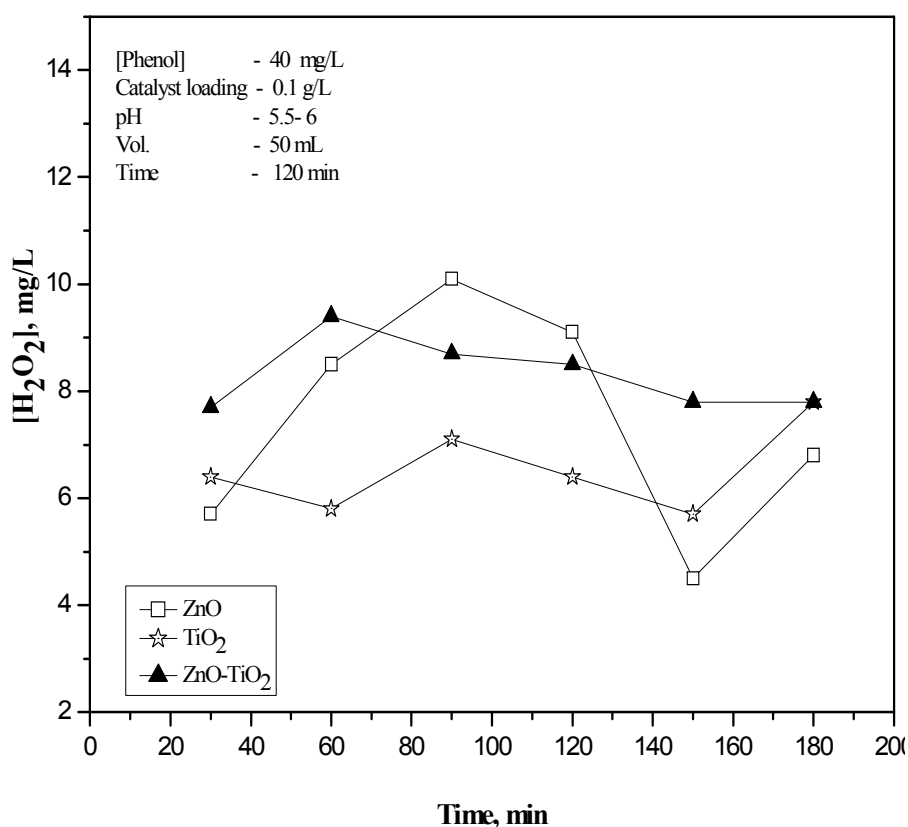
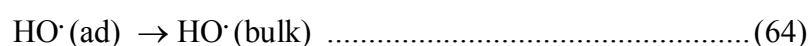
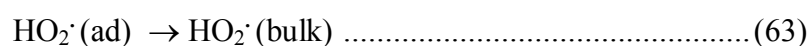
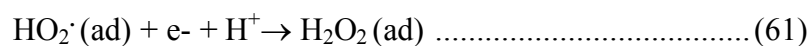
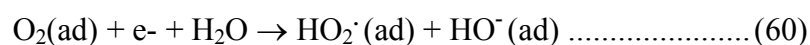
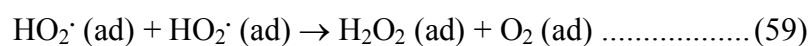
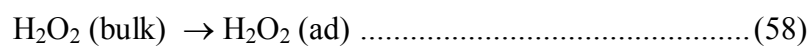
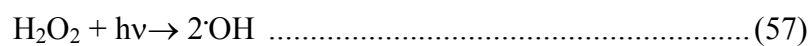
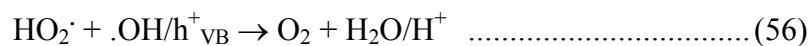


Fig.3.15: Fate of H₂O₂ formed during the photocatalytic degradation of phenol.

The concentration of H₂O₂ does not have any correlation with the degradation/mineralization of phenol. The degradation of phenol continues to increase with time. However the concentration of H₂O₂ is fluctuating with time in the case of ZnO and TiO₂. In the case of ZnO-TiO₂ it remains almost stable after initial increase. The concentration of H₂O₂ formed in situ increases initially, reaches a maximum, starts decreasing, reaches a minimum and then it starts rising again. This periodic increase and decrease in the concentration of H₂O₂ (oscillation) indicates its concurrent formation and decomposition. In the case of ZnO-TiO₂, after moderate increase in the beginning, the rates of formation and decomposition of H₂O₂ balance and hence its concentration remains steady. When the rate of formation dominates, the concentration increases and reaches a maximum. From this point onwards, the decomposition dominates and the concentration of H₂O₂ decreases.

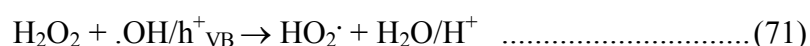
Hydrogen peroxide can be formed either through the reduction of O₂ by electron in the conduction band (e⁻_{cb}) or by the oxidation of H₂O by holes in the valence band (h⁺_{vb}). H₂O₂ is formed from both H₂O and OH⁻ ions by surface oxidation caused by the photogenerated holes and also by the disproportionation of the superoxide radical anion. Various steps involved in the formation of H₂O₂ can be as follows:





ad: adsorbed

However, concurrent decomposition of H₂O₂ is caused by reduction by the conduction band electron [94, 95] and the reactions are as follows:



The radicals as well as H_2O_2 can accelerate the degradation of phenol. The radicals can also interact with H_2O_2 resulting in decomposition and formation of even more free radicals. So the concentration of H_2O_2 increases initially and decreases thereafter showing that the H_2O_2 formed are undergoing simultaneous decomposition.

The acceleration of the degradation of phenol by H_2O_2 and/or the free radicals resulting from it, is tested by adding H_2O_2 at the beginning of the experiment and evaluating the phenol at various intervals. The results are shown in Table 3.2.

Table 3.2: Effect of added H_2O_2 on the Photocatalytic degradation of phenol under UV.

[Catalyst]: 0.1g/L; [phenol]: 40 mg/L; pH: 5.5-6; Reaction Volume: 50 mL; Time: 120 min

Catalyst	% Degradation of phenol without added H_2O_2 at the end of				% Degradation of phenol with added H_2O_2 at the end of				% Enhancement by added H_2O_2 at the end of			
	30 min	60 min	90 min	120 min	30 min	60 min	90 min	120 min	30 min	60 min	90 min	120 min
ZnO	5.8	14.6	26.3	62	10.5	24.8	34.6	75.41	81.0	70.0	31.6	20.9
TiO ₂	7.0	17.5	33.2	55	14.3	31.2	44.7	61.53	104.3	78.3	34.6	9.5
ZnO-TiO ₂	9.2	18.3	36.6	67	16.1	29.5	45.8	79.46	75.0	61.2	25.1	18

H_2O_2 enhances the degradation of phenol significantly in the beginning. This enhancement is due to the faster decomposition of added H_2O_2 in presence of UV producing maximum OH radicals which can degrade phenol. However, the decomposition of H_2O_2 to water and oxygen also occurs in parallel which restricts the continued availability of

the oxidizing species for phenol degradation resulting in a decrease in degradation rate at a later stage. Further, it must be noted that even in those experiments without externally added H_2O_2 , the H_2O_2 formed in-situ has been already accelerating the reaction rate [166].

The effect of initially added H_2O_2 is not that prominent in the later stages of the reaction. H_2O_2 accelerates the degradation in all cases following a fairly uniform pattern. The degree of enhancement varies in the case of the three catalysts with maximum in the case of TiO_2 and the minimum in the case of ZnO-TiO_2 . However, the trend remains the same showing that the mechanism of degradation of phenol as well as the formation and decomposition of H_2O_2 is more or less the same in all three cases.

3.6 Effect of anions

In industrial waste waters, phenols and other pollutants are present along with many other natural/man-made organic and inorganic materials which can affect the photocatalytic degradation. In this context, the effect of few added salts/anions like Cl^- , I^- , SO_4^{2-} , F^- , CO_3^{2-} , NO_3^- , Br^- and PO_4^{3-} on the rate of photocatalytic degradation was investigated. Fig.3.16 (a, b and c) show the results obtained with different anions in the case of ZnO , TiO_2 and ZnO-TiO_2 as catalysts.

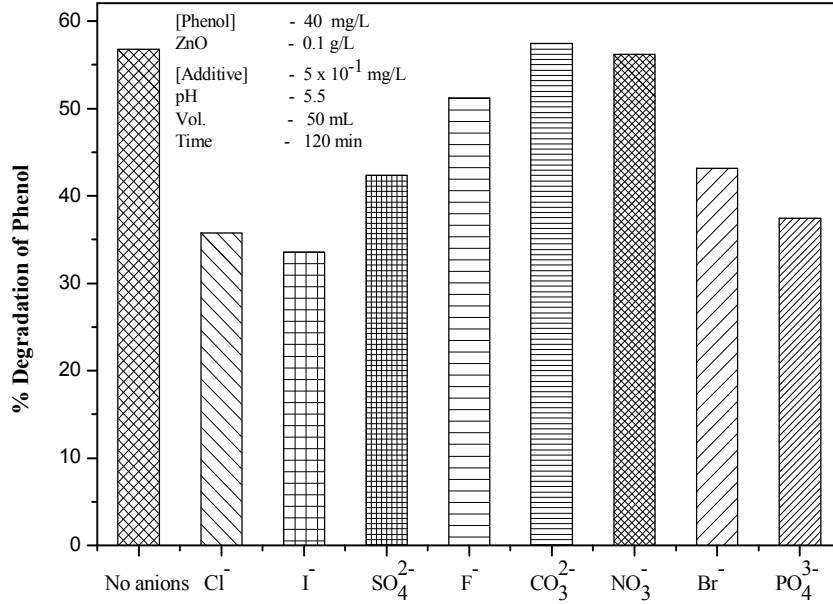


Fig.3.16(a): Effect of anions on the photocatalytic degradation of phenol over ZnO.

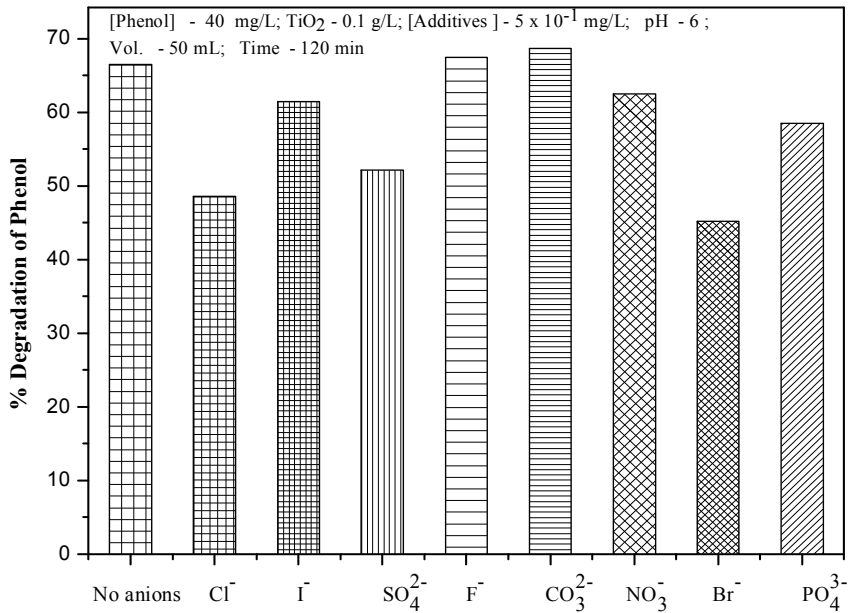


Fig.3.16(b): Effect of anions on the photocatalytic degradation of phenol over TiO₂.

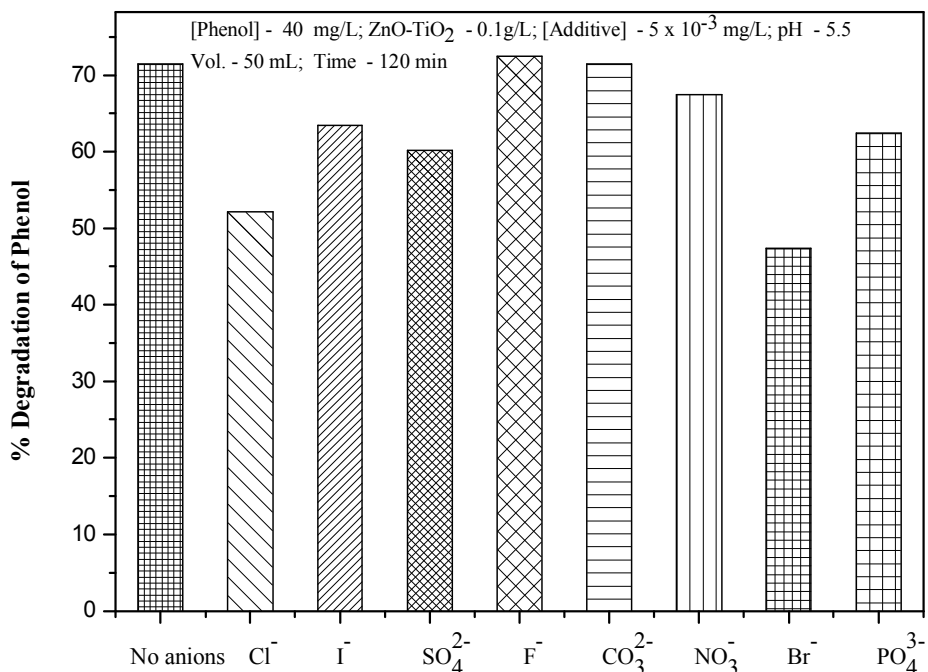


Fig.3.16(c): Effect of anions on the photocatalytic degradation of phenol over ZnO-TiO₂.

In the case of ZnO catalyst, Cl⁻, I⁻, SO₄²⁻, Br⁻ and PO₄³⁻ inhibit the reaction in the order I⁻ > Cl⁻ > PO₄³⁻ > SO₄²⁻ ≥ Br⁻ while CO₃²⁻ and NO₃⁻ do not have much effect on the reaction rate. The effect of F⁻ also can be treated as insignificant or slight inhibition. In the case of TiO₂ catalyst, Cl⁻, I⁻, SO₄²⁻, NO₃⁻, Br⁻, PO₄³⁻ inhibit the reaction in the order Br⁻ > Cl⁻ > SO₄²⁻ > PO₄³⁻ > NO₃⁻ ≥ I⁻ while CO₃²⁻ and F⁻ do not have any significant effect. The effect of NO₃⁻ and I⁻ can be considered as negligible within the limits of experimental error.

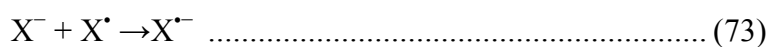
In the case of ZnO-TiO₂, inhibition decreases in the order Br⁻ > Cl⁻ > SO₄²⁻ > PO₄³⁻ > I⁻ while NO₃⁻, CO₃²⁻ and F⁻ have no effect. Thus the anions have more or less similar effect on ZnO-TiO₂ as in the case of

TiO₂. Though the effect is not quite identical in the case of these three catalysts, a general trend is obvious. Analysis of the effect of each of the anion on each catalyst requires in depth study on the role of a number of parameters which is beyond the scope of the current study. Such investigation are in progress in our laboratory at present.

The inhibition by anions can be broadly explained by the general mechanism of photocatalysis. The experiments were conducted at pH 5.5, which is below the PZC of ZnO and TiO₂. Hence, the semiconductor particles will be carrying positive charge. Consequently, the anions can be strongly adsorbed onto these particles through ionic forces. The reaction of surface holes with these undesirable ions leads to a decrease in the formation of hydroxyl radicals, resulting in low photocatalytic efficiency.

The inhibition by halide ion I⁻, Cl⁻ and Br⁻, though in varying degrees, may be explained as follows:

The halide ions(X⁻) scavenge the photoproduced holes and the hydroxyl radicals more effectively as in reaction 72-75.

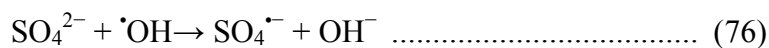


Scavenging the highly reactive hydroxyl radical, results in their decreased role in the degradation of phenol.

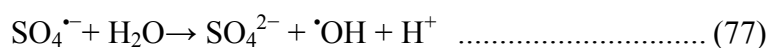
In this respect, the relatively lower inhibition by F^- is surprising. However, instances of similar behaviour by F^- in TiO_2 photocatalysis have been reported earlier also. Calsa and Pelizetti [155] explained this phenomenon as given below:

The holes formed during the irradiation of the semiconductors responsible for the photocatalytic degradation can be either in the bulk or trapped on the surface. When F^- ions get strongly adsorbed on the surface, the holes are bound and effectively ^-OH is replaced from the surface. The reactive ^-OH interacts with the hole in the bulk resulting in enhanced formation of $\cdot\text{OH}$ radicals. These $\cdot\text{OH}$ radicals can compensate at least partially for the surface sites lost to F^- . The redox potential of the coupled F/F^- is 3.6 eV which makes fluoride stable against valence band holes. Hence the negligible effect of fluoride may be due to the bulk homogeneous OH reaction and the direct electron transfer from the organic compound to the relatively more abundant valence band hole. However, this may not be the complete picture and the effect may be more complex and not amenable to simple explanation.

The deactivation and decrease in the concentration of hydroxyl radicals caused by SO_4^{2-} can be explained as follows:



The sulphate radical ions ($SO_4^{\cdot -}$) can react with water to produce more sulphate ions



$\text{SO}_4^{\bullet-}$ is also a strong oxidant which can contribute to the degradation of phenol



Of the two reactions (76) and (77), the latter will be more facile resulting in regeneration of SO_4^{2-} which will again lead to trapping of hydroxyl radicals as in (76). Further, the anion gets adsorbed on to the surface of the catalyst thereby denying access to the phenol molecule. Decreased access to surface sites and reduced the availability of active OH radicals result in a decreased degradation in presence of sulphate ions. However, this is partially compensated by the parallel regeneration of OH radicals as in reaction (77). Hence, the inhibition is relatively less in the case of SO_4^{2-} .

PO_4^{3-} ions are well known to get strongly adsorbed on the surface of semiconductor oxide. They compete with phenol for the adsorption sites on the surface of the photocatalyst. They can also scavenge OH to form the corresponding anion radicals $\text{PO}_4^{3\bullet-}$, which leads to a decrease in the oxidation process. However, in this case also, simple competitive adsorption and blocking of surface sites may not be sufficient to explain the role of PO_4^{3-} . The strong inhibition by PO_4^{3-} , reported in the case of many photocatalytic processes is absent in the current instance, probably because the bulk process is also equally dominating. In the case of NO_3^- and CO_3^{2-} the effect on the degradation of phenol is negligible. Both the anions are known to be weakly adsorbed on the surface of semiconductors [155-159,167-169]. They are also not known as strong OH radical scavengers. Hence, these anions do not influence the semiconductor

catalysed photodegradation of phenol, at least under the conditions of the current study.

3.7 Conclusions

The photocatalytic degradation of phenol pollutant in water in presence of ZnO, TiO₂ and ZnO-TiO₂ catalyst is investigated. The efficiency of the catalysts is in the order ZnO-TiO₂ > TiO₂ > ZnO. H₂O₂ formed during the photocatalytic degradation undergoes simultaneous formation and decomposition resulting in oscillation in its concentration. Major intermediates of phenol degradation are catechol, hydroquinone and p-benzoquinone. Ultimately they also degrade fully resulting in the complete mineralization of the pollutant into relatively harmless end products, i.e., CO₂ and H₂O. Possible mechanism for the photocatalytic degradation of phenol, formation and decomposition of H₂O₂ and the enhanced activity of coupled ZnO-TiO₂ are discussed. Various anions likely to be present in water influences the photocatalytic degradation differently. However, there is no general trend indicating the complexity of the effect of anions in photocatalysis.

.....✂.....

**SEMICONDUCTOR OXIDES MEDIATED SONOCATALYTIC
DEGRADATION OF PHENOL IN WATER**

- 4.1 *Introduction*
- 4.2 *Experimental Details*
- 4.3 *Results and Discussion*
- 4.4 *General Mechanism of sonocatalysis*
- 4.5 *Effect of anions*
- 4.6 *Conclusions*

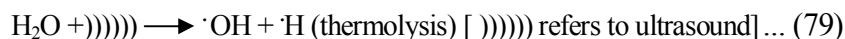
4.1 Introduction

As explained in Chapter 3, the photocatalytic degradation needs high power ultraviolet light to induce excitation of the semiconductor. This restricts the application of photocatalysis for the treatment of turbid/opaque waste waters of low transparency. The photocatalytic activity cannot be enhanced by increasing catalyst dosage beyond a limit due to ineffective light penetration and its scattering. The substrate itself can absorb part of the light in many cases reducing the radiation available for catalyst activation. In order to overcome these drawbacks, ultrasound was examined instead of ultraviolet light as the irradiation source for the activation of various semiconductor oxides for the degradation of organic pollutants. This method was reported to yield positive result for the treatment of different types of pollutants in water. However, the

degradation rate is slow when compared to other established methods and needs substantial improvement in the reaction system as a whole to be considered as a viable wastewater treatment method.

Basic principles of the application of ultrasound for the degradation of pollutants in water are already discussed in Chapter 1. The chemical effect of acoustic cavitation consists of nucleation, growth and collapse of bubbles. The collapse of bubbles results in localized supercritical conditions such as high temperature, high pressure, electrical discharges and plasma effects. The temperature of the gaseous contents of a collapsing cavity can reach approximately 5500⁰C and that of the liquid immediately surrounding the cavity reaches upto 2100⁰C. The localized pressure is estimated to be around 500 atmospheres resulting in the formation of transient supercritical water. Thus these cavities are capable of functioning like high energy micro reactors [81,166]. The consequence of these extreme conditions is the cleavage of dissolved oxygen molecules and water molecules into radicals such as H[·], OH[·] and O[·] [Eqs. 79 to 82] which will react with each other as well as with H₂O and O₂ during the rapid cooling phase giving HO₂[·] and H₂O₂. Ultrasound also contributes to the pyrolysis that takes place within the cavitation bubbles in which very high temperature and pressure exist. The free radicals formed in the hot regions diffuse to the bulk solution and react with the pollutants. The addition of soluble and insoluble particles (heterogeneous catalysts) such as metallic oxides (eg. TiO₂ or ZnO) and mixture of metals to an ultrasonic reaction system promotes the formation of cavities and generation of free radicals. The sonocatalytic effect is based on enhancement of the oxidative power of US by the solid, which increased

with increase in the surface area of the catalyst. This leads to the formation of more ·OH by heterogeneous nucleation of the bubbles. Sonoluminescence caused by the bubble or cavity implosion may induce the excitation in the semiconductor which initiates photocatalytic process in the ultrasonic system. In this highly reactive nuclear environment, organic pollutants can be decomposed and inorganic pollutants can be oxidised or reduced. The ultrasonic formation of reactive free radicals from water can be summarized as follows:



Furthermore, the production of OH radical is promoted when O₂ is present in water as shown in the following equations [Eqs.83 and 84]



Recently, many studies have been reported on the application of sonochemical reaction for wastewater treatment with and without catalysts. Semiconductors such as, TiO₂ and ZnO are the most frequently tested materials. Of these, ZnO has received relatively less attention possibly due to its corrosive nature under extreme pH conditions. Comparative study of the activity of TiO₂, ZnO and composite TiO₂/ZnO powders for the

photocatalytic degradation of phenol described in the previous chapter showed that the composite powder is more effective. Similarly Tb_7O_{12}/TiO_2 composite was reported to perform better as sonocatalyst compared to the individual oxides for the degradation of Amaranth [170]. However, not many reports are available on the use of ZnO or coupled ZnO-TiO₂ as sonocatalysts for the removal of water pollutants [170,171]. In this chapter, investigations and results on the sonocatalytic activity of ZnO, TiO₂ and ZnO-TiO₂ for the removal of trace amounts of phenol in water are presented. The influence of various parameters on the efficacy of the process also is investigated and the findings are critically assessed.

4.2 Experimental Details

4.2.1 Materials

The sources of various materials used, their characteristics etc are the same as provided in Chapter 3.

4.2.2 Equipment Used

Ultrasonic bath (Equitron make) was used as the irradiation source. Its frequency and power were 42 kHz and of 100W respectively. Rest of the equipment used for this study is same as described in Chapter 3. The analytical procedures are also the same.

4.2.3 Experimental set up

The experiments were performed using aqueous solutions of phenol of the desired concentration in presence of specified quantity of the catalyst suspended in the solution. Sonication was sufficient to ensure adequate mixing of the suspension. Additional mechanical mixing did not

make any notable consistent difference in the reaction rate. The ultrasonic bath was operated at a frequency of 42 kHz and a power of 100 W unless indicated otherwise. Water from the sonicator was continuously replaced by circulation from a thermostat maintained at the required temperature, ($29\pm 1^\circ\text{C}$). The position of the reactor in the ultrasonic bath was always kept the same. Typical reaction assembly is shown in Fig. 4.1. In most cases, simple glass beakers of 250 mL capacity were used as reactors for convenience as well as comparison with other AOPs.

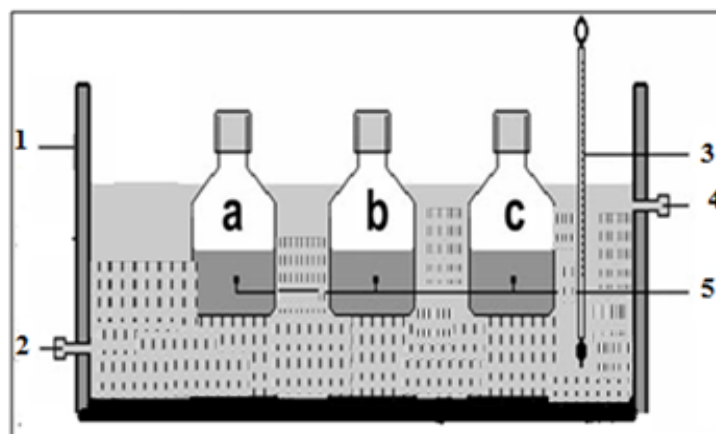


Fig.4.1: Experimental set-up for: (1) Ultrasonic bath, (2) Inlet, (3) Thermometer, (4) Outlet, (5) (a, b and c) Reactors.

4.2.4 Analytical Methods used

Sampling and analysis were done as explained in Chapter 3.

4.3 Results and Discussion

The catalysts were characterized as explained in Chapter 3. Preliminary investigations on the sonocatalytic degradation of phenol were made using ZnO, TiO₂ and ZnO-TiO₂ combination catalysts under identical conditions. The results show that ZnO-TiO₂ [1:1] is the most efficient closely

followed by ZnO and then TiO₂ with 15%, 14% and 7% degradation respectively in 2 hr time under otherwise identical conditions as shown in Fig.4.2. The catalytic activity is in the order ZnO-TiO₂ > ZnO > TiO₂.

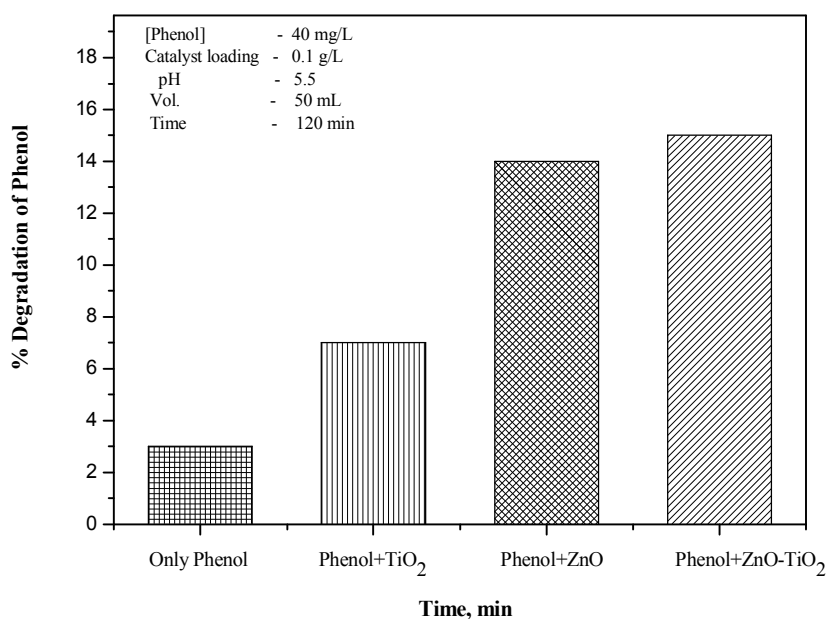


Fig.4.2: Comparison of sonocatalytic activities of on ZnO, TiO₂ and ZnO-TiO₂.

No significant degradation of phenol took place in the absence of US or the catalyst suggesting that both catalyst and ultrasound are essential to effect degradation. Small quantity of phenol degraded under US irradiation even in the absence of the catalysts. This is understandable, since sonolysis of water is known to produce the free radicals H[•] and OH[•] (Eq.79) which are capable of attacking the organic compounds in solution. This process is facilitated in a heterogeneous environment in presence of ZnO, TiO₂ and ZnO-TiO₂. The solid particles help to break up the microbubbles created by US into smaller ones, thus increasing the number of regions of high temperature and pressure. This leads to an

increase in the number of OH radicals and other reactive oxygen species which will interact with the organic molecules present in water and oxidize them, resulting in mineralization.



Since ZnO-TiO₂ is the most efficient of the three catalysts, it is essential to identify the optimum ratio of the individual oxides in the composite. A series of experiments were conducted for this purpose by varying the ratio of ZnO and TiO₂. The percentage degradation varies with the composition of ZnO-TiO₂ with a maximum degradation of 15% in presence of ZnO-TiO₂ at the weight ratio 4:6 as shown in Fig. 4.3. Incidentally it is the same composition of ZnO-TiO₂ that gives optimum degradation of phenol under photocatalytic conditions also.

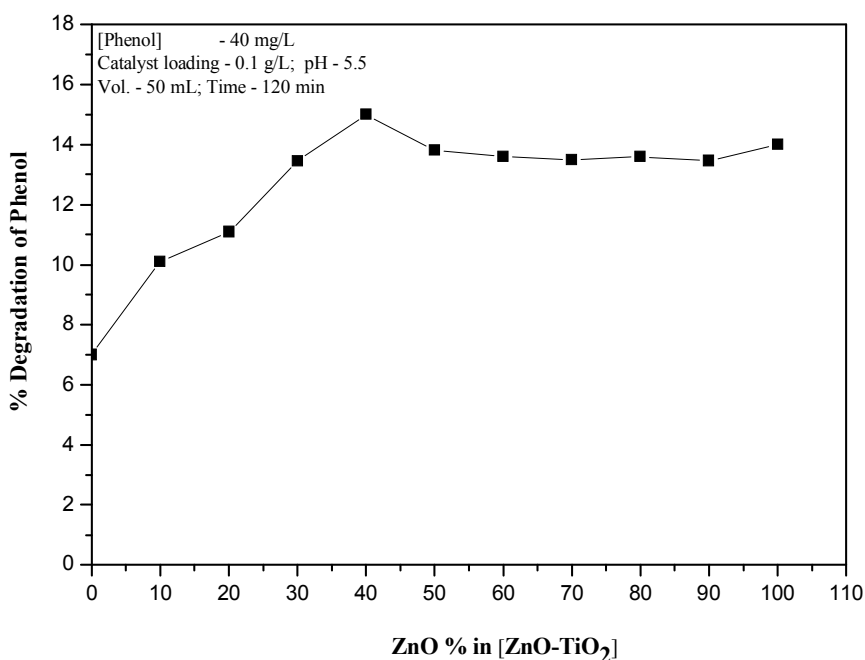


Fig.4.3: Effect of variation of ZnO in ZnO-TiO₂ ratio on the sonocatalytic activity.

Pure TiO₂ powder gives the lowest degradation (7 %) of phenol under ultrasonic irradiation. The degradation increases as the content of ZnO increases. When the weight ratio of ZnO and TiO₂ reaches 4:6, the activity is maximum. The similarity in optimum catalyst composition for degradation under photocatalysis and sonocatalysis shows that the mechanism of degradation also may be similar. Since the degradation is primarily initiated by ·OH and ROS, it may be presumed that the concentration of ·OH radicals produced by ZnO is more than that produced by TiO₂ of the same weight under US irradiation. When the proportion of ZnO and TiO₂ is appropriate (e.g. 4:6), maximum degradation occurs. At the same time the combination of ZnO-TiO₂ is slightly more effective than pure ZnO when the % of ZnO in the composite is >40%. Hence the effectiveness of combination is not simply additive. This is further confirmed from the observation that at the catalyst weight of 0.05g/L of individual loading the sum of degradation achieved in presence of ZnO (~7%) and TiO₂ (~2%) is less than the degradation of ~ 15 % achieved in presence of composite ZnO-TiO₂ (0.05g+0.05g). The Interparticulate Electron Transfer, responsible for enhanced effectiveness of ZnO-TiO₂ composite under photocatalysis is functional in this case also. Therefore, the proportion of 4:6 (ZnO-TiO₂) was used for further studies.

4.3.1 Effect of irradiation time

The effect of irradiation time on the sonocatalytic degradation of phenol was studied by varying the US irradiation time, keeping other parameters constant. The results are shown in Fig. 4.4.

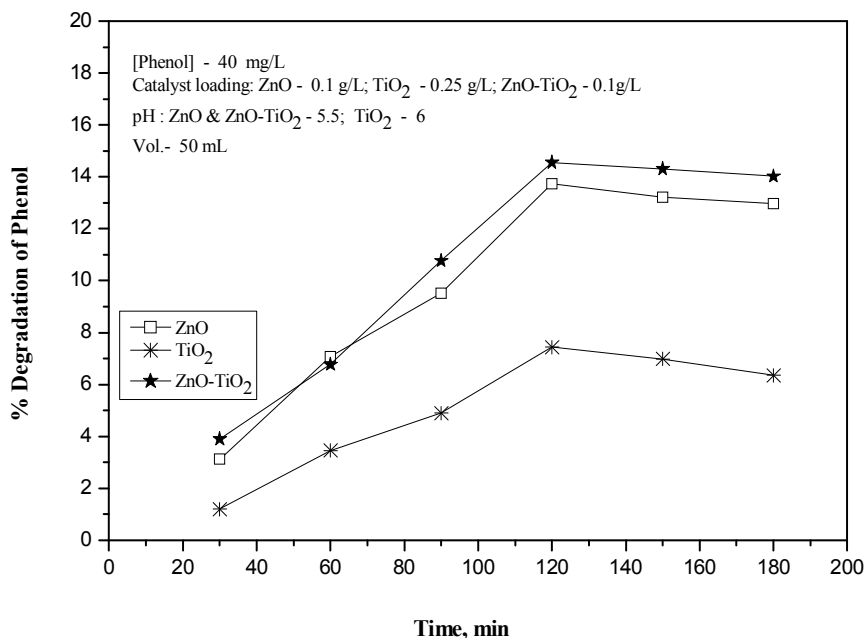


Fig.4.4: Effect of irradiation time on the sonocatalytic degradation of phenol over ZnO, TiO₂ and ZnO-TiO₂

The percentage degradation of phenol increases as the ultrasonic irradiation time increases. The mixed catalyst, ZnO-TiO₂, has slightly better degradation efficiency than either of the individual's catalysts. The degradation may be taking place on the surface of the catalyst as well as in the bulk [87,130,131,143,172-176]. The degradation levels off with time of irradiation probably due to saturation of the surface of the catalyst, accumulation of intermediates which compete with the substrate and decrease in the concentration of substrate [177-180].

4.3.2 Effect of catalyst dosage

The effect of catalyst dosage on the sonocatalytic degradation of phenol was studied at different loadings of ZnO, TiO₂ and ZnO-TiO₂. The results showed that with increase in the catalyst loading from 0.02 to

0.10 g/L the degradation increases steadily in the case of ZnO and ZnO-TiO₂ and reaches an optimum. In case of TiO₂ the degradation increases relatively slowly from 0.02 to 0.25 g/L and levels off thereafter as shown in Fig.4.5.

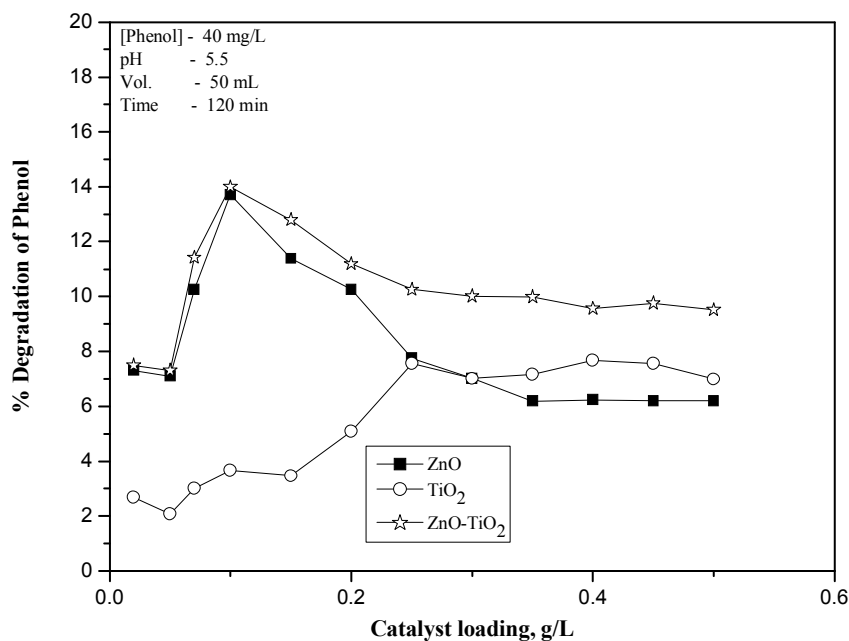


Fig.4.5: Effect of catalyst loading on the sonocatalytic degradation of phenol over ZnO, TiO₂ and ZnO-TiO₂.

In all three cases, beyond the respective optimum dosage of catalyst, the degradation slows down and thereafter remains more or less steady. The enhanced degradation efficiency with increase in the dosage is probably due to increased number of catalytic sites, higher production of OH radicals and more effective interaction with the substrate. It is known that the addition of particles of appropriate size and amount into the liquid system results in an increase in the acoustic noise and a rise in

temperature in the irradiated liquid. Introduction of more catalyst particles in the solution provides more nucleation sites for cavitation bubbles at their surface. This will result in decrease in the cavitation thresholds responsible for the increase in the number of bubbles when the liquid is irradiated by US. The increase in the number of cavitation bubbles increases the pyrolysis of water that results in the sonocatalytic degradation of phenol. Any further increase in catalyst concentration beyond the optimum will only result in the particles coming too close to each other or aggregating thereby limiting the number of accessible active sites on the surface. Higher concentration of the suspended particles may also disturb the transmission of ultrasound in aqueous medium. Hence no further increase in the degradation of the pollutant is observed beyond the optimum dosage. However, the number of particles alone or the effect of ultrasound on them is not the only factors leading to increased degradation with increase in catalyst dosage, as seen in the difference in the optimum amount of ZnO, TiO₂ and ZnO-TiO₂ with comparable particle size and surface area. Surface and bulk interactions of the reactant molecules also play an important role in the sonocatalytic degradation of organics in a suspended system.

The enhanced degradation in presence of ZnO-TiO₂ compared to individual ZnO or TiO₂ powder under identical conditions can be attributed partially to the combination of better adsorption by TiO₂ and better catalytic activity of ZnO. The adsorption of phenol on the catalysts is determined at the optimum degradation dosages and the values are 8.8, 3.6 and 4.4 mg/g in the case of TiO₂, ZnO and ZnO-TiO₂ respectively. TiO₂ is a better adsorber compared to the other two catalysts. However,

its sonocatalytic activity is less compared to ZnO thereby confirming that adsorption is not the only factor controlling sonocatalysis. At the same time increase in the degradation rate with increase in catalyst loading for all three catalysts as observed in the current study shows that adsorption does not inhibit the degradation altogether. Adsorption helps the surface initiated degradation on one hand and protects at least partly, the adsorbed species from cavitation effects on the other. At the same time, cavitation is known to alter the adsorption/desorption/degradation rates. The current study shows that ZnO is more efficient than TiO₂ for the degradation of phenol. Combination of ZnO and TiO₂ is having almost the same activity as ZnO. This also shows that the effect of particles is not limited to cavitation or its consequences alone. Irradiation of aqueous solution by ultrasound is known to produce ultraviolet light by sonoluminescence. Since ZnO is known to be a better harvester of light, the higher sonocatalytic activity can be at least partly attributed to the photocatalysis occurring during US irradiation. The presence of suspended particles upto a critical maximum leads to better propagation of the ultrasonic wave in the suspended medium resulting in the production of cavitation bubbles and emission of light throughout the reactor. This light can activate ZnO leading to the production of OH radicals which can either react with phenol and degrade it or recombine to produce H₂O₂. Higher adsorption of the pollutant on the surface of the catalysts is known to retard the absorption of light resulting in lower degradation. At the same time, lower adsorption can result in decreased reaction rate, prolonged degradation time and even incomplete degradation. Hence, reasonable degree of adsorption combined with good absorption of light resulting from

sonoluminescence lead to good sonocatalytic activity of semiconductor oxides. The higher activity of ZnO-TiO₂ indicates that the better adsorption capacity of TiO₂ and the light absorption capability of ZnO can be suitably exploited to achieve maximum degradation of the pollutant in water by sonocatalysis using such composites.

4.3.3 Effect of concentration

The effect of initial concentration of phenol in the range of 10-60mg/L on the sonocatalytic degradation on ZnO, TiO₂ and ZnO- TiO₂ was investigated. The results are plotted in Fig. 4.6 (a).

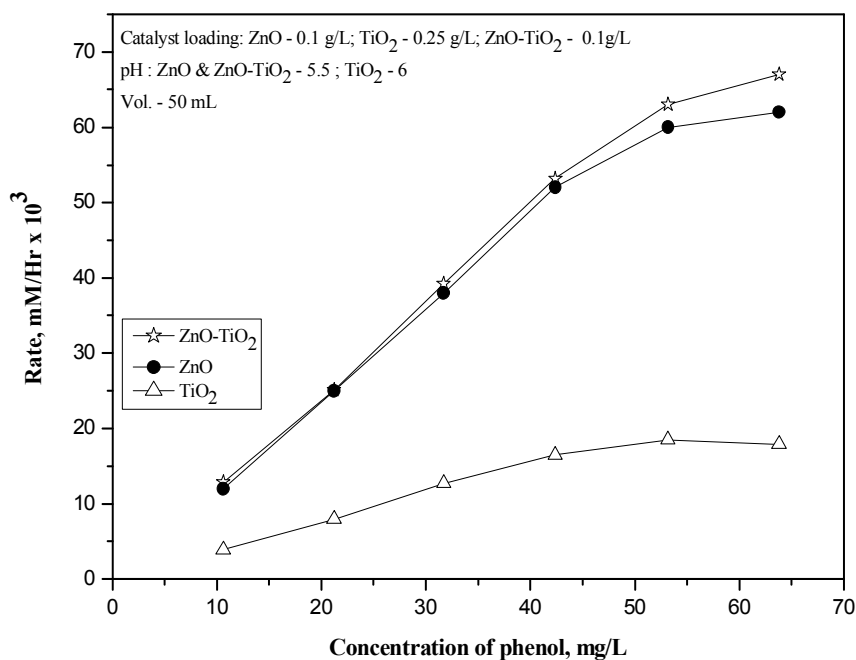


Fig.4.6(a): Effect of concentration on the sonocatalytic degradation of phenol over ZnO, TiO₂ and ZnO-TiO₂.

In the case of ZnO, TiO₂ as well as ZnO-TiO₂, the rate increases linearly with increase in concentration and levels off eventually at

~ 55 mg/L. The kinetics of the sonocatalytic degradation of phenol on the three catalysts at lower concentration range (10-30 mg/L) is further computed from the logarithmic plot as shown in Fig.4.6 [b-d]. It is observed that in the case of all three catalysts the plots are similar indicating that the kinetics and mechanism of degradation also may be similar. As in the case of photocatalysis, in sonocatalysis also the reaction is following variable kinetics; pseudo first order at lower concentration which decreases progressively and eventually becomes zero order.

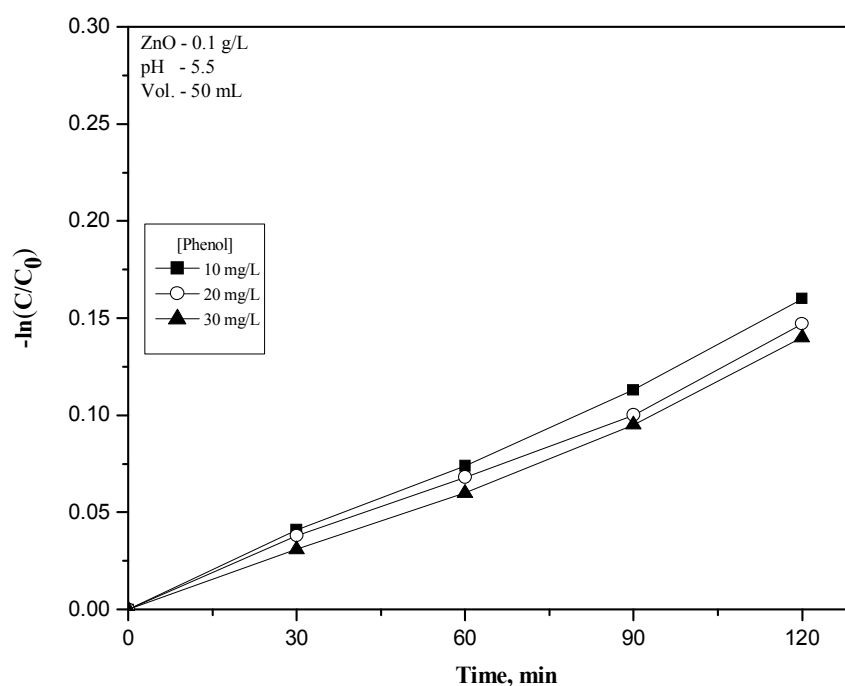


Fig.4.6(b): Kinetics of ZnO mediated sonocatalytic degradation of phenol.

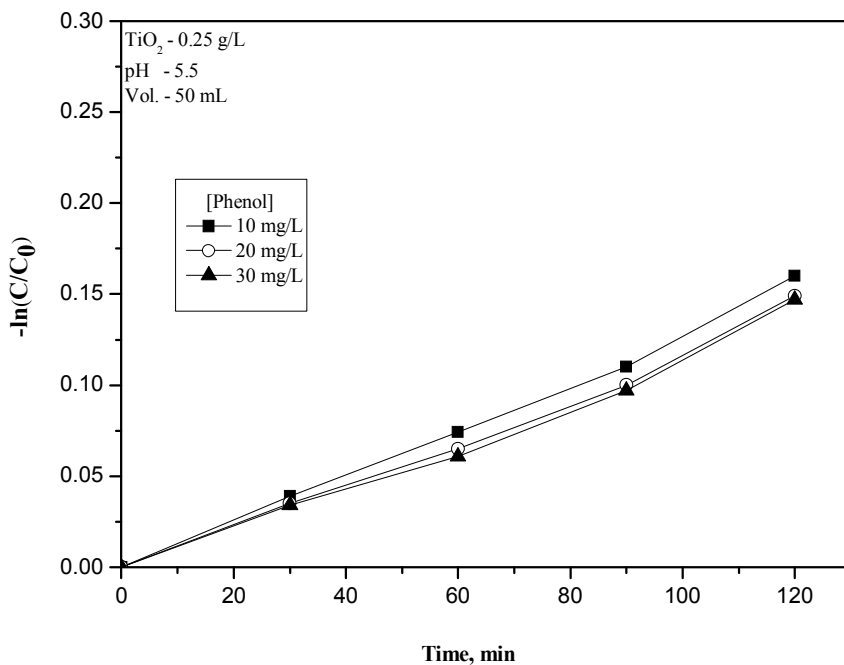


Fig.4.6(c): Kinetics of TiO₂ mediated sonocatalytic degradation of phenol

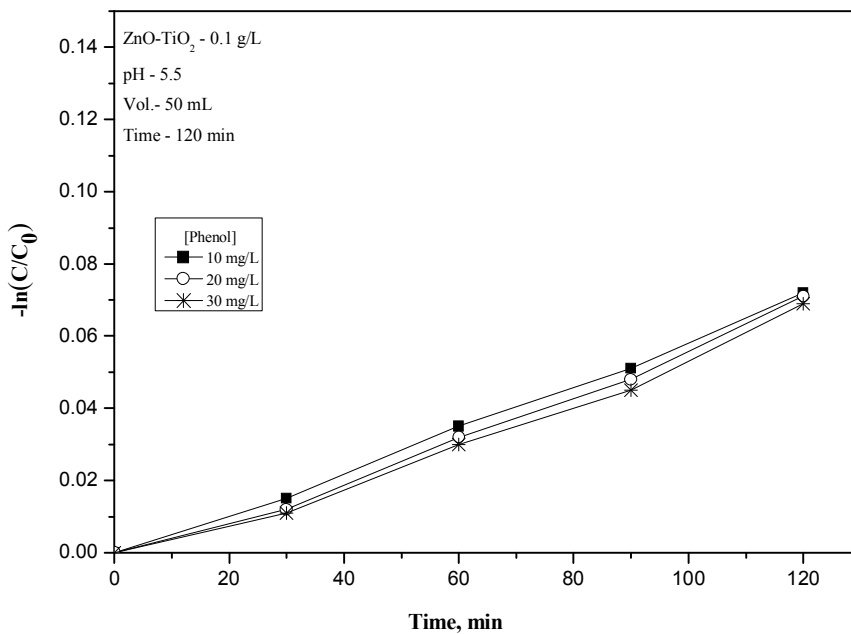


Fig.4.6(d): Kinetics of ZnO-TiO₂ mediated sonocatalytic degradation of phenol.

Change in the order of the reaction at higher concentration of the reactant has already been reported in the case of photocatalysis [130,148] and sonocatalysis [176]. Generally the L-H model in which the reaction rate depends on the initial solute concentration is applied to many sono and photo catalytic reactions. Several modifications to the L-H model based on irradiation intensity, catalyst dosage, O₂ concentration etc., also have been proposed [130]. The lower order at higher concentration can be attributed to the saturation of dissolved or adsorbed state of the reactant or the formation of relatively stable intermediates. However, the kinetics can be complex due to the presence of different adsorption sites, presence of pores which results in complex adsorption isotherms and mass transfer problems. The recombination of active species also contributes to the complex kinetics.

In any case, it may be generally concluded that L-H mechanism and first order rate equation can explain the semiconductor mediated photo and sonocatalytic degradation of pollutants in water at ppm and ppb levels. The fact that the degradation rate increases proportionally with increase in concentration at least in the lower range despite the increased competition for OH radicals from various intermediates and other species in the bulk solution shows decomposition occurs not only in the bulk liquid and catalyst liquid interface but also at the bubble-liquid interface. The degradation rate in presence of TiO₂ was lower than that in the case of either ZnO-TiO₂ or ZnO. The similarity in the rate of degradation on ZnO and ZnO/TiO₂ and its variation from TiO₂ shows that surface characteristics and adsorption are also relevant. The result clearly demonstrates that sonocatalytic reactions occur at the

surface and in the bulk as well as at the interface of the cavitation bubble. At the surface of the collapsed bubble, the concentration of the OH radicals is relatively high. At low concentration, when the amount of phenol at the surface or in the bulk is low, a considerable part of the OH radicals recombine yielding H₂O₂. Only about 10% of the OH radicals generated in the bubble can diffuse into the bulk solution [176]. These factors lead to lower degradation of phenol. With increase in concentration, the probability of interaction of OH radicals with phenol increases on the surface as well as in the bulk resulting in increased rate of degradation. The degradation rate slows down and reaches almost a constant level when the concentration of phenol on the catalyst surface as well as at the bubble surface reach a saturation limit during the persistence of the bubble. This is in agreement with earlier findings [181].

The general mechanism of sonocatalytic degradation in aqueous medium involves the formation of OH and other reactive free radicals and their attack on the organic substrate. The radicals are generated as shown in Eqs. 79-84 as well as in the following steps.



The reactive free radicals interact with phenol resulting in the degradation and eventual mineralization of the latter

Phenol + ROS (OH, HO₂, H₂O₂ etc) → Intermediates Mineralization.....(89)

This can also explain the decrease in the recombination of OH radicals resulting in lower concentration of H₂O₂ at higher concentration of phenol [27]. At higher concentration of the substrate, the surface is fully covered as a result of which it cannot effectively absorb the light produced by ultrasound (sonoluminescence), resulting in a decrease in photocatalytic effect and eventual stabilization. Also at higher concentrations, the phenol molecules can act as mutual screens thereby preventing effective interaction of all molecules with the ultrasound [182,183].

4.3.4 Effect of pH

The pH of the reaction medium is known to have a strong influence on US degradation of organic pollutants. In sonocatalytic reaction, pH can alter the distribution of the pollutants in the bulk region, on the surface and at the site of the cavity collapse. The surface charge of semiconductors, the interfacial electron transfer and the photoredox processes occurring in their presence are also affected by pH. Hence the effect of pH on sonocatalytic degradation of phenol is investigated in the pH range 3-11. The pH of the suspension was adjusted initially and was not controlled during the irradiation. The results are presented in Fig. 4.7.

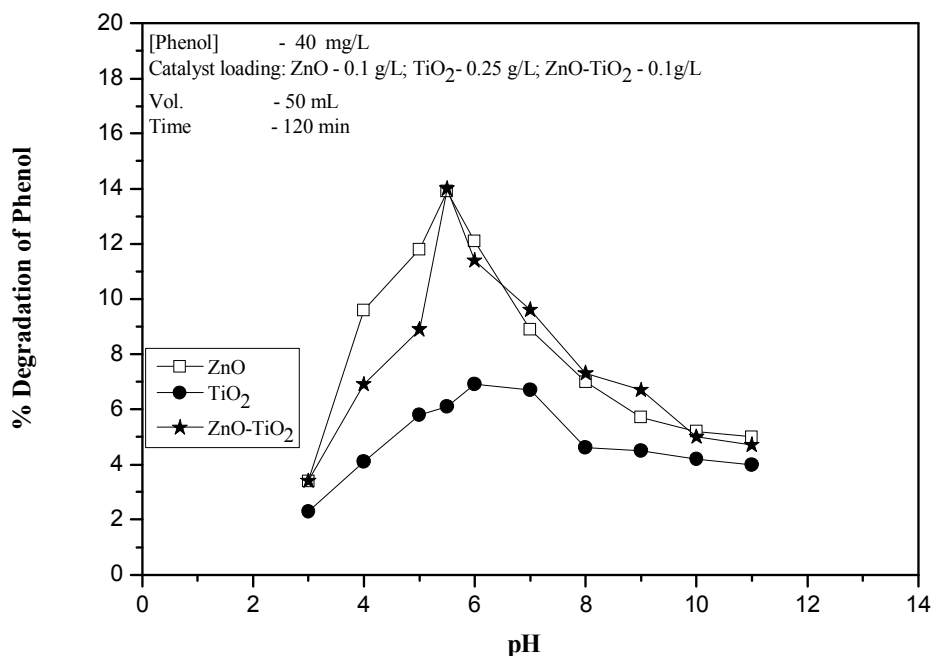


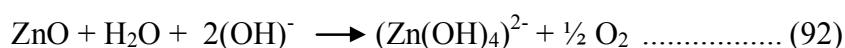
Fig.4.7: Effect of pH on the sonocatalytic degradation of phenol over ZnO, TiO₂ and ZnO-TiO₂.

The degradation is more in the acidic pH region of 4-6 in the case of all the three catalysts tested. In the case of ZnO and ZnO-TiO₂, maximum degradation is observed in the acidic pH range of 4-6, which peaks at pH 5.5. In the case of TiO₂ also similar trend follows with the maximum at pH 6. This observation can be correlated to the electrostatic interaction between the substrate and the catalyst surface, depending on the pH of the suspension. Higher degradation efficiency in the acidic range has been reported by other authors also with different types of phenol using TiO₂ as the catalyst. The steep fall in degradation rate below pH 4 in the case of ZnO and ZnO-TiO₂ can be attributed to the corrosion of ZnO under acidic conditions. The dissolution of ZnO is due to a classical chemical process and the mechanism describing the dissolution of ZnO under acid

conditions is available in literature [149,151,184]. In the acidic range, the photocorrosion takes place through self oxidation. ZnO powder has the tendency to dissolve with decrease in pH:



In alkaline range also the possibility of dissolution of ZnO cannot be ruled out



This reduction in ZnO concentration also leads to a decrease in the degradation at alkaline pH. Similar degradation trend has also been observed by other researchers. The pH of the reaction medium can also influence the surface properties of semiconductor oxide particles, including the surface charge, size of the aggregation and the band edge position. Consequently the adsorption – desorption characteristics of the surface of the catalyst also will be affected. However, in the case of sonocatalysis, adsorption is not the only factor leading to the degradation for reasons explained earlier. Maximum adsorption is observed in the range 5.5–7.0 and it decreases thereafter in the alkaline range as shown in Fig. 3.9(b) in Chapter 3. The results further indicate that the pH dependence of sonocatalytic degradation of phenol cannot be fully attributed to the adsorption characteristics even though the trend shows some similarities. In addition to affecting the surface properties of the catalyst, pH also influences direct sonolysis of phenol and the reactive

$\cdot\text{OH}$ radical formation. Alkaline range is expected to favour the formation of more OH radicals from the large quantity of OH ions present which could enhance the degradation significantly. However, this is not reflected in the actual degradation rate possibly due to the poor adsorption. Further the acid–base property of metal oxides can also influence the catalytic activity at varying pH as explained in Chapter 3. Significant enhancement in the degradation in the acidic range can also be attributed to the effect of US in reducing the distance between the substrate molecule and the surface of the catalyst particles. This is not feasible in the alkaline range where repulsion between like charges of the substrate and the catalyst particles keep them far apart.

4.3.5 Formation and Decomposition of H_2O_2

The mechanism of sonochemical degradation of phenol involves the production of free radicals and their subsequent attack on pollutant species. Formation of H_2O_2 is observed in the case of sonocatalytic degradation of phenol in presence of ZnO, TiO_2 and ZnO- TiO_2 . Small amount of hydrogen peroxide is formed even in the absence of phenol indicating the formation of free radicals $\cdot\text{OH}$ and $\text{HO}_2\cdot$ in liquid water by US. The results are shown in Fig. 4.8 (a & b) which clearly demonstrate that just as in the case of photocatalysis, H_2O_2 undergoes concurrent formation and decomposition in sonocatalysis also, especially in the presence of phenol.

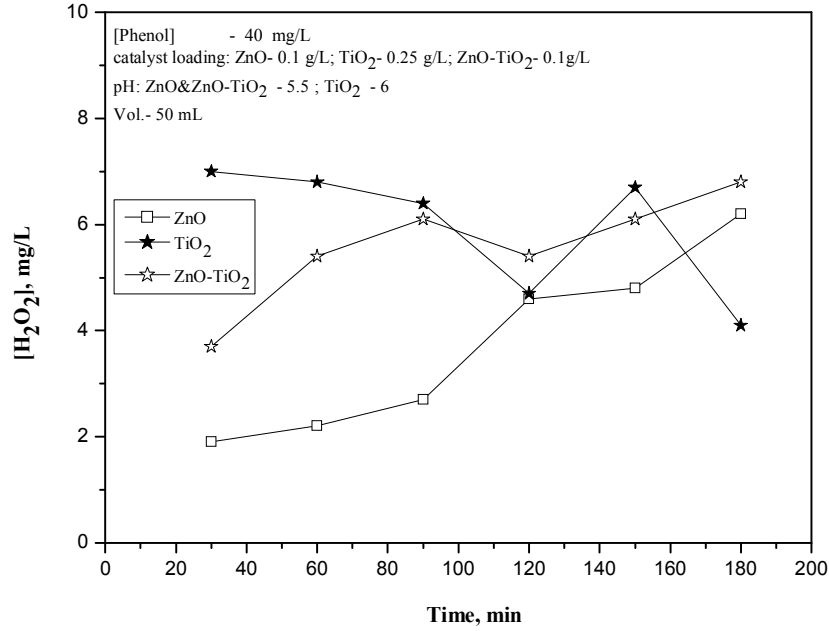


Fig.4.8(a): Oscillation in the concentration of H₂O₂ formed in presence of phenol under sonocatalytic condition on various catalysts.

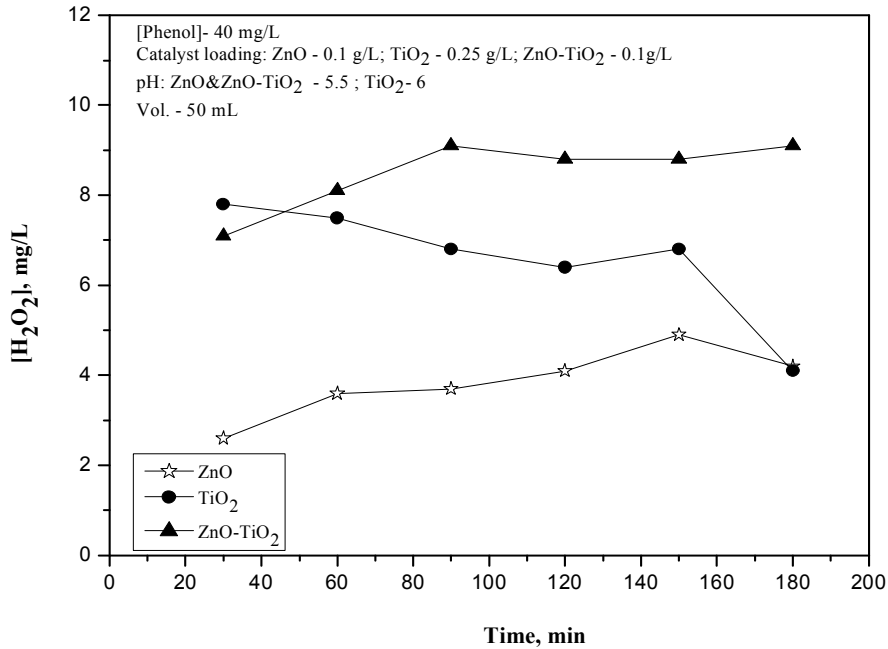


Fig.4.8(b): Oscillation in the concentration of H₂O₂ formed in absence of phenol under sonocatalytic condition on various catalysts.

The generation of H_2O_2 was found to increase with time of US irradiation in case of ZnO and ZnO-TiO₂. It is noteworthy that the H_2O_2 concentration is almost the same irrespective of the presence of phenol. This may be because in presence of phenol, many of the hydroxyl radicals produced by sonication react with phenol before they could combine to form H_2O_2 . In pure water, due to the absence of organic substrates, the hydroxyl radicals combine to form H_2O_2 without any competition. The results also indicate that during the initial stage, H_2O_2 formation is more in presence of TiO₂ than in presence of ZnO or ZnO- TiO₂. It is a well accepted fact that in sonolysis, H_2O_2 is formed from the reaction of OH and HO₂ radicals in the liquid phase around the cavitation bubble. In fact, the formation of H_2O_2 is sometimes used to quantify the efficiency of reactor in generating the desired cavitation intensities. Also in this case, thermal decomposition of H_2O_2 yields only water and oxygen rather than reactive radical species [185]. In the case of TiO₂, in presence of phenol, concentration of H_2O_2 formed in the reaction system remains fairly stable for sometime before it starts decreasing and oscillating. In this case, the degradation of phenol is also found to be less. The periodic increase and decrease in the concentration of H_2O_2 happen in the presence of all three catalysts showing that simultaneous formation and decomposition of H_2O_2 is taking place irrespective of the composition of the semiconductor oxide. At the same time, the degradation of phenol continues without break, though the rate of degradation slows down with time. The decomposition and consequent decrease/stabilization in the concentration of H_2O_2 is more evident even in the initial stages in the case of TiO₂. There is some kind of an optimum concentration for H_2O_2 in each system, at which the rates of decomposition will start dominating. The

minimum concentration of H_2O_2 reached is different for different catalysts irrespective of the period when it occurs indicating that it is dependent on the nature of the catalyst. In any case, since the formation and decomposition of H_2O_2 is very slow and ongoing continuously in sonocatalysis, the net concentration at any point of time is often inconsistent and irreproducible. Oscillatory behavior in the concentration of H_2O_2 during photocatalysis is reported in the earlier Chapter. In the absence of phenol the H_2O_2 formation / decomposition follows different trend in the case of ZnO, TiO_2 and ZnO- TiO_2 . In this case, once certain minimum concentration of H_2O_2 is reached it remains steady, showing comparable rates of formation and decomposition. Experiments with added H_2O_2 show that H_2O_2 enhances the sonocatalytic degradation of phenol significantly in the beginning. The results are summarized in Table 4.1.

Table 4.1: Effect of added H_2O_2 on the sonocatalytic degradation of phenol.

[ZnO] - 0.1g/L [TiO₂] - 0.25g/L & [ZnO-TiO₂] - 0.1g/L; pH: 5.5; Reaction Volume: 50 mL;

Catalyst	% Degradation of phenol without added H_2O_2 at the end of				% Degradation of phenol with added H_2O_2 at the end of				% Enhancement by added H_2O_2 at the end of			
	30 min	60 min	90 min	120 min	30 min	60 min	90 min	120 min	30 min	60 min	90 min	120 min
ZnO	1.1	6.0	9.5	13.7	3.0	7.1	11.2	16.9	172.7	18.3	17.9	23.0
TiO ₂	0.8	3.7	5.2	7.0	1.8	4.7	5.8	9.5	125.0	27.0	11.5	39.9
ZnO- TiO ₂	1.1	6.2	10.1	14.6	2.7	7.4	11.4	17.1	145.5	19.4	12.9	19.5

[Phenol]: 40 mg/L

This enhancement by added H_2O_2 can be explained in two possible ways: i) H_2O_2 molecules that enter the cavitation bubbles during sonication are broken into OH radicals, which enter the solution and

degrade phenol. ii) It is possible that H_2O_2 oxidizes phenol directly, perhaps catalyzed by particles suspended in the solution. However this high rate of enhancement is not sustained later on. This can be explained as follows: In the beginning, added H_2O_2 decomposes faster in presence of US producing maximum OH radicals which can degrade phenol. However, the decomposition of H_2O_2 to water and oxygen also occurs in parallel which restricts the continued availability of the oxidizing species for phenol degradation. Further, even in those experiments without externally added H_2O_2 , the H_2O_2 formed in-situ will be accelerating the reaction rate. Hence the effect of initially added H_2O_2 is not that prominent in the later stages of the reaction [23,143,148]. H_2O_2 accelerates the degradation in all cases following a fairly uniform pattern. The enhancement effect is comparable more in the case of ZnO and ZnO-TiO₂. This shows that in the case of the coupled catalyst, the mechanism of degradation of phenol as well as the formation and decomposition of H_2O_2 is more or less dictated by ZnO since it has higher sonocatalytic activity compared to TiO₂. This is consistent with the observations on the similarity in ZnO and ZnO-TiO₂ reported in previous chapter as well as in the earlier part of this chapter.

4.3.6 Effect of reactant volume

Sonolysis rate has been reported to be dependent on the volume of the reaction system. In order to verify this, experiments were conducted by varying the reactant solution volume from 25-100 mL. The results show that the % degradation increases with decrease in reaction volume [Fig. 4.9(a)].

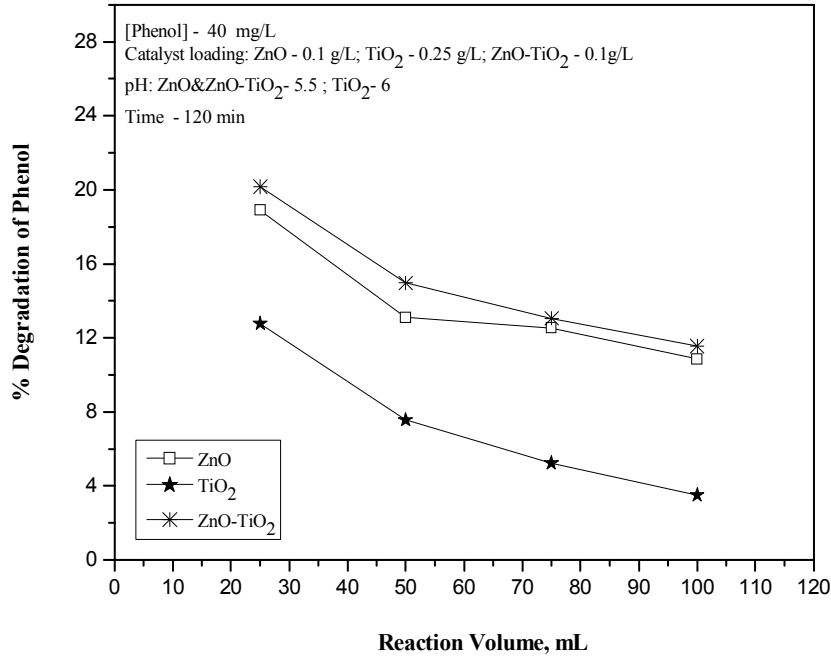


Fig.4.9(a): Effect of reaction volume on the sonocatalytic degradation of phenol over ZnO, TiO₂ and ZnO-TiO₂.

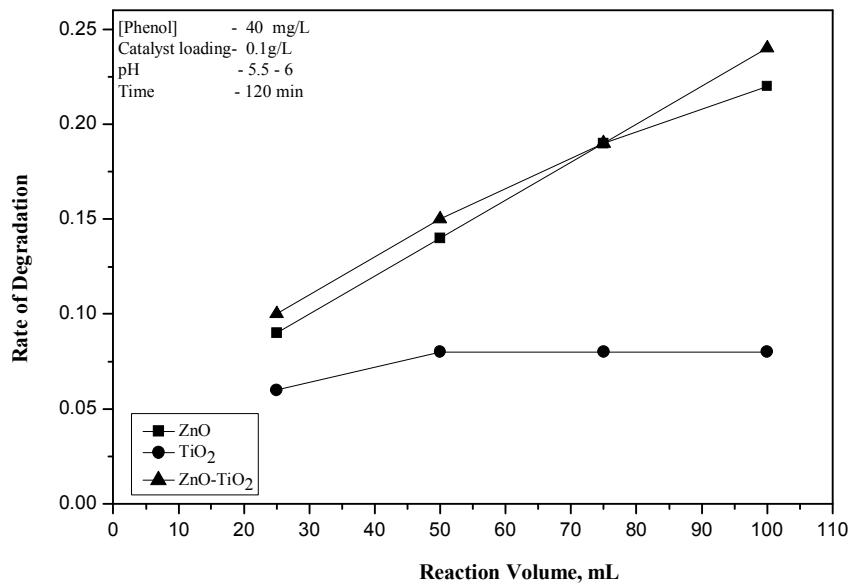


Fig.4.9(b): Effect of reaction volume on the rate of degradation of phenol.

The % degradation decreases fairly steeply with increase in volume up to 50 mL, slows down or stabilizes thereafter. However, the actual degradation rate in terms of the number of molecules of phenol remains the same in the case of TiO₂ at all volumes, while it increases with volume in the case of ZnO and ZnO-TiO₂ [Fig. 4.9(b)].

The rate of increase with volume slows down, in the case of ZnO as in the case of photocatalysis. The increase in degradation rate with increasing volume can be attributed to the increase in the relative number of active cavitation bubbles and consequent generation of more OH radicals. The slow rate of increase at higher reaction volumes may be caused by eventual absorption of ultrasonic energy by the surrounding apparatus, i.e. the reactor wall and cooling water. When volume is increased, beyond a limit, the transmission of waves also becomes slow and the energy available for the formation of reactive species gets scattered. The tendency of increasing rate of degradation with increase in volume remains in the case of ZnO-TiO₂, probably due to the IPET, as discussed earlier

4.3.7 Effect of particle size

In any particulate system, decrease in the average particle size is expected to increase the rate of interfacial charge transfer. Lower particle size increases the specific surface area that in turn increases the number of active surface sites where the charge carriers are able to react with absorbed molecule to form hydroxyl and superoxide radicals. Hence, lower particle size is expected to enhance the degradation. Experiments were conducted with ZnO, TiO₂ and ZnO-TiO₂ of various particle sizes keeping other variables constant and the results are shown in Fig. 4.10.

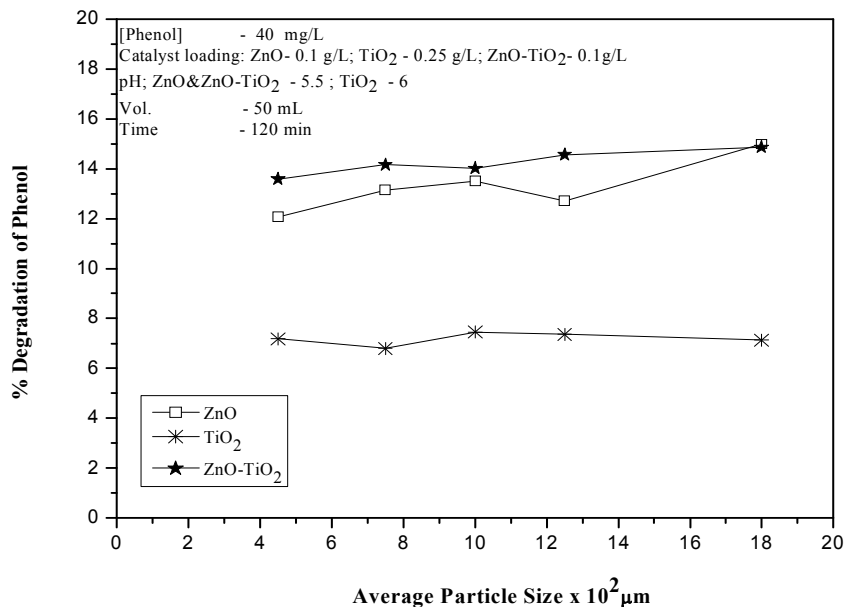


Fig.4.10: Effect of particle on the sonocatalytic degradation of phenol over ZnO, TiO₂ and ZnO-TiO₂.

It is seen that particle size variation within limited range as in the current study does not have any significant effect on sonocatalysis. With increase in particle size in the range of 4.5-18 μm, respective degradation remains more or less unchanged in the case of ZnO, TiO₂ as well as ZnO-TiO₂. Decrease in particle size generally leads to increase in surface area, more surface sites for adsorption of the pollutant and better surface promoted interaction between the reactants, resulting in higher conversion. In the case of US, the radiation itself causes decrease in particle size and enhanced surface area due to deagglomeration. The US also increases the mass transfer between the liquid phase and the catalyst surface, making the surface more readily available for reactants. Further, the US reduces the charge recombination and promotes the production of additional •OH from the residual H₂O₂. As a result of these US effects, the negative impact of

increasing particle size of the catalyst on the rate of degradation of phenol is compensated. Hence the effect of initial particle size of the catalyst on the sonocatalytic degradation is practically insignificant.

4.3.8 Effect of ultrasonic frequency

It is also worthwhile to compare the effect of varying the frequencies of US on the sonocatalytic degradation of phenol. US with frequencies 32 kHz, 42 kHz and 53 kHz were used for the irradiation of a phenol solution of initial concentration of 40 mg/L for 120 min and the results obtained are shown in Table 4.2.

Table 4.2: Effect of Ultrasonic Frequency on the sonocatalytic degradation of phenol.

[ZnO] - 0.1g/L [TiO₂] - 0.25g/L & [ZnO-TiO₂] - 0.1g/L; pH: 5.5; Reaction Volume: 50 mL; [Phenol]: 40 mg/L; Irradiation time: 120 min

Ultrasonic frequency, kHz	Percentage Degradation of Phenol on		
	ZnO	TiO ₂	ZnO-TiO ₂
32	4	2	6
42	14	7	15
53	14	11	15

It is observed that phenol removal efficiency increases with increase in frequency of the US. Highest efficiency is obtained at 53 kHz US frequency. The degradation of phenol is around 14% in case of ZnO, 11% in the case of TiO₂ and 15% in the case of ZnO-TiO₂ in 120 min at this frequency. Higher frequency increases the amount of free radicals that are produced in the reactor. However, the rate of increase is less at higher frequency as seen from the increase in the range 32-42 and 42-53 kHz. This behaviour can be explained on the basis of power dissipation levels at

different frequencies. At higher frequencies, unless suitable modifications are made in the reactor, the full potential of enhanced frequency may not be realized and wastage of energy also is possible. For every system there may be optimum reactant volume/frequency ratio. For a fixed volume, there will be an optimum frequency beyond which the energy is not efficiently utilized. Identification of the optimum reactant volume-frequency combination is important in ensuring the efficiency of the process. The volume and the availability of substrate molecules have to be properly balanced to economically utilize the reactive free radicals and other ROS generated by the enhanced frequency.

4.3.9 Effect of aeration/deaeration

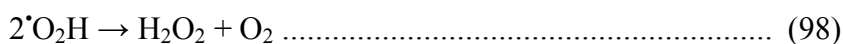
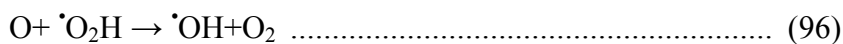
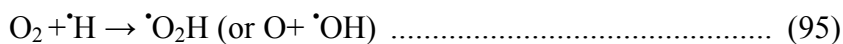
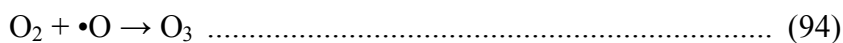
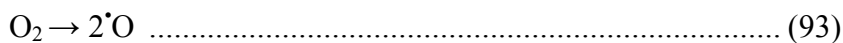
The effect of dissolved O₂/air on the sonocatalytic degradation of phenol was tested by bubbling N₂ through the suspension for one hour before the ultrasound irradiation. The degradation was inhibited by N₂ bubbling thereby confirming the role of dissolved O₂. This is further confirmed by enriching the suspension with more O₂ by bubbling air. In this case the degradation is more. The results are tabulated in Table 4.3.

Table 4.3: Effect of aeration/deaeration on the sonocatalytic degradation of phenol.

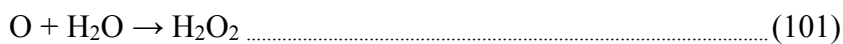
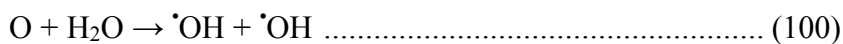
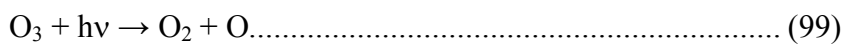
[ZnO] - 0.1g/L; [TiO₂] - 0.25g/L; [ZnO-TiO₂] - 0.1g/L pH: 5.5; Reaction Volume: 50 mL; [Phenol]: 40 mg/L; Purging time- 120 min; Irradiation time: 120 min

Purging gas	Percentage Degradation of Phenol on		
	ZnO	TiO ₂	ZnO-TiO ₂
None	14	7	15
N ₂	9	4	10
Air	19	12	21

As explained in Chapter III, O₂ retards the electron-hole recombination rate during sonocatalysis and the sonoluminescence initiated photocatalysis and facilitates the formation of Reactive Oxygen Species. Presence of air/O₂ also enhances the formation of H₂O₂ which in turn accelerates the degradation of phenol. Various reactions involving the role of O₂ in sonocatalysis can be summarized as follows:



Various active species produced as above react with phenol in the bulk solution or at the interface between the bubbles and the liquid phase. The ozone produced as above can also promote the degradation of phenol in combination with UV via the direct and indirect production of hydroxyl radicals.



4.4 General Mechanism of sonocatalysis

Sonocatalytic degradation of organic compounds is generally explained based on sonoluminescence and hot spot theory as described earlier. Acoustic cavitation produces highly reactive primary radicals such as $\cdot\text{OH}$ and $\cdot\text{H}$ as shown in Eq.79. Recombination of the radicals and a number of other reactions occur within the bubble as shown in Eqs.80 to 84 following this primary radical generation. Hydroxyl radical is a nonselective oxidant with a high redox potential (2.8 eV) which is able to oxidize most organic pollutants.

Ultrasonic irradiation results in the formation of light of comparatively wide wavelength range of 200-500 nm, resulting in sonoluminescence. Wavelengths below 375 nm can excite the semiconductor catalyst and generate highly active OH radicals on the surface and photocatalysis follows. At the same time, the more complex phenomenon of formation of hotspots upon implosion of some bubbles on the catalyst surface also leads to the formation of electron-hole pairs and OH radicals. The mechanism of $\cdot\text{OH}$ radical formation during sonolysis is shown in Fig. 1.10 under Chapter 1.

Since the formation of electron-hole pairs is the first step in both photocatalysis and sonocatalysis, the efficiency of the process depends on the ability to prevent their recombination. Enhanced efficiency of ZnO-TiO₂, though moderate, is due to the ability of the combination to inhibit electron-hole recombination by electron transport within the composite. Because the TiO₂ and ZnO possesses same band gap (3.2 eV), the electrons can be transferred easily from TiO₂ to ZnO through the

crystal interface between the two which results in separation of electrons and holes. Such electron transport through the crystal interface of composite oxides has been reported earlier also [170]. The possible mechanism of sonocatalytic degradation in presence of ZnO-TiO₂ is shown in Fig. 4.11.

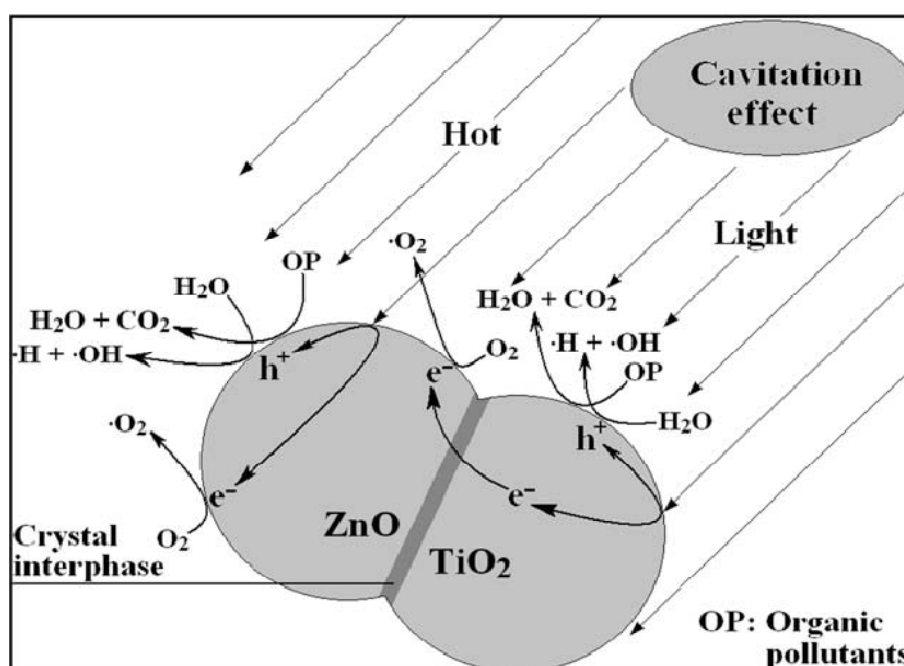
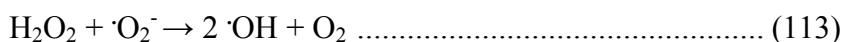
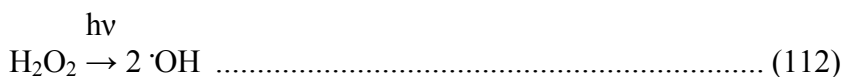
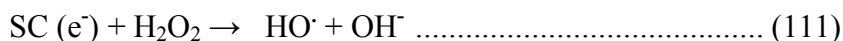


Fig.4.11: Mechanism of degradation of organic pollutant on composite ZnO- TiO₂ particle under ultrasonic irradiation.

Because of the difference in adsorption capacity, the TiO₂ part is inclined to the hole oxidation and ZnO tends towards radical oxidation. However, since sonocatalysis itself is relatively less efficient compared to photocatalysis this expected enhancement is not significant in the presence of ZnO-TiO₂



The OH^\cdot radicals thus formed from H_2O_2 also can contribute to the degradation of phenol.

4.5 Effect of anions

Sonication/ sonocatalysis has been proven to be a potential environment-friendly process for the degradation of trace amounts of organic pollutants such as phenol in the present case. But the rates of phenol degradation under sonication have been observed to be low. In order to increase the rate, various modifications of the catalyst-reaction system have been tested. Addition of anions has been reported to influence AOPs positively and negatively. Anions are often present in natural water systems and hence the study of the effect of added anions on the sonocatalytic degradation of pollutants is important, especially in the context of commercial application of the technique. In this context, the effect of some of the common anions likely to be present in water such as Cl^- , I^- , SO_4^{2-} , CO_3^{2-} , NO_3^- , Br^- and PO_4^{3-} on the sonocatalytic degradation of phenol is investigated using the corresponding sodium salts. Experiments were conducted with aqueous suspensions containing 5×10^{-3} mg/L of the selected inorganic salt and the phenol degradation is observed under optimized conditions as explained earlier. The results are plotted in Fig.4.12 (a, b & c).

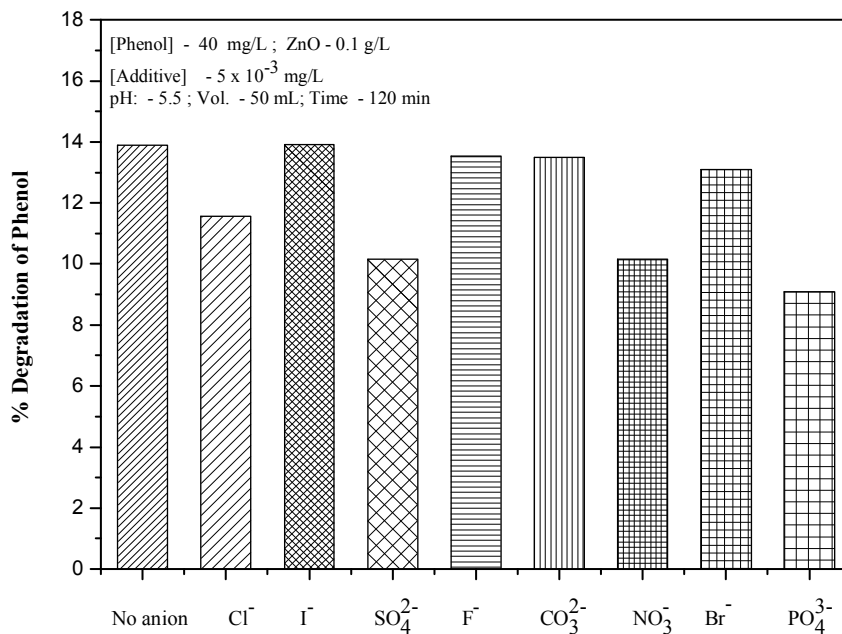


Fig.4.12(a): Effect of anions on the sonocatalytic degradation of phenol over ZnO

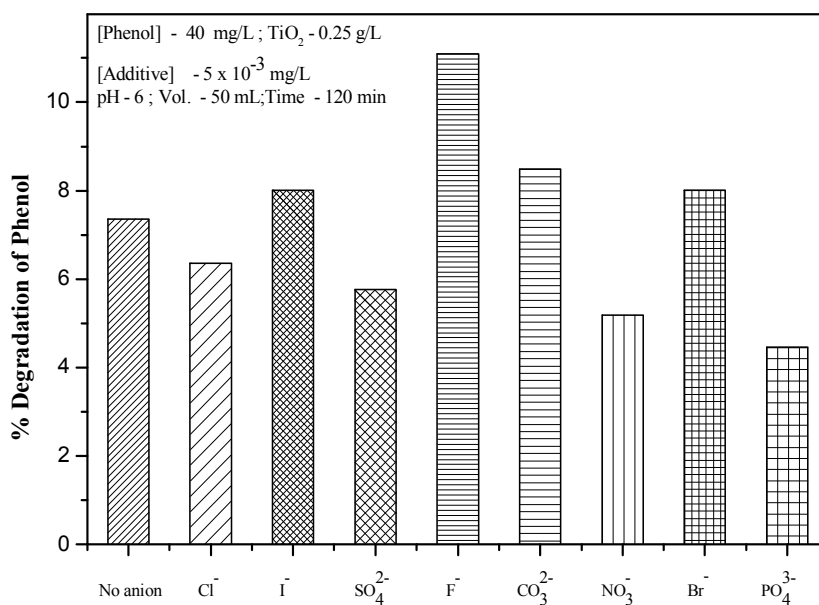


Fig.4.12(b): Effect of anions on the sonocatalytic degradation of phenol over TiO_2 .

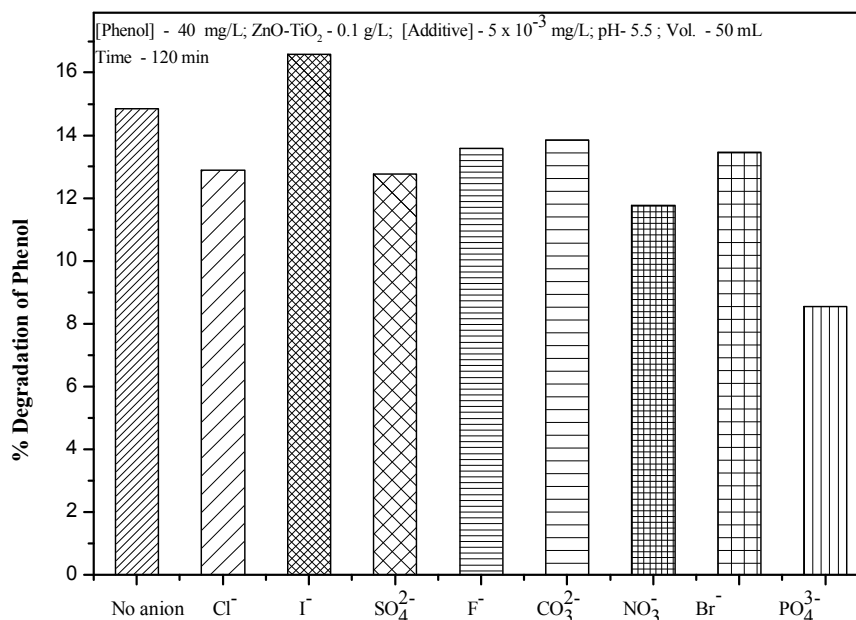


Fig.4.12(c): Effect of anions on the sonocatalytic degradation of phenol over ZnO-TiO₂.

There is a pattern in the effect of the anion on the degradation of phenol in presence of the catalysts though it is not very consistent in presence of ZnO. For eg. Cl⁻, SO₄²⁻, NO₃⁻ and PO₄³⁻ inhibit the degradation moderately, while I⁻, CO₃²⁻, F⁻ and Br⁻ have no effect. In presence of TiO₂, F⁻ has good enhancing effect while there is slight to moderate enhancement by I⁻, CO₃²⁻ and Br⁻. In this case also, Cl⁻, SO₄²⁻, NO₃⁻ and PO₄³⁻ inhibit the degradation as in the case of ZnO. The behaviour of anions in presence of ZnO-TiO₂ appears to be average of the behavior in presence of ZnO and TiO₂. The most distinct and consistent observation is the clear inhibition in presence of PO₄³⁻ anion. The effect may be summarized as in Table 4.4. Irrespective of the degree of

enhancement/inhibition; the trend appears similar in all cases suggesting similar mechanism for the effect of anion.

Table 4.4: Effect of anions on the sonocatalytic degradation of phenol.

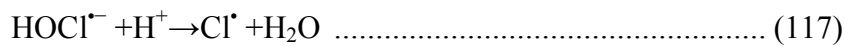
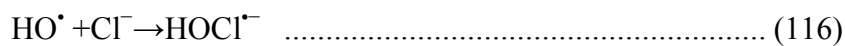
Catalyst	Effect of anions	
	Inhibition	Enhancement/ No effect
ZnO	$\text{PO}_4^{3-} > \text{NO}_3^- > \text{SO}_4^{2-} > \text{Cl}^-$	I^- , CO_3^{2-} , F^- and Br^- have no effect
TiO_2	$\text{PO}_4^{3-} > \text{NO}_3^- > \text{SO}_4^{2-} > \text{Cl}^-$	F^- , I^- , CO_3^{2-} and Br^- cause enhancement
ZnO- TiO_2	$\text{PO}_4^{3-} > \text{NO}_3^- > \text{SO}_4^{2-} > \text{Cl}^-$	I^- causes enhancement Br^- , F^- , CO_3^{2-} no effect

Addition of ions to the solution decreases the solubility and consequently, increases the hydrophobicity of the substrate due to the “salting out effect” where fewer water molecules form hydration spheres around the salt ions. This phenomenon pushes the substrate phenol toward the bubble–bulk solution interface and, therefore is expected to lead to a higher degradation rate. The addition of salt also increases the ionic strength of the aqueous phase. This is expected to drive the organic substrate towards the bubble-bulk interface where majority of the sonodegradation takes place [155-159,167-169,186-191]. The increase in surface tension caused by the anion can affect the nucleation process and the cavitation threshold. Presence of salt will also increase the partitioning of the organic species upon cavitation implosion. Thus the interfacial concentrations of the pollutants are likely to increase which could enhance the overall degradation rate. However, this enhancing effect is evident only in the case of some of the anions tested here and cannot be generalized. Hence other factors also have to be taken into consideration under the experimental conditions. Almost all the anions

tested here are known to be strongly adsorbed on the surface of the catalyst, thereby depriving the substrate molecules from interacting with the surface. This can lead to inhibition. The current study shows that Cl^- , SO_4^{2-} , PO_4^{3-} and NO_3^- inhibit the sonocatalytic degradation by varying degrees. The experiments were carried out in the acidic pH range of 5.5-6. In this range ZnO , TiO_2 and ZnO-TiO_2 will be positively charged. Consequently, all these anions can get strongly adsorbed on the surface through ionic forces. The reaction of the surface holes with these undesirable ions leads to a decrease in the formation of reactive $\cdot\text{OH}$ radical resulting in reduced activity. NO_3^- adsorption is relatively weaker and hence the inhibition is less compared to PO_4^{3-} .

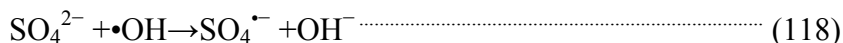
The inhibition caused by two typical anions Cl^- and SO_4^{2-} can be explained as follows:

The chloride ions scavenge the photoproduced holes and the hydroxyl radical more effectively leading to decrease in the $\cdot\text{OH}$ initiated degradation



The deactivation and decrease in the concentration of hydroxyl radicals caused by SO_4^{2-} can be explained as follows:

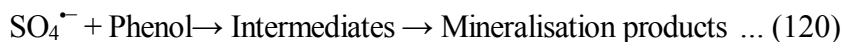
Scavenging of $\cdot\text{OH}$ radicals:



Interaction of sulphate radicals with water:



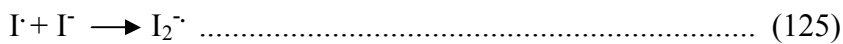
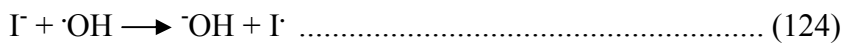
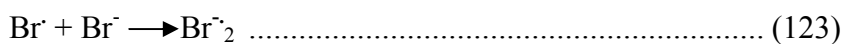
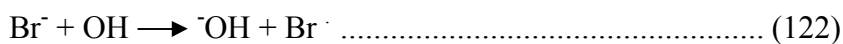
$\text{SO}_4^{\cdot-}$ is also a strong oxidant which can contribute to the degradation of phenol as follows:



Of the two competing reactions (119) and (120), the former will be more facile resulting in regeneration of $(\text{SO}_4)^{2-}$ which will again get adsorbed on to the surface thereby denying access to the phenol molecule. This, together with reaction (118) which reduces the availability of active OH radicals will result in decreased degradation in the presence of sulphate ions. The highest inhibition due to PO_4^{3-} can be explained based on the preferential adsorption on the surface and prevention of the activation of the catalyst. The surface coverage will be more than that of other anions due to steric factors also. Further each PO_4^{3-} anion brings 3 cations of Na which also can block the surface sites and accelerate the inhibition.

The enhancement of sonocatalytic degradation of phenol by I^- , CO_3^{2-} and Br^- in presence of TiO_2 , lack of any influence by these anions in presence of ZnO and the average (of ZnO and TiO_2) effect in presence of ZnO-TiO_2 even though these anions are known to be

scavengers of the reactive $\cdot\text{OH}$ radicals shows that a general single mechanism cannot explain the effect of anions fully. Normally in sonocatalysis, the surface of the cavitation bubbles as well as the solution bulk is rich in $\cdot\text{OH}$ radicals. In the absence of $\cdot\text{OH}$ scavengers like anions, the degradation is mainly driven by the $\cdot\text{OH}$ radicals present at the bubble surface and in the bulk. The surface of the cavitation bubble will be much richer in $\cdot\text{OH}$ compared to the bulk. Thus the air-water interface of the cavitation bubbles is a very reactive environment. This together with the factor explained earlier can be contributing towards enhancement of degradation. But not all $\cdot\text{OH}$ will be available for substrate degradation and at least a part of $\cdot\text{OH}$ will be reacting to form H_2O_2 and H_2O . Further, the anion gets preferentially adsorbed on the catalytically active site reducing the formation of surface promoted ROS and other free radicals. Another possibility is the interaction of the anion with $\cdot\text{OH}$ radicals and the formation of radical species such as $\text{CO}_3^{\cdot-}$, $\text{Br}^{\cdot-}$, $\text{I}^{\cdot-}$ etc.



These radical species formed from the anion are less reactive compared to $\cdot\text{OH}$. However, their recombination is not as facile as $\cdot\text{OH}$ on the surface of the cavitation bubbles. Hence, they are more available for

the degradation of the substrate compared to $\cdot\text{OH}$. Thus the anion transforms at least some of the reactive $\cdot\text{OH}$ into less reactive species. But these less reactive species can be more involved with the degradation of the substrate apart from $\cdot\text{OH}$. Interaction of the inorganic anions with the substrate is only a secondary process which has only limited impact on its interaction with $\cdot\text{OH}$. Hence the relative concentration of $\cdot\text{OH}$, the anion derived free radical species, the surface concentration of the anion, recombination of $\cdot\text{OH}$ radical etc, affect the number of effective interactions with the substrate. Thus, a multitude of factors responsible for enhancement and inhibition of the degradation of phenol coexist in the system and the domination of specific factors determine the rate of degradation/mineralization. It may hence be concluded that the effect of anion on the sonocatalytic degradation needs in depth analysis individually and no general prediction is possible due to the complexity of the system.

4.6 Conclusions

The sonocatalytic activity of ZnO, TiO₂ and ZnO- TiO₂ for the degradation of phenol pollutant in water is investigated. The efficiency of the catalysts for the degradation is in the order ZnO-TiO₂ > ZnO > TiO₂. Reaction parameters such as the catalyst loading, irradiation time, initial pH, concentration of the substrate, presence of O₂, anions etc. affect the rate of degradation. The degradation follows variable kinetics, depending on the concentration of the substrate. H₂O₂ formed during the degradation of phenol undergoes simultaneous decomposition as well. After initial accumulation upto a certain concentration, decomposition of H₂O₂

dominates resulting in decrease in its concentration. Once a minimum is reached formation process dominates again. This cycle leads to oscillation in the concentration of H_2O_2 . The effect of anion on the rate of sonocatalytic degradation is very complex. Anions can act as inhibitors or promoters of the degradation depending on the nature of their interaction with the surface and the reactions that follow. The size of catalyst particles has little impact on sonocatalytic degradation. The study illustrates that semiconductor mediated sonocatalysis is a potential environment-friendly tool for the removal of phenol pollutant from water.

.....❧.....

SEMICONDUCTOR OXIDES MEDIATED SONOPHOTOCATALYTIC DEGRADATION OF PHENOL IN WATER

- 5.1 *Introduction*
- 5.2 *Experimental Details*
- 5.3 *Results and Discussion*
- 5.4 *Mechanism of the Sonophotocatalytic degradation*
- 5.5 *Effect of added anions*
- 5.6 *Conclusions*

5.1 Introduction

As highlighted in Chapters 3 and 4, semiconductor mediated photocatalysis and sonocatalysis respectively have been investigated extensively as viable techniques for the removal of organic and inorganic pollutants from aqueous streams. The techniques have been proven moderately effective for the oxidative destruction of recalcitrant organic compounds such as dyes [61], pesticides [192], phenols [62,193,194] and the reduction of several heavy metals [195]. However, sonocatalysis has still not gained acceptance as an adequately efficient and effective stand-alone technology for the commercial level decontamination of wastewater. Photocatalysis is used at commercial level for limited application though its potential as an efficient waste management technology is still not fully explored. Attempts to enhance the efficiency

of photocatalytic treatment of wastewater by adding H_2O_2 , $\text{H}_2\text{O}_2/\text{Fe}^{2+}$, Fe^{3+} , cations, anions, dyes, etc. to the reaction system and modification of catalyst characteristics by doping, supporting and coating have also been reported [196-200].

Recently, combination of sonocatalysis and photocatalysis (sonophotocatalysis) has been receiving attention as a promising technique for the treatment of hazardous organic pollutants in wastewater [171, 177, 201]. It has been reported that combining US with Ultraviolet (UV) irradiation enhances the efficiency of semiconductor mediated degradation of aqueous pollutants synergistically [56, 59, 112, 140, 202-207, 208]. Similarity in the mechanism of photocatalytic and sonocatalytic reactions, enhances the advantage of combining these techniques. However, very few reports are available on this combination, which have been summarized in a recent review [208]. The degradation of phenol under photo and sonocatalytic conditions in presence of ZnO , TiO_2 and ZnO-TiO_2 is investigated and reported in previous chapters. Hence, a detailed study is undertaken on the degradation of trace amounts of phenol contaminant in water under simultaneous presence of US and UV irradiation in presence of ZnO , TiO_2 and ZnO-TiO_2 . The photo and sonocatalytic degradation data from chapters 3 and 4 respectively are compared with the results in this chapter, wherever relevant.

5.2 Experimental Details

5.2.1 Materials

Materials used for the studies in this chapter are as described in Chapters 3 and 4

5.2.2 Equipment Used

The Mercury Vapor lamp for UV light and the Ultrasonic bath for US are the same as described in Chapters 3 and 4, section 3.2.4 and 4.2.2. respectively. Rest of the equipments used for this experiments are also described in Chapters 3 and 4

5.2.3 Experiments and Analytical Methods

The experiments were performed using aqueous solutions of phenol of desired concentration. Specified quantity of the catalyst was suspended in the solution. The reaction set up was a combination of those used in Chapters 3 and 4. The reactors were same as those used in photocatalysis. They were placed in an ultrasonic bath in which water from a thermostat at the required temperature was circulated. Unless otherwise mentioned, the reaction temperature was maintained at 29 ± 1 °C. The position of the reactor in the ultrasonic bath was always kept the same. A high intensity UV lamp (400 W medium pressure mercury vapor quartz lamp) mounted above was used as the UV irradiation source. The ultrasonic bath was operated at a frequency of 40 kHz and a power of 100 W unless indicated otherwise. Rest of the experimental procedure, sampling and analysis methods etc were the same as described in Chapters 3 and 4. Typical reactor set up is shown in Fig. 5.1.

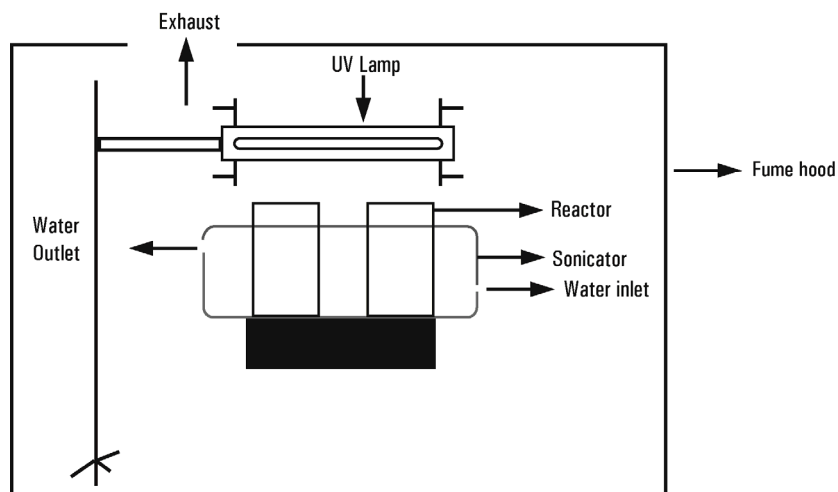


Fig.5.1: A schematic diagram of the sonophotocatalytic experimental set up.

5.3 Results and Discussion

Preliminary investigations on the sonophotocatalytic degradation of phenol were made using ZnO, TiO₂ and ZnO-TiO₂ catalysts under identical conditions. The results are presented in Fig. 5.2.

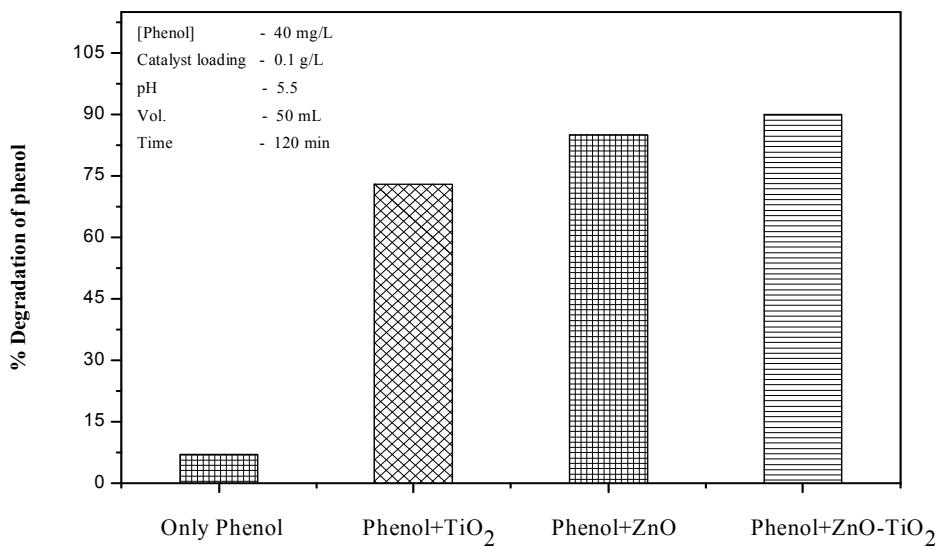


Fig.5.2: Comparison Sonophotocatalytic activities of ZnO, TiO₂ and ZnO-TiO₂.

The results show that ZnO-TiO₂ combination [1:1] with 89.0% degradation of phenol is the most efficient closely followed by ZnO with 85% degradation. The percentage degradation in presence of TiO₂ is ~ 63.1% and is hence the least active of the three.

It was already demonstrated in Chapters 3 and 4 that catalyst and light or catalyst and sound are essential to effect significant degradation. The results in Fig.5.3 show that the presence of the semiconductor catalyst in combination with light and sound (sonophotocatalysis) enhances the degradation of phenol significantly. The degradation under (UV + US) irradiation is more than the sum of degradation under individual UV and US irradiation, thereby showing a synergistic effect. The synergy can be explained at least partially based on the effects of microstreaming and increased mass transport associated with the interaction of US with solid matter. Microstreaming provides in situ regeneration of the catalyst surface as the cavitation near the solid surface causes a jet of fluid directed onto the particle [82]. Thus the blockage of active adsorption sites on the catalyst can be partially cleared. US also increases the mass transfer on the solid-liquid interface [82,181,198] leading to the generation of more ROS, enhanced adsorption and faster degradation.

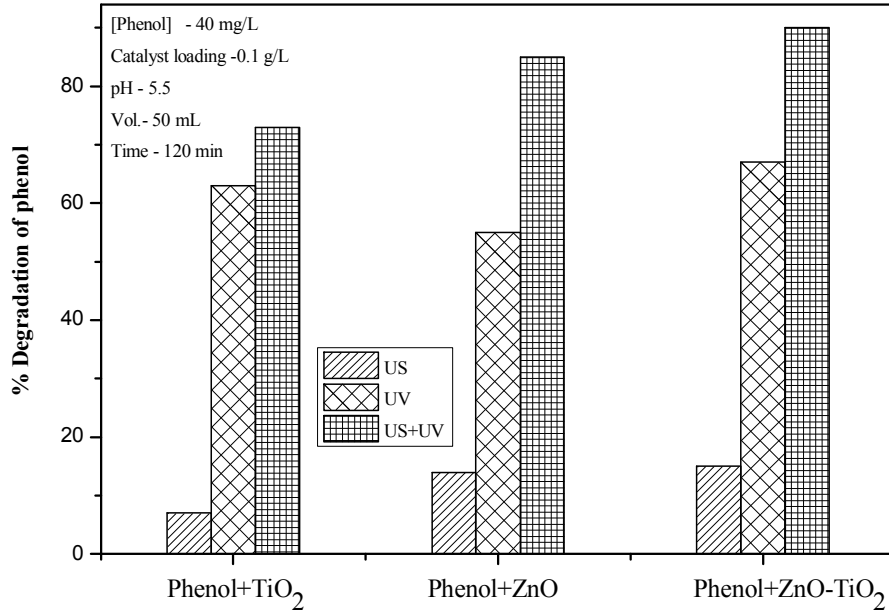


Fig.5.3: Comparative degradation of phenol under sono, photo and sonophotocatalysis under ZnO, TiO₂ and ZnO-TiO₂

The synergy index under sonophotocatalysis irradiation is calculated from the rates of degradation under different conditions using the following equation :

$$\text{Synergy Index (US+UV)} = \frac{R_{US+UV}}{R_{US}+R_{UV}} \dots\dots\dots (126)$$

where R_{US}, R_{UV} and R_{US+UV} are sono, photo and sonophoto catalytic degradation rates respectively. The synergy index thus calculated is 1.12 for ZnO- TiO₂, 1.25 for ZnO and 1.12 for TiO₂.

The results further showed that just as in the case of sonocatalysis, ZnO is more efficient for the sonophotocatalytic degradation of phenol compared to TiO₂ under identical conditions. This implies that the effect

of the combination of US and UV on respective catalyst, is not much different from that of individual US or UV [56, 59].

The effect of ZnO-TiO₂ ratio in the combination catalyst on the degradation is verified and the results are presented in Fig. 5.4. Maximum degradation of $\approx 90\%$ is seen in presence of ZnO-TiO₂ in the ratio 4:6. Pure TiO₂ powder (ZnO/TiO₂ = 0:1) gives the lowest degradation of 73 % of phenol under UV+US irradiation. The degradation increases slowly with increase in ZnO, reaches an optimum, then decreases slightly and stabilizes. The optimum ZnO/TiO₂ ratio is same as in the case of US or UV irradiation, once again confirming that there is not much mechanistic difference in the effect of UV+US combination other than synergy in the combined effect.

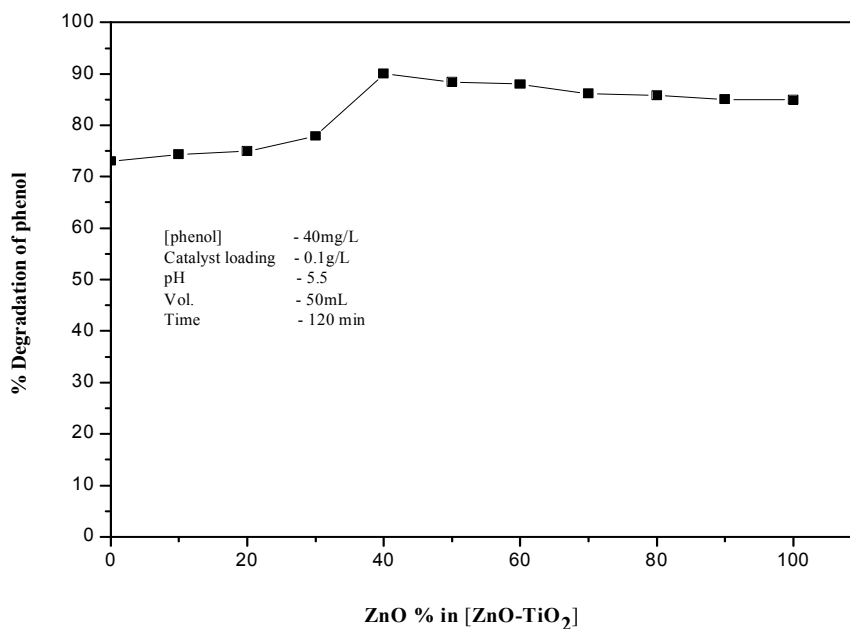


Fig.5.4: Effect of percentage of ZnO in ZnO-TiO₂ composite on the sonophotocatalytic activity.

Summary of the effect of ZnO content in ZnO-TiO₂ on US, UV and US+UV degradation of phenol is shown in Table 5.1

Table 5.1: Effect of percentage of ZnO in ZnO-TiO₂ on US, UV and US+UV.
[Phenol]: 40 mg/L; pH: 5.5; Reaction Volume: 50 mL; Irradiation time: 120 min

% ZnO in ZnO-TiO ₂	US	UV	US+UV
0	6.8	64.7	73.0
10	10.1	63.7	74.3
20	11.0	63.4	74.9
30	12.0	65.7	77.8
40	14.0	68.1	90.0
50	13.5	65.4	88.3
60	13.1	64.1	87.9
70	13.8	63.4	86.1
80	13.6	62.7	85.7
90	13.4	60.1	85.0
100	14.0	57.4	85.0

5.3.1 Effect of Catalyst loading

It is necessary to determine the optimum catalyst dosage in order to avoid the use of excess catalyst, and to design appropriate reactor system. The sonophotocatalytic degradation of phenol is studied at different loadings of ZnO, TiO₂ and ZnO-TiO₂ (4:6) keeping all the other parameters identical. The results plotted in Fig. 5.5 show that in all three cases when the catalyst loading is increased from 0.02 to 0.50 g/L, the phenol degradation increases initially. This is followed by a slow and steady decrease at higher loadings. The optimum loading is 0.1 g/L in the case of ZnO and ZnO-TiO₂ and 0.25 g/L in the case of TiO₂. The maximum degradation attained in sonophotocatalysis is significantly higher than that in the case of photocatalysis and sonocatalysis for all catalyst loadings, thereby

suggesting that the catalyst as well as the source of irradiation is important for the efficiency of degradation. This is also evident from the nearly identical synergy index value for all the catalysts even though the actual degradation efficiency is more in the case of ZnO-TiO₂. The decrease in degradation with increase in catalyst loading beyond a particular maximum is more pronounced in sonocatalysis and sonophotocatalysis when compared to photocatalysis. However, the optimum loading and the trend remain fairly the same suggesting that US induced increase in rate of photocatalysis is resulting at least partly from the increase in light absorbed by the reaction system. This leads to a higher concentration of active species. At higher catalyst loading when filtering and/or scattering of light becomes important, the amount of photo produced active species does not increase anymore and the synergy between photocatalysis and sonocatalysis also remains almost constant or even decreases. This is understood from the observation that efficiency of photocatalysis which is determined by the processes occurring at the semiconductor-water interface also starts decreasing at around the same catalyst dosage as in the case of sonophotocatalysis. In the case of TiO₂, the optimum catalyst loading is higher compared to ZnO and ZnO-TiO₂. At higher catalyst loadings; the aggregation of particles is one factor responsible for the decrease in rate. Sonication helps to deaggregate the particles which will be more efficient in the case of TiO₂. This will result in the availability of more active light absorbing and adsorbing sites for longer periods.

The optimum catalyst loading will also depend on the size, shape and geometry of the reaction assembly. Hence, for each reactor configuration, the optimization has to be done separately.

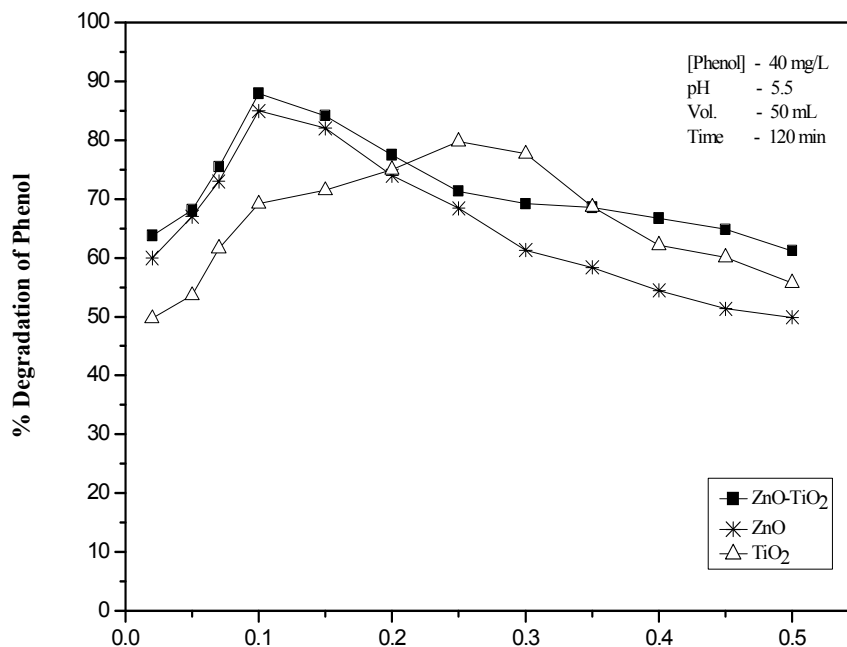


Fig.5.5: Effect of catalyst loading on the sonophotocatalytic degradation of phenol over ZnO, TiO₂ and ZnO-TiO₂

Comparison of the optimum catalyst loading under sono, photo and sonophotocatalysis in the case of ZnO, TiO₂ and ZnO-TiO₂ is tabulated in Table 5.2. In the case of ZnO the optimum is 0.10 g/L for sono, photo as well as sonophotocatalysis. However, in the case of TiO₂ the optimum dosage for sono and sonophotocatalysis is 0.25g/L while for photocatalysis, it is 0.1g/L. In the case of ZnO-TiO₂ the optimum loading is same as in the case of ZnO i.e., 0.1g/L for sono, photo and sonophotocatalysis. This clearly show that ZnO plays a major role in the sono or photocatalytic behaviour of ZnO-TiO₂. The higher optimum dosage in the case of TiO₂ as well as its higher photoactivity indicates that it is capable of absorbing more of UV light compared to ZnO.

Table 5.2: Effect of catalyst loading on the US, UV and US+UV induced degradation of phenol in presence of ZnO, TiO₂ and ZnO-TiO₂.
 [Phenol]: 40 mg/L; pH: 5.5; Reaction Volume: 50 mL; Irradiation time: 120 min

Catalyst loading (g/L)	Percentage Degradation of phenol on								
	ZnO			TiO ₂			ZnO- TiO ₂		
	US	UV	US+UV	US	UV	US+UV	US	UV	US+UV
0.02	7.3	45.8	60.0	2.0	43.3	49.7	7.5	41.7	63.7
0.05	7.1	46.5	67.0	2.6	49.7	53.6	7.3	47.1	68.1
0.07	10.2	54.8	73.0	3.0	59.4	61.6	11.4	60.4	75.4
0.1	13.7	55.0	85.0	3.4	63.0	69.1	15.0	67.0	89.0
0.15	11.3	50.9	82.0	3.6	59.5	71.5	12.8	57.3	84.1
0.2	10.2	46.6	74.0	5.0	57.0	72.5	11.1	54.4	77.4
0.25	7.7	44.7	68.4	7.1	57.8	75.0	10.2	51.0	71.3
0.3	7.0	43.4	61.3	7.0	58.0	74.1	10.0	50.8	69.1
0.35	6.1	43.0	58.3	7.1	56.5	68.6	9.9	50.4	68.5
0.4	6.2	43.0	54.4	7.6	56.0	62.1	9.5	49.7	66.7
0.45	6.2	42.7	51.3	7.5	55.9	60.1	9.7	49.0	64.8
0.5	6.2	43.1	49.9	6.9	55.6	55.7	9.5	47.9	61.1

5.3.2 Effect of concentration

The effect of initial concentration of phenol in the range of 10-60 mg/L on the sonophotocatalytic degradation was investigated in presence of ZnO, TiO₂ and ZnO –TiO₂. The results are plotted in Fig. 5.6(a). As in the case of sonocatalysis and photocatalysis, sonophotocatalysis also appears to follow pseudo-first order kinetics. At higher concentrations, the rate slows down as the concentration increases. The first order kinetics of the reaction is confirmed by the logarithmic plot given in Fig. 5.6(b-d). In the case of all three catalysts, the reaction follows similar kinetics, indicating that the mechanism of degradation may be the same. The linear plot of $-\ln C/C_0$ versus time shows that the reaction obeys first order kinetics at

lower concentrations of 10-30 mg/L in the case of ZnO, TiO₂ and ZnO - TiO₂. Above this concentration, the order decrease, the decrease being steeper above 40 mg/L which is in line with the observations in most sono and photocatalytic processes [130,198-201].

Davydov *et al.*, [113] reported zero order kinetics in the sonophotocatalytic degradation of salicylic acid on TiO₂. However, the authors worked in the low conversion regime only. In the present case also, the shift from zero to first order takes place only at higher conversion ranges. The first order kinetics at lower concentrations and higher conversion ranges is understandable from both photocatalytic and sonocatalytic angles. In photocatalysis, with increase in concentration, more reactant molecules get adsorbed onto the catalyst site, get activated and interact with correspondingly more OH radicals. This will continue until all the surface sites are occupied. Thereafter, increase in concentration cannot result in increased surface occupation and the phenol removal becomes independent of concentration. The sonocatalytic degradation takes place in the bulk of the solution where the concentration of OH radicals is relatively smaller [29]. Hence, increase in concentration of phenol can more effectively utilize the otherwise limited OH radicals leading to increased degradation. This will continue until the phenol concentration remains sufficiently high to interact with optimum number of OH radicals.

It is also possible that some of the reaction products and intermediates may remain attached to the surface for relatively longer period towards the later stages of reaction or at higher concentration of the substrate resulting in non-availability of the surface sites for fresh

reactant molecules. Higher substrate concentration can also absorb more photons thereby decreasing the photons available for catalyst activation. In pure photocatalytic systems, complete domination of the surface by the reactant/intermediates/products can result in suppression of the generation of surface initiated OH radicals. However, in presence of US, the saturation of catalyst surface takes place at a relatively later stage due to deaggregation. Further, the reaction can also take place at the cavitation bubble interface where the OH concentration can reach a higher limit. However, the contribution from deaggregation of catalyst particles and the higher $\cdot\text{OH}$ concentration at the cavitation bubble interface do not influence the kinetics of the degradation of phenol which remains similar under sono, photo and sonophotocatalysis.

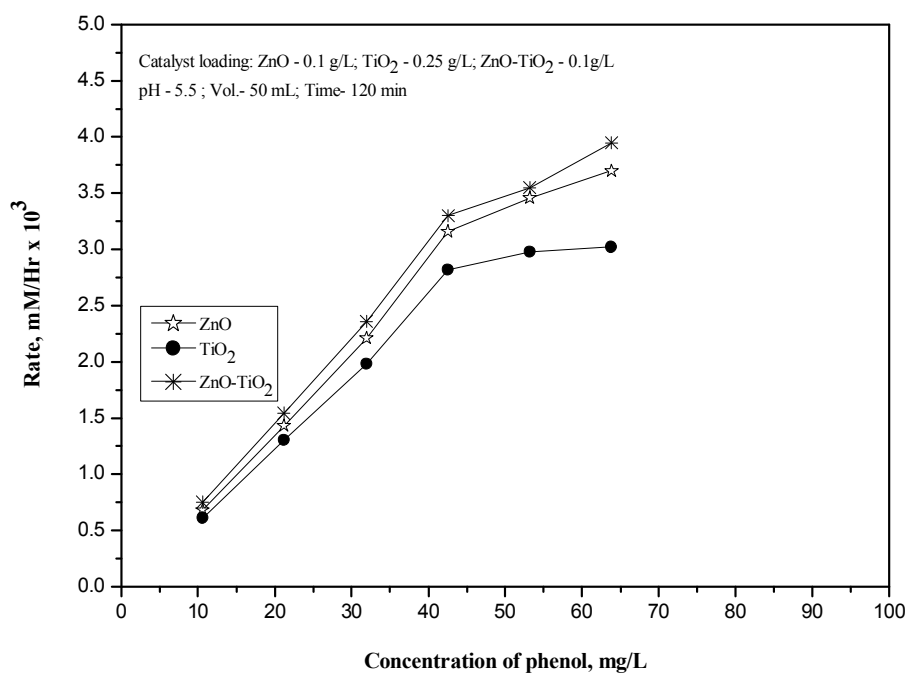


Fig.5.6(a): Effect of concentration on the sonophotocatalytic degradation of phenol over ZnO, TiO₂ and ZnO- TiO₂

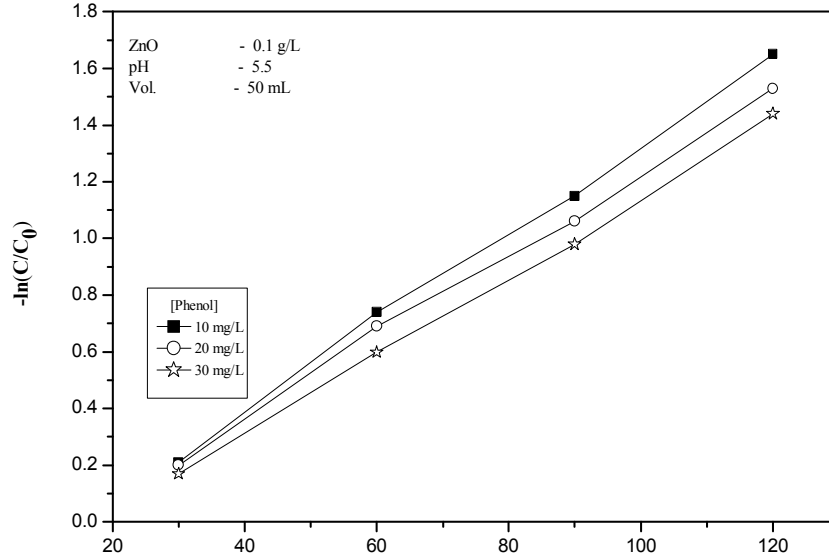


Fig.5.6(b): Kinetics of ZnO mediated sonophotocatalytic degradation of phenol

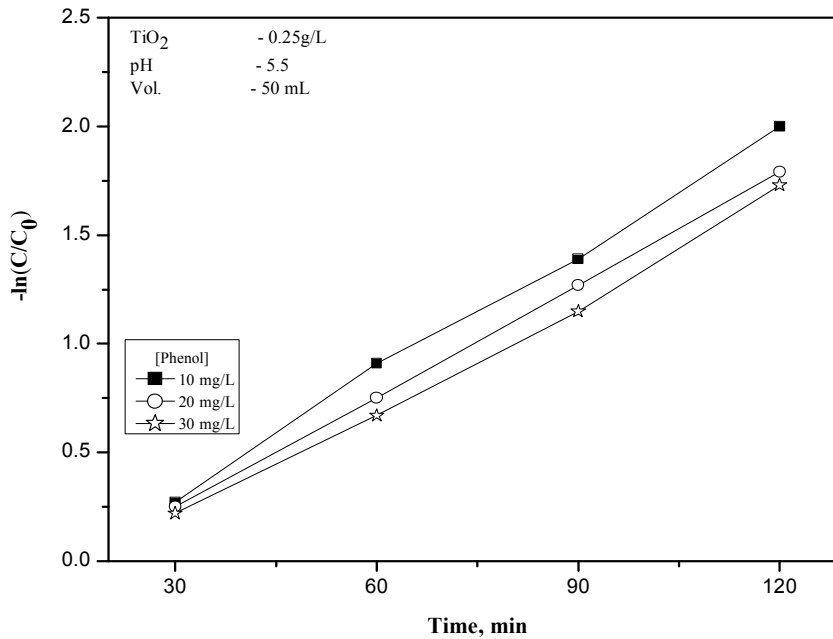


Fig.5.6(c): Kinetics of TiO₂ mediated sonophotocatalytic degradation of phenol

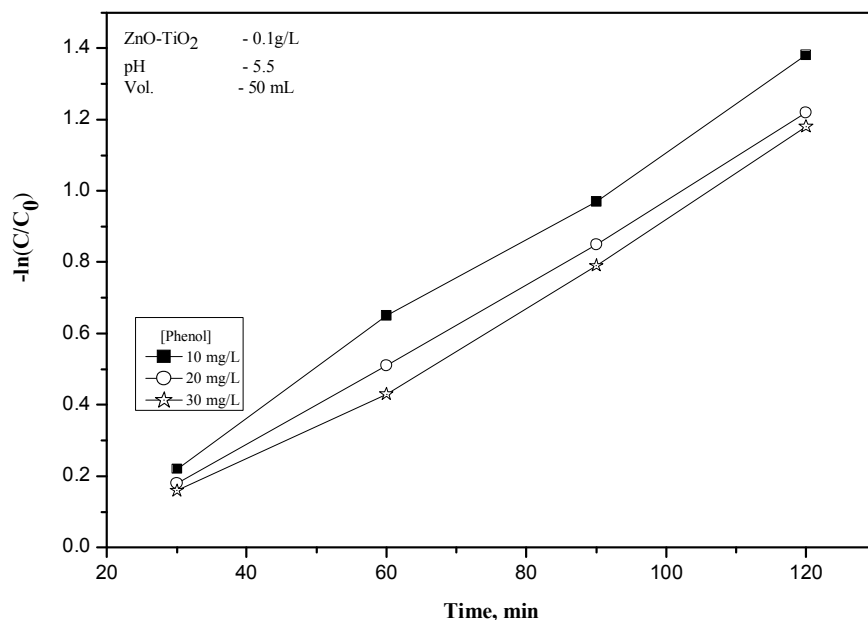


Fig.5.6(d): Kinetics of ZnO-TiO₂ mediated sonophotocatalytic degradation of phenol

5.3.3 Effect of pH

pH of the reaction medium has significant effect on the sono and photocatalytic degradation of phenol as seen in earlier chapters. pH affects the properties of semiconductor oxide particles, including the surface charge, size of the aggregation and the band edge position. pH can also affect the adsorption–desorption characteristics of the surface of the catalyst. Hence the effect of pH on sonophotocatalytic degradation of phenol is investigated in the range 3–11. The pH of the suspension was adjusted before irradiation and it was not controlled during the experiment. The results are presented in Fig. 5.7. Maximum degradation is in the acidic region. In the acidic pH range of 4–6, over ≈88% (ZnO-TiO₂), 85% (ZnO) and 74 % (TiO₂) conversion is effected in 2 hr

while it is around 62% (ZnO-TiO₂), 54% (ZnO) and 63 % (TiO₂) in the alkaline range (9-11). The pH for optimum degradation of phenol is 5.5 in presence of ZnO-TiO₂ and ZnO and 6 in presence of TiO₂ as catalysts. This observation is similar to that of Wu et.al [206]. Higher degradation efficiency in the acidic pH has been reported by other authors also [133,150,151,202]. The adsorption of phenol from aqueous solution on ZnO, TiO₂, and ZnO-TiO₂ was studied at different pH values and the results are plotted and described in Chapter 3 Fig. 3.9(b). The effect of pH can be explained at least partially based on the amphoteric behaviour and surface charge of the semiconductors. The acid-base property of metal oxides is known to have considerable influence on their photocatalytic activity, as explained in earlier chapters.

Significant enhancement in the degradation of phenol under sonophotocatalysis can also be attributed to the effect of US in reducing the distance between the substrate molecule and the surface of the catalyst particles. This is not feasible in the alkaline range where repulsion between like charges of the substrate and the catalyst particles is much greater [203]. Two important factors responsible for the efficiency of degradation are adsorption of the substrate on the catalyst surface and the reactive OH radical formation. These are affected conversely by the pH resulting in a balancing effect, though to a limited extent. Hence the degradation appears to be stabilized in the alkaline range.

The synergy in the sonophotocatalytic degradation is seen at all pH values. The synergy is more at extreme acidic and alkaline pH compared to that at the respective optimum pH in the presence of ZnO, TiO₂ as well

as ZnO-TiO₂. Hence the combination of US and UV is highly effective to assist in overcoming at least partially, the negative impact on degradation caused by the pH effect. The simultaneous sono and photo activation of the catalyst serves to lessen the effect of pH on the surface characteristics of the catalyst. However, it is rather complex to analyze or predict the precise effect of the pH on the sono, photo or sonophotocatalytic degradation of phenol on semiconductor oxides. Effect of pH on the US, UV and US+UV induced activation of ZnO, TiO₂ and ZnO-TiO₂ is summarized in Table 5.3.

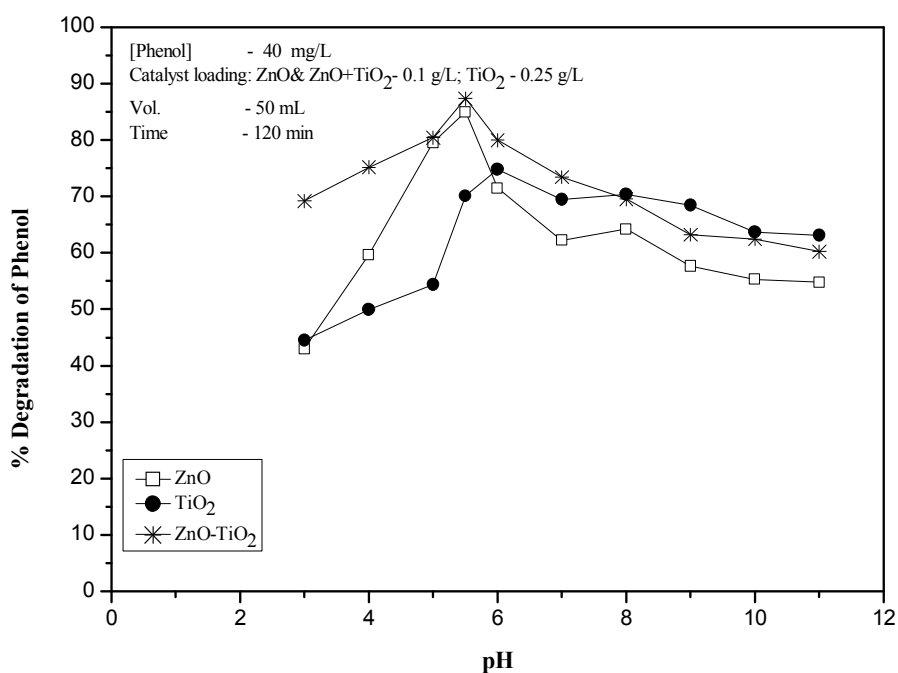


Fig.5.7: Effect of pH on the sonophotocatalytic degradation of phenol ZnO, TiO₂ and ZnO-TiO₂.

Table 5.3: Effect pH on the US, UV and US+UV induced degradation of phenol in presence of ZnO, TiO₂ and ZnO-TiO₂.

[Catalyst]: [0.1g/L (ZnO-TiO₂ & ZnO) & 0.25g/L (TiO₂)]; Reaction Volume: 50 mL; [Phenol]: 40 mg/L; Irradiation time: 120 min

pH	Percentage Degradation of phenol on								
	ZnO			TiO ₂			ZnO- TiO ₂		
	US	UV	US+UV	US	UV	US+UV	US	UV	US+UV
3	3.4	22.0	43.0	2.3	26.0	44.5	3.4	32.4	69.1
4	9.6	33.1	59.6	4.1	40.4	49.9	6.9	48.3	75.1
5	11.8	44.7	79.5	5.8	50.1	54.3	8.9	56.7	80.4
5.5	13.9	55.0	85.0	6.1	57.4	70.1	14.0	65.7	87.3
6	12.1	53.7	71.5	6.9	63.0	74.8	11.4	64.7	79.9
7	8.9	52.2	62.2	6.7	57.4	69.4	9.6	58.4	73.4
8	7.0	51.2	64.2	4.6	54.1	70.3	7.3	56.1	69.5
9	5.7	43.4	57.6	4.5	47.1	68.4	6.7	50.7	63.1
10	5.2	36.7	55.2	4.2	44.3	63.7	5.0	47.5	62.4
11	5.0	32.6	54.7	4.0	37.7	63.0	4.7	40.1	60.1

5.3.4 Effect of reaction volume

The effect of reaction volume on sonophotocatalytic degradation of phenol on ZnO, TiO₂ and ZnO-TiO₂, is investigated by varying the reaction volume keeping the other parameters constant.

The results obtained are presented in Fig. 5.8(a). It is seen that the % degradation in presence of each catalyst (ZnO, TiO₂ and ZnO-TiO₂) decreased with increase in reaction solution volume. The synergistic effect of sonophotocatalysis is visible in all cases irrespective of the volume as shown in Table 5.4. The % degradation decreases with increase in volume upto 75 mL and stabilizes thereafter. However, the actual rate of degradation in terms of the number of phenol molecules disappearing increases with increase in volume [see Fig. 5.8(b)].

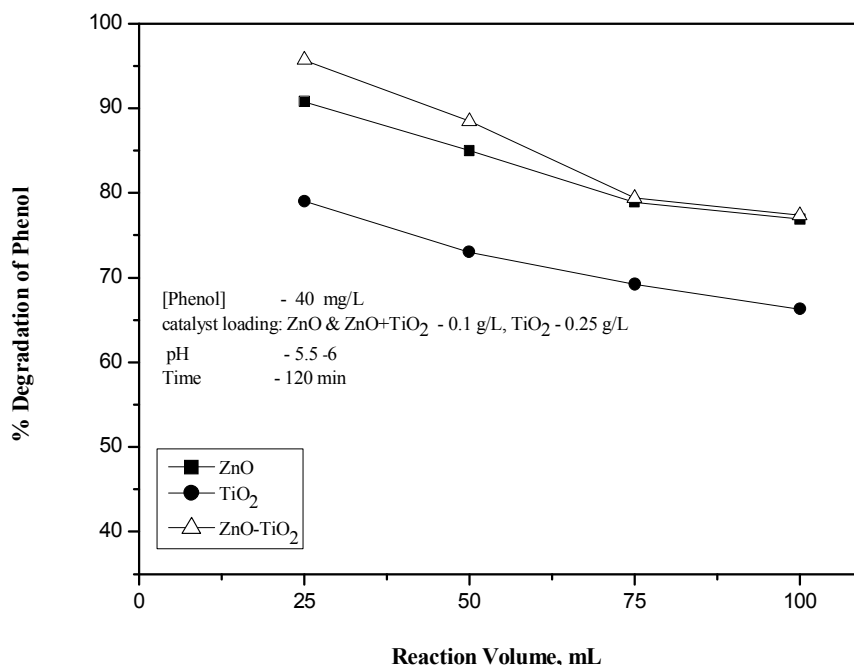


Fig.5.8(a): Effect of reaction volume on the sonophotocatalytic degradation of phenol over ZnO, TiO₂ and ZnO-TiO₂.

Table 5.4: Effect of reaction volume on the US, UV and US+UV induced degradation of phenol in presence of ZnO, TiO₂ and ZnO-TiO₂.
[Catalyst]: [0.1g/L (ZnO-TiO₂ & ZnO) & 0.25g/L (TiO₂)]; pH: 5.5-6;
[Phenol]: 40 mg/L; Irradiation time: 120 min

Reaction volume (mL)	Percentage Degradation of phenol on								
	ZnO			TiO ₂			ZnO- TiO ₂		
	US	UV	US+UV	US	UV	US+UV	US	UV	US+UV
25	18.9	70.1	90.7	12.7	71.1	79.0	20.1	79.4	95.7
50	13.1	54.3	85.0	7.5	63.5	73.0	14.9	69.4	88.4
75	12.5	42.4	78.9	5.2	54.4	69.2	13.0	59.1	79.4
100	10.8	31.1	76.9	3.5	40.3	66.3	11.5	47.3	77.3

The rate of increase with volume slows down at higher volumes. The increase in rate with increase in volume can be attributed to the increase in the number of active cavitation bubbles per unit volume and

consequent increase in the number of reactive free radicals formed in the system and their interaction with the increasingly available substrate.

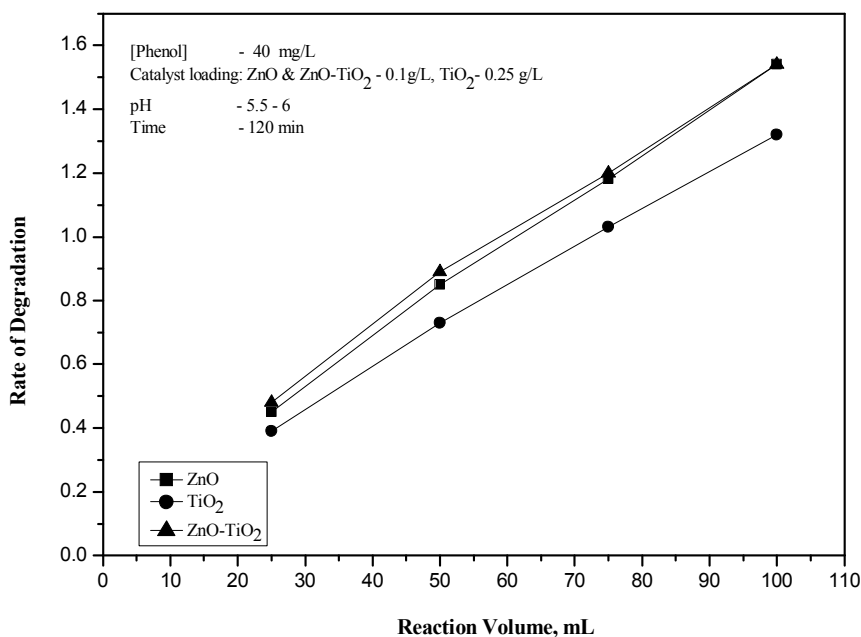


Fig.5.8(b): Effect of reaction volume on the rate of degradation of phenol.

This reduction of the rate increase with increase in volume in the same reactor is attributed to the increase in the thickness of the irradiated region which results in attenuation of the UV/US intensity through the solution [203]. The slowdown in the rate is also caused possibly by eventual absorption of ultrasonic energy by the medium and its dissipation less productively. The enhancement in the degradation of phenol by (US+UV) over the degradation in presence of US or UV individually is higher at all volumes. This again confirms the potential of the combination of US and UV to accelerate the degradation of organic pollutants in water even under unfavorable conditions.

5.3.5 Effect of particle size

The particle size of catalyst influences the catalyst activity inversely mainly due to decreasing surface area with increase in particle size. This has been proven in the case of sono and photocatalysis in earlier chapters. The influence of catalyst loading also points to the possibility of surface availability related effect on the degradation. Hence, degradation experiments were conducted with ZnO, TiO₂ and ZnO-TiO₂ of various particle sizes and the results obtained are shown in Fig 5.9. The effect is not significant for any of the catalysts, at least in the range of 4 to 16 μm studied.

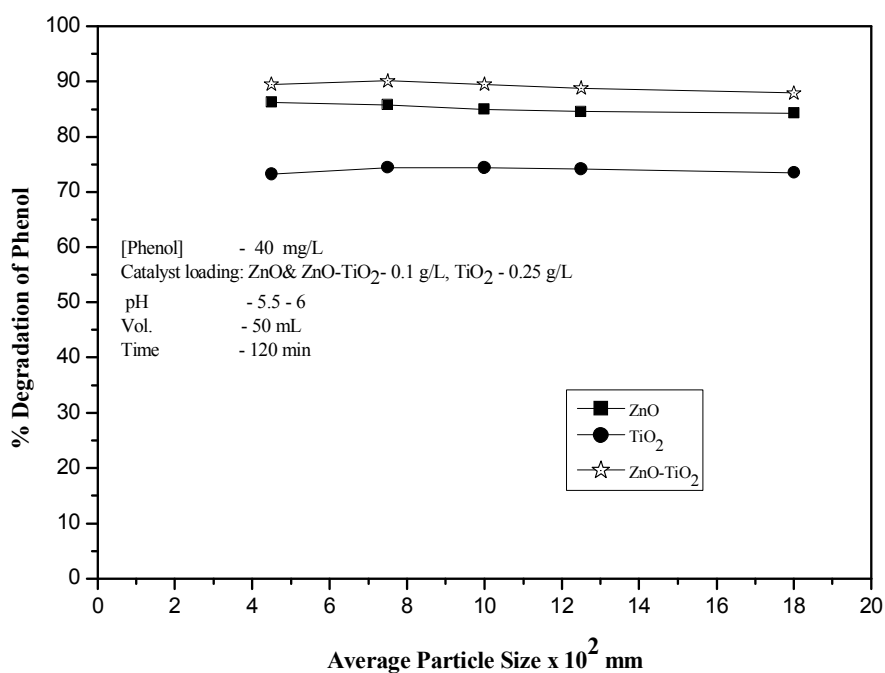


Fig.5.9: Effect of particle size on the sonophotocatalytic degradation of phenol over ZnO, TiO₂ and ZnO-TiO₂

The inverse relation between particle size of the catalyst and the degradation of phenol is more significant in photocatalysis as shown in chapter 3. Decrease in particle size leads to increase in surface area, more surface sites for adsorption of the pollutant, more efficient absorption of light and better surface promoted interaction between the reactants resulting in higher conversion. However, in the case of sonophotocatalysis, the synergy as a result of the combination of UV and US is adequate to compensate for the decrease in photocatalysis due to increase in particle size. Further, the US itself leads to deaggregation as well as decrease in particle size and enhanced surface area. Hence, the particle size effect is not very significant in sono or sonophotocatalysis.

5.3.6 Effect of aeration/deaeration

The important role of dissolved O₂ in sono and photocatalysis was discussed in previous chapters. The effect of dissolved air/oxygen on the sonophotocatalytic degradation of phenol was also tested by purging the system with N₂ for 1 hr in the presence of each of the three catalysts. The results are as shown in Table 5.5. The degradation is inhibited in the system purged with N₂. Bubbling with air enhances the degradation because of increased supply of O₂ including the replenishment of consumed O₂. This confirms that dissolved oxygen has a significant role in the sonophotocatalytic degradation of phenol also for the reasons explained and discussed in earlier chapters.

Table 5.5: Effect of N₂/air/purging of the reaction system on the sonophotocatalytic degradation of phenol.

[Catalyst]: [0.1g/L (ZnO-TiO₂ & ZnO) & 0.25g/L (TiO₂)]; [phenol]: 40 mg/L; pH: 5.5; Reaction Volume: 50 ml; Irradiation Time: 120 min

Purging gas	Percentage Degradation of phenol under US+UV on		
	ZnO	TiO ₂	ZnO-TiO ₂
None	85	73	89
N ₂	41	34	41
Air	96	85	98

Comparative effect of purging the reaction solution with N₂ and air on the sono, photo and sonophotocatalytic degradation of phenol is given in Table 5.6.

Table 5.6: Comparative effect of N₂/air/purging of the reaction system on the US, UV and US+UV degradation of phenol.

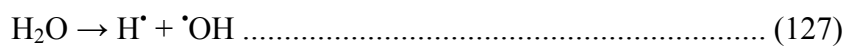
[Catalyst]: [0.1g/L (ZnO-TiO₂ & ZnO) & 0.25g/L (TiO₂)]; [phenol]: 40 mg/L; pH: 5.5; Reaction Volume: 50 ml; Irradiation Time: 120 min

Purging Gas	Percentage Degradation of phenol on								
	ZnO			TiO ₂			ZnO- TiO ₂		
	US	UV	US+UV	US	UV	US+UV	US	UV	US+UV
None	14	55	85	7	62	73	15	67	89
N ₂	9	23	41	4	30	34	10	37	41
Air	19	65	96	12	79	85	21	83	98

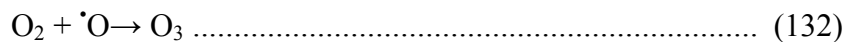
5.4 Mechanism of the Sonophotocatalytic degradation

The mechanism of sonophotocatalysis is essentially a combination of sono and photocatalysis which have been explained in earlier chapters. The combination of the two processes provides synergy and consequently, the combined effect is more than the simple additive effect. The general mechanism of sonophotocatalysis can be summarized as follows:

Sonolysis of water produces active radicals H^\bullet and OH^\bullet via cavitation which attack organic compounds in solution. The presence of a highly heterogeneous environment such as the catalyst particles in the reaction mixture enhances this phenomenon as the microbubbles tend to break up into smaller ones. This will increase the total number of regions of high temperature and pressure. Dissolved oxygen present in the system serves as a source for nucleus cavitation. Thus the number of OH radicals produced by the system increases leading to oxidation of phenol even in the absence of light. In addition to the production of free radicals, sonolysis can also result in the pyrolysis of vaporized molecules and shear stress. Sonication of pure water has been shown to result in the following chain reactions which are accelerated by the presence of suspended solid particles [32].



Further, the following reactions (which are shown in section 4.3.9. chapter 4) can occur in presence of oxygen.



Various active species produced as above react with phenol in the bulk solution or at the interface between the bubbles and the liquid phase. The ozone produced as above can also promote the degradation of phenol in combination with UV via the direct and indirect production of hydroxyl radicals.



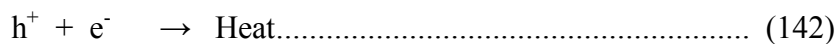
H₂O₂ as well as the reactive radical species can interact with phenol, leading to its degradation and eventual mineralization.

Further sonolysis of the semiconductor is also known to lead to sonoluminescence which can result in photocatalytic degradation. Under concurrent UV irradiation, the direct photocatalytic reaction becomes the most dominant route making the sonoluminescence initiated photocatalysis a minor player. The overall photocatalytic process can be summarized as:

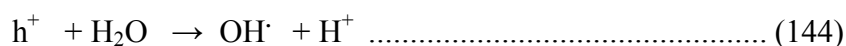
Generation of electron – hole pairs from UV radiation striking the semiconductor (SC)



Recombination of electron – hole pairs



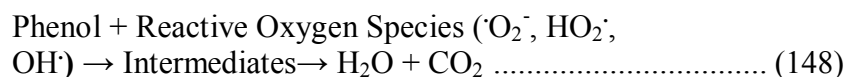
Formation of primary radicals by valence band holes



Scavenging of conduction band electrons by O₂



Formation of multiple peroxide species



US is known to have the ability to disperse agglomerated particles. Deagglomeration of catalyst particles can increase the overall surface area, provide more active sites for adsorption of the reactant, enhance the absorption of US/UV and generate more reactive species. This can lead to synergy in the degradation. In order to verify this, the photocatalytic reaction was interrupted periodically (for 3 min each after 15, 45, 75 and 105 min of UV irradiation) by removing the reaction system from UV light and subjecting it to US during the interruption. The results are summarized in Table 5.7.

Table 5.7: Photocatalytic removal of phenol with and without interruption of UV irradiation [ZnO]: 0.1 g/L; pH: 5.5; volume: 50 mL; [Phenol]: 40 mg/L.

UV irradiation time (min)	Percentage removal of phenol	
	Uninterruption of UV	With interruption of UV
30	21.2	29.0 (3 min interruption of UV with US)
60	43.1	49.5 (6 min interruption of UV with US)
120	56.9	65.4 (12 min interruption of UV with US)

In the case of experiments with periodic short interruption of UV with US, there is enhancement in the degradation of phenol. Since the US was used only for a short period, the influence of sonolysis other than deagglomeration is expected to be minimal. Hence, the enhancement can be attributed to deagglomeration and associated advantages. The extent of enhancement remains more or less the same (6–8%) in all cases, indicating that US has only limited influence when applied independently. Further, the enhancement is much less compared to that from simultaneous (UV + US) irradiation (~ 85% after 120 min) thereby confirming the synergistic role of US in presence of UV. Hence deagglomeration is not the only factor that contributes to the US induced synergy even though its contribution could be important. Another major factor for the synergy may be the ability of US to prevent the deactivation of the catalyst by removing adsorbed moieties from the surface by microstreaming and microbubbles' eruption [19]. This kind of surface cleaning can contribute to enhanced reaction only by the simultaneous use of US and UV because microstreaming and microbubbling can only occur in the solution during the instantaneous moment when US is applied. The current observation that the increase in degradation, when the UV is interrupted by US is only marginal irrespective of the duration of US irradiation, suggests that the synergy is operational only when US and UV are applied simultaneously.

According to Naffrechoux et al. [209] the synergy in sonophotocatalytic systems can be attributed to the US induced physical changes in the catalyst and consequent benefits coupled with concurrent action of three oxidation mechanisms – (i) photodegradation,

(ii) sonodegradation and (iii) ozone oxidation. This is consistent with the observation made here and the mechanism proposed.

5.5 Effect of anions

The importance of investigating the effect of anions on the degradation of water pollutants by AOPs has been discussed earlier. In this context, the effect of some of the anions commonly found in water on the sonophotocatalytic degradation of phenol in presence of ZnO, TiO₂ and ZnO-TiO₂ is investigated. The results are presented in Fig.5.10 (a,b and c).

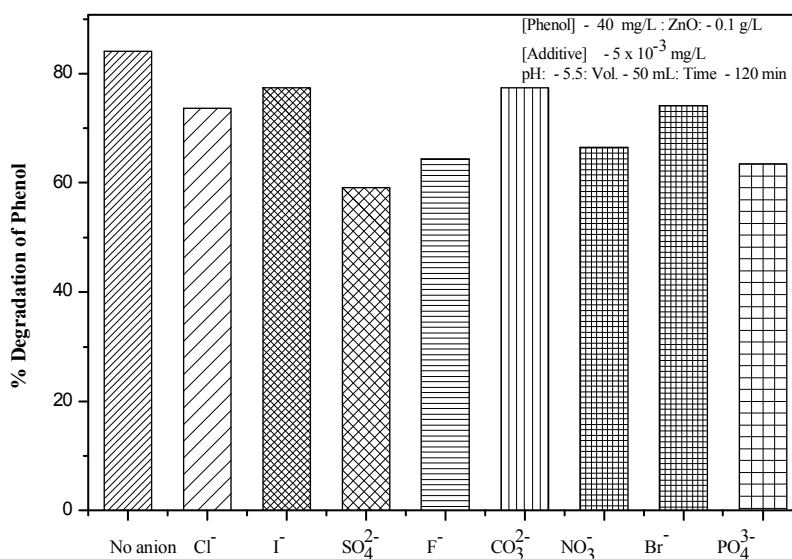


Fig.5.10(a): Effect of anions on the sonophotocatalytic degradation of phenol over ZnO

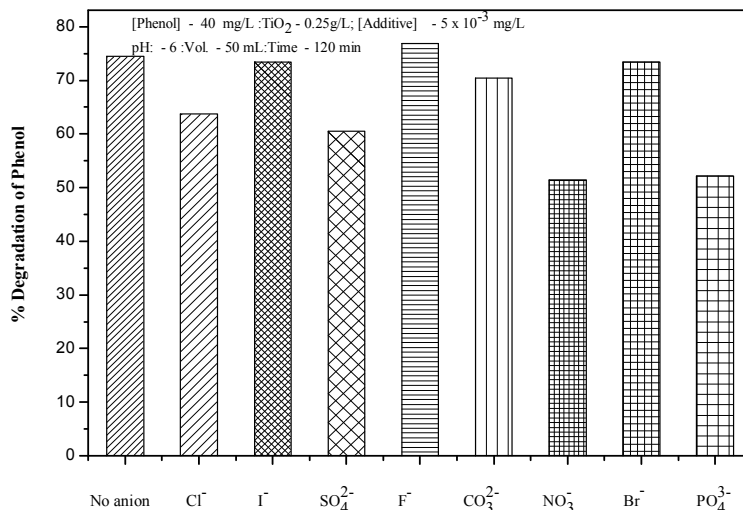


Fig.5.10(b): Effect of anions on the sonophotocatalytic degradation of phenol over TiO₂

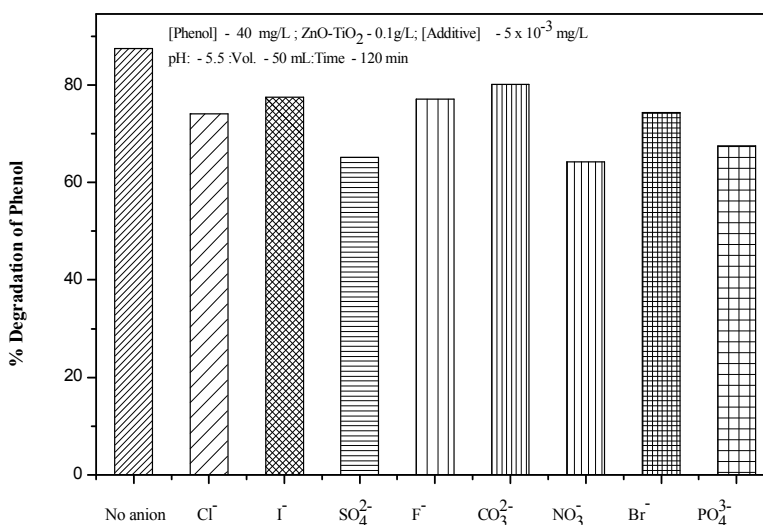
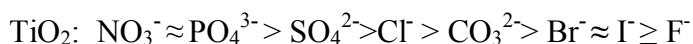


Fig.5.10(c): Effect of anion on the sonophotocatalytic degradation of phenol over ZnO-TiO₂

Unlike in the case of sono and photocatalysis in which some anions enhance the degradation of phenol, in the case of sonophotocatalysis almost all anions investigated inhibit the degradation. The inhibition by I⁻, Br⁻ and

CO_3^{2-} is relatively less and may be treated as almost insignificant in the case of ZnO and TiO_2 . In the case of ZnO- TiO_2 also, the inhibition by these ion is not much. It may be generally stated that in the case of all three catalysts the anion I^- , Br^- and CO_3^{2-} do not have any significant effect on the sonophotocatalytic degradation of phenol. In the case of F^- , the effect is not consistent, with inhibition in presence of ZnO and ZnO- TiO_2 and no significant effect in the case of TiO_2 . The inconsistent behaviour of F^- is seen in photocatalysis also. Anions PO_4^{3-} , SO_4^{2-} , Cl^- and NO_3^- inhibit the degradation in all cases. The inhibition can be partially attributed to the scavenging of reactive $\cdot\text{OH}$ radicals by the anions. The radical anion formed by interaction of $\cdot\text{OH}$ and the anion are not as effective as the $\cdot\text{OH}$ to effect the degradation of the pollutant, thus leading to the inhibition. Being relatively large in size, they can also form layers on the catalyst surface thereby inhibiting the activation of the catalyst surface. In any case, the highly efficient sonophotocatalysis is capable of overcoming the inhibitor effect by most anions as seen in the case of all three catalysts.

The inhibition follows the order:



However, the influence of anion on AOPs, as brought out in earlier chapters also, is very complex and inconsistent and hence cannot be generalized. Factors such as concentration of the anion, concentration of substrate, catalyst loading, type of intermediates formed, interaction in the bulk as well as on the surface can influence the effect of anions.

The comparative effect of these anions on the sono, photo and sonophotocatalytic degradation of phenol is summarized in Fig. 5.11 (a - x)

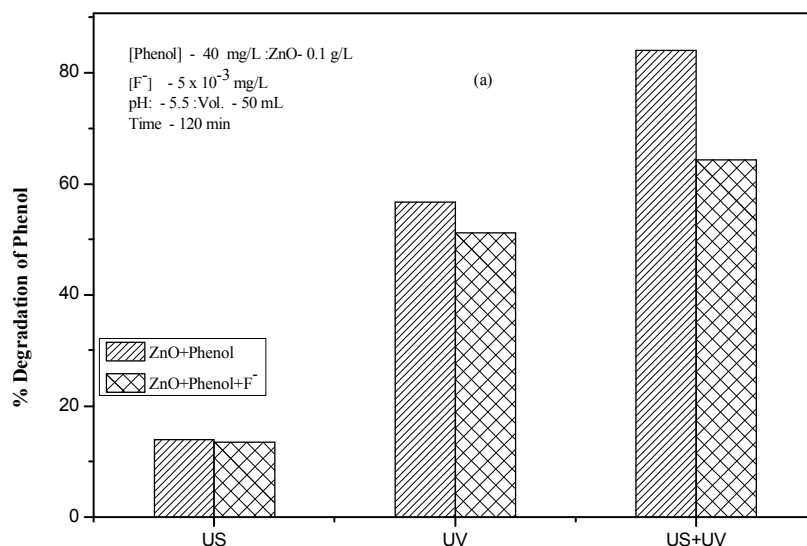


Fig. 5.11 (a): Effect of F⁻ on US, UV and US+UV initiated degradation of phenol in presence of ZnO.

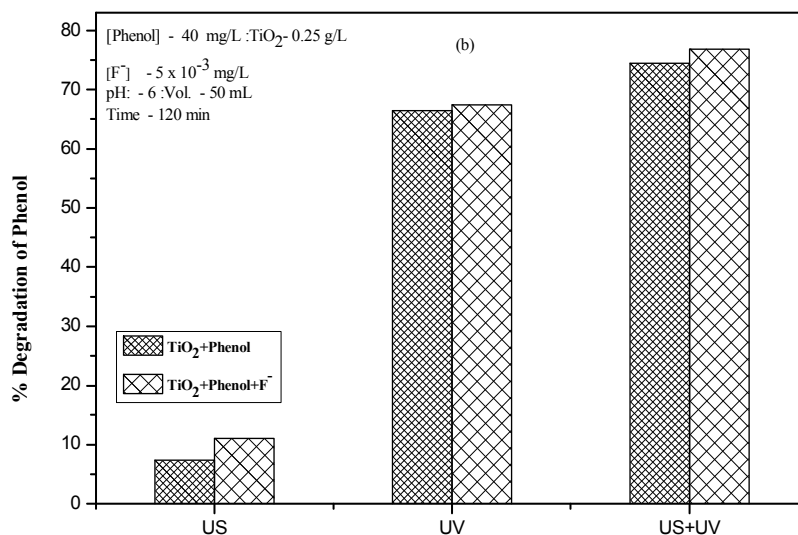


Fig. 5.11 (b): Effect of F⁻ on US, UV and US+UV initiated degradation of phenol in presence of TiO₂.

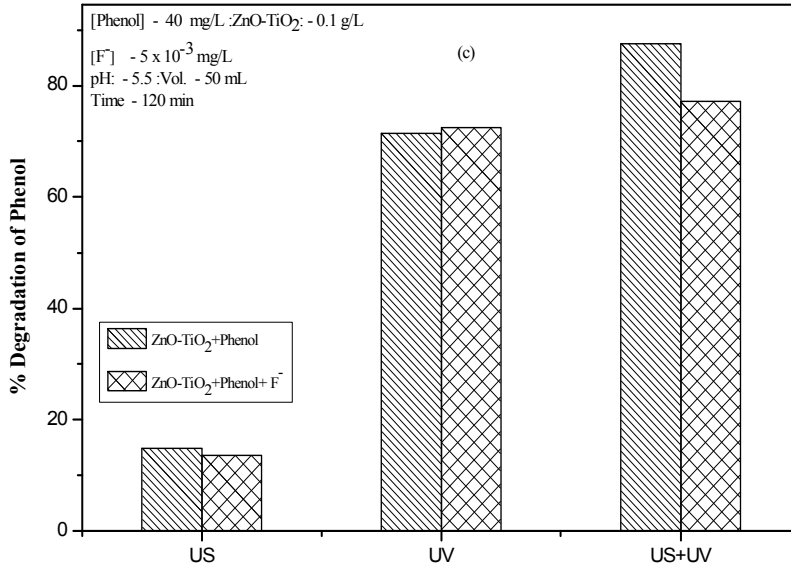


Fig. 5.11 (c): Effect of F⁻ on US, UV and US+UV initiated degradation of phenol in presence of ZnO-TiO₂.

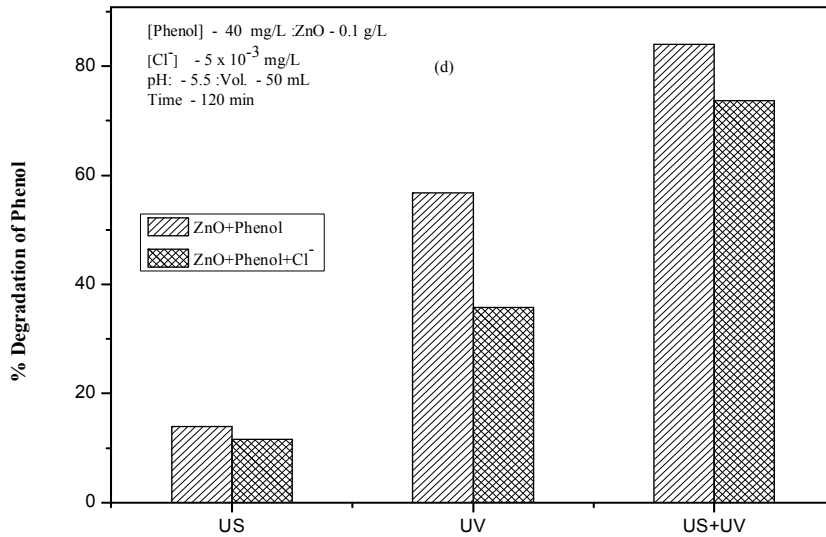


Fig. 5.11 (d): Effect of Cl⁻ on US, UV and US+UV initiated degradation of phenol in presence of ZnO.

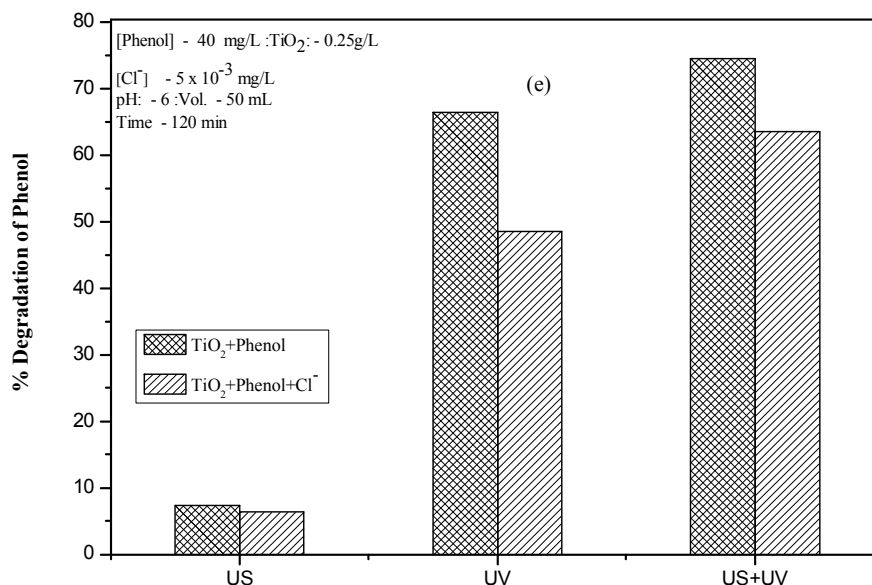


Fig. 5.11 (e): Effect of Cl⁻ on US, UV and US+UV initiated degradation of phenol in presence of TiO₂.

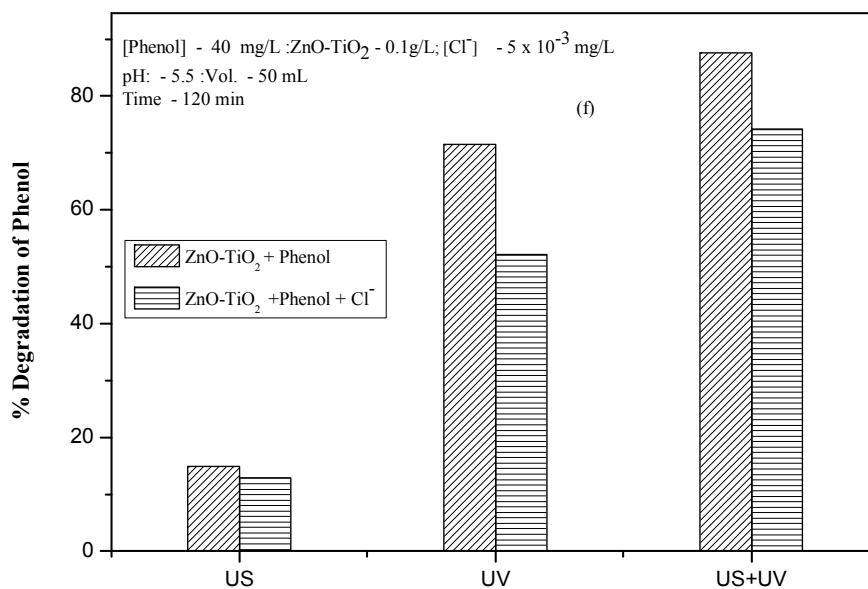


Fig. 5.11 (f): Effect of Cl⁻ on US, UV and US+UV initiated degradation of phenol in presence of ZnO-TiO₂.

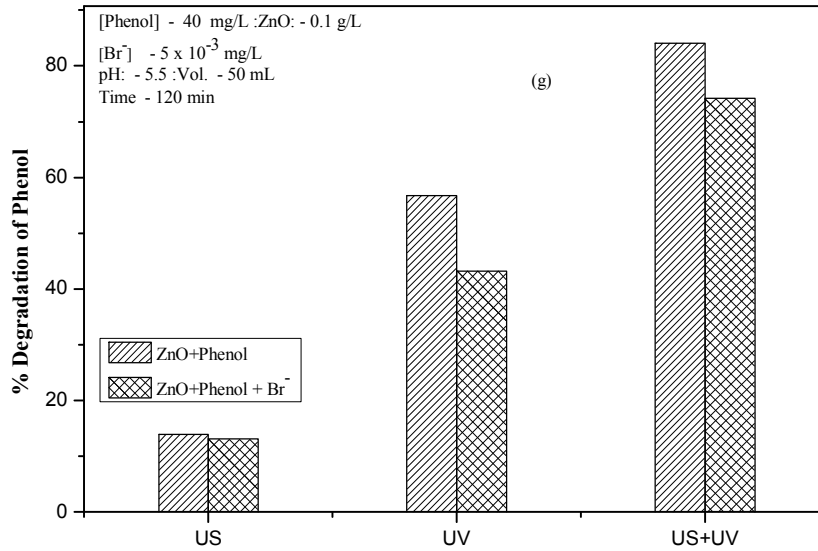


Fig. 5.11 (g): Effect of Br⁻ on US, UV and US+UV initiated degradation of phenol in presence of ZnO.

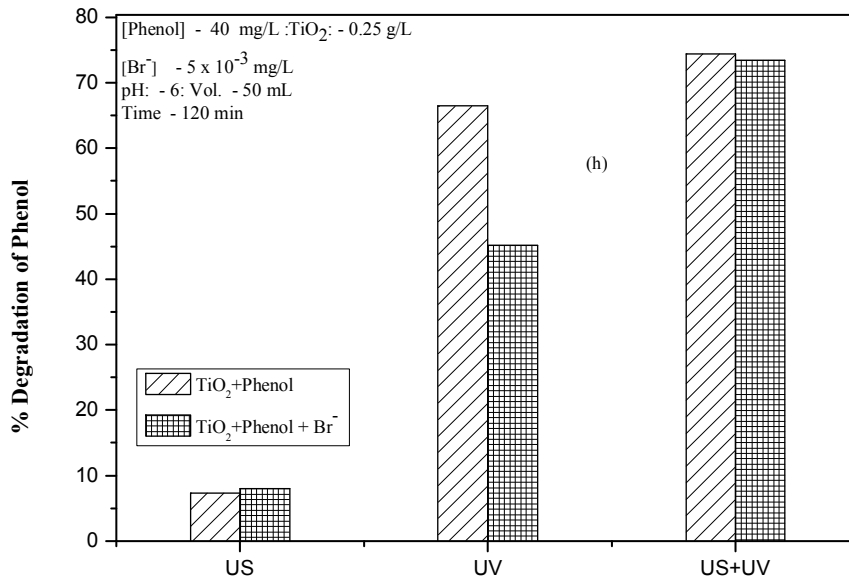


Fig. 5.11 (h): Effect of Br⁻ on US, UV and US+UV initiated degradation of phenol in presence of TiO₂.

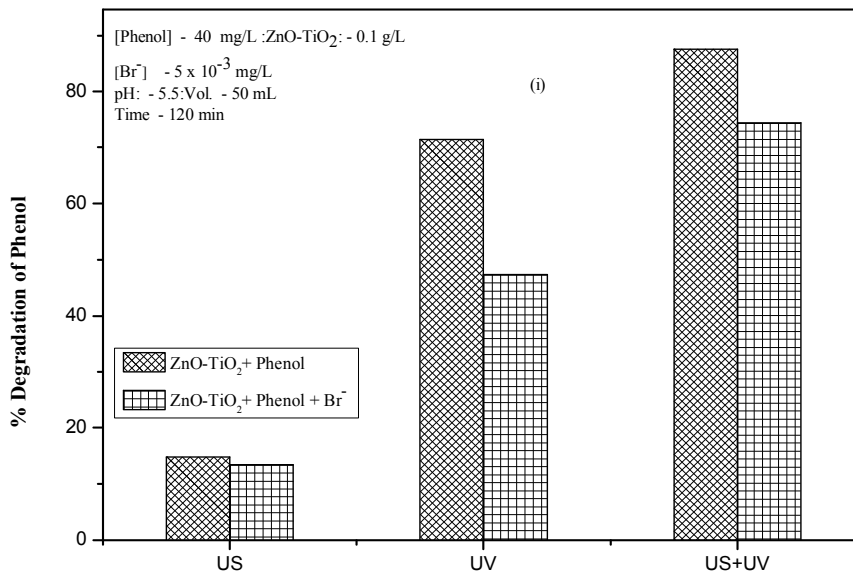


Fig. 5.11 (i): Effect of Br⁻ on US, UV and US+UV initiated degradation of phenol in presence of ZnO-TiO₂.

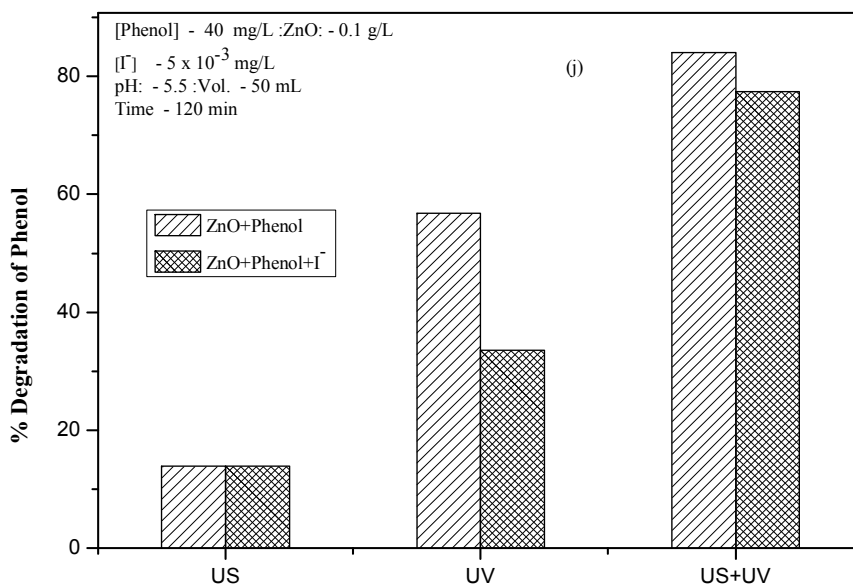


Fig. 5.11 (j): Effect of I⁻ on US, UV and US+UV initiated degradation of phenol in presence of ZnO.

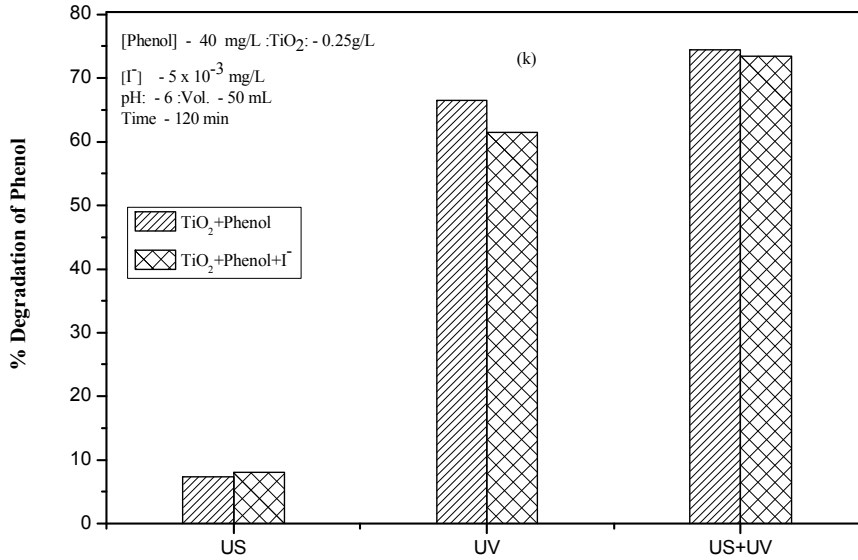


Fig. 5.11 (k): Effect of I⁻ on US, UV and US+UV initiated degradation of phenol in presence of TiO₂.

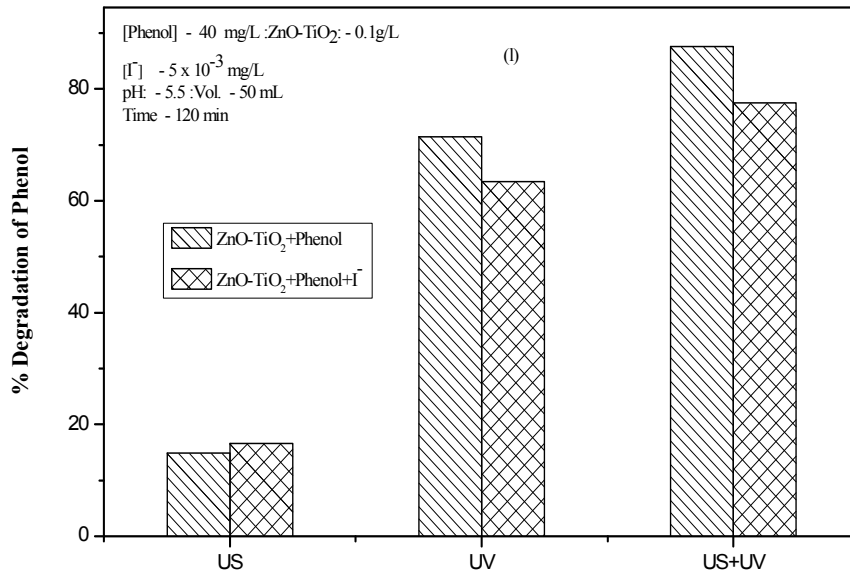


Fig. 5.11 (l): Effect of I⁻ on US, UV and US+UV initiated degradation of phenol in presence of ZnO-TiO₂.

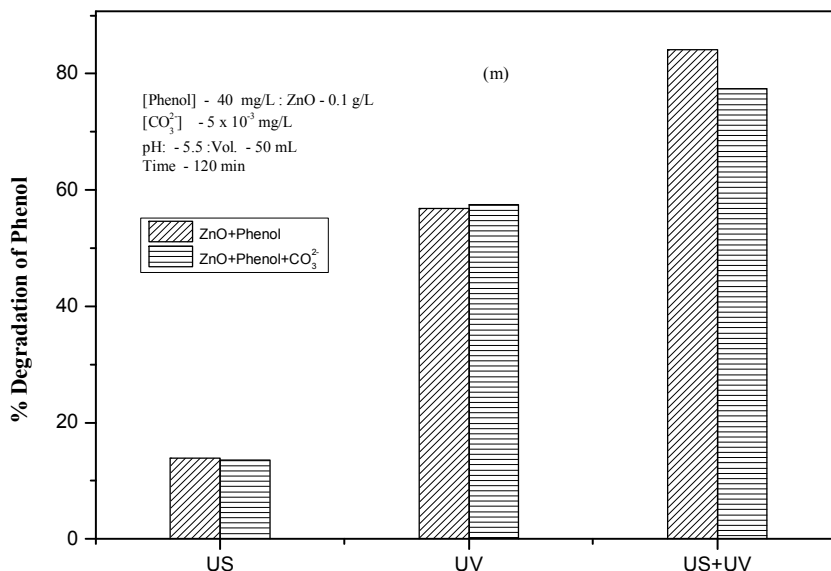


Fig. 5.11 (m): Effect of CO₃²⁻ on US, UV and US+UV initiated degradation of phenol in presence of ZnO.

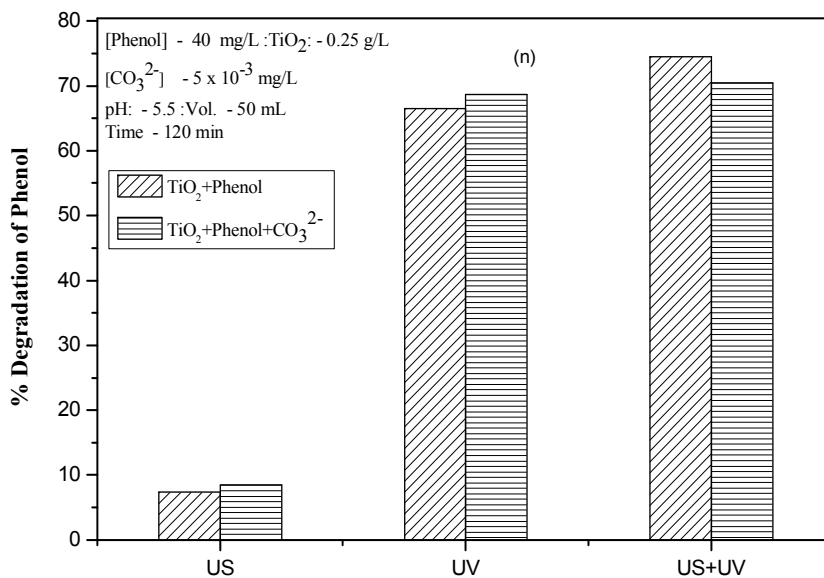


Fig. 5.11 (n): Effect of CO₃²⁻ on US, UV and US+UV initiated degradation of phenol in presence of TiO₂.

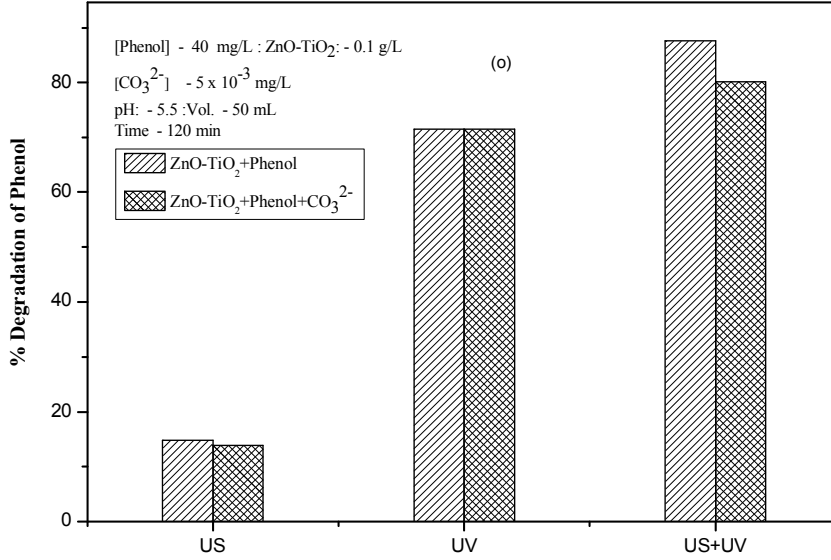


Fig. 5.11 (o): Effect of CO₃²⁻ on US, UV and US+UV initiated degradation of phenol in presence of ZnO-TiO₂.

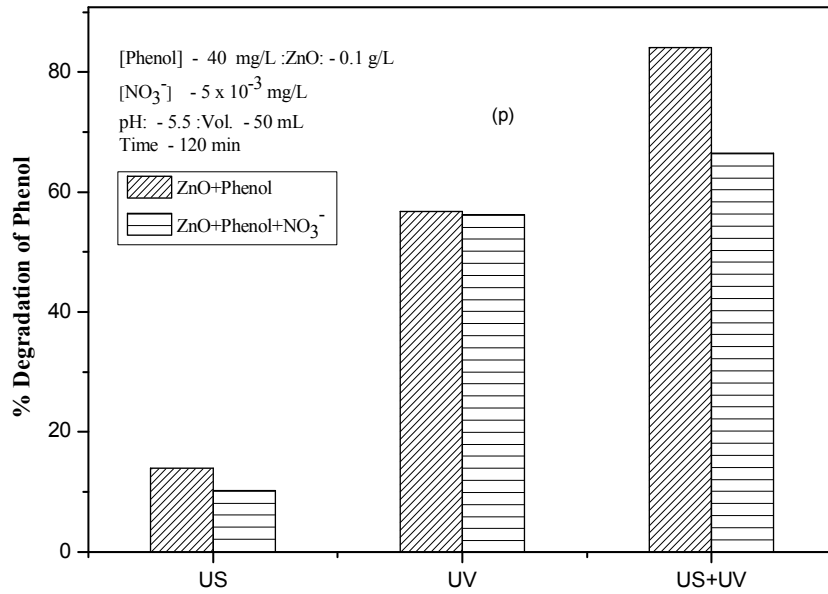


Fig. 5.11 (p): Effect of NO₃⁻ on US, UV and US+UV initiated degradation of phenol in presence of ZnO.

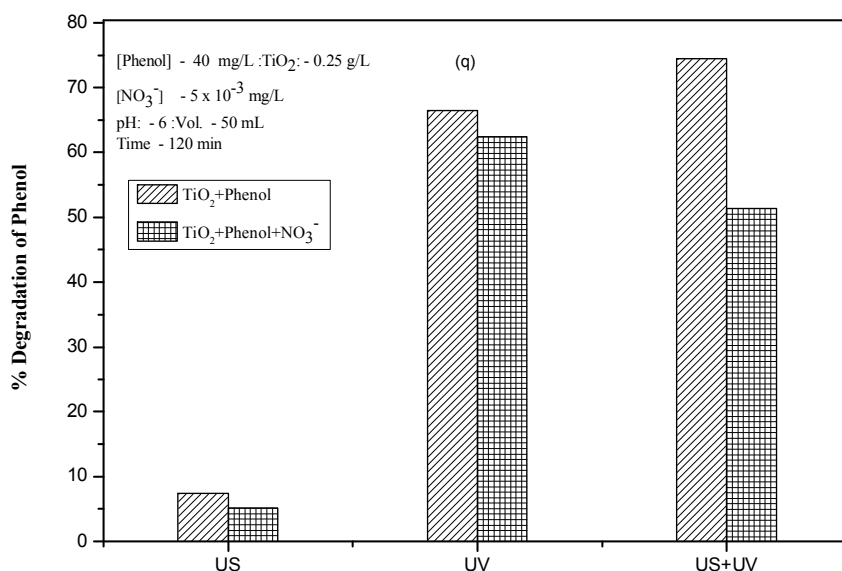


Fig. 5.11 (q): Effect of NO₃⁻ on US, UV and US+UV initiated degradation of phenol in presence of TiO₂.

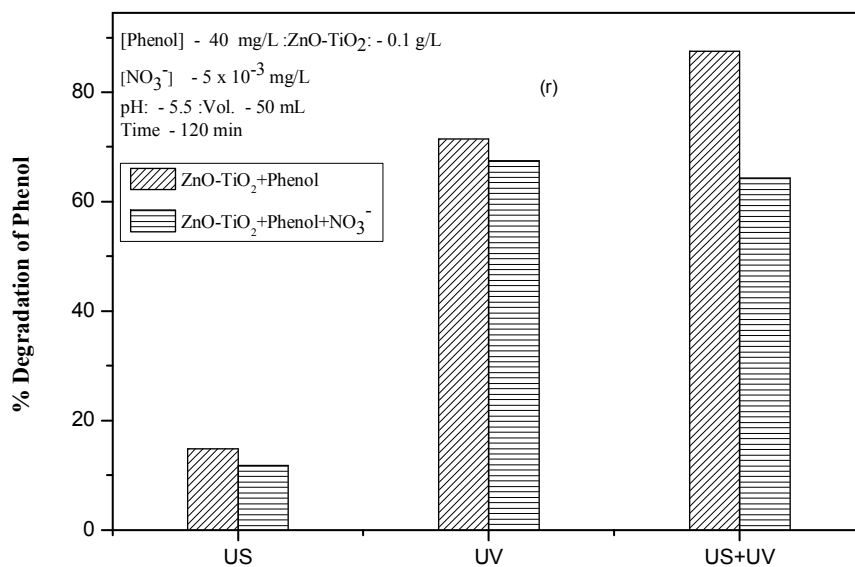


Fig. 5.11 (r): Effect of NO₃⁻ on US, UV and US+UV initiated degradation of phenol in presence of TiO₂.

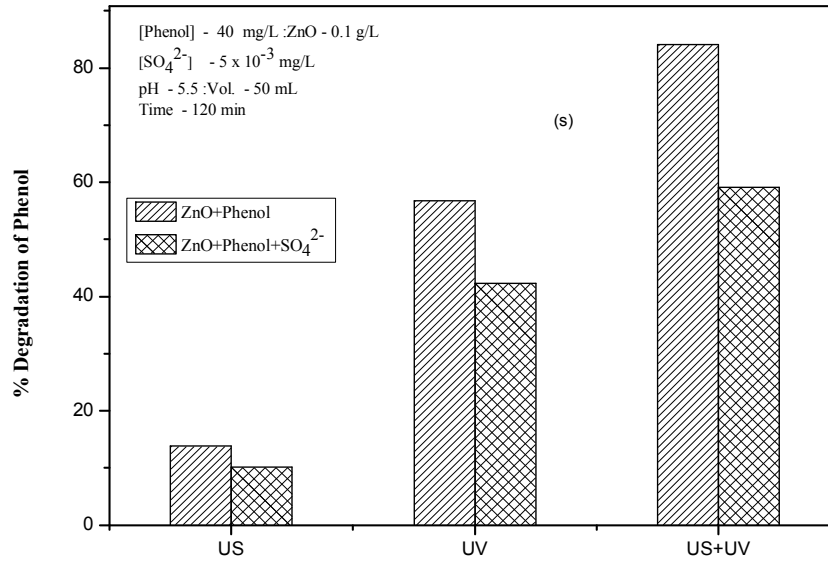


Fig. 5.11 (s): Effect of SO₄²⁻ on US, UV and US+UV initiated degradation of phenol in presence of ZnO.

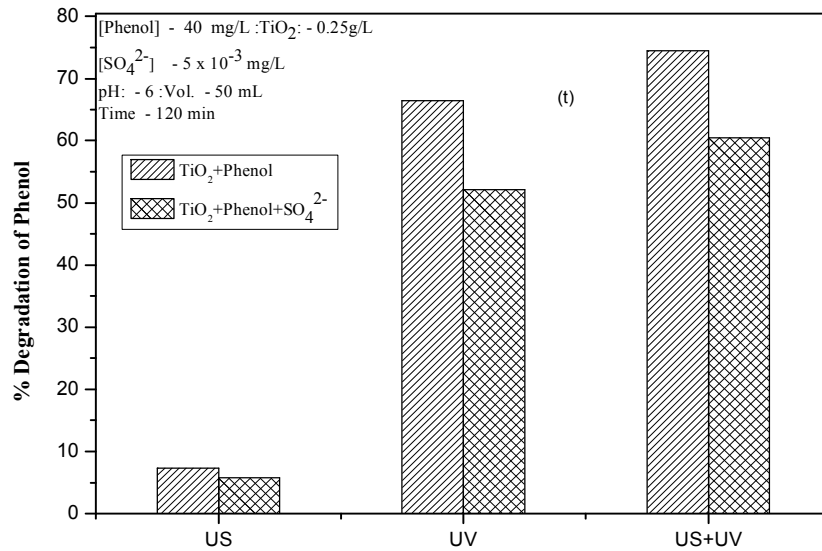


Fig. 5.11 (t): Effect of SO₄²⁻ on US, UV and US+UV initiated degradation of phenol in presence of TiO₂.

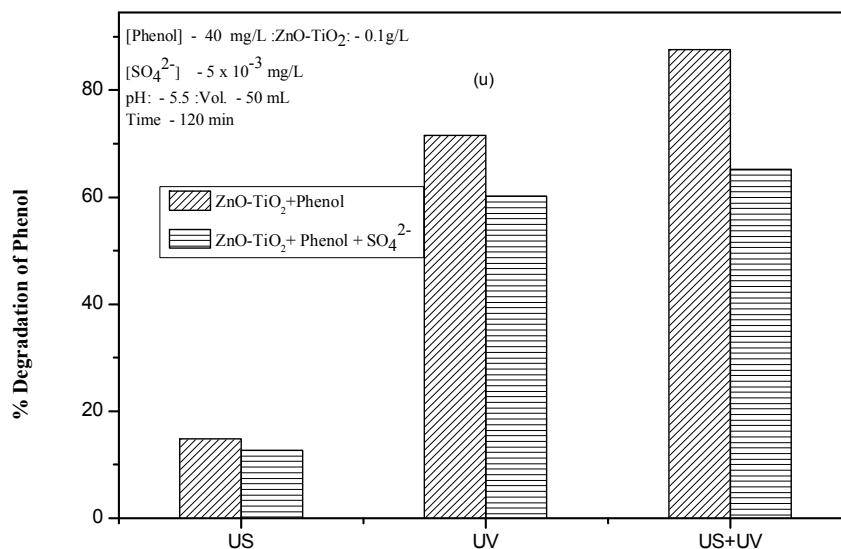


Fig. 5.11 (u): Effect of SO_4^{2-} on US, UV and US+UV initiated degradation of phenol in presence of ZnO-TiO_2 .

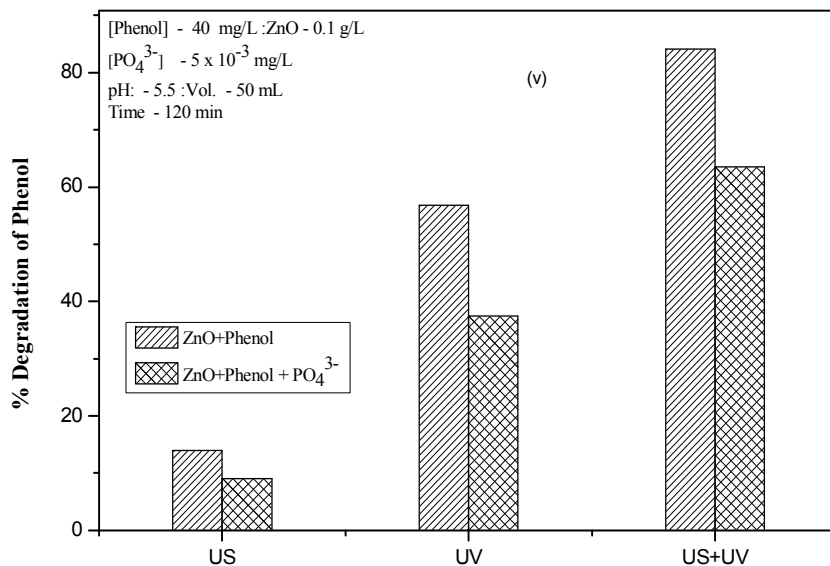


Fig. 5.11 (v): Effect of PO_4^{3-} on US, UV and US+UV initiated degradation of phenol in presence of ZnO .

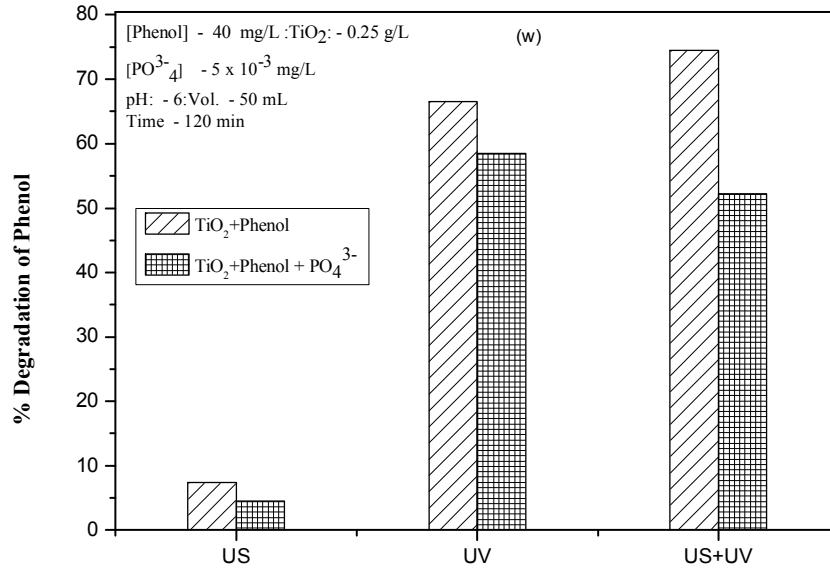


Fig. 5.11 (w): Effect of PO₄³⁻ on US, UV and US+UV initiated degradation of phenol in presence of TiO₂.

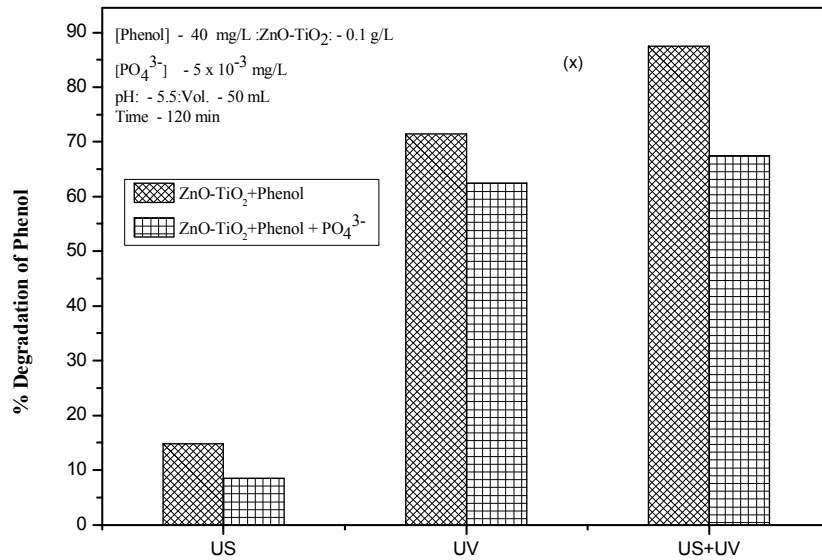


Fig. 5.11 (x): Effect of PO₄³⁻ on US, UV and US+UV initiated degradation of phenol in presence of ZnO-TiO₂.

5.6 Conclusions

Sonophotocatalytic degradation of phenol in water is investigated in presence of ZnO, TiO₂ and ZnO-TiO₂ catalysts. Combination of UV light and Ultrasound provides synergy for the degradation. Possible reasons for this phenomenon which are significant in the context of the commercial feasibility of the technique are explored. Optimum parameters for the sonophotocatalytic degradation of phenol were identified in terms of concentration of the substrate, catalyst loading, pH, reactant volume, oxygen concentration etc. Particle size does not have any impact in the narrow range studied here. The sonophotocatalytic degradation is found to follow variable kinetics, depending on the concentration of the substrate. pH effect on the reaction is rather complex and is dependent on a number of factors. Maximum degradation is observed in the pH range 4-5.5. Presence of anions can have enhancing, inhibiting or insignificant effect, depending on the reaction conditions. However, a general explanation applicable to the effect of all anions on all catalysts, is not possible due to the complexity of AOPs involving sono, photo and sonophotocatalysis.

.....✪.....

ZINC OXIDE MEDIATED SONOCATALYTIC REMOVAL OF BACTERIAL CONTAMINANTS FROM WATER

- 6.1 *Introduction*
- 6.2 *Experimental Details*
- 6.3 *Results and Discussion*
- 6.4 *Mechanism of disinfection*
- 6.5 *Mechanism of disinfection*
- 6.6 *Conclusions*

6.1 Introduction

Over the last two decades, researchers have found that microorganisms are becoming resistant to conventional disinfection techniques such as chlorination and ozonation. Further, these methods generate disinfection byproducts (DBPs) with carcinogenic and mutagenic potential that are harmful to the environment and human beings. Semiconductor mediated photocatalysis has been investigated extensively as a viable technique for the removal of organic and inorganic pollutants from water and waste water [34, 95,96,192]. Photocatalytic deactivation of bacterial pollutants from aqueous streams has also been reported extensively in recent years [208,210,211]. Other Advanced Oxidation Processes (AOPs) under investigation in this context are sonolysis and sonocatalysis in which ultrasound (US) is used as the energy source in place of conventional

heat or light [101,208,212,213]. Ultrasound irradiation, if and when perfected, will be one of the most attractive treatment techniques since the inactivation of biohazardous microorganisms can be achieved under ambient conditions without any chemical compound. Major observations in this respect till 2003 were summarized by Piyasena *et al.*, [101]. US is able to inactivate bacteria and de-agglomerate bacterial clusters or flocs through a number of physical, mechanical and chemical effects arising from cavitation [84, 213]. The microbial disintegration and destruction by ultrasonic waves result from the microorganisms' interaction with the cavitation bubbles. When ultrasound is applied to a liquid medium, the ultrasonically induced cavitations produce bubbles in solution. The result of the bubble collapse is a localized reaction field of high temperature and pressure called "hot spot". The violent collapse of the transient cavitations during the compression phase of the ultrasonic wave generates physical effects such as the shock wave and chemical effects due to the OH radicals generated.

The mechanism underlying ultrasonic inactivation of bacteria involves both chemical and physical effects as in the case of destruction of chemical pollutants [84]. The mechanism involving cavitation, collapse of bubbles, creation of supercritical conditions enabling complete destruction of the target molecules etc is discussed in detail in earlier chapters. ROS formed from the cleavage of dissolved oxygen and water molecules such as OH \cdot , HO $_2$ \cdot and O \cdot radicals and H $_2$ O $_2$ can disrupt or damage various cellular functions or structures of microorganisms and play a significant role in the cell deactivation process through DNA damage [208]. Mediation by semiconductor oxides has been proven to be effective in enhancing the

rate of chemical and bacterial decontamination of water under sono and photochemical conditions [214-216]. However, most of these studies used titanium dioxide as the catalyst. Earlier studies from our laboratories including those described in previous chapters revealed that zinc oxide is an efficient sonocatalyst and photocatalyst for the removal of chemical and bacterial pollutants from water [104]. In this chapter, the results of our study on the zinc oxide mediated sonocatalytic removal of four common bacterial pollutants, i.e. *Escherichia coli* (*E. coli*), *Vibrio harveyi* (*V.harveyi*), *Pseudomonas aeruginosa* (*P.aeruginosa*) and *Bacillus subtilis* (*B.subtilis*) are presented. *E. coli*, *V.harveyi* and *P.aeruginosa* are of gram-ve type while *B.subtilis* is of gram +ve type.

6.2 Experimental Details

6.2.1 Materials

Yeast extract, Peptone (CAS No. 91076-46-8), and NaCl (CAS No. 7647-14-5) (High Media). Other materials used in the experiments are described in Chapter 3 Section 3.2.

6.2.2 Analytical Methods Used

Ultrasonic bath specifications are the same as described earlier in Chapter 4 Section 4.2.

6.2.3 Microorganisms chosen for the study

- (i) *Escherichia coli* (*E. coli*) is one of the major species of bacteria that lives in the lower intestine of warm-blooded animals (including birds and mammals) and is necessary for the proper digestion of food. It belongs to the family *Enterobacteriaceae*. It is a non-spore

forming gram negative organism existing in the form of straight rods arranged singly or in pairs. *E. coli* [Fig. 6.1(a)] is usually harmless, but can cause clinical syndromes like diarrhea, urinary tract infection, pyrogenic infection and septicemia.

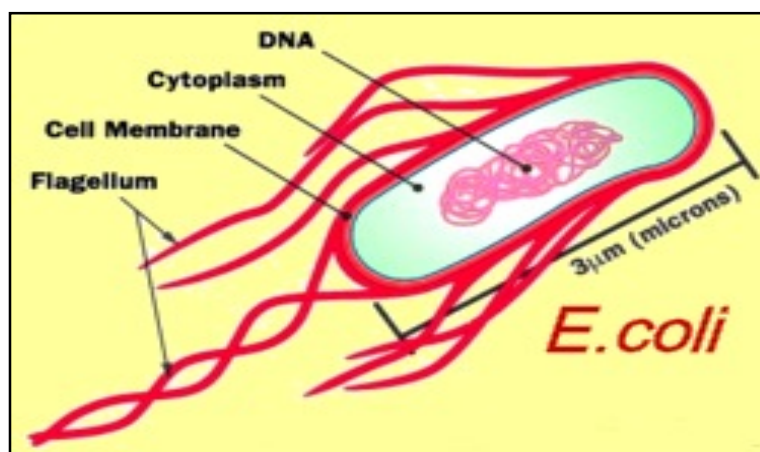


Fig.6.1(a): Image of *E. coli*

- (ii) *Bacillus subtilis* (*B.subtilis*) [Fig. 6.1(b)] belongs to the family Bacillaceae. It is a spore forming, gram positive rod widely adopted as a model organism. It is not considered to be a human pathogen, but it can contaminate food and rarely cause food poisoning. It is capable of forming a tough, protective endospore which allows it to tolerate extreme environmental conditions. It is not biologically active. It produces the enzyme that has been reported to cause dermal allergic or hypersensitivity reaction in individuals.

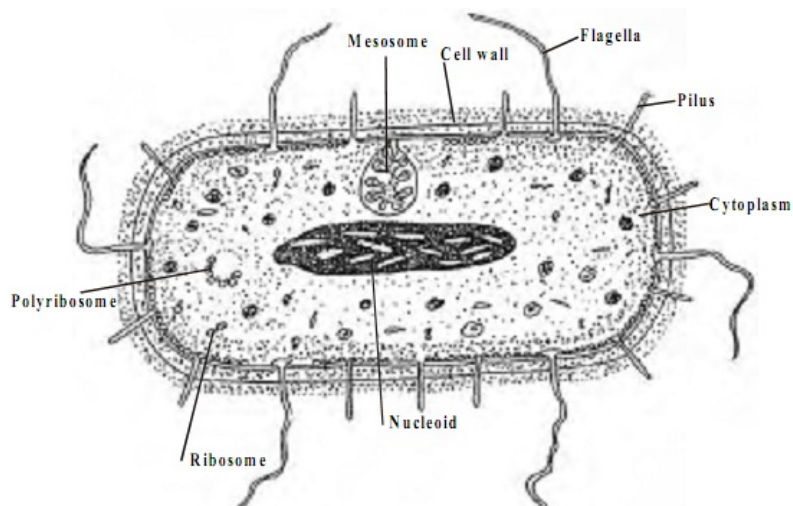


Fig.6.1 (b): Image of *B.subtilis*.

(iii) *Vibrio harveyi* (*V.harveyi*) is a rod-shaped marine bioluminescent gram- negative bacterium in the genus *Vibrio*. *V.harveyi* is a potential pathogen, a more common cause of luminous vibriosis in commercially farmed marine invertebrates. It belongs to the family of Vibrionaceae [Fig. 6.1(c)].

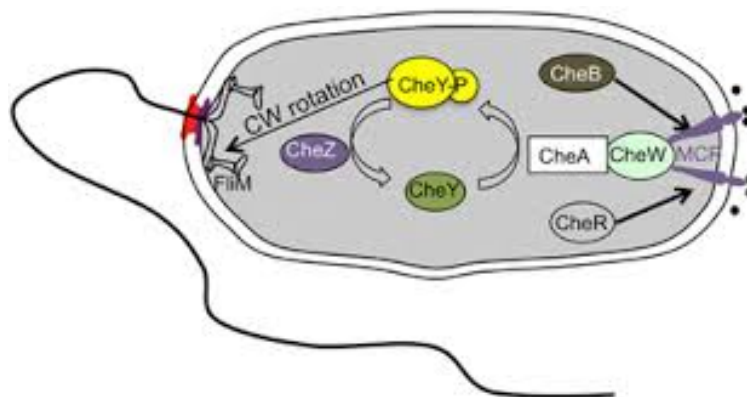


Fig.6.1(c): Image of *V.harveyi*.

- (iv) *Pseudomonas aeruginosa* (*P.aeruginosa*) is a gram negative Bacillus that is typically 1-3 μm in length. The organism is typically a strict aerobe. It is generally found in moist environments. It can also be found in water and soil as well as on fruits, vegetables and flowers. *P.aeruginosa* may cause acute pneumonia or may be a chronic colonizer of the lungs [Fig.6.1(d)].



Fig.6.1(d): Image of *P.aeruginosa*.

6.2.4 Culture conditions

Microorganisms *E.coli*, *B.subtilis*, *P.aeruginosa* and *V. harveyi* were obtained from Environmental Biotechnology Laboratory, School of Environmental Studies, Cochin University of Science and Technology.

The culture medium for stock cultures of *E. coli*, *B. subtilis* and *P.aeruginosa* is the nutrient broth containing 5 g L⁻¹ yeast extract, 5 g L⁻¹ peptone and 5 g L⁻¹ NaCl in distilled water at pH 7.5. The culture

medium of *V.harveyi* consists of 1 g L⁻¹ yeast extract, 5 gL⁻¹ peptone and 0.1gL⁻¹ ferric phosphate in sea water at pH 7.5. The bacterial cells were inoculated and subcultured under sterile conditions, grown overnight at ~37°C for 24 hr in 100mL of the nutrient broth under aerobic conditions by constant agitation in a shaker incubator at 140 rpm. The cells were then sedimented by centrifugation at 8000 rpm for 15 minutes at 4°C and the bacterial pellet obtained was washed with sterile distilled water. It was then resuspended in sterile distilled water and the absorbance was measured at 600 nm using a UV-Visible spectrophotometer. The cell suspensions were diluted with sterile distilled water in Pyrex glass beakers to the required cell density corresponding to 10⁵-10⁷ colony forming units per milliliter (CFU/mL). This suspension in required volume was taken in bottles containing weighed amounts of the catalysts (0.1g/L) and irradiated using US of frequency 40 KHz and a power of 100W. The samples were covered with aluminum foil before and after irradiation to eliminate the effects of diffused light illumination, if any. The temperature was kept at ~37°C during US irradiation by circulating water maintained at appropriate temperature. Sampling was done at predetermined time intervals by pipetting out 1mL of the experimental solution into 9 mL sterile saline and serially diluting. After mixing, 0.1 mL aliquot of each dilution was spread plated. The cell inactivation was monitored by counting the CFU/mL after 24 h incubation at ~37°C. Since *V. harveyi* is a marine bacterium, sterile seawater was used in place of distilled water. All experiments were repeated thrice and the average count was taken.

6.3 Results and Discussion

Preliminary investigations on the sonocatalytic disinfection of organisms were made using ZnO, TiO₂ and ZnO-TiO₂ composite as catalysts under identical conditions. The results show that ZnO is a more efficient sonocatalyst when compared to TiO₂ for the deactivation of organisms in 2 hr time under otherwise identical conditions as shown in Fig. 6.2. ZnO-TiO₂ (4:6) is slightly more active than ZnO. For all organisms, the sonocatalytic activity for deactivation is in the order ZnO-TiO₂ > ZnO > TiO₂.

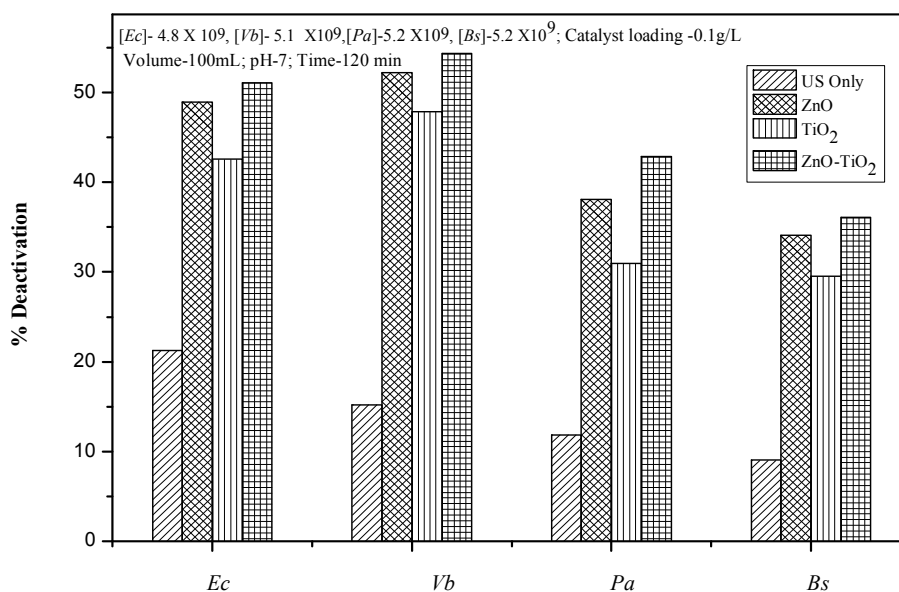


Fig.6.2: Comparison of sonocatalytic activities of various catalysts
Ec: E.coli, Vb: V.harveyi, Pa: P.aeruginosa, Bs: B.subtilis

As expected, no significant deactivation of any of the organisms was observed in the absence of US, with catalyst. However, moderate deactivation of the organism was observed under US irradiation even in the

absence of the catalysts, in the order *E.coli* > *V.harveyi* > *P.aeruginosa* > *B.subtilis*. The enhancing effect in presence of the catalyst is not due to aggregation or adsorption of the cells as no such reduction was observed during the incubation of the organisms, under identical conditions in the absence of irradiation in the presence of catalyst. The enhancement in presence of the catalyst can be attributed to the increased production of OH radicals on the surface of the semiconductor. SEM images of the organisms [Fig. 6.3(a)–(l)] before and after US irradiation and with and without catalyst show that irradiation causes morphological changes and possibly cell-wall disruption. Before illumination, the cells had cylindrical shape. After illumination, many of the cells were completely damaged and the cells lost their viability, as observed from the number of CFU/mL. The damage caused by the US in presence of catalyst is significantly more than that in the absence of the catalyst under otherwise identical conditions.

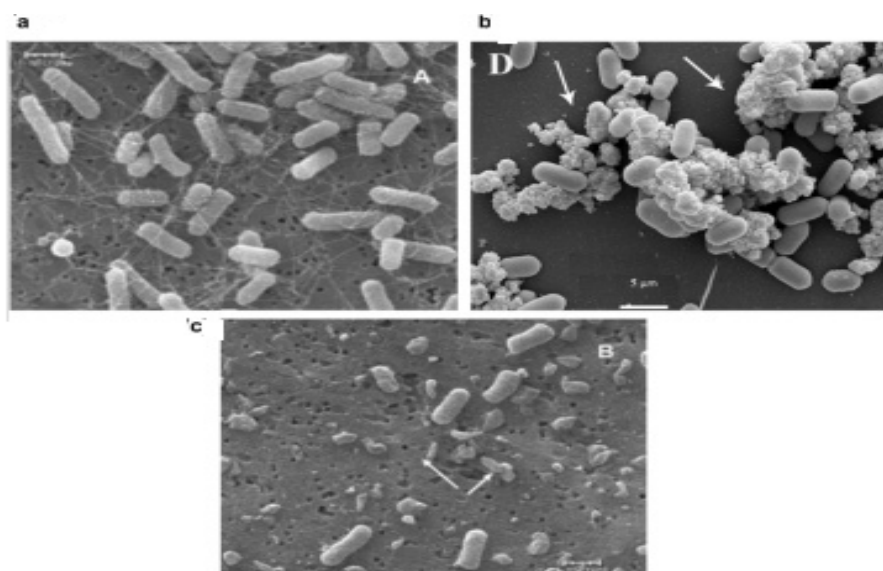


Fig. 6.3(a, b& c): SEM image of *E. coli*: (a) before US irradiation, (b) after US irradiation, and (c) after US irradiation in presence of ZnO.

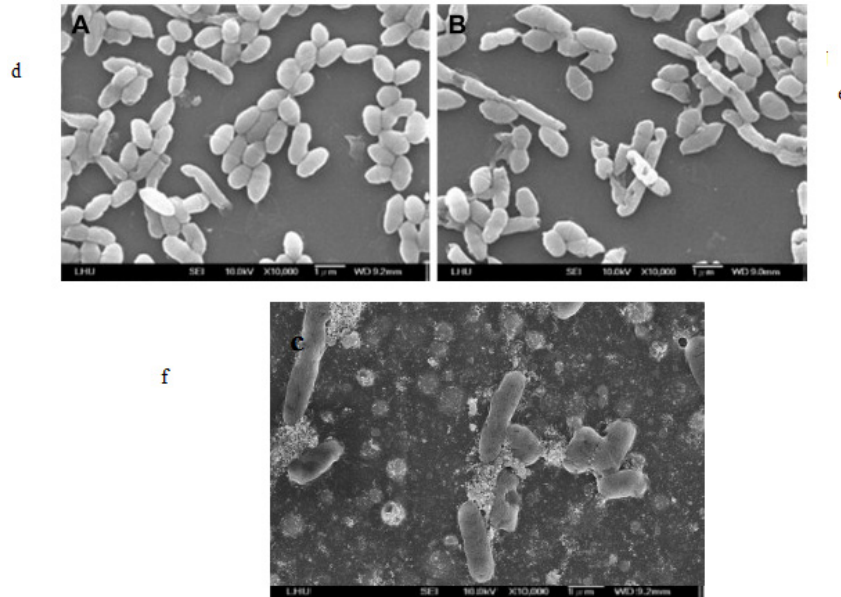


Fig. 6.3 (d, e & f): SEM image of *B.subtilis*: (d) before US irradiation,(e) after US irradiation, and (f) after US irradiation in presence of ZnO.

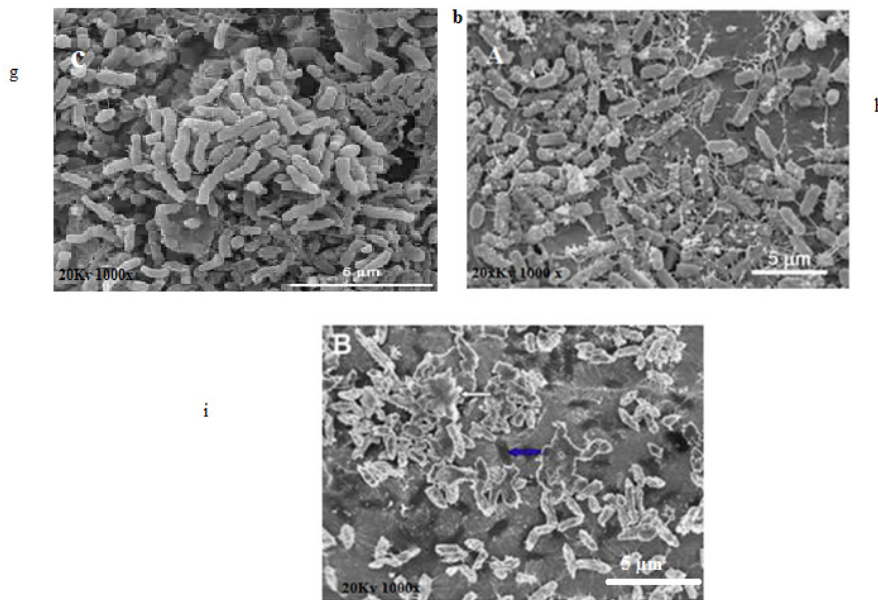


Fig. 6.3 (g, h & i): SEM image of *V.harveyi*: (g) before US irradiation, (h) after US irradiation, and (i) after US irradiation in presence of ZnO.

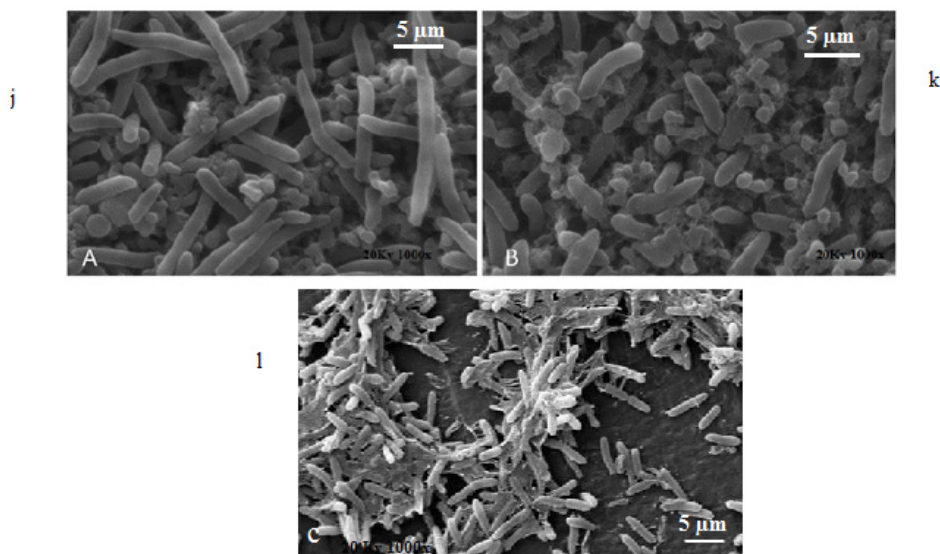


Fig. 6.3 (j, k & l): SEM image of *P.aeruginosa*: (j) before US irradiation, (k) after US irradiation and (l) after US irradiation in presence of ZnO.

Detailed investigation on the deactivation of bacterial organisms by a series of semiconductors is in progress in our laboratory at present. Of them, studies in presence of ZnO are reported here. The effect of various reaction parameters on the sonocatalytic deactivation of the organisms in presence of ZnO is investigated and the findings are as follows:

6.3.1 Effect of catalyst loading

The effect of catalyst loading on the bactericidal activity was examined by varying the ZnO concentration from 0.02 to 0.15g/L keeping all other reaction parameters constant. The results are shown in Fig.6.4 (a, b, c & d), Fig.6.5 (a, b, c & d), Fig.6.6 (a, b, c & d) and Fig.6.7 (a, b, c & d). The deactivation increased with increase in catalyst loading.

However, above 0.1 g/L, the increase was less pronounced as seen by comparing the results of 0.1 and 0.15 g/L towards the later stages of the reaction. The optimum catalyst loading remains more or less same irrespective of the initial cell count present in the system. The data in the figures is translated into percentage deactivation and presented in table 6.1 (a)-(d).

E.coli

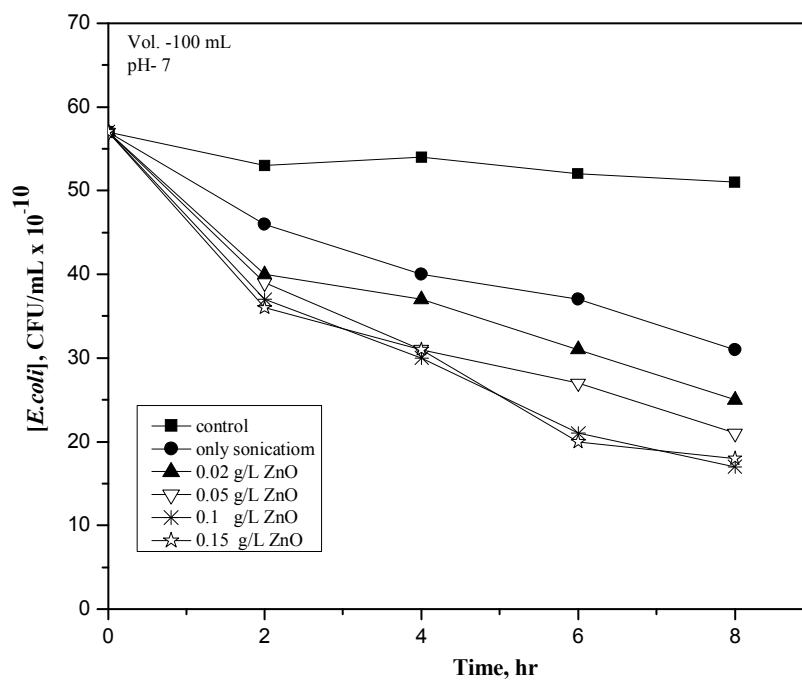


Fig.6.4(a): Effect of catalyst loading on the sonocatalytic deactivation of *E. coli* (57×10^{10} CFU/mL) by ZnO.

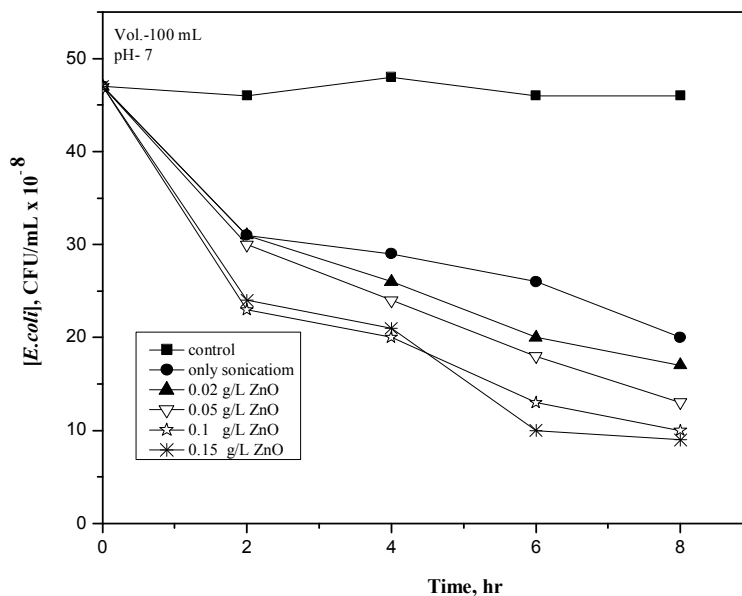


Fig.6.4(b): Effect of catalyst loading on the sonocatalytic deactivation of *E. coli* (47×10^8 CFU/mL) by ZnO.

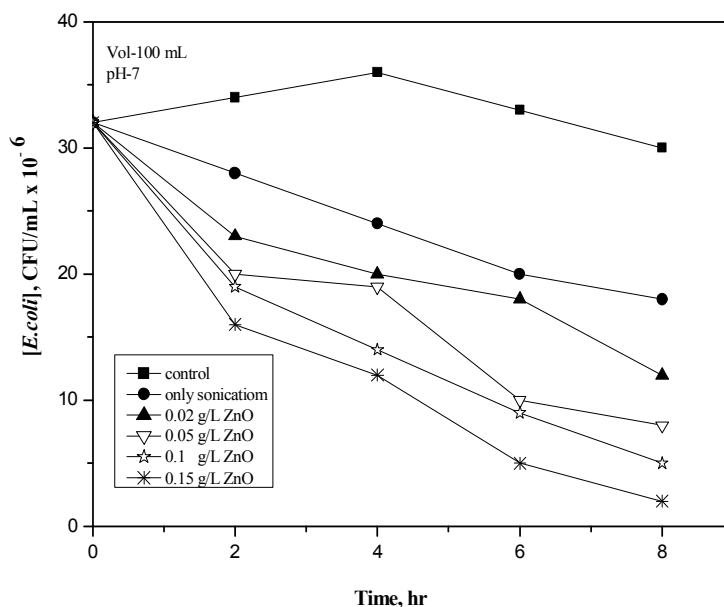


Fig.6.4(c): Effect of catalyst loading on the sonocatalytic deactivation of *E. coli* (33×10^6 CFU/mL) by ZnO.

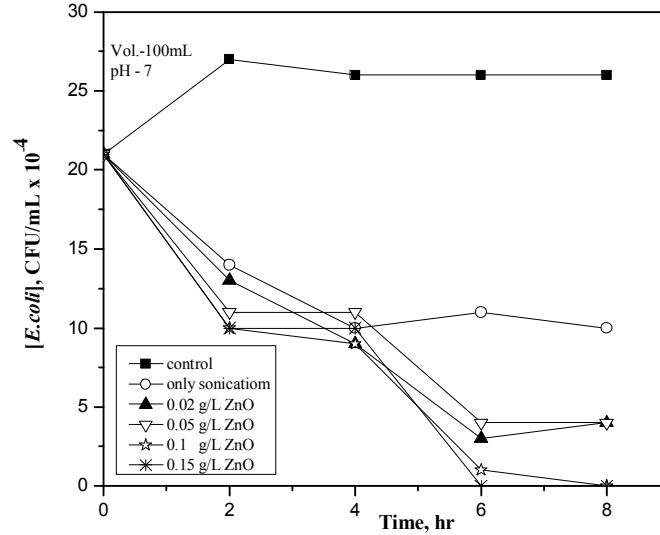


Fig.6.4(d): Effect of catalyst loading on the sonocatalytic deactivation of *E. Coli* (21×10^4 CFU/mL) by ZnO.

Table 6.1(a): Sonocatalytic deactivation (%) of *E coli* vs catalyst loading (ZnO)

[<i>E.coli</i>] CFU/mL	Time (hr)	Control	US only	0.02 g/L ZnO+US	0.05g/L ZnO+US	0.10g/L ZnO+US	0.15 g/L ZnO+US
57×10^{10}	0	0	0	0	0	0	0
	2	3.0	19.0	29.0	31.0	35.0	36.0
	4	3.0	29.0	35.0	45.0	47.0	45.0
	6	3.0	35.0	45.0	52.0	63.0	64.0
	8	3.0	45.0	56.0	63.0	70.0	68.0
47×10^8	0	0	0	0	0		0
	2	3.0	34.0	34.0	36.0	51.0	48.0
	4	3.0	38.0	44.0	48.0	57.0	55.0
	6	3.0	44.0	57.0	61.0	72.0	78.0
	8	3.0	57.0	63.0	72.0	78.0	80.0
33×10^6	0	0	0	0	0	0	0
	2	3.0	34.0	34.0	40.0	45.0	54.0
	4	3.0	42.0	42.0	45.0	60.0	65.0
	6	3.0	49.0	49.0	71.0	74.0	85.0
	8	3.0	65.0	65.0	77.0	85.0	94.0
21×10^4	0	0	0	0	0	0	0
	2	3.0	50.0	53.0	60.0	64.0	64.0
	4	3.0	64.0	67.0	60.0	67.0	64.0
	6	3.0	60.0	89.0	85.0	96.0	100
	8	3.0	64.0	85.0	85.0	100	100

B. subtilis

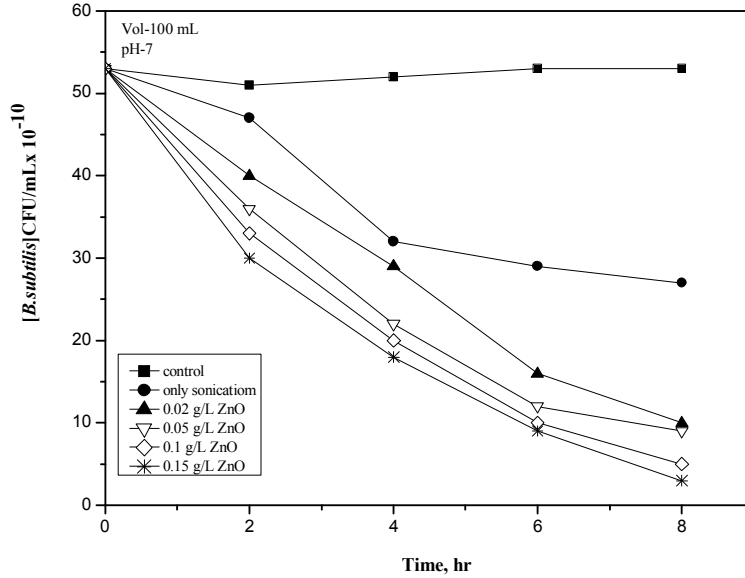


Fig.6.5 (a): Effect of catalyst loading on the sonocatalytic deactivation of *B. subtilis* (53×10^{10} CFU/mL) by ZnO.

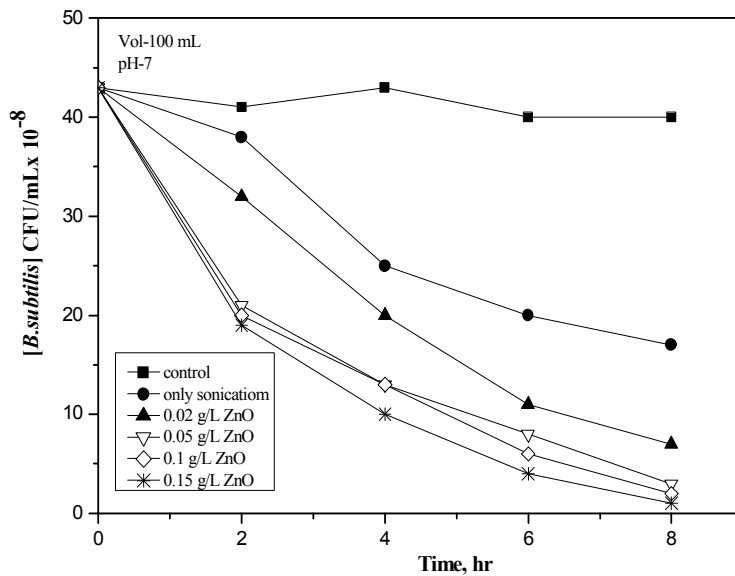


Fig.6.5 (b): Effect of catalyst loading on the sonocatalytic deactivation of *B. subtilis* (43×10^8 CFU/mL) by ZnO.

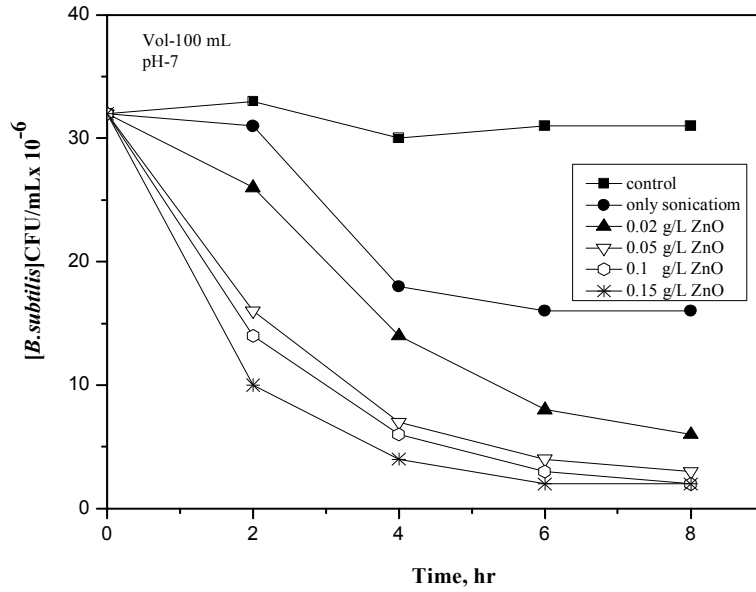


Fig.6.5 (c): Effect of catalyst loading on the sonocatalytic deactivation of *B. subtilis* (32×10^6 CFU/mL) by ZnO

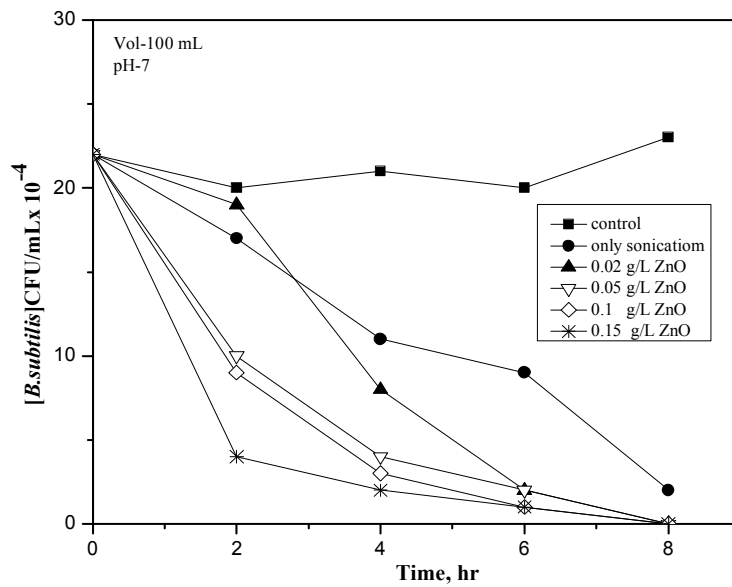


Fig.6.5 (d): Effect of catalyst loading on the sonocatalytic deactivation of *B. subtilis* (22×10^4 CFU/mL) by ZnO.

Table 6.1.(b): Sonocatalytic deactivation (%) of *B.subtilis* vs catalyst loading (ZnO)

[<i>B.subtilis</i>] CFU/mL	Time (hr)	Control	US only	0.02 g/L ZnO+US	0.05g/L ZnO+US	0.10g/L ZnO+US	0.15 g/L ZnO+US
53 x 10 ¹⁰	0	0	0	0	0	0	0
	2	3.0	11.0	24.0	32.0	37.0	43.0
	4	3.0	39.0	45.0	58.0	62.0	66.0
	6	3.0	45.0	69.0	77.0	81.0	83.0
	8	3.0	49.0	81.0	83.0	90.0	94.0
43 x 10 ⁸	0	0	0	0	0	0	0
	2	1.0	11.0	25.0	51.0	53.0	55.0
	4	2.0	41.0	53.0	69.0	69.0	76.0
	6	6.0	53.0	74.0	81.0	86.0	90.0
	8	6.0	60.0	83.0	93.0	95.0	97.0
32 x 10 ⁶	0	0	0	0	0	0	0
	2	1.0	31.0	16.0	50.0	56.0	68.0
	4	1.0	43.0	56.0	78.0	81.0	87.0
	6	1.0	50.0	75.0	87.0	90.0	93.0
	8	1.0	50.0	81.0	90.0	93.0	93.0
22 x 10 ⁴	0	0	0	0	0	0	0
	2	1.0	22.0	13.0	54.0	59.0	81.0
	4	1.0	50.0	63.0	81.0	86.0	90.0
	8	1.0	59.0	90.0	90.0	95.0	95.0
		1.0	90.0	100	100	100	100

V.harveyi

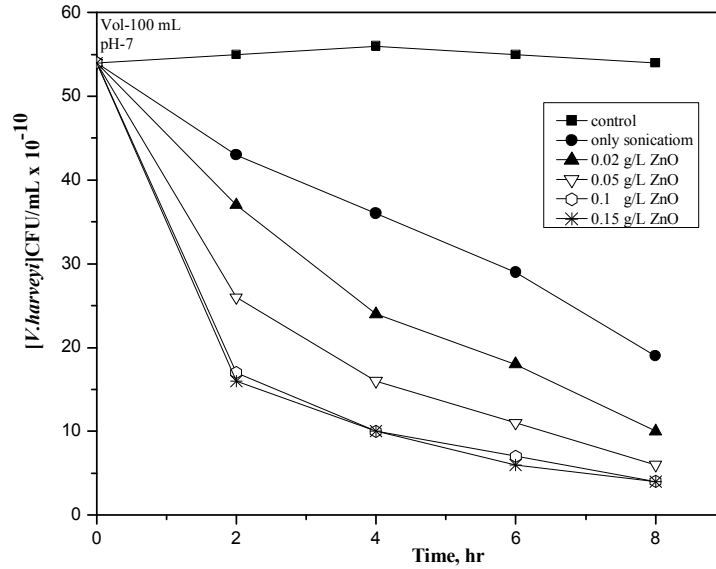


Fig.6.6(a): Effect of catalyst loading on the sonocatalytic deactivation of *V.harveyi* (54×10^{10} CFU/mL) by ZnO.

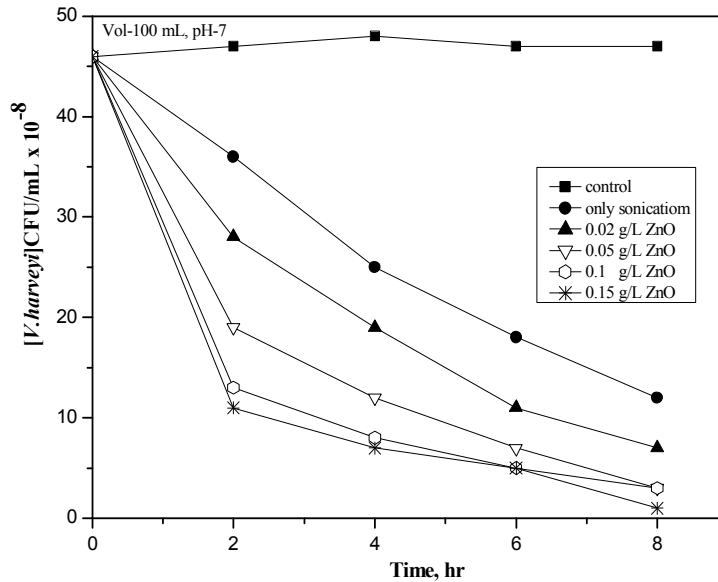


Fig.6.6(b): Effect of catalyst loading on the sonocatalytic deactivation of *V.harveyi* (46×10^8 CFU/mL) by ZnO.

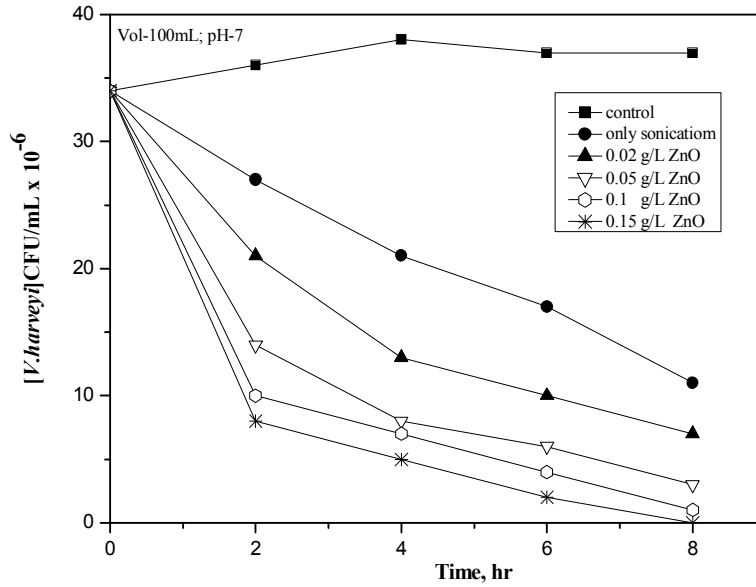


Fig.6.6(c): Effect of catalyst loading on the sonocatalytic deactivation of *V.harveyi* (34×10^6 CFU/mL) by ZnO.

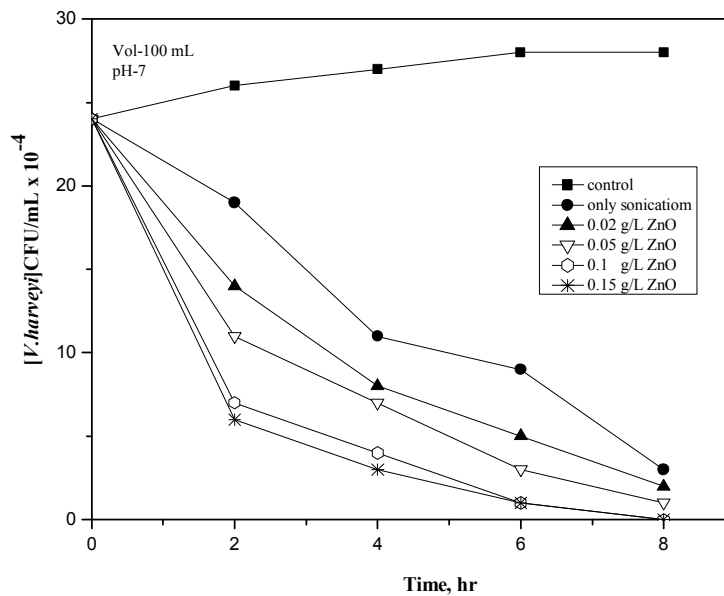


Fig.6.6(d): Effect of catalyst loading on the sonocatalytic deactivation of *V.harveyi* (24×10^4 CFU/mL) by ZnO.

Table 6.1(c): Sonocatalytic deactivation (%) of *V.harveyi* vs catalyst loading (ZnO)

[<i>V.harveyi</i>]/CF U/mL	Time (hr)	Control	US only	0.02 g/L ZnO+US	0.05g/L ZnO+US	0.10g/L ZnO+US	0.15 g/L ZnO+US
54 x 10 ¹⁰	0	0	0	0	0	0	0
	T2	3.0	23.0	33.0	53.0	69.0	71.0
	4	3.0	35.0	57.0	71.0	82.0	82.0
	6	3.0	48.0	67.0	80.0	87.0	89.0
	8	3.0	66.0	82.0	89.0	92.0	92.0
46 x 10 ⁸	0	0	0	0	0	0	0
	2	2.0	25.0	41.0	60.0	72.91	77.0
	4	2.0	47.0	60.0	75.0	83.33	85.0
	6	2.0	62.0	77.0	85.0	89.58	89.0
	8	2.0	75.0	85.0	93.0	93.75	97.0
34 x 10 ⁶	0	0	0	0	0	0	0
	2	3.0	25.0	41.0	61.0	72.22	77.0
	4	3.0	41.0	63.0	77.0	80.55	86.0
	6	3.0	52.0	72.0	83.0	88.88	94.0
	8	3.0	69.0	80.0	91.0	97.22	100
24 x 10 ⁴	0	0	0	0	0	0	0
	2	3.0	26.0	46.0	57.0	73.07	76.0
	4	3.0	57.0	69.0	73.0	84.61	88.0
	6	3.0	65.0	80.0	88.0	96.15	91.0
	8	3.0	88.0	92.0	96.0	100	100

P.aeruginosa

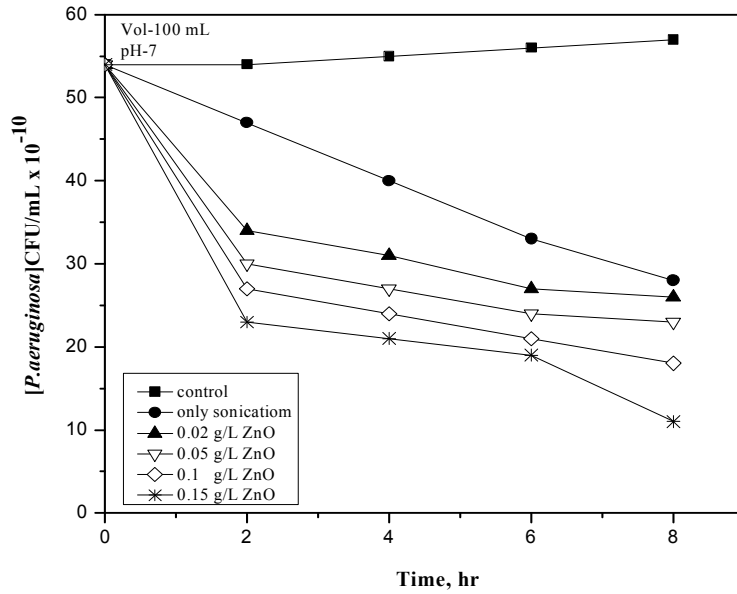


Fig.6.7(a): Effect of catalyst loading on the sonocatalytic deactivation of *P.aeruginosa* (54×10^{10} CFU/mL) by ZnO.

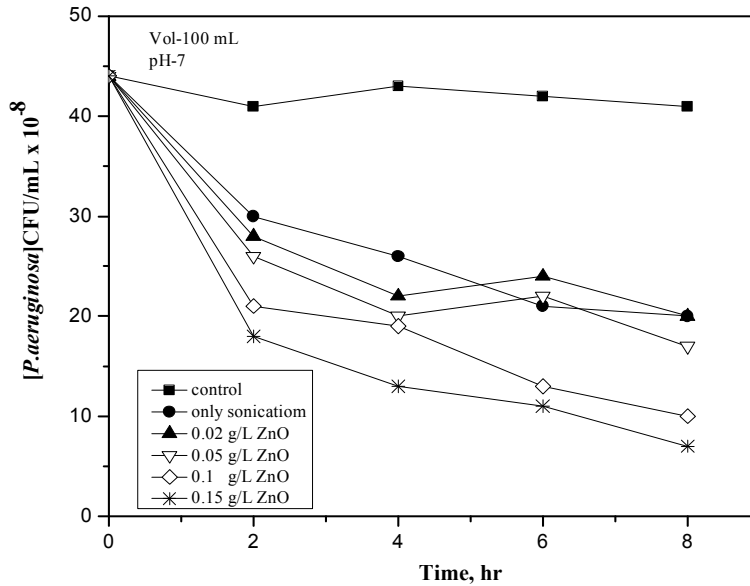


Fig.6.7(b): Effect of catalyst loading on the sonocatalytic deactivation of *P.aeruginosa* (44×10^8 CFU/mL) by ZnO.

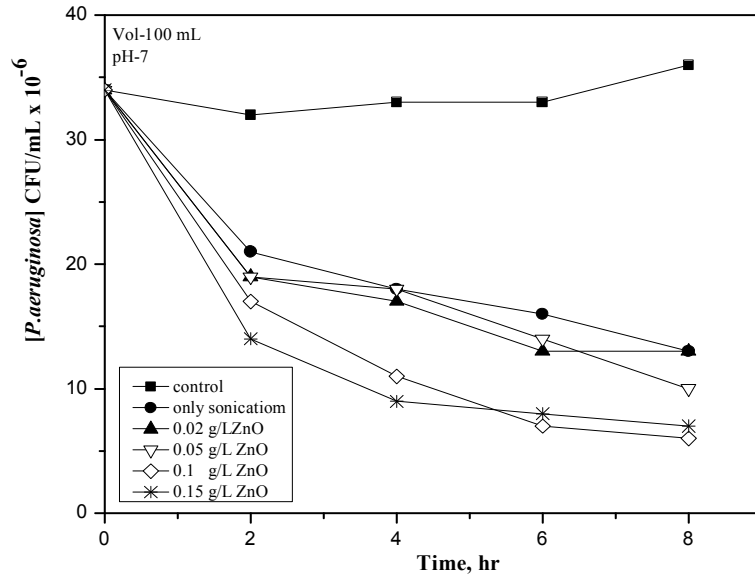


Fig.6.7(c): Effect of catalyst loading on the sonocatalytic deactivation of *P.aeruginosa* (34×10^6 CFU/mL) by ZnO.

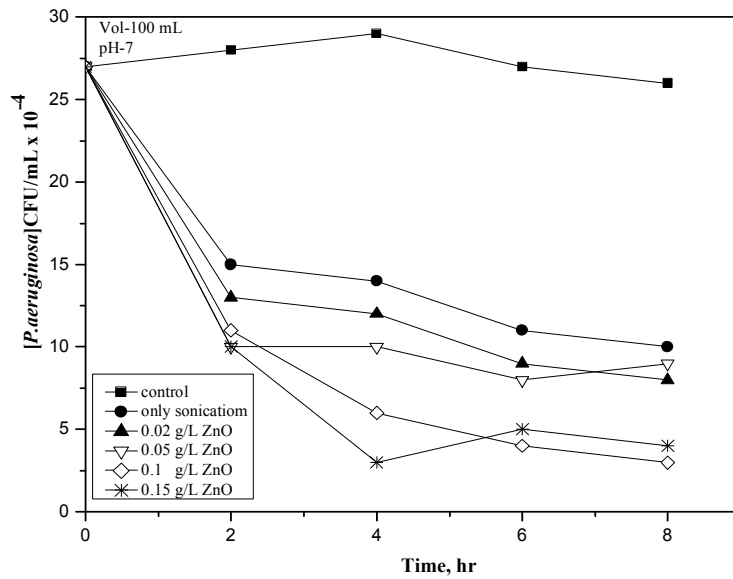


Fig.6.7(d): Effect of catalyst loading on the sonocatalytic deactivation of *P.aeruginosa* (27×10^4 CFU/mL) by ZnO.

Table 6.1(d): Sonocatalytic deactivation (%) of *P.aeruginosa* vs catalyst loading

[<i>P.aeruginosa</i>] CFU/mL	Time (hr)	Control	US only	0.02 g/L ZnO+US	0.05g/L ZnO+US	0.10g/L ZnO+US	0.15 g/L ZnO+US
54 x 10 ¹⁰	0	0	0	0	0	0	0
	2	0	12.96	37.03	44.4	50	57.40
	4	2.7	25.92	4.59	50	55.5	61.11
	6	3.7	38.88	50	55	61.11	64.81
	8	4.3	48.14	51	57	66.66	79.62
44 x 10 ⁸	0	0	0	0	0	0	0
	2	1.7	31.81	36.36	40.90	52.27	59.09
	4	1.7	40.90	50	54.54	56.81	70.45
	6	7.7	52.27	45.45	50	70.45	75
	8	3.7	54.54	54.54	61.36	77.27	84.09
34 x 10 ⁶	0	0	0	0	0	0	0
	2	0	38.23	44.11	44.11	50	58.82
	4	2.7	47.05	50	47.05	67.64	73.52
	6	2.7	52.94	61.76	58.52	79.41	76.47
	8	2.7	61376	61.76	70.58	82.35	79.41
27 x 10 ⁴	0	0	0	0	0	0	0
	2	0	44.44	51.85	62.96	59.25	62.96
	4	1.8	48.14	55.55	62.96	77.77	88.88
	6	1.8	59.25	66.66	70.39	85.18	81.46
	8	2.0	62.96	70.37	66.66	88.88	85.85

Based on the data, for convenience, the optimum loading is taken as 0.1 g/L for all cases. The disinfection was significant in the initial stage. However, the rate of disinfection decreased as time progressed. Increased deactivation with increase in catalyst loading may be due to increased number of active sites available for interaction between the semiconductor particles and the bacterial cells in suspension together with the increased ROS production from the enhanced surface area. However, at higher loadings there is a rapid saturation of the interaction between the surface

and the micro-organisms which results in stabilized or even decreased rate of deactivation. This saturation by the organisms or their damaged remnants on the catalyst surface also can cause decreased rate (number of organisms deactivated per unit time,) of deactivation with time. The screening effect seen in photocatalysis which spatially limits the photoactive region is not seen in sonocatalysis as the ultrasonic energy is propagated throughout the entire region in the vessel. Hence, the optimum dosage is much higher in sonocatalysis compared to photocatalysis under identical conditions in reaction vessels of the same size and geometry for the mineralization of chemicals [Results from our laboratory]. In any case, there is an optimum beyond which the activity is lower which may be due, at least partially, to the shielding effect of these overcrowded particles from the energy source.

6.3.2 Effect of concentration

The effect of change in the population of the organisms on the rate of deactivation is shown in Fig. 6.8 (a,b,c&d). The concentration for optimum effectiveness may vary with time of irradiation. Since the concentration of the organism is varying by orders of magnitude with time, the rate is transformed into comparable arbitrary unit. The rate decreased with time of irradiation and stabilized later in all cases for all organisms. The initial rate of deactivation increased with increase in concentration. This showed that the rate is dependent on the concentration of the organism and the availability of catalyst sites. As the reaction progressed, the effective concentration of organism decreased and the concentration dependent deactivation rate also decreased correspondingly.

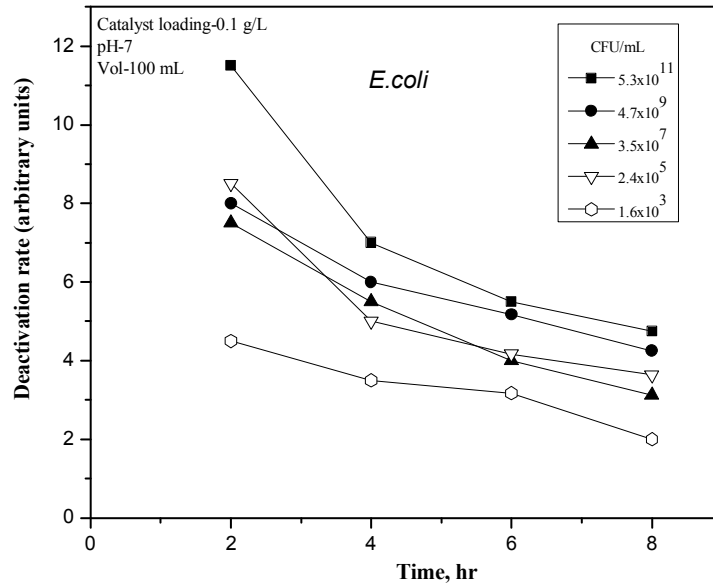


Fig.6.8(a): Effect of concentration of *E.coli* on its sonocatalytic deactivation by ZnO.

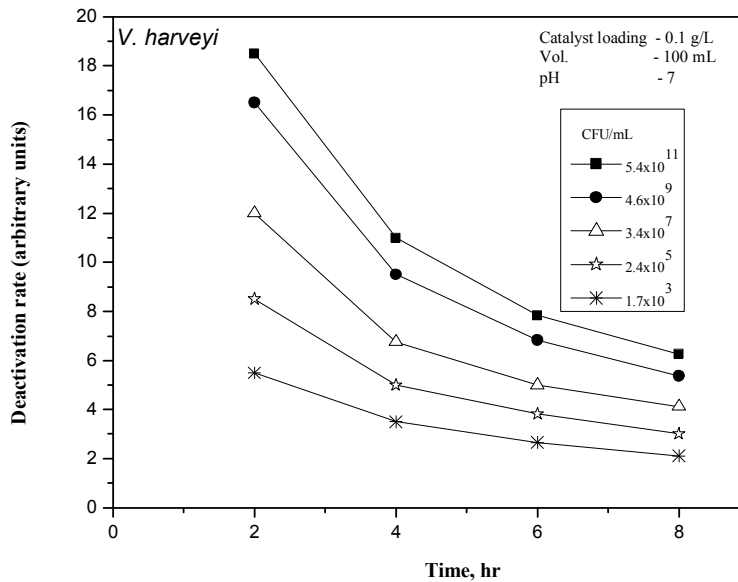


Fig.6.8(b): Effect of concentration of *V.harveyi* on its sonocatalytic disinfection by ZnO.

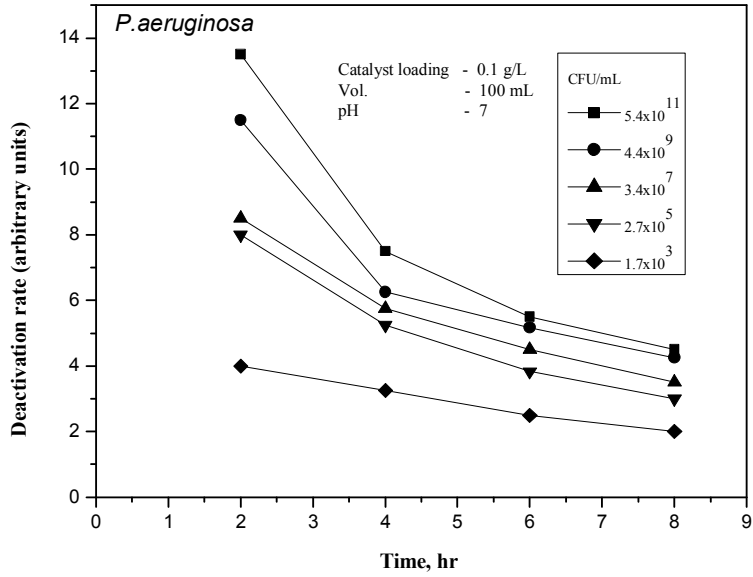


Fig.6.8 (c): Effect of concentration of *P.aeruginosa* on its sonocatalytic deactivation by ZnO.

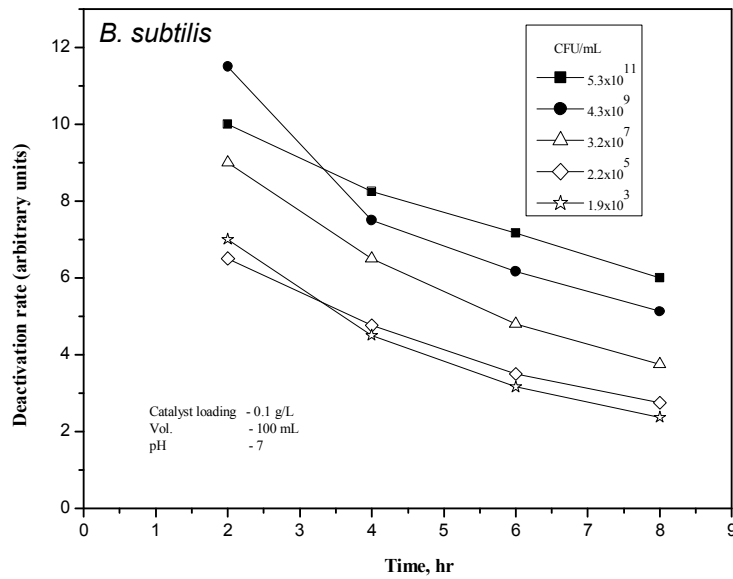


Fig.6.8(d): Effect of concentration of *B.subtilis* on its sonocatalytic disinfection by ZnO.

No clear concentration of respective organism to achieve optimum rate of initial deactivation is seen at least in the range investigated here. The rate of deactivation continues to increase with increase in population of the organism. Hence for convenience of experiments and better consistency, concentration in the range of $\sim 10^9$ CFU/mL is chosen for further studies.

6.3.3 Effect of pH

The effect of initial pH of the reaction system on the sonocatalytic deactivation of the organism is investigated at two different time periods of irradiation and the results are shown in Fig. 6.9 (a-h). The organisms are destroyed under extreme acidic and alkaline conditions in all cases as seen in the figures. US enhances the deactivation at all pH, even in the absence of the catalyst. In the case of *E.coli*, the deactivation at neutral pH is $\sim 19\%$ in 2 hr. In presence of catalyst and US, the deactivation is $\sim 52\%$. In presence of US only, the deactivation is around 35% in 2 hr. However, in the absence of US or US/ZnO, the deactivation does not increase with time and remains fairly same even after 4 hr. The extent of US/ZnO induced enhancement is more at all pH compared to the absence of ZnO or US. The degree of enhancement of deactivation by US/ZnO is maximum at neutral pH. Earlier studies on the photocatalytic deactivation of *E. coli* in presence of TiO_2 showed that the deactivation is followed by a decrease in the pH of the system. In the current study, also decrease in pH is observed, though to a much lesser extent, i.e, from 7 to 6.5 in the case of neutral system. The survival of some of the bacteria in the otherwise lethal acidic pH in the absence of US irradiation or US/ZnO is due to the presence of acid-induced proteins that protect the cells from an acid shock and the tolerance of acid

adapted cells towards osmotic stress [217]. However, in presence of the high energy US radiation, such protection will not be fully effective as seen from the enhanced deactivation at all pH. The effect of ZnO/US is the least at acidic or alkaline pH compared to neutral pH, probably because the concentration of ZnO in the system will slowly diminish under the extreme conditions, as explained in earlier chapters. Hence, the real enhancement in the efficiency of ZnO/US compared to the absence of US or ZnO is more visible at the neutral pH.

The results are similar in the case of the other three organisms also as seen in Fig. 6.9(c-h). However, minor variation can be seen especially in the pH range of 5-8 for organisms *P.aeruginosa* and *V. harveyi*. In these cases, the deactivation is more at pH ~7 compared to pH 5 or 8 in presence of US/ZnO. The reason for the unusual phenomenon needs to be explored separately.

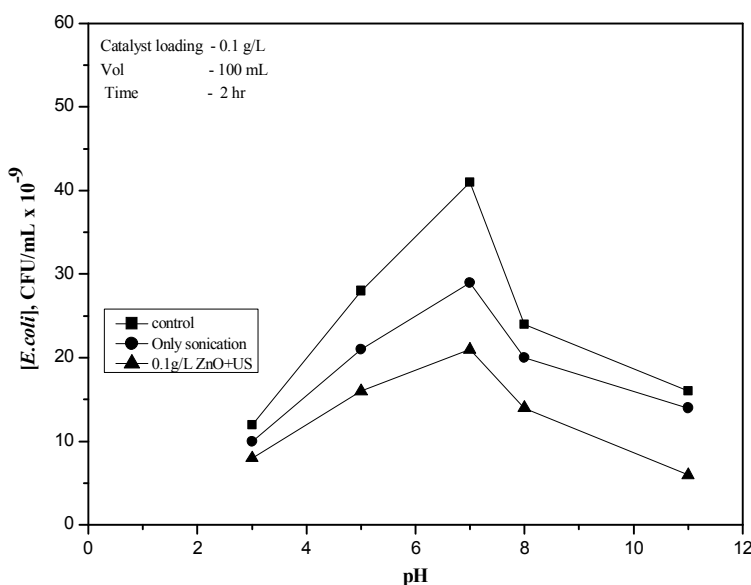


Fig.6.9 (a): Effect of pH on the sonocatalytic disinfection of *E.coli* in two hours.

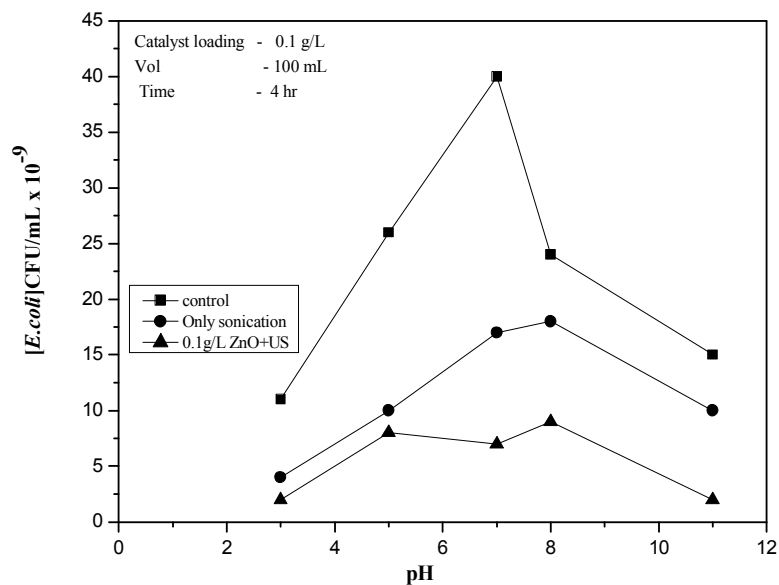


Fig.6.9 (b): Effect of pH on the sonocatalytic disinfection of *E.coli* in four hours.

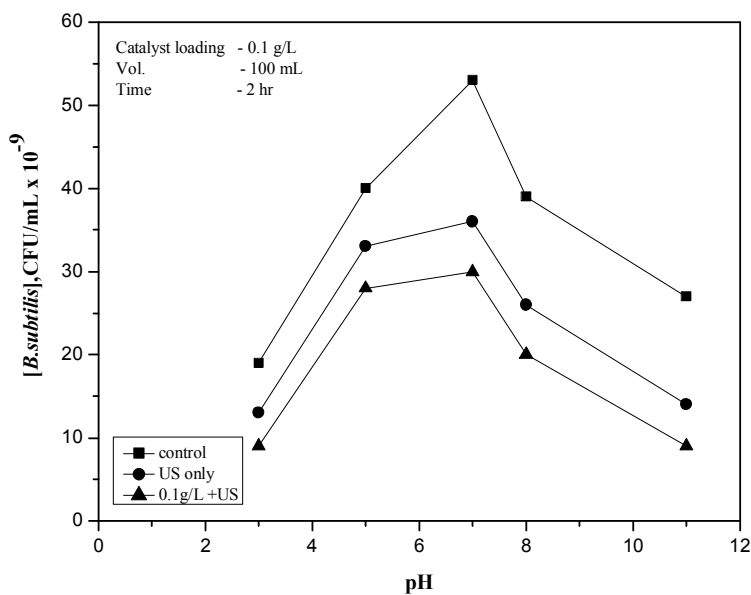


Fig.6.9 (c): Effect of pH on the Sonocatalytic disinfection of *B.subtilis* in two hours.

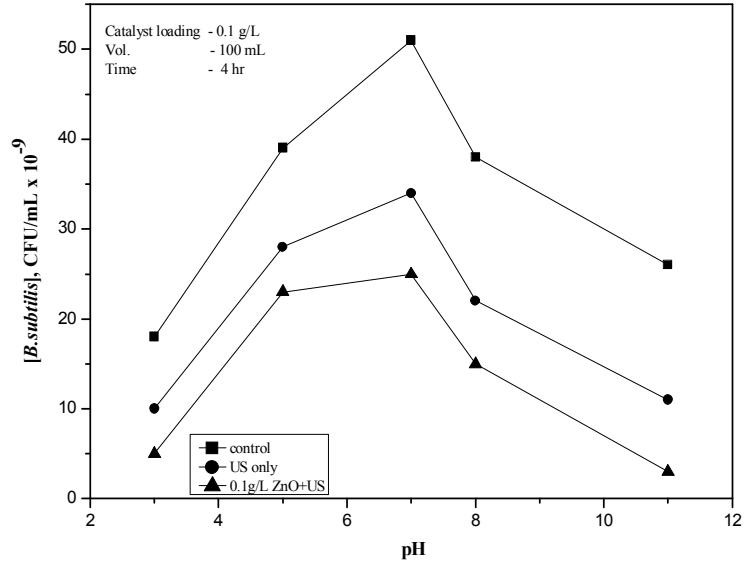


Fig.6.9 (d): Effect of pH on the Sonocatalytic disinfection of *B.subtilis* in four hours.

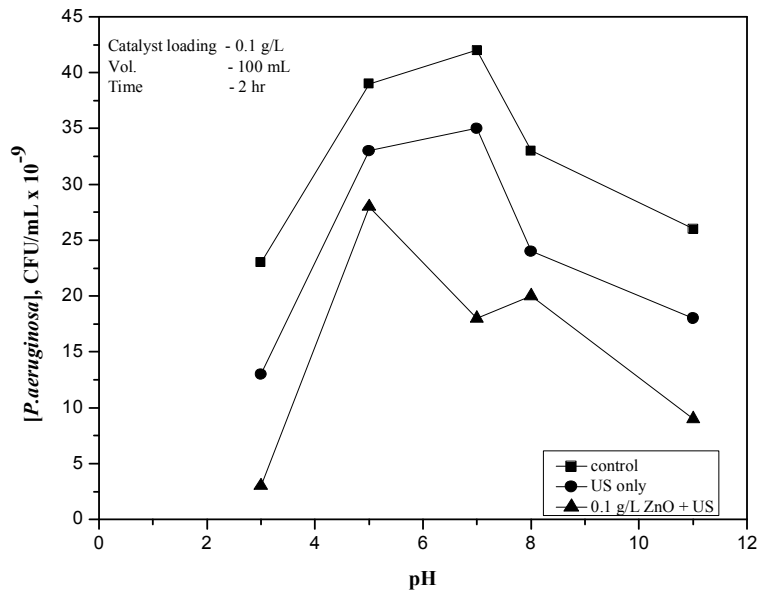


Fig.6.9 (e): Effect of pH on the Sonocatalytic disinfection of *P.aeruginosa* in two hours.

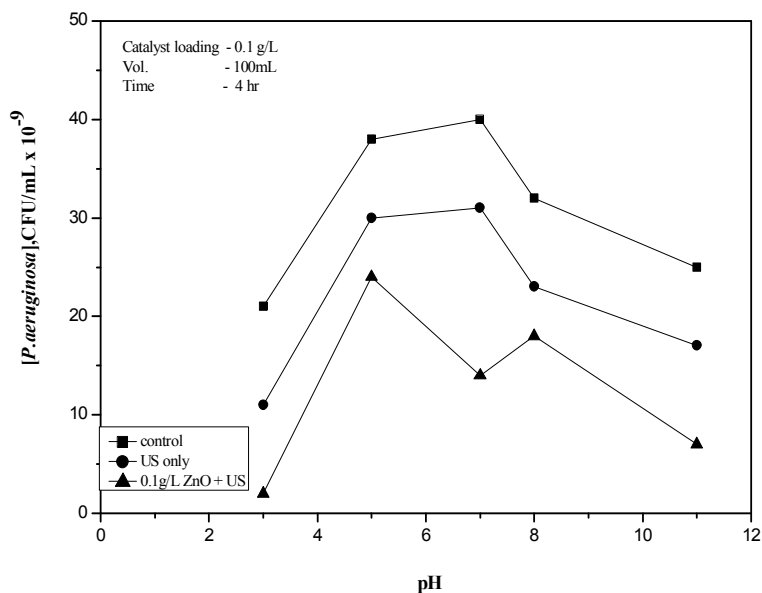


Fig.6.9 (f): Effect of pH on the Sonocatalytic disinfection of *P.aeruginosa* in four hours.

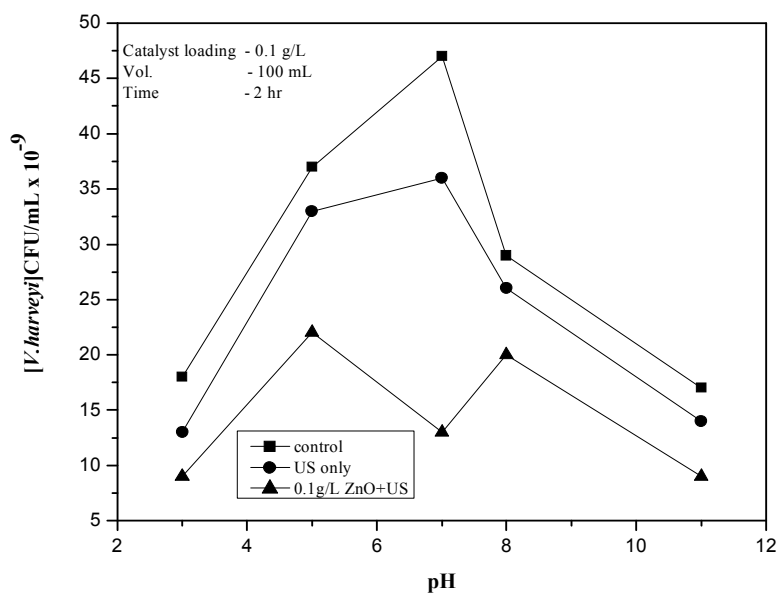


Fig.6.9 (g): Effect of pH on the Sonocatalytic disinfection of *V.harveyi* in two hours.

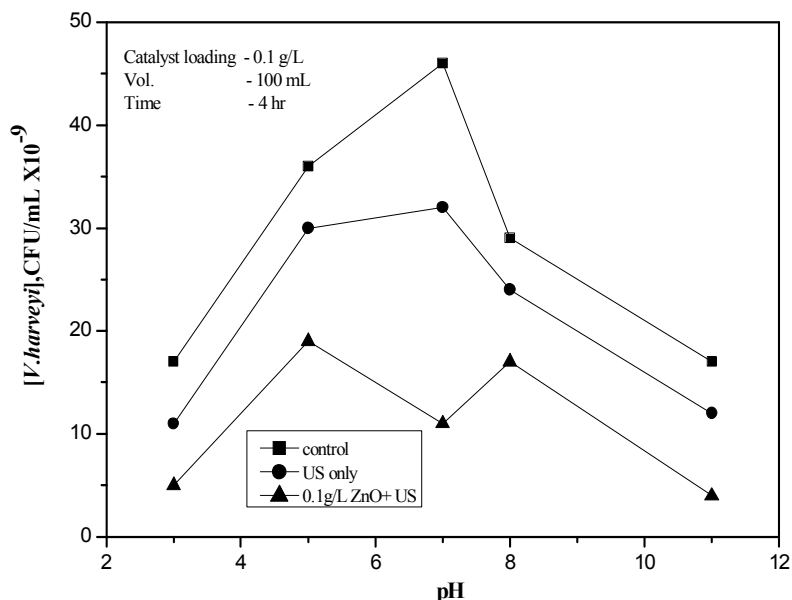


Fig.6.9 (h): Effect of pH on the Sonocatalytic disinfection of *V.harveyi* in four hours.

6.3.4 Effect of H₂O₂

As H₂O₂ is an important intermediate as well as end product in the sono and photocatalytic degradation of organic pollutants in water, experiments were carried out to study the effect of H₂O₂ on the sonocatalytic deactivation of microorganisms in presence of ZnO. A definite concentration of the microorganism in water with no sonication was used as the Control Reactive System (CRS). The effect of H₂O₂ was studied by conducting the following experiments: (i) CRS+H₂O₂ (ii) CRS+H₂O₂+US (iii) CRS+ZnO+US (iv) CRS+ZnO+H₂O₂+US. The concentration of microorganisms was followed at regular intervals in each case. The results obtained for the different microorganisms are shown in Fig.6.10 (a-d). Though H₂O₂ itself induces the disinfection, it did not

show any significant extra enhancing effect in presence of ZnO and US irradiation. In fact, the disinfection in presence of H₂O₂, catalyst, and US irradiation together was less than the sum of disinfections achieved individually by (i) H₂O₂ (ii) US + ZnO only (iii) US only (iv) H₂O₂ + US + ZnO, as applicable, as shown in Fig. 6.10 (a,b,c & d). Hence, added H₂O₂ contributes to only moderate extra effect in the case of sonocatalytic decontamination of bacterial pollutants. Though H₂O₂ is a meta-stable molecule of high redox potential (1.77 V), its disinfecting properties are derived mostly from the free radicals formed in presence of catalysts. H₂O₂ enhances the sensitivity of bacteria to heat, light, and sound. However, the benefits of added H₂O₂ are not fully reflected in the sonocatalytic system possibly because H₂O₂ formed in situ in the sonocatalytic system is already enhancing the rate of deactivation making the added effect of H₂O₂ superfluous. It has been reported that both the formation and decomposition of H₂O₂ take place concurrently in sonocatalytic systems leading to oscillation in its concentration [104]. Hence, the concentration of H₂O₂ either formed in situ or externally added cannot increase beyond a critical limit, thereby restricting the enhanced detrimental effect on bacterial organisms.

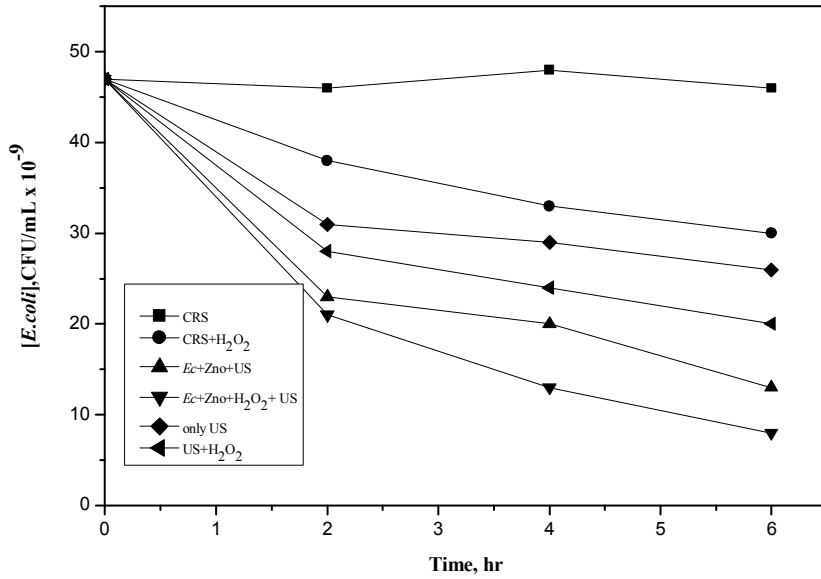


Fig.6.10 (a): Effect of H₂O₂ on the sonocatalytic disinfection of *E.coli*.

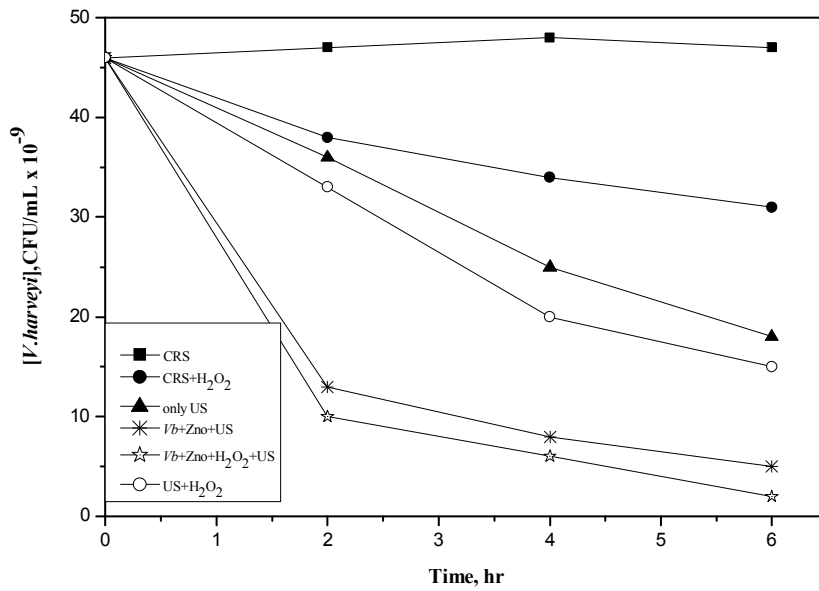


Fig.6.10 (b): Effect of H₂O₂ on the sonocatalytic disinfection of *V.harveyi*.

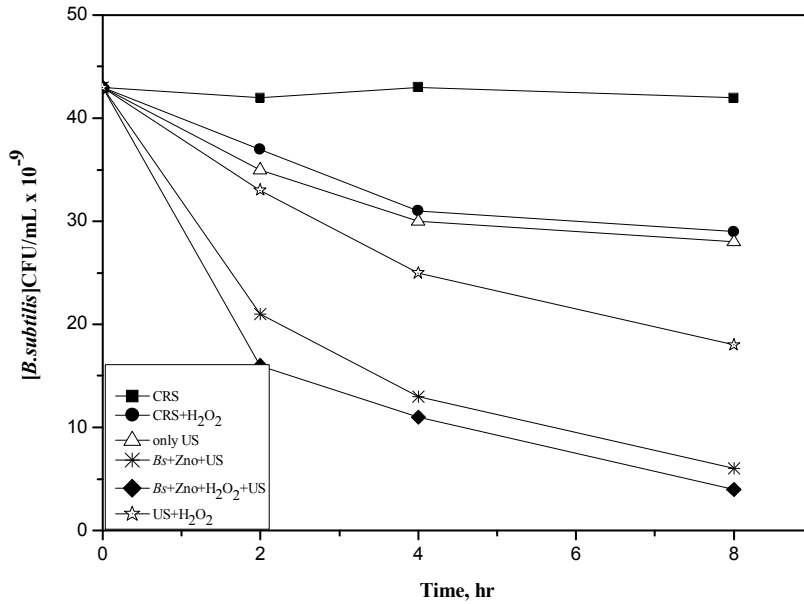


Fig.6.10 (c): Effect of H₂O₂ on the sonocatalytic disinfection of *B. subtilis*.

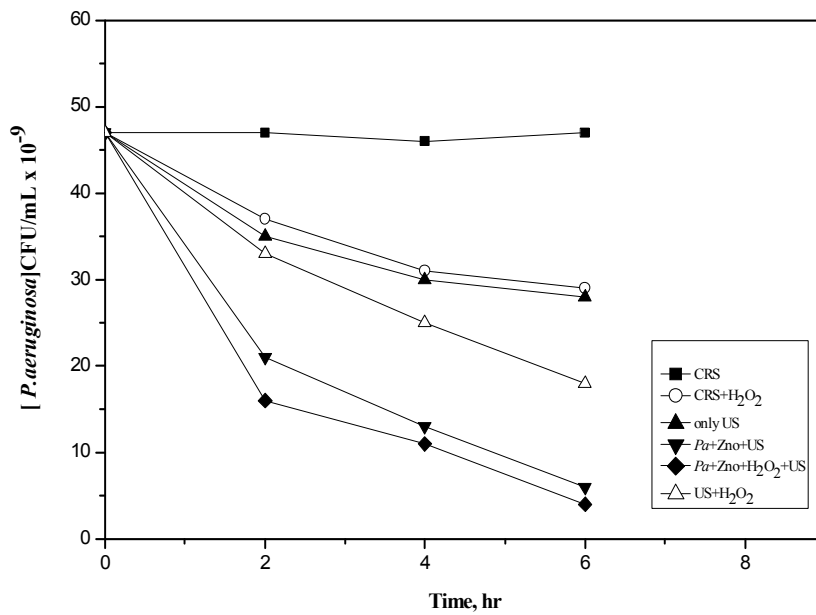


Fig.6.10 (d): Effect of H₂O₂ on the sonocatalytic disinfection of *P. aeruginosa*.

6.4 Re-emergence

One of the major problems associated with environment-friendly deactivation of bacterial agents by solar energy without the use of chemical disinfectants, is its re-emergence, once the source of energy is discontinued. The possibility of such reemergence of the organism deactivated by sonication and sonocatalysis is examined by measuring the bacterial concentration after the sonication has been put off. In this case, the concentration of organism is $\sim 2 \times 10^5$ CFU/mL. The deactivation continued for some more time after the US irradiation is discontinued after 8 hrs, possibly because the free radicals generated in the process continue to be active for some more time until they are totally consumed by various processes taking place. In the case of sonocatalysis, no significant re-emergence is noticed even after 16 hr as shown in Fig. 6.11 (a, b, c& d). Hence, the destruction can be considered complete and irreversible in this case. This is in contrast with the bacterial deactivation by sunlight or other softer techniques where a sizeable population of the bacteria re-emerges once the source of irradiation is off. The regrowth occurs probably because not all of the bacteria have been deactivated by the soft process. In such cases the bacteria may have entered a viable but non-culturable state and then recovered their culturability after a period, under more favorable conditions.

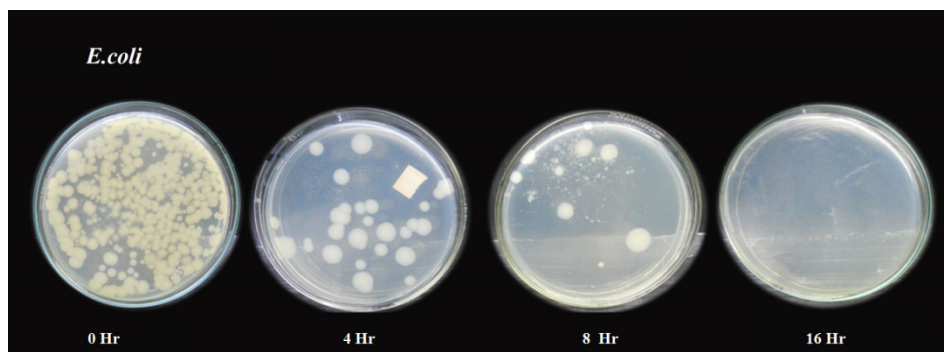


Fig.6.11(a): TRDeactivation of *E.coli* by ZnO sonocatalysis
[*E.coli*]: 2.1×10^5 CFU/mL; [ZnO]:0.1 g/L; Sonication discontinued after 8 hr

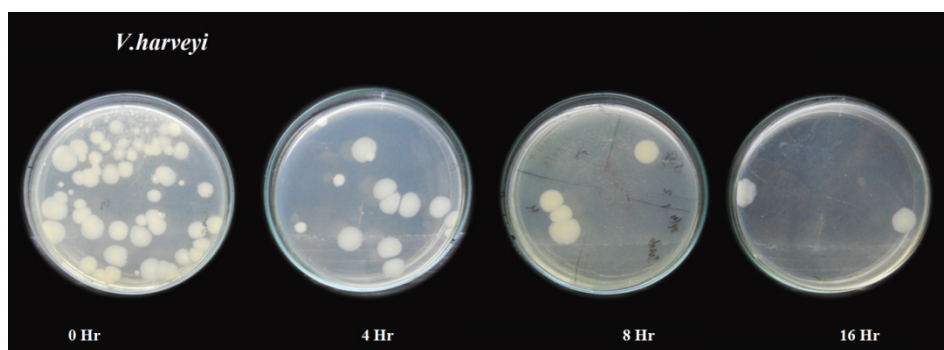


Fig.6.11(b): Deactivation of *V.harveyi* by ZnO sonocatalysis
[*V.harveyi*]: 2.4×10^5 CFU/mL; [ZnO]:0.1 g/L; Sonication discontinued after 8 hr

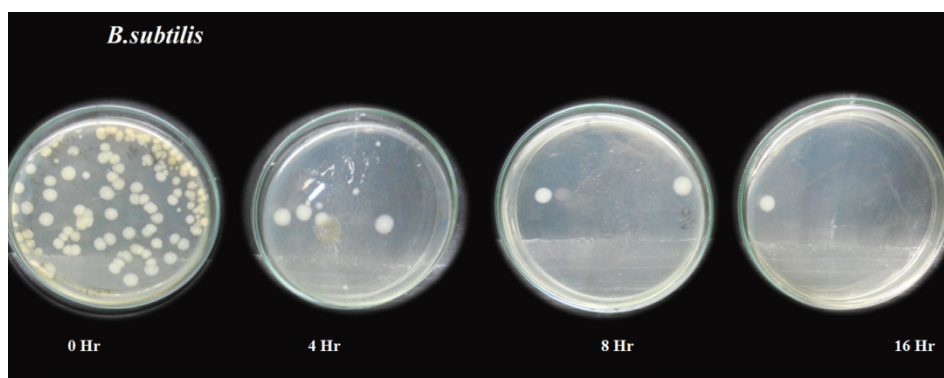


Fig.6.11(c): Deactivation of *B.subtilis* by ZnO sonocatalysis
[*B.subtilis*]: 2.2×10^5 CFU/mL; [ZnO]:0.1 g/L; Sonication discontinued after 8 hr

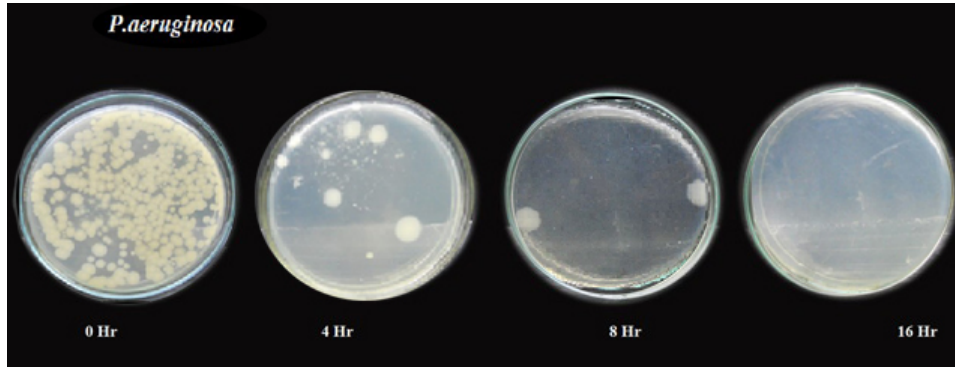
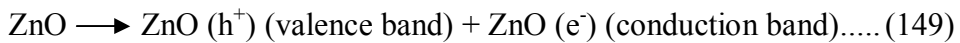


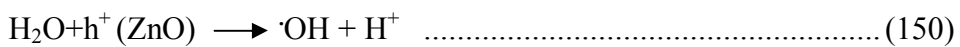
Fig.6.11(d): Deactivation of *P.aeruginosa* by ZnO sonocatalysis
 [*P.aeruginosa*]: 2.7×10^5 CFU/mL; [ZnO]:0.1 g/L; Sonication discontinued after 8 hr

6.5 Mechanism of disinfection

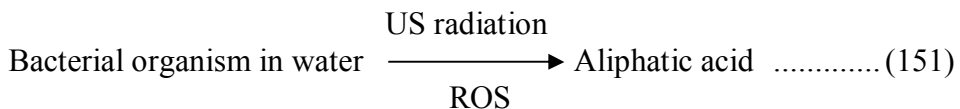
Sonocatalysis and the photocatalysis promoted by US induced sonoluminescence results in transfer of electron from the valence band of ZnO to its conduction band as in reaction.



The superoxide anion O_2^- and its protonated form OH_2^- And H_2O_2 are formed, as explained in earlier chapters. The hole in the valence band also causes the formation of reactive $\cdot\text{OH}$ as in reaction.



Various reactive oxygen species (ROS) such as HO_2^\cdot , H_2O_2 , $\cdot\text{OH}$ etc formed during the sono and resultant photo processes interact with bacterial organism as follows [218].



Of the various ROS, the most prominent and reactive is the $\cdot\text{OH}$.

During sonocatalysis, the disinfection can occur both in the bulk phase and at the catalyst surface. In the bulk phase, the bacterial cells are inactivated by the micro jet shear stress and the reactive OH radicals. At the catalyst surface, bacterial cells are deactivated by the OH radicals generated by sonocatalytic excitation of the semiconductor. The amount of OH radicals produced in the presence of semiconductor was significantly greater than the amount generated by US alone [219].

In aqueous phase sonolysis, there are four potential sites for sonochemical activity [220]:

- (i) The gaseous region of the cavitation bubble where volatile and hydrophobic species are easily degraded through pyrolytic reactions as well as reactions involving the participation of hydroxyl radicals with the latter being formed through water sonolysis:
- (ii) The bubble—liquid interface where hydroxyl radicals are localized and therefore radical reactions predominate although pyrolytic reactions also may occur to a lesser extent.
- (iii) The liquid bulk where secondary sonochemical activity may take place mainly by free radicals that escaped from the interface and migrated to the liquid bulk.
- (iv) Catalyst-liquid interface where OH radicals initiate reaction. OH radicals can recombine to produce H_2O_2 which may in turn interact with free radicals to generate more radicals:

Reactions initiated by OH radicals primarily in the liquid bulk, at the bubble interface and the catalyst surface may be the dominant deactivation pathways. The catalyst particles, in addition to promoting the OH radicals, may also stabilize the reactive species resulting in a more intensive disinfection. The photocatalytic characteristics of ZnO induced by the US-initiated sonoluminescence caused by the implosion of bubbles also will result in disinfection. It is known that flashes of single bubble sonoluminescence (SBSL) involve intense UV light which can activate ZnO photocatalytically [221]. The semiconductor particles can also lead to strong jet streams and physical stresses in the ultrasonic system which can affect the cell structure as well as the cell membrane of the organisms [208,219]. US can also increase catalyst surface area producing more active sites for reactions with target species. Further, smaller catalyst particles may enter the bacterial cells which may have already damaged cell membranes and cause additional damage to intracellular components. Sonication itself can also cause greater intracellular damage in the already damaged bacterial cells. Other factors leading to disinfection include pressure gradient resulting from bubble collapse causing cell damage due to mechanical fatigue and shear forces induced by microstreaming. Intrinsic oxygen vacancies on the catalyst surface can also lead to more cavitation [222].

The photocatalytic disinfection of *E. coli* in water has been modeled with kinetic equations based on a simplified reaction mechanism which consists of three different stages; i.e. (i) initial delay or smooth decay at the beginning of the reaction, usually called “shoulder,” (ii) a log-linear disinfection region that covers most part of the reaction, and (iii) a

deceleration of the process at the end of the reaction, usually called “tail” [220]. Kinetic constant, pseudo-adsorption constant, and inhibition coefficient were the three key parameters used in the model. It was seen that the inhibition coefficient is not influenced by the experimental conditions while the other two are more sensitive. The presence of different inorganic anions and cations in water strongly influences the efficiency of the disinfection process as has been observed by preliminary studies in this context. This aspect needs more extensive investigation which needs to be taken up as an independent project. This indicates the possibility of different mechanisms for the disinfection and thus different values of kinetic and pseudo-adsorption constants depending on the characteristics of water. However, the model cannot be applied as such in the current instance of sonocatalytic deactivation because the “shoulder” is not observed here. The long-linear inactivation region that covers over 50% of the reaction and the “tail” are observed here also. Hence in sonocatalysis, the physical and chemical effects of sonolysis may be the dominant driving forces of disinfection initially. As the reaction proceeds, the SBSL sets in making the disinfection a complex process involving a combination of sonolysis, sonocatalysis, photocatalysis and possibly sonophotocatalysis.

In many instances, it has been reported that gram +ve bacteria is deactivated slowly due to its thick cell wall structure. But in the current instance, the gram +ve organism *B.subtilis* is getting deactivated as efficiently as the gram –ve organism. Hence, the conventional destruction mechanism based on the thickness of the cell wall alone may not be relevant here.

Gram –ve bacteria have triple layer cell wall with an inner membrane (IM), a thin peptidoglycan (PG) layer and an outer membrane (OM). Gram +ve bacteria have thicker PG and no OM. The higher efficiency of deactivation of gram –ve bacteria shows that the lethal action is primarily due to membrane and cell wall damage. The indestructibility of the thicker PG when subjected to local hotspots and pressure gradients is often cited as the reason for the poor deactivation of the gram +ve bacteria. However, the equal efficiency of destruction of gram +ve and gram –ve organisms has shown that the mechanism of sonocatalytic destruction of bacteria is not that simple. It is possible that the extreme local temperature and pressure conditions created by sonication would disintegrate gram positive and gram negative bacterial cells and /or denature any enzymes present. The imploding cavitation bubbles also produce high sheer forces and liquid jets in the solvent that may also have sufficient energy to physically damage the cell walls/membrane. It is also possible that, bubbles induce microstreaming in the surrounding liquid that can induce stress in any microbiological species present without the bubbles having to burst. However, the mechanism of sonocatalytic destruction of bacterial organism may involve a combination of this and other factors which need detailed investigation which is beyond the scope of the present study.

6.6 Conclusions

Sonication and in particular, sonocatalysis as a means of bacterial decontamination of water is investigated using ZnO as the catalyst. The technique is effective for the destruction of both gram –ve and gram +ve

organisms. The influence of various parameters on the rate of sono-deactivation of organisms is evaluated. The rate of deactivation increases with increase in catalyst loading as well as concentration of the organism. In the case of catalyst dosage, there is an optimum beyond which the deactivation is leveled off or even decreases. In the case of concentration of the organism the deactivation continues to increase with concentration ,at least in the range of our study. Externally added H₂O₂ does not accelerate the sonocatalytic deactivation significantly, though by itself, it is a good disinfectant. This may be because the H₂O₂ formed insitu in sonocatalytic system may have already played the role. Acidic and alkaline pH are detrimental to the organisms even without catalyst or sonication. Sonocatalysis in presence of ZnO enhances the decontamination of the organism in the entire pH range of 3-11. The sonocatalytic deactivation is irreversible and the bacteria do not reemerge as in the case of other deactivation processes. The study reveals conclusively that ZnO-mediated sonocatalysis has the potential to be used as an effective tool for the irreversible deactivation of bacterial organisms in water.

.....✪.....

SUMMARY AND CONCLUSIONS

The main objective of the current investigation was to identify suitable reaction conditions for the removal of chemical and bacterial pollutants from water using Advanced Oxidation Processes. Sonocatalysis, Photocatalysis and Sonophotocatalysis were the AOPs subjected to the investigation. The semiconductor oxides tested as catalysts were ZnO, TiO₂ and ZnO-TiO₂ composite. The chemical pollutant chosen for the study was phenol, a trace pollutant found in waste water discharges of most petrochemical industries. The bacterial pollutants subjected to the investigation were *E.coli*, *B.subtilis*, *P.aeruginosa* and *V.harveyi*. The catalysts were characterized by standard wet analytical, adsorption and instrumentation techniques. The reaction was followed by UV-VIS spectrophotometry and other standard methods. The parameters subjected to detailed investigation and finally identified as relevant for optimum efficiency of the process include catalyst dosage, concentration of pollutant, pH, presence of other contaminants, dissolved oxygen, reactor geometry and design, catalyst life cycle etc.,

Relevant findings of the study and the conclusions are as follows:

- i) ZnO, TiO₂ and composite ZnO-TiO₂ are very efficient photocatalysts for the degradation and complete mineralization of trace amounts of Phenol, the order of efficiency being ZnO-TiO₂ > TiO₂ > ZnO. The rate of degradation is dependent on a number of factors including the concentration of the substrate, catalyst loading, pH, presence of other contaminants in water, dissolved O₂ etc. H₂O₂ is formed in the reaction as a co-product and it undergoes simultaneous decomposition, leading to periodic increase and decrease in its concentration (oscillation). Major intermediates of phenol degradation are catechol, hydroquinone and p-benzoquinone. Ultimately they also degrade and mineralize into relatively harmless end products, i.e., CO₂ and H₂O. Anions such as Cl⁻, I⁻, SO₄²⁻, Br⁻ and PO₄³⁻ inhibit the photocatalytic degradation of phenol over semiconductor oxides. However, the extent of inhibition and the efficiency of each anion is dependent on the nature of the catalyst. Possible mechanism for the photocatalytic degradation of phenol, formation of intermediates, enhanced activity of coupled ZnO-TiO₂ and oscillation in the concentration of insitu formed H₂O₂ is proposed and discussed.
- ii) ZnO, TiO₂ and ZnO-TiO₂ can also function as sonocatalysts for the degradation and mineralization of Phenol with efficiency in the order ZnO-TiO₂ > ZnO > TiO₂. The degradation is much less compared to photocatalysis. Reaction parameters such as the catalyst loading, irradiation time, initial pH, concentration of the substrate, presence of anions, reaction volume, US power etc affect the rate of degradation in this case also.

The degradation follows variable kinetics, depending on the concentration of the substrate. H_2O_2 formed during the degradation undergoes simultaneous decomposition resulting in oscillation in the concentration as in the case of photocatalysis. The maxima and minima in the oscillation curve are not constant and vary from experiment to experiment.

The effect of anions on the rate of sonocatalytic degradation is very complex. They can either inhibit or promote the degradation depending on the nature of their interaction with the surface and the reactions that follow. The size of catalyst particles has little impact on sonocatalytic degradation. Possible mechanisms for the sonocatalytic degradation of phenol, formation and decomposition of H_2O_2 , enhanced activity of coupled ZnO-TiO₂, and the effect of anions are proposed and discussed.

- iii) Simultaneous illumination by UV light and Ultrasound (US) results in enhanced degradation of phenol compared to that achieved in presence of either of them individually. In fact, the combination has a synergistic effect. Optimum parameters for the combination induced sonophotocatalytic degradation of phenol were identified as in the case of sonocatalysis or photocatalysis. Particle size does not have much impact on the rate of degradation in the narrow range studied here.

The sonophotocatalytic degradation also follows variable kinetics, depending on the concentration of the substrate as in the case of sonocatalysis and photocatalysis. Maximum degradation is observed in the pH range 4.0-5.5. Presence of anions can have enhancing,

inhibiting or insignificant effect, depending on other reaction parameters as well as possible interactions on surface and homogeneous bulk. However, no consistent universally applicable explanation for the effect of all anions is possible with the limited data available and also due to the complexity of AOPs involving sono-, photo- and sonophotocatalysis. The study clearly proved the synergy of sonophotocatalysis and the advantages of coupling two AOPs. Sonophotocatalysis provides a potentially viable option for the removal of trace chemical pollutants from water.

- iv) Sonocatalysis using ZnO as the catalyst is an efficient process for the bacterial decontamination of water. Gram –ve organism such as *E.coli* and gram +ve organism like *B.subtilis* can be destroyed with comparable efficiency by the technique. The advantage of this novel technique over other methods of bacterial destruction is that the destruction is irreversible and the reemergence of the bacteria is practically nil. The rate of deactivation increases with increase in catalyst dosage. Externally added H₂O₂ does not accelerate the sonocatalytic deactivation significantly, though by itself it is a good disinfectant.

Sonocatalysis in presence of ZnO enhances the decontamination of the organism in the pH range of 3-11. The study reveals conclusively that ZnO-mediated sonocatalysis has the potential to be used as an effective tool for the irreversible deactivation of bacterial organisms in water. Probable mechanisms for the destruction of the bacterial contaminants are discussed.

To sum up, sono-, photo- and sonophotocatalysis can be used as effective AOPs for the removal of chemical and bacterial pollutants from water. Being environment-friendly without the use of any toxic or hazardous additives, the techniques will increase the chance of safe reuse of water. Once scaled up, optimum parameters reconfirmed and a suitable reactor assembly designed, the technique can be considered as a major candidate for providing contamination – free drinking water in water scarce remote areas, especially in developing and less developed world.

.....✻.....

References

- [1] J.H. Baxendale, J.A. Wilson, The photolysis of hydrogen peroxide at high light intensities, *Trans. Faraday Soc.* 53 (1957) 344-356.
- [2] A. Roberto, C. Vincenzo, I. Amedeo, M. Raffaele, Advanced oxidation processes (AOP) for water purification and recovery, *Catal. Today* 53 (1999) 51-59.
- [3] O. Legrini, E. Oliveros, A. M. Braun, Photochemical processes for water treatment, *Chem. Rev.* 93 (1993) 671-698.
- [4] P.R. Gogate, A.B. Pandit, A review of imperative technologies for wastewater treatment II: Hybrid methods, *Adv. Environ. Res.* 8 (2004) 553-597.
- [5] A.S. Stasinakis, Use of selected advanced oxidation processes (AOP's) for wastewater treatment – A mini review, *Global NEST J.* 10 (2008) 376-385.
- [6] N. Daneshvar, S. Aber, F. Hosseinzadeh, Study of C.I. Acid Orange 7 removal in contaminated water by photo oxidation processes, *Global NEST J.* 10 (2008) 16-23.
- [7] A. Rezaee, M.T. Ghaneian, S.J. Hashemian, G. Moussavi, A. Khavanin, G. Ghanizadeh, Decolorization of Reactive Blue 19 dye from textile wastewater by the UV/H₂O₂ process, *J. Appl. Sci.* 8 (2008) 1108-1122.
- [8] P.C. Fung, Q. Huang, S.M. Tsui, C.S. Poon, Treatability study of organic and colour removal in desizing/dyeing wastewater by UV/US system combined with hydrogen peroxide, *Water Sci. Technol.* 40 (1999) 153-160.

- [9] M.A. Behnajady, N. Modirshahla, M. Shokri, B. Vahid, Investigation of the effect of ultrasonic waves on the enhancement of efficiency of direct photolysis and photooxidation processes on the removal of a model contaminant from textile industry, *Global NEST J.* 10 (2008) 8-15.
- [10] F.J. Benitez, A.J. Beltran-Heredia, J.L. Acero, Oxidation of vanillic acid as a model of polyphenolic compounds in olive mill wastewaters III. Combined UV radiation-hydrogen peroxide oxidation, *Toxicol. Environ. Chem.* 56 (1996) 199-210.
- [11] A.de O. Martins, V.M. Canalli, C.M.N. Azevedo, M. Pires, Degradation of Pararosaniline (C.I. Basic Red 9 monohydrochloride) dye by ozonation and sonolysis, *Dyes & Pigments* 68 (2006) 227-234.
- [12] W.H. Glaze, J.W Kang, D.H. Chapin, The chemistry of water treatment processes involving ozone, hydrogen peroxide and ultraviolet radiation, *Ozone Sci. Eng.* 9 (1987) 335-352.
- [13] T.L. Prasad, M. Smitha, C. Srinivas, Advanced oxidation processes for treatment of spent organic resins in nuclear industry, *BARC Newsletter* (2001) 55-58.
- [14] S. Guittonneau, W.H. Glaze, J.P. Duguet, O. Wable, J. Mallevalle, Characterization of natural waters for potential to oxidize organic pollutants with ozone, *Ozone Sci. Eng.* 14 (1992) 185-196.
- [15] F.J Beltran, J.M. Encinar, M.A. Alonso, T. Gonzalez, Nitroaromatic hydrocarbon ozonation in water. 2. Combined ozonation with hydrogen peroxide or UV radiation, *Ind. Eng. Chem. Res.* 37 (1998) 32-40.
- [16] T. Oppenlander, Photochemical purification of water and air; advanced oxidation processes (AOPs): Principles, reaction mechanisms, reactor concepts – *Wiley-VCH* (2003).

- [17] S. Contreras, M. Rodríguez, E. Chamarro, S. Esplugas, J. Casado, Oxidation of nitrobenzene by O_3 /UV: The influence of H_2O_2 and Fe (II). Experiences in a pilot plant, *Water Sci. Technol.* 44 (2001) 39-46.
- [18] M. D. Gurol, R. Vatistas, Oxidation of phenolic compounds by ozone and ozone/UV radiation: A comparative study, *Water Res.* 21 (1987) 895-903.
- [19] P.L. Yue, O. Legrini, Photochemical Degradation of organics in water, *Water Pollut. Res. J. Canada* 27 (1992) 123-137.
- [20] S. Esplugas, J. Gimenez, S. Contreras, E. Pascual, M. Rodríguez, Comparison of different advanced oxidation processes for phenol degradation, *Water Res.* 36 (2002) 1034-1042.
- [21] J. Hoigne, H. Bader, Rate constants of reaction of ozone with organic and inorganic compounds in water-I: Non-dissociating organic compounds, *Water Res.* 17 (1983) 173-83.
- [22] J. Hoigne, H. Bader, Rate constants of reaction of ozone with organic and inorganic compounds in water-II: Dissociating organic compounds, *Water Res.* 17 (1983) 185-94.
- [23] J. D. Zeff, J. T. Barich, Symposium on advanced oxidation processes and treatment of contaminated water and air, *Wastewater Technol. Center, Ontario (Canada)* (1990).
- [24] A. Mokrini, D. Oussi, S. Esplugas, Oxidation of aromatic compounds with UV radiation/ozone/hydrogen peroxide, *Water Sci. Technol.* 35 (1997) 95-102.
- [25] W.H. Glaze, J.W. Kang, Advanced oxidation processes. Description of a kinetic model for the oxidation of hazardous materials in aqueous media with ozone and hydrogen peroxide in a semi batch reactor, *Ind. Eng. Chem. Res.* 28 (1989) 1573-1580.

- [26] M. Trapido, Y. Veressinina, J. Kallas, Degradation of aqueous nitrophenols by ozone combined with UV-radiation and hydrogen peroxide, *Ozone Sci. Eng.* 23 (2001), 333-342.
- [27] W. Spacek, R. Bauer, G. Heisler, Heterogeneous and homogeneous wastewater treatment Comparison between photodegradation with TiO₂ and the photo-Fenton reaction, *Chemosphere* 30 (1995) 477-484.
- [28] F.J. Benitez, A.J. Beltran-Heredia, T. Gonzalez, F. Real, Kinetics of the elimination of vanillin by UV radiation catalyzed with hydrogen peroxide, *Fresen. Environ. Bull.* 7 (1998) 726-73.
- [29] M. Ugurlu, I. Kula, Decolourization and removal of some organic compounds from olive mill wastewater by advanced oxidation processes and lime treatment, *Environ. Sci. Poll. Res.* 14(2007) 319-325.
- [30] F. Torrades, J. Garcia-Montano, J.A. Garcia-Hortal, X. Domenech, J. Peral, Decolorization and mineralization of commercial reactive dyes under solar light assisted photo-Fenton conditions, *Sol. Energy* 77 (2004) 573-581.
- [31] M. I. Litter, Introduction to photochemical advanced oxidation processes for water treatment, *Hdb. Env. Chem.* 2 (2005) 325-366.
- [32] J. J. Pignatello, Dark and photoassisted Fe³⁺ catalyzed degradation of chlorophenoxy herbicides by hydrogen peroxide, *Environ. Sci. Technol.* 26 (1992) 944-951.
- [33] M. P. G. De. S. Lucas, Application of advanced oxidation processes to waste water Treatment, *Thesis*, University of Tras-os-Montes and Atto Douro, Oct (2009).
- [34] M. N. Chong, B. Jin, W. K. C. Chow, C. Saint, Recent developments in photocatalytic water treatment technology: A review, *Water Res.* 44 (2010) 2997 -3027.

- [35] C. Walling, A. Goosen, Mechanism of ferric ion catalyzed decomposition of hydrogen peroxide. Effect of organic substrates, *J. Am. Chem. Soc.* 95 (1973) 2987–2991.
- [36] A. S. Amiri, J.R. Bolton, S.R. Cater, Ferrioxalate mediated photo degradation of organic pollutants in contaminated water, *Water Res.* 31 (1997) 787-798.
- [37] J. E. F. Moraes, F. H. Quina, C.A.O. Nascimento, D.N. Silva, O. C. Filho, Treatment of saline wastewater contaminated with hydrocarbons by the photo-Fenton process, *Environ. Sci. Technol.* 38 (2004) 1183-1187.
- [38] R. Mosteo, J. Sarasa, M.P. Ormad, J.L. Ovelleiro, Sequential solar photo-fenton biological system for the treatment of winery wastewater, *J. Agric. Food Chem.* 56 (2008) 7333-7338.
- [39] J.J. Pignatello, E. Oliveros, A. Mackay, Advanced oxidation processes for organic contaminant destruction based on the Fenton reaction and related chemistry, *Crit. Rev. Environ. Sci. Technol.* 36 (2006) 1-84.
- [40] R.W. Mathews, S.R. MeEvoy, Destruction of phenol in water with sun, sand, and photocatalysis, *Sol. Energy* 49 (1992) 507-513.
- [41] S. Tunesi, M. Anderson, Influence of chemisorptions on the photodecomposition of salicylic acid and related compounds using suspended titania ceramic membranes, *J. Phys. Chem.* 95 (1991) 3399-3405.
- [42] A. Fujishima, K. Honda, Electrochemical photolysis of water at a semiconductor Electrode, *Nature* 238 (1972) 37–38.
- [43] D.S. Bhatkhande, V.G. Pangarkar, A.C.M. Beenackers, Photocatalytic degradation for environmental applications - A Review, *J. Chem. Technol. Biotech.* 77 (2002) 102-116.

- [44] U. I. Gaya, A. Halim Abdullah, Heterogeneous photocatalytic degradation of organic contaminants over titanium dioxide: A review of fundamentals, progress and problems, *J. Photochem. Photobiol. C: Photochem. Reviews* 9 (2008) 1–12.
- [45] W. Chu, W.K. Choy, T.Y. So, The effect of solution pH and peroxide in the TiO₂-induced photocatalysis of chlorinated aniline, *J. Hazard. Mater.* 141 (2007) 86-91.
- [46] S. Cheng, S. J. Tsai, Y. F. Lee, Photocatalytic decomposition of phenol over titanium oxide of various structures, *Catal. Today* 26 (1995) 87-96.
- [47] C. Kittel, Introduction to Solid State Physics, Wiley Eastern Limited, New Delhi (1976).
- [48] W. Han, W. Zhu, P. Zhang, Y. Zhang, L. Li, Photocatalytic degradation of phenols in aqueous solutions under irradiation of 254 and 185 nm UV light, *Catal. Today* 90 (2004) 319-324.
- [49] D. Chen, A. K. Ray, Photocatalytic kinetics of phenol and its derivatives over UV irradiated TiO₂, *Appl. Catal. B* 23 (1999) 143–157.
- [50] A. Dobosz, A. Sobczynski, The influence of silver additives on titania photoactivity in the photooxidation of phenol, *Water Res.* 37 (2003) 1489-1496.
- [51] M. Moonsiri, P. Rangsunvigit, S. Chavadej, E. Gulari, Effects of Pt and Ag on the photocatalytic degradation of 4-chlorophenol and its by-products, *Chem. Eng. J.* 97 (2004) 241-248.
- [52] L. Lhomme, S. Brosillon, D. Wolbert, J. Dussaud, Photocatalytic degradation of a phenylurea, chlortoluron in water using an industrial titanium dioxide coated media, *Appl. Catal B: Environ.* 61 (2005) 227- 235.

- [53] L. Liu, L. A. Lawson, B. Cornish, P. K. J. Robertson, Mechanistic and toxicity studies of the photocatalytic oxidation of microcystin -LR, *J. Photochem. Photobiol. A: Chem.* 148 (2002) 349-354.
- [54] A. Mills, S. Le Hunte, An overview of semiconductor photocatalysis, *J. Photochem. Photobiol. A: Chem.* 108 (1997)1-35.
- [55] A. Mills, A. Belghazi, D. Rodman, Bromate removal from drinking water by semiconductor photocatalysis, *Water Res.* 30 (1996) 1973-1978.
- [56] I. Poullos, A. Avranas, E. Rekliti, A. Zouboulis, Photocatalytic oxidation of Auramine O in the presence of semiconducting oxides, *J. Chem. Technol. Biotechnol.* 75 (2000) 205–212.
- [57] B. Neppolian, H.C. Choi, S. Sakthivel, B. Aurobindo, B. Murugesan, Solar/UV induced photocatalytic degradation of three commercial textile dyes, *J. Hazard. Mater.* 89 (2002) 303–317.
- [58] D.G. Mirat, R. Vatisstas, Oxidation of phenolic compounds by ozone and ozone-UV radiation: A comparative study, *Water Res.* 21 (1997) 895-900.
- [59] S. Sakthivel, H. Kish, Photocatalytic and photoelectrochemical properties of nitrogen doped TiO₂, *Chem. Phys. Chem.* 4 (2003) 487–490.
- [60] S. Jain, R. Yamgar, R.V. Jayram, Photolytic and photocatalytic degradation of atrazine in the presence of activated carbon, *Chem. Eng. J.* 148 (2009) 342–347.
- [61] M.S.T. Gonsalves, A.M.F. Oliveira-Campos, E.M.M.S. Pinto, P.M.S. Plasencia, M.J.R.P. Queiroz, Photochemical treatment of solutions of azo dyes containing TiO₂, *Chemosphere* 39 (1999) 781–786.
- [62] Z.B. Guo, R. Ma, G.H. Li, Degradation of phenol by nanomaterial TiO₂ in wastewater, *Chem. Eng. J.* 119 (2006) 55–61.

- [63] L. Davydov, P.G. Smirniotis, Quantification of the primary processes in aqueous heterogeneous photocatalysis using single stage oxidation reactions, *J. Catal.* 191 (2000) 105–112.
- [64] A. Fujishima, N. T. Rao, A.D. Tryk, Titanium dioxide photocatalysis, *J. Photochem. Photobiol. C: Photochem. Reviews* 1 (2000) 1–21.
- [65] J.M. Herrmann, Heterogeneous photocatalysis: fundamentals and applications to the removal of various types of aqueous pollutants, *Catal. Today* 53 (1999) 115-129.
- [66] M. Muneer, D. Bahnemann, Semiconductor mediated photocatalysed degradation of two selected pesticide derivatives, terbacil and 2,4,5-tribromoimidazole in aqueous suspension, *Appl. Catal. B: Environ.* 36 (2002) 95-111.
- [67] T. Pandiyan, O.M. Rivas, J. O. Martinez, G. B. Amezcua, M.A. Martinez-Carrillo, Comparison of methods for the photochemical degradation of chlorophenols, *J. Photochem. Photobiol. A: Chem.* 146 (2002) 149-155.
- [68] J. M. Wu, T. W. Zhang, Photodegradation of Rhodamine B in water assisted by titania films prepared through a novel procedure, *J. Photochem. Photobiol. A: Chem.* 162 (2004) 171-177.
- [69] G. G. Liu , X. Z. Zhang , Y. J. Xu, X. S. Niu, L. Q. Zheng, X. J. Ding, Effect of $ZnFe_2O_4$ doping on the photocatalytic activity of TiO_2 , *Chemosphere* 55 (2004) 1287-91.
- [70] Y. Chen, S.W. Kan, L. Liping, Role of primary active species and TiO_2 surface characteristic in UV-illumination photodegradation of acid orange 7, *J. Photochem Photobiol. A:Chem.* 172 (2005) 47-54.
- [71] Li. Youji, L. Junwen, Y. Jing, Photocatalytic degradation of methyl orange in a sparged tube reactor with TiO_2 -coated active carbon composites, *Cataly. Communi.* 6 (2005) 650-655.

- [72] C.C. Chang, L. C. Shin, C.Y. Chien, Photocatalytic degradation of ethyl violet in aqueous solution mediated by TiO₂ suspensions, *J. Photochem. Photobiol. A: Chem.* 181 (2006) 120-125.
- [73] S. K. Dubey, Solar photocatalytic treatment biodegradability enhancement (heterogeneous), *M.Tech. Thesis*, Thapar University, Patiala, (2006) 12-18.
- [74] C. Minero, C. Pelizzetti, P. Piccini, M.Vinceti, Photocatalytic water decontamination - degradation of Photocatalysed transformation of nitrobenzene on TiO₂ and ZnO, *Chemosphere* 28 (1994) 1229-1244.
- [75] R.W. Matthews, Purification of water with near-UV illuminated suspensions of titanium dioxide, *Water Res.* 24 (1990) 653-660.
- [76] M.V. Shankar, N. S. Anandan, B. Venkatachalam, B. Arabind, V. Murugesan, Fine route for an efficient removal of 2,4, dichlorophenoxyacetic acid (2,4 D) by zeolite-support TiO₂, *Chemosphere* 63 (2006) 1014-1021.
- [77] T. Oyama, A. Aoshima, S. Horikoshi, S. Hidaka, J. Zhao, N. Serpone, Solar photocatalysis, photodegradation of a commercial detergent in aqueous TiO₂ dispersions under sunlight irradiation, *Sol. Energy* 77 (2004) 525-532.
- [78] O. Horvath, R. Huszank, Degradation of surfactants by hydroxyl radicals photogenerated from hydroxoiron (III) complexes, *Photochem. Photobiol. Sci.* 2 (2003) 960-966.
- [79] K. Djebbar, A. Zertal, T. Sehili, Photocatalytic Degradation of 2,4-dichlorophenoxyacetic acid and 4-chloro-2-methylphenoxyacetic acid in water by using TiO₂, *Environ. Technol.* 27 (2006)1191-1197.
- [80] C. Hariharan, Photocatalytic degradation of organic contaminants in water by ZnO nanoparticles: Revisited, *Appl. Catal. A: General* 304 (2006) 55-61.

- [81] K.S. Suslick, The chemical effects of ultrasound, *Sci. Am.* 260 (1989) 80-86.
- [82] Y. G. Adewuyi, Sonochemistry in environmental remediation 2, heterogeneous sonophotocatalytic oxidation processes for the treatment of pollutants in water, *Environ. Sci. Technol.* 39 (2005) 8557–8570.
- [83] Y. G. Adewuyi, Sonochemistry: Environmental Science and Engineering Applications, *Ind. Eng. Chem. Res.* 40 (2001) 4681–4715.
- [84] K. S. Suslick, Sonochemistry, *Science* 247 (1990) 1439-1445.
- [85] K. S. Suslick, Sonochemistry and sonoluminescence in encyclopedia of physical science and technology, 3rd ed. *Academic Press*. San Diego, 17 (2001) 363-376.
- [86] Y. C. Chen, Enhancement on photocatalytic degradation of phenol by ultrasound, *Ind. Eng. Chem. Res.* 41 (2002) 5958–5965.
- [87] J. Hartmann, P. Bartels, U. Mau, M. Witter, W. V. Tumpling, J. Hofmann, E. Nietzsche, Degradation of the drug diclofenac in water by sonolysis in presence of catalysts, *Chemosphere* 70 (2008) 453-61.
- [88] Y. Jiang, C. Petrier, T.D Waite, Sonolysis of 4-chlorophenol in aqueous solution: effects of substrate concentration, aqueous temperature and ultrasonic frequency, *Ultrason. Sonochem.* 13 (2006) 415-22.
- [89] J.D. Schramm, I. Hua, Ultrasonic irradiation of dichlorvos decomposition mechanism, *Water Res.* 35 (2001) 665-674.
- [90] M. Dukkanci, G. Gunduz, Ultrasonic degradation of oxalic acid in aqueous solutions, *Ultrason. Sonochem.* 13 (2006) 517-522.
- [91] K. Okitsu, K. Iwasaki, Y. Yobiko, H. Bandow, R. Nishimura, Y. Maeda, Sonochemical degradation of azo dyes in aqueous solution: A new heterogeneous kinetics model taking into account the local concentration of OH radicals and azo dyes, *Ultrason. Sonochem.* 12 (2005) 255-262.

- [92] N.N. Mahamuni, A.B. Pandit, Effect of additives on ultrasonic degradation of phenol, *Ultrason. Sonochem.* 13 (2006)165-174.
- [93] Z. Guo, Z. Zheng, S. Zheng, W. Hu, F. Ruo, Effect of various sono-oxidation parameters on the removal of aqueous 2, 4-dinitrophenol, *Ultrason. Sonochem.* 12 (2005) 461-465.
- [94] J. Yano, J. Matsuura, H. Ohura, S. Yamasaki, Complete mineralization of propylamide in aqueous solution containing TiO₂ particles and H₂O₂ by the simultaneous irradiation of light and ultrasonic waves, *Ultrason. Sonochem.* 12 (2005) 197-203.
- [95] D. Ollis, P. Pichat, N. Serpone, TiO₂ photocatalysis – 25 years preface, *Appl. Catal. B: Environ.* 99 (2010) 377-387.
- [96] M. Hoffmann, S. Martin, W. Choi, D. Bahnemann, Environmental applications of semiconductor catalysis, *Chem. Rev.* 95 (1995) 69-96.
- [97] C. Mccullagh, J.M.C. Robertson, D.W. Bahnemann, P.K.J. Robertson, The application of TiO₂ photocatalysis for disinfection of water contaminated with pathogenic microorganisms: A review, *Res. Chem. Interned.* 33 (2007), 359-375.
- [98] R.K. Amarnath, Ultrasonic chemistry, A survey and energy assessment, TR-109974, Final report, (1998).
- [99] E.N. Harvey, A.L. Loomis, The destruction of luminous bacteria by high frequency sound waves, *J. Bacteriol.* 17(1929) 373-376.
- [100] M. Furuta, M. Yamaguchi, T. Tsukamoto, B. Yim, C.E. Stavarache, K. Hasiba, Y. Maeda, Inactivation of *Escherichia coli* by ultrasonic irradiation, *Ultrason. Sonochem.* 11 (2004) 57-60.
- [101] P. Piyasena, E. Mohareb, R.C. McKellar, Inactivation of microbes using ultrasound: A review, *Int. J. Food Microbiol.* 87 (2003) 207-216.

- [102] E. Ananta, D. Voight, M. Zenker, V. Heinz, D. Knorr, Cellular injuries upon exposure of *Escherichia coli* and *Lactobacillus rhamnosus* to high-intensity ultrasound, *J. Appl. Microbiol.* 99 (2005) 271-278.
- [103] U.M. Alvarez, A.M. Loske, E. Castano-Tostado, F.E. Prieto, Inactivation of *Escherichia coli* 0157.H7, *Salmonella Typhimurum* and *Listeria monocytogenes* by underwater shock waves, *Innovative Food Sc. Emerging Technol.* 5 (2004) 459-463.
- [104] N.H. Ince, R. Belen, Aqueous phase disinfection with power ultrasound: Process kinetics and effect of solid catalysts, *Environ. Sci. Technol.* 35 (2001) 1885– 1888.
- [105] S. Koda, M. Miyamoto, M. Toma, T. Matsuoka, M. Maebayashi, Inactivation of *Escherichia coli* and *Streptococcus mutans* by ultrasound at 500 kHz, *Ultrason. Sonochem.* 16 (2009) 655–659.
- [106] C. G. Joseph, Y. L. S. Liew, D. Krisnaiah, A. Bono, Application of a semiconductor oxide-based catalyst in heterogeneous wastewater treatment: A green technology approach, *J. Appl. Sci.* 12 (2012) 1966-1971.
- [107] C. Berberidou, I. Poullos, N.P. Xekoukoulotakis, D. Mantzavinos, Sonolytic, photocatalytic and sonophotocatalytic degradation of malachite green in aqueous solutions, *Appl. Catal. B: Environ.* 74 (2007) 63–72.
- [108] H. Harada, C. Hosoki, A. Kudo, Overall water splitting by sonophotocatalytic reaction: the role of powdered photocatalyst and an attempt to decompose water using a visible-light sensitive photocatalyst. *J. Photochem. Photobiol. A: Chem.* 141 (2001) 219-224.
- [109] E. Selli, Synergistic effects of sonolysis combined with photocatalysis in the degradation of an azo dye, *Phys. Chem. Chem. Phys.* 4 (2002) 6123-6128.

- [110] N.J.B. Pe´rez, M.F Sua´rez-Herrera, Sonochemical and sonophotocatalytic degradation of malachite green: The effect of carbon tetrachloride on reaction rates, *Ultrason. Sonochem.* 15 (2008) 612–617.
- [111] A.A. Kulkarni, M. Deshpande, A.B.Pandit, Techniques of wastewater treatment. 1. Introduction to effluent treatment and industrial methods resonance, *J. Sci. Edu.* 5 (2000) 56-68.
- [112] S.S Martinez, A.S. González, Study of the sonophotocatalytic degradation of basic blue 9 industrial textile dye over slurry titanium dioxide and influencing factors, *Ultrason. Sonochem.* 15 (2008) 1038–1042.
- [113] L. Davydov, E. P. Reddy, P. France, P. G. Smirniotis, Sonophotocatalytic destruction of organic contaminants in aqueous systems on TiO₂ powders, *Appl. Catalysis B: Environ.* 32 (2001) 95–105.
- [114] A.M.T. Silva, E. Nauli, C. Angela, A-Carmo, X.P. Nikolaos, M. Dionissios Sonophotocatalytic/H₂O₂ degradation of phenolic compounds, *Catal. Today* 124 (2007) 232-239.
- [115] T. An, H. Gu, Y. Xiong, W. Chen, X. Zhu, G. Sheng, J. Fu, Decolourization and COD removal from reactive dye-containing wastewater using sonophotocatalytic technology, *J. Chem. Technol. Biotechnol.* 78 (2003) 1142–1148.
- [116] V.A. Coleman, C. Jagadish, Basic properties and applications of ZnO, Zinc oxide bulk, thin films & nano structures, Elseiver 2006.
- [117] F. Tamaddon, M. A. Amrollahi, L. Sharafat, A green protocol for chemo selective O-acylation in the presence of zinc oxide as a heterogeneous, reusable and eco-friendly catalyst, *Tetrahedron Letters* 46 (2005) 7841–7844.
- [118] T. Chungui, Q. Zhang, A. Wu, M. Jiang, Z. Liang, B. Jiang ,H. Fu. Cost-effective large-scale synthesis of ZnO photocatalyst with excellent performance for dye photodegradation, *Chem. Commun.* 48 (2012) 2858–2860.

- [119] J. Lahiri, M. Batzill, Surface functionalization of ZnO photocatalysts with monolayer ZnS, *J. Phy. Chem. C* 112 (2008) 4304-4307.
- [120] A.S. Shriwas, D. Aparna, M. Sonali, M.E. Wankhede, C. Jayashree, P. Renu, J. Urban, S.K. Haram, S.W. Gosawi, S.K. Kulkarni, Synthesis and analysis of ZnO and CdSe nanoparticles, *Parmana J. Phy.* 65 (2005) 615-620.
- [121] R. B. H. Tahar, N. B. H. Tahar, Boron-doped zinc oxide thin films prepared by sol-gel technique, *J. Mat. Sci.* 40 (2005) 5285-5289.
- [122] J. Yu, X. Yu, Hydrothermal synthesis and photocatalytic activity of zinc oxide hollow spheres, *J. Enviorn. Sci. Technol.* 42 (2008) 4902-4907.
- [123] B.A. Mohammad, M. Nasser, S. Mohammad, Z. Arezoo, A. Z. Hassan, Enhancement photocatalytic activity of ZnO nanoparticles by silver doping with optimization of photodeposition method parameters, *J. Enviorn. Sc. Health* 44 (2009) 666-672.
- [124] K. Byrappa, A. K. Subramani, S. Ananda, K.M.L. Rai, R. Dinesh, M. Yoshimura, Photocatalytic degradation of Rhodamine B dye using hydrothermally synthesized ZnO, *J. of Bulletin Mat. Sci.* 29 (2008) 433-438.
- [125] K.M. Parida, S.S. Dash, D.P. Das, Physico-chemical characterization and photocatalytic activity of zinc oxide prepared by various methods, *J. Colloid Interface Sci.* 298 (2006) 787-793.
- [126] S. M Zhu, J.Y Li, Y.S Li, Y Wang, Y.L Jiang, Reactive ion exchange synthesis of high purity ZnO nanoparticles, *J. Nano Eng. Nano systems* 221 (2009) 121-124.
- [127] A.A. Gribb, J.F. Banfield, Particle size effects on transformation kinetics and phase stability in nanocrystalline TiO₂, *American Mineralogist* 82 (1997) 717-728.

- [128] A.G. Agrios, P. Pichat, State of the art and perspectives on materials and applications of photocatalysis over TiO₂: Reviews, *Appl. Electrochem.* 58 (2005) 655–63.
- [129] K. Demeestere, J. Dewulf, V.H. Langenhove, Heterogeneous photocatalysis as an advanced oxidation process for the abatement of chlorinated, monocyclic aromatic and sulfurous volatile organic compounds in air: state of the art. Critical reviews, *Environ. Sci. Technol.* 37 (2007) 489–538.
- [130] S. Rabindranathan, S. Devipriya, S. Yesodharan, Photocatalytic degradation of phosphamidon on semiconductor oxides, *J. Hazard. Mater.* 102 (2003) 217–229.
- [131] K.E. O’Shea, I. Garcia, M. Aguilar, Titanium dioxide photocatalytic degradation of dimethyl and diethyl methyl phosphonate: Effect of catalyst and environmental factors, *Res. Chem. Intermed.* 23 (1997) 325–339.
- [132] N. Serpone, P. Maruthamuthu, P. Pichat, E. Pelizzetti, H. Hidaka, Exploiting the interparticle electron transfer process in the photocatalysed oxidation of phenol, 2-chlorophenol and pentachlorophenol: Chemical evidence for electron and hole transfer between coupled semiconductors, *J. Photochem. Photobiol. A: Chem.* 85 (1995) 247–255.
- [133] A. Khodja, T. Sehili, J. F. Pilichowski, P. Boule, Photocatalytic degradation of 2-phenylphenol on TiO₂ and ZnO in aqueous suspensions, *J. Photochem. Photobiol. A: Chem.* 141 (2001) 231–236.
- [134] L. Liao, C.A. Badour, B.Q. Liao, Preparation of nano sized TiO₂/ZnO composite catalyst and its photocatalytic activity for degradation of methyl orange, *J. Photochem. Photobiol. A: Chem.* 194 (2008) 11–19.
- [135] M. Zhang, T. An, X. Hu, C. Wang, G. Sheng, J. Fu, Preparation and photocatalytic properties of a nanometer ZnO-SnO₂ coupled Oxide, *Appl. Catal. A: Gen.* 260(2004) 215–222.

- [136] M. Qamar, M. Muneer, A comparative photocatalytic activity of titanium dioxide and zinc oxide by investigating the degradation of vanillin, *Desalination* 249 (2009) 535–540.
- [137] U. Stafford, K.A. Gray, P.V. Kamat, Photocatalytic degradation of 4-chlorophenol the effects of varying TiO₂ concentration and light wavelength, *J. Catal.* 167 (1997) 25–32.
- [138] M. Muneer, H.K. Singh, D.W. Bahnemann, Semiconductor mediated photocatalysed degradation of two selected priority organic pollutants, benzidine and 1, 2-diphenylhydrazine in aqueous suspension, *Chemosphere* 49 (2002) 193–203.
- [139] M. Qamar, M. Saquib, M. Muneer, Photocatalytic degradation of two selected dye derivatives, chromotrope 2B and amido black 10B, in aqueous suspensions of titanium dioxide, *Dyes and Pigments* 65 (2005) 1–9.
- [140] K. Krishnakumar, K. Selvam, R. Velmurugan, M. Swaminathan, Influence of operational parameters on photodegradation of Acid Black 1 with ZnO, *Desalin. Water Treat.* 24 (2010) 132–139.
- [141] A.M.T. Silva, E. Nouli, Nikolaos, P. Xekoukoulotakis, D. Mantzavinos, Effect of key operating parameters on phenols degradation during H₂O₂-assisted TiO₂ photocatalytic treatment of simulated and actual olive mill wastewaters, *Appl. Catal. B* 73 (2007) 11–22.
- [142] G. Heit, A.M. Braun, UV photolysis of aqueous systems: Spatial differentiation between volumes of primary and secondary reactions, *Water Sci. Technol.* 35 (1997) 25–30.
- [143] N. Daneshvar, S. Aber, M.S.S. Dorraji, A.R Khataee, M.H. Rasoulifard, Preparation and investigation of photocatalytic properties of ZnO nanocrystals: Effect of operational parameters and kinetic study, *World Acad. Sci. Eng. Technol.* 29 (2007) 267-272 .

- [144] X.H. Ou, S.L. Lo, C. H. Wu, Exploring the interparticular electron transfer process in the photocatalytic oxidation of 4-chlorophenol, *J Hazard. Mater.* 137 (2006) 1362-1370.
- [145] D.E. Kritikos, N.P. Xekoukoulotakis, E. Psillakis, D. Mantzavinos, Photocatalytic degradation of reactive black 5 in aqueous solutions: Effect of operating conditions and coupling with ultrasound irradiation, *Water Res.* 41 (2007) 2236-2246.
- [146] A. Akyol, M. Bayramoglu, Photocatalytic degradation of Remazol Red F3B using ZnO catalyst, *J. Hazard. Mater. B* 124 (2005) 241–246.
- [147] S. Kaneco, H. Katsumata, T. Suzuki, K. Funasaka, K. Ohta, Solar photo-catalytic degradation of endocrine disruptor di-n-butyl phthalate in aqueous solution using ZnO, *Bull. Catal. Soc. Ind.* 6 (2007) 22–33.
- [148] S. Zhou, A.K. Ray, Kinetic studies for photocatalytic degradation of Eosin B on a thin film of Titanium dioxide, *Ind. Eng. Chem. Res.* 42 (2003) 6020-6033.
- [149] D.H. Kim, M.A. Anderson, Solution factors affecting the photocatalytic and photoelectron catalytic degradation of formic acid using supported TiO₂ thin films, *J. Photochem. Photobiol. A: Chem.* 94 (1996) 221–229.
- [150] T.J. Mason, J.L. Luche, Chemistry under extreme or nonclassical conditions, John Wiley & Sons, New York (1997) 317.
- [151] P.N. Vijayalaxmi, P. Saritha, N. Rambabu, V. Himabindu, Y. Anjaneyulu, Sonochemical degradation of 2 chloro-5methyl phenol assisted by TiO₂ and H₂O₂, *J. Hazard. Mater.* 174 (2010) 151–155.
- [152] I.M. Khokhawala, P.R. Gogate, Degradation of phenol using a combination of ultrasonic and UV irradiations at pilot scale operation, *Ultrason. Sonochem.* 17 (2010) 833–838.

- [153] J. Yi, C. Bahrini, C. Schoemaeker, C. Fittschen, W. Choi, Photocatalytic decomposition of H_2O_2 on different TiO_2 surfaces along with the concurrent generation of HO_2 radicals monitored using cavity ring down spectroscopy, *J. Phys. Chem. C*. 116 (2012) 10090-10097.
- [154] A.C. Dodd, A.J. McKinley, M. Saunders, T. Tsuzuki, Effect of particle size on the photocatalytic activity of nanoparticulate zinc oxide, *J. Nanoparticles Res.* 8 (2006) 43–51.
- [155] P. Calza, E. Pelizzetti, Photocatalytic transformation of organic compounds in the presence of inorganic ions, *Pure Appl. Chem.* 73 (2001) 1839–1848.
- [156] C. Minero, V. Maurino, E. Pelizzetti, D. Vione, An empirical, quantitative approach to predict the reactivity of some substituted aromatic compounds towards reactive radical species ($\text{Cl}_2^{\cdot-}$, $\text{Br}_2^{\cdot-}$, $^{\cdot}\text{NO}_2$, $\text{SO}_3^{\cdot-}$, $\text{SO}_4^{\cdot-}$) in Aqueous Solution, *Environ. Sci. Pollut. Res.* 13 (2006) 212-214.
- [157] C. Minero, S. Chiron, G. Falletti, V. Maurino, E. Pelizzetti, R. Ajassa, M.E. Carlotti, D. Vione, Photochemical processes involving nitrite in surface water samples, *Aquat. Sci.* 69 (2007) 71.
- [158] N. Serpone, R. Terzian, P. Colarusso, Sonochemical oxidation of phenol and three of its intermediate products in aqueous media: Catechol, hydroquinone and benzoquinone. Kinetic and mechanistic aspects, *Res. Chem. Intermed.* 18 (1992) 183-202.
- [159] C. Pétrier, R. Torres-Palma, E. Combet, G. Sarantakos, S. Baup, C. Pulgarin, Enhanced sonochemical degradation of bisphenol-A by bicarbonate ions, *Ultrason. Sonochem.* 17 (2010) 111–115.
- [160] D.W. Bahnemann, D. Bockelmann, R. Goslich, Mechanistic studies of water detoxification in illuminated TiO_2 suspensions, *Sol. Energy Mater.* 24 (1991) 564–583.

- [161] S. Sakthivel, B. Neppolian, M.V. Shankar, B. Arabindoo, M. Palanichamy, V. Murugesan, Solar photocatalytic degradation of azodye: Comparison of photocatalytic efficiency of ZnO and TiO₂, *Sol. Energy Mater. Sol. Cells* 77 (2003)65–82.
- [162] J. Saien, A.R. Soleymani, Degradation and mineralization of Direct blue 71 in a circulating up-flow reactor by UV/TiO₂ process and employing a new method in kinetic study, *J. Hazard. Mater.* 14 (2007) 507–512.
- [163] J. Saien, H. Delavari, A.R. Soleymani, Sono-assisted photocatalytic degradation of styrene-acrylic acid copolymer in aqueous media with nano titania particles and kinetic studies, *J. Hazard. Mater.* 177 (2010) 1031–1038.
- [164] R. Comparelli, E. Fanizza, M.L. Curri, P.D. Cozzoli, G. Mascolo, A. Agostiano, UV induced photocatalytic degradation of azo dyes by organic capped ZnO nano crystals immobilized onto substrate, *Appl. Catal. B: Environ.* 60 (2005) 1–11.
- [165] C. Karunakaran, R. Dhanalakshmi, Semiconductor catalysed degradation of phenols by sunlight, *Sol. Energy Mater. Sol. Cells* 92 (2008) 1315–1321.
- [166] K. P Jyothi, S. Joseph, S. Yesodharan, E.P Yesodharan, Periodic change in the concentration of hydrogen peroxide formed during the semiconductor mediated sonocatalytic treatment of wastewater: Investigations on pH effect and other operational variables, *Res. J. of Recent Sci.* 2 (2013)136-149.
- [167] P. Neta, R.E. Huie, A.B. Ross, Rate constants for reactions of inorganic radicals in aqueous solution, *J. Phys. Chem.* 17 (1988) 1027–1258.
- [168] G. V. Buxton, C. L. Greenstock, W. P. Helman, A. B. Ross, Critical review of rate constants for reactions of hydrated electrons, hydrogen atoms and hydroxyl radicals ($\cdot\text{OH}/\text{O}^-$) in aqueous solution, *J. Phys. Chem.* 17(2) (1988) 513–886.

- [169] X. Zhua, M.A. Nanny, E.C. Butler, Effect of inorganic anions on the titanium dioxide-based photocatalytic oxidation of aqueous ammonia and nitrite, *J. Photochem. Photobiol. A: Chem.* 185 (2007) 289–294.
- [170] L. Song, C. Chen, S. Zhang, Sonocatalytic performance of Tb_7O_{12}/TiO_2 composite under ultrasonic irradiation, *Ultrason. Sonochem.* 18, (2011) 713-717.
- [171] J. Wang, Z. Jiang, L. Zhang, P. Kang, Y. Xie, Y. Lv, R. Xu, X. Zhang, Sonocatalytic degradation of some dyestuffs and comparison of catalytic activities of nano sized TiO_2 , nano-sized ZnO and composite TiO_2/ZnO powders under ultrasonic irradiation, *Ultrason. Sonochem.* 16 (2009) 225-231.
- [172] M H. Priya, G Madras, kinetics of TiO_2 -catalyzed ultrasonic degradation of Rhodamine B dyes, *Ind. Eng. Chem. Res.* 45 (2006) 913-921.
- [173] Y.L. Pang, A.Z. Abdullah, S. Bhatia, Comparison of sonocatalytic activities on the degradation of Rhodamine B in the presence of TiO_2 powder and nanotubes, *J. Appl. Sci.* 10 (2010)1068-1075.
- [174] Z. Meng, W. C. Oh, Sonocatalytic degradation and catalytic activities for MB solution of Fe treated fullerene/ TiO_2 composite with different ultrasonic intensity, *Ultrason. Sonochem.* 18 (2011) 757–764.
- [175] W. Zheng, M. Maurin, M.A.Tarr, Enhancement of sonochemical degradation of phenol using hydrogen atom scavengers, *Ultrason. Sonochem.* 12(2005) 313-317.
- [176] M. Goel, H. Hongqiang, A.S. Majumdar, M.B. Ray, Sonochemical decomposition of volatile and nonvolatile organic compounds: A comparative study, *Water Res.* 38 (2004) 4247-4261.
- [177] J.D. Seymour, R.B. Gupta, Oxidation of aqueous pollutants using ultrasound: Salt induced enhancement, *Ind. Eng. Chem. Res.* 36 (1997) 3453–3459.

- [178] E. Evgenidou, I. Konstantinou, K. Fytianos, I. Poulios, Oxidation of two organophosphorous insecticides by the photo-assisted Fenton reaction, *Water Res.* 41 (2007) 2015–2027.
- [179] M.A. Rauf, S.S. Ashraf, Fundamental principles and application of heterogeneous photocatalytic degradation of dyes in solution, *Chem. Eng. J.* 151 (2009) 10–18.
- [180] A. Henglein, C. Kormann, Scavenging of OH radicals produced in the sonolysis of water, *Int. J. Radiat. Biol.* 48 (1985) 251–258.
- [181] S. Marouani, O. Hamdaoui, F. Saoudi, M. Chiha, Sonochemical degradation of Rhodamine B in aqueous phase: effect of additives, *J. Chem. Eng.* 158 (2010) 550-557.
- [182] J. Madhavan, F. Grieser, M. Ashokkumar, Combined advanced oxidation processes for the synergistic degradation of ibuprofen in aqueous environments, *J. Hazard. Mater.* 178 (2010) 202-208.
- [183] J. Wang, Y. Jiang, Z. Zhang , G. Zhao ,G. Zhang , T. Ma , W. Sun , Investigations on the sonocatalytic degradation of Congo red catalysed by nanometer rutile powder and various influencing factors, *Desalination* 216 (2007) 196-208.
- [184] S. Kaur, V. Singh, Visible light induced sonocatalytic degradation of Reactive Red dye 198 using dye sensitized TiO₂, *Ultrason. Sonochem.* 14 (2007) 531-537.
- [185] R. Chand, N.H. Ince, P.R. Gogate, D.H. Bremner, Phenol degradation using 20, 300 and 520 kHz ultrasonic reactors with hydrogen peroxide, ozone and zero valent metals, *Sep. Puri. Technol.* 67 (2009) 103-109.
- [186] A. Piscopo, D. Robert, J. V. Weber, Influence of pH and chloride anion on the photocatalytic degradation of organic compounds Part I. Effect on the benzamide and para - hydroxybenzoic acid in TiO₂ aqueous solution, *Appl. Catal. B: Environ.* 35 (2001) 117–124.

- [187] M. Dukkanci, G. Gunduz, Ultrasonication degradation of oxalic acid in aqueous solution, *Ultrason. Sonochem.* 13 (2006) 517-522.
- [188] C. Minero, P. Pellizzari, V. Maurino, E. Pelizzetti, D. Vione, Enhancement of dye sonochemical degradation by some inorganic anions present in natural waters, *Appl. Catal. B: Environ.* 77 (2008) 308–316.
- [189] J.-J. Yao, N.-Y. Gao, Y. Deng, Y. Ma, H.-J. Li, B. Xu, L. Li, Sonolytic degradation of parathion and the formation of byproducts, *Ultrason. Sonochem.* 17 (2010) 802–809.
- [190] M. Chiha, O. Hamdaoui, S. Baup, N. Gondrexon, Sonolytic degradation of endocrine disrupting chemical 4-cumylphenol in water, *Ultrason. Sonochem.* 18 (2011) 943–950.
- [191] O. Moumeni, O. Hamdaoui, Intensification of sonochemical degradation of malachite green by bromide ions, *Ultrason. Sonochem.* 19 (2012) 404–409.
- [192] S. Devi Priya, S. Yesodharan, Photocatalytic degradation of pesticide contaminants in water, *Sol. Energy Mater. Sol. Cells* 86 (2005) 309–348.
- [193] A. Sobczyk, L. Duczmal, W. Zmudzinski, Phenol destruction by photocatalysis on TiO₂: An attempt to solve the reaction mechanism, *J. Mol. Catal. A* 213 (2004) 225–232.
- [194] P.A. Deshpande, G. Madras, Photocatalytic degradation of phenol by base metal substituted orthovanadates, *Chem. Eng. J.* 161 (2010) 136–145.
- [195] M.I. Litter, Heterogeneous photocatalysis: Transition metal ions in photocatalytic systems, *Appl. Catal. B* 23 (1999) 89–97.
- [196] R. Doong, W. Chang, Photodegradation of parathion in aqueous TiO₂ and zero valent iron solutions in the presence of hydrogen peroxide, *J. Photochem. Photobiol. A: Chem.* 116 (1998) 221–228.

- [197] T. Chen, R. Doong, W. Lei, Photocatalytic degradation of parathion in aqueous TiO₂ dispersion: The effect of hydrogen peroxide and light intensity, *Water Sci. Technol.* 37 (1998) 187–194.
- [198] M.G. Antoniou, P.A. Nicolaou, J.A. Shoemaker, A.A. de la Cruz, D.D. Dionysiou, Detoxification of water contaminated with cyanotoxin microcystin-LR by utilizing thin TiO₂ photocatalyst films, *Appl. Catal. B: Environ.* 91 (2009) 165–173.
- [199] L. Andronic, A. Enesca, C. Vladuta, A. Duta, Photocatalytic activity of cadmium doped TiO₂ films for photocatalytic degradation of dyes, *Chem. Eng. J.* 152 (2009) 64–71.
- [200] Y. Chen, D.D. Dionysiou, A comparative study of physicochemical properties and photocatalytic behavior of macroporous TiO₂-P25 composite films and macroporous TiO₂ films coated on stainless steel substrates, *Appl. Catal. A: Gen.* 317 (2007) 129–137.
- [201] Z.D. Meng, W.C. Oh, Sonocatalytic degradation and catalytic activities for MB solution of Fe treated fullerene/TiO₂ composite with different ultrasonic intensity, *Ultrason. Sonochem.* 18 (2011) 757–764.
- [202] R.A. Torres-Palma, E. Combet, C. Petrier, C. Pulgarin, An innovative ultrasound, Fe²⁺ and TiO₂ photoassisted process for bisphenol A mineralization, *Water Res.* 44 (2010) 2245–2252.
- [203] P.R. Gogate, Treatment of wastewater streams containing phenolic compounds using hybrid techniques based on cavitation: A review of the current status and the way forward, *Ultrason. Sonochem.* 15 (2008) 1–15.
- [204] S. K. Kavitha, P. N. Palanisamy, Photocatalytic and sonophotocatalytic degradation of reactive red 120 using dye sensitized TiO₂ under visible light, *Inter. J. Civil Environ. Eng.* 3 (2011) 365-378.

- [205] M. Mrowetz, C. Pirola, E. Selli, Degradation of organic water pollutants through sonophotocatalysis in the presence of TiO₂, *Ultrason. Sonochem.* 10 (2003) 247–254.
- [206] C. Wu, X. Liu, D. Wei, J. Fan, L. Wang, Photo sonochemical degradation of phenol in water, *Water Res.* 35 (2001) 3927–3933.
- [207] M.A. Beckett, I. Hua, Elucidation of the 1, 4-dioxane decomposition pathway at discrete ultrasonic frequencies, *Environ. Sci. Technol.* 34 (2000) 3053–3944.
- [208] C.G. Joseph, G.L. Puma, A. Bono, D. Krishniah, Sonophotocatalysis in advanced oxidation process: A short review, *Ultrason. Sonochem.* 16 (2009) 583–589.
- [209] E. Naffrechoux, S. Chanoux, C. Petrier, J. Suptil, Sonochemical and photochemical oxidation of organic matter, *Ultrason. Sonochem.* 7 (2000) 255–259.
- [210] C. McCullagh, J.M.C. Robertson, D.W. Bahnemann, P.K.J. Robertson, The application of TiO₂ photocatalysis for disinfection of water contaminated with pathogenic microorganisms: A review, *Res. Chem. Intermed.* 33 (2007) 359–375.
- [211] S. Devipriya, Y. Suguna, E.P. Yesodharan, Solar photocatalytic removal of chemical and bacterial pollutants from water using Pt/TiO₂, *Int. J. Photoenergy* (2012) 1-8.
- [212] C. Ogino, M. Farshbaf Dadjour, K. Takaki, N. Shimizu, Enhancement of sonocatalytic cell lysis of *Escherichia coli* in the presence of TiO₂, *Biochem. Eng. J.* 32 (2006) 100–105.
- [213] E. Joyce, S.S. Phull, J.P. Lorimer, T.J. Mason, The development and evaluation of ultrasound for the treatment of bacterial suspensions: A study of frequency, power and sonication time on cultured *Bacillus* species, *Ultrason. Sonochem.* 10 (2003) 315–318.

- [214] N. Shimizu, K. Ninomiya, C. Ogino, M. Rahman, Potential uses of titanium dioxide in conjunction with ultrasound for improved disinfection, *Biochem. Eng. J.* 48 (2010) 416–423.
- [215] K. Ninomiya, M. Arakawa, C. Ogino, N. Shimizu, Inactivation of *Escherichia coli* by sono electrocatalytic disinfection using TiO₂ as electrode, *Ultrason. Sonochem.* 20 (2013) 762–767.
- [216] M.F. Dadjour, C. Ogino, S. Matsumura, N. Shimizu, Kinetics of disinfection of *Escherichia coli* by catalytic ultrasonic irradiation with TiO₂, *Biochem. Eng. J.* 25 (2005) 243–248.
- [217] A.G. Rincon, C. Pulgarin, Effect of pH, inorganic ions, organic matter and H₂O₂ on *E. coli* K12 photocatalytic inactivation by TiO₂: Implications in solar water disinfection, *Appl. Catal., B: Environ.* 51 (2004) 283–302.
- [218] S. Drakopoulou, S. Terzakis, M.S. Fountoulakis, D. Mantzavinos, T. Manios, Ultrasound-induced inactivation of gram-negative and gram-positive bacteria in secondary treated municipal wastewater, *Ultrason. Sonochem.* 16 (2009) 629–634.
- [219] A. Nakajima, H. Sasaki, Y. Kameshima, K. Okada, H. Harada, Effect of TiO₂ powder addition on sonochemical destruction of 1,4-dioxane in aqueous systems, *Ultrason. Sonochem.* 14 (2007) 197–200.
- [220] J. Maruga'n, R. van Grieken, C. Sordo, C. Cruz, Kinetics of the photocatalytic disinfection of *Escherichia coli* suspensions, *Appl. Catal. B: Environ.* 82 (2008) 27–36.
- [221] R.W. Watts, S. Kong, M.P. Orr, G.C. Miller, B.E. Henry, Photocatalytic inactivation of coliform bacteria and viruses in secondary wastewater effluent, *Water Res.* 29 (1995) 95–100.
- [222] S.I. Nikitenko, L. Venault, R. Pflieger, T. Chave, I. Bisel, P. Moisy, Potential applications of sonochemistry in spent nuclear fuel reprocessing: a short review, *Ultrason. Sonochem.* 17 (2010) 1033–1040.



ANNEXURE I

LIST OF ABBREVIATIONS AND SYMBOLS

h	Planck's constant
c	Velocity of light.
AOP	Advanced Oxidation Process
AOT	Advanced Oxidation Technology
EOP	Enhanced Oxidation Process
GAC	Granulated Activated Carbon
UV	Ultraviolet
US	Ultrasound
VB	Valence Band
CB	Conduction Band
MW	Microwave
E_g	BandGap Energy
MTBE	Methyl tertiary butyl ether
NHE	Normal Hydrogen Electrode
SPC	Sonophotocatalysis
4-CP	4-chlorophenol
DPA	2,4-dichlorophenoxyacetic acid
DNP	2,4- Dinitrophenol
ppm	Parts per million
ppb	Parts per billion
ROS	Reactive Oxygen Species
AO7	Acid Orange 7
EV	Ethyl Violet
MCP	Monocrotophos
CTA+	Cationic cetyltrimethyl ammonium

List of Abbreviation and Symbols

LS-	Anionic lauryl sulfate
UNESCO	United Nations Educational, Scientific and Cultural Organization
$\cdot\text{OH}$	Hydroxyl Radical
H_2O_2	Hydrogen Peroxide
O_3	Ozone
eV	Electron Volt



ANNEXURE II

RESEARCH PAPERS BASED ON THE CURRENT INVESTIGATIONS

A. List of research papers published in journals

- [1] S.G. Anju, S. Yesodharan, E.P. Yesodharan, Zinc oxide mediated sonophotocatalytic degradation of phenol in water, *Chem. Eng. J.* 189–190 (2012) 84–93.
<http://www.sciencedirect.com/science/article/pii/S138589471200246X>
- [2] S. G. Anju, K. P. Jyothi, S. Joseph, Y. Suguna, E.P. Yesodharan, Ultrasound assisted semiconductor mediated catalytic degradation of organic pollutants in water: Comparative efficacy of ZnO, TiO₂ and ZnO-TiO₂, *Research J. Recent Sci.* 1 (2012) 191-201.
<http://www.isca.in/rjrs/archive/iscsi/30.ISCA-ISC-2011-8EnvS-79>
- [3] N. Hariprasad, S.G. Anju, S. Yesodharan, E.P. Yesodharan, Sunlight Induced removal of Rhodamine B from water through semiconductor photocatalysis: Effects of Adsorption, Reaction Conditions and Additives, *Research J. Mat. Sci.* 1(4) (2013) 9-17.
http://www.isca.in/MATERIAL_SCI/Archive/v1/i4/2.ISCA-RJMatS-2013-019.pdf
- [4] S.G. Anju, I.S. Bright Singh, E.P. Yesodharan, S. Yesodharan, Investigations on semiconductor sonocatalysis for the removal of pathological micro-organisms in water, *Desalination and Water Treat.* 1–8 (2014).
<http://www.tandfonline.com/doi/pdf/10.1080/19443994.2014.908417>

- [5] P.D. Phonsy, S. G. Anju, K. P. Jyothi, S. Joseph, Y. Suguna, E.P. Yesodharan, Semiconductor Mediated Photocatalytic Degradation of Plastics and Recalcitrant Organic Pollutants in Water: Effect of Additives and Fate of Insitu Formed H₂O, *J. Adv. Oxidation Teach.* 18(1) 85-97(13) 2015.
<http://www.ingentaconnect.com/content/stn/jaots/2015/00000018/00000001/art00013>

B. Presented in Conferences

- [1] S. Devipriya, S.G. Anju, S. Yesodharan, E.P. Yesodhara, Photocatalytic degradation of plastic waste using semiconductor oxide catalysts, 1st Kerala Women's Science Congress, Ernakulam, Kerala (2010).
- [2] S.G. Anju, S. Yesodharan, E.P. Yesodhara, Semiconductor Mediated Sonophotocatalytic Degradation of Organic Pollutants in Water in 23rd Kerala Science congress, 2011 p.156.
- [3] S.G. Anju, K.P. Jyothi, S. Joseph, Y. Suguna, E.P. Yesodharan, Ultrasound assisted semiconductor mediated catalytic degradation of organic pollutants in water: Comparative efficacy of ZnO, TiO₂ and ZnO-TiO₂, 1st International Science Congress 2011 p.179.
- [4] S.G. Anju, E.P. Yesodharan, S. Yesodharan, Sunlight Induced Degradation of Plastic Bag Waste Using Photocatalysis. 99th Indian Science Congress, 2012 p. 265.
- [5] K.P.Jyothi, S. Joseph, S.G. Anju, S. Yesodharan, E.P.Yesodharan, Role and Fate Of Hydrogen Peroxide In The Sono And Photocatalytic Transformation Of Organic Pollutants In Water. National Conference in Climate Change: Challenges and Strategies, 2012 p.19.

- [6] N. Hariprasad, S.G. Anju, E.P. Yesodharan, S. Yesodharan, Sunlight Induced removal of Rhodamine B from water through semiconductor photocatalysis: Effects of Adsorption, Reaction Conditions and Additives, 2nd International Science Congress, 2013 p. 194.
- [7] B. Rajeev, P.D. Phonsy, S. G. Anju, Y. Suguna,, Investigations on Zinc oxide as solar photocatalyst for the removal of chemical pollutant from water, Proc.25th Kerala Science Congress, Thiruvananthapuram, 2013, p. 32.
- [8] P.D. Phonsy, S. G. Anju, K. P. Jyothi, S. Joseph, Y. Suguna, E.P. Yesodharan, Semiconductor mediated photocatalytic degradation of plastics and recalcitrant organic pollutants in water: Effect of additives and Fate of insitu formed H₂O₂, Proc. of the 18th International conference on Semiconductor Photocatalysis and Solar Energy Conversion(SPASEC-18), San Diego, USA 2013, p. 172.
- [9] S.G. Anju, I.S Bright Singh, E.P. Yesodharan, S. Yesodharan, Investigations on semiconductor sonocatalysis for the removal of pathological microorganisms in water, Proc.1st National Conference on Advance Oxidation Process, AOP 2013, Punjab 2013, p. 42.
- [10] S.G. Anju, E.P. Yesodharan, S. Yesodharan, Advanced Oxidation Processes for the chemical and bacterial decontamination of water: Inactivation of *Bacillus subtilis* by sonocatalysis, Proc. Of the 3rd Int. Science Congress, Coimbatore, India 2013, p. 83.

- [11] S.G. Anju, E.P. Yesodharan, S. Yesodharan, Augmentation of the photoactivity of semiconductor oxides: Investigations on the coupling of ZnO and TiO₂, Proc. 26th Kerala Science Congress, Wayanad, 2014, p. 210.
- [12] S.G. Anju, E.P. Yesodharan, S. Yesodharan, Irreversible sonocatalytic deactivation of *Bacillus subtilis* in water, 2nd Asia-Oceania Sonochemical Society conference, Malaysia, 2015, p.71.

ANNEXURE III

REPRINTS OF PAPER PUBLISHED

Provided for non-commercial research and education use.
Not for reproduction, distribution or commercial use.



This article appeared in a journal published by Elsevier. The attached copy is furnished to the author for internal non-commercial research and education use, including for instruction at the authors institution and sharing with colleagues.

Other uses, including reproduction and distribution, or selling or licensing copies, or posting to personal, institutional or third party websites are prohibited.

In most cases authors are permitted to post their version of the article (e.g. in Word or Tex form) to their personal website or institutional repository. Authors requiring further information regarding Elsevier's archiving and manuscript policies are encouraged to visit:

<http://www.elsevier.com/copyright>

Author's personal copy

Chemical Engineering Journal 189–190 (2012) 84–93



Contents lists available at SciVerse ScienceDirect

Chemical Engineering Journal

journal homepage: www.elsevier.com/locate/cejChemical
Engineering
Journal

Zinc oxide mediated sonophotocatalytic degradation of phenol in water

S.G. Anju, Suguna Yesodharan, E.P. Yesodharan*

School of Environmental Studies, Cochin University of Science and Technology, Kochi 682022, India

ARTICLE INFO

Article history:

Received 29 September 2011
 Received in revised form 10 February 2012
 Accepted 10 February 2012

Keywords:

Photocatalysis
 Sonocatalysis
 Sonophotocatalysis
 Zinc oxide
 Phenol
 Hydrogen peroxide

ABSTRACT

The degradation of trace amounts of phenol pollutant in water in presence of Zinc oxide catalyst under Ultraviolet (UV), Ultrasonic (US) and combination of UV and US irradiation has been investigated and optimum parameters for the mineralization of the pollutant have been identified. ZnO is more active than TiO₂ for the sonophotocatalytic (UV + US) degradation of phenol. The extent of sonophotocatalytic degradation was higher compared to the individual sono or photocatalytic degradation or even their sum, thereby demonstrating a synergistic effect. The effect of different parameters, viz. dosage and particle size of the catalyst, concentration of pollutant, volume of reaction system, pH, US power density and presence of anions on the degradation rate has been evaluated. The degradation follows variable kinetics depending on the concentration of the substrate. The degradation is facilitated at lower reaction volume and acidic pH. The concentration of hydrogen peroxide formed in the reaction is fluctuating with time, indicating simultaneous formation and decomposition. Anions such as chloride and sulphate inhibit the sonophotocatalytic activity of ZnO. The kinetics and mechanism of the process and possible reasons for the synergy are presented.

© 2012 Elsevier B.V. All rights reserved.

1. Introduction

Semiconductor mediated photocatalysis has been investigated extensively as a viable technique for the removal of organic and inorganic pollutants from aqueous streams. The technique has been proven effective for the oxidative destruction of recalcitrant organic compounds such as dyes [1], pesticides [2], phenols [3–5] and the reduction of several heavy metals [6]. However, photocatalysis has still not gained acceptance as an adequately efficient and effective stand-alone technology for the commercial level decontamination of wastewater. Attempts to enhance the efficiency of photocatalytic treatment of wastewater by adding H₂O₂, H₂O₂/Fe²⁺, Fe³⁺, cations, anions, dyes, etc. to the reaction system and modification of catalyst characteristics by doping, supporting and coatings have also been reported [7–11].

Recently, Ultrasonic (US) irradiation mediated by suitable catalysts (sonocatalysis) has been receiving attention as a promising technique for the treatment of hazardous organic pollutants in wastewater [12–14]. However the degradation rate is slow compared to other established methods. Studies are in progress in many laboratories around the world to enhance the efficiency of US promoted decontamination of water. It has been reported that combining US and Ultraviolet (UV) irradiation enhances the efficiency

of semiconductor mediated degradation of aqueous pollutants synergistically [15–22].

The chemical effects of US in liquid include cavitation which consists of nucleation, growth and collapse of bubbles. The collapse of the bubbles results in localized supercritical condition such as high temperature, pressure, electrical discharges and plasma effects [19]. The gaseous contents of a collapsing cavity reach temperatures of approximately 5500 °C and the liquid immediately surrounding the cavity reaches up to 2100 °C. The localized pressure is estimated to be around 500 atmospheres resulting in the formation of transient supercritical water [23]. The cavities thus serve the purpose of high energy micro reactors. The consequence of these extreme conditions is the cleavage of dissolved oxygen molecules and water molecules. The H•, OH• and O• radicals formed in the process will react with each other as well as with H₂O and O₂ during the rapid cooling phase giving HO₂• and H₂O₂. In this highly reactive nuclear environment, organic pollutants can be decomposed and inorganic pollutants can be oxidised or reduced. This phenomenon is being explored in the emerging field of sonocatalysis for the removal of pollutants.

In photocatalytic systems photo excitation of the semiconductor promotes valence band electrons to the conduction band thereby creating electron deficiency or hole in the valence band. Dioxygen provides a sink for conduction band electron forming superoxide •O₂⁻ which leads to the formation of hydroperoxide HO₂•. Holes in the valence band can react with water molecules or hydroxide anion to form OH radicals. The holes can also be filled by an adsorbed organic donor.

* Corresponding author. Tel.: +91 484 2862557; fax: +91 484 2577311.
 E-mail address: epyesodharan@gmail.com (E.P. Yesodharan).

The similarity in the mechanisms of photocatalytic and sonocatalytic reactions opens up the possibility of combining the techniques for enhancing the degradation of organic pollutants in water. However, very few reports are available on this combination, also known as sonophotocatalysis, which were summarized in a recent review [18]. Almost all these studies are made using TiO_2 as the catalyst. To date no detailed investigation has been reported on the sonophotocatalytic degradation of phenol in presence of ZnO (UV/US/ZnO). Hence we have undertaken a detailed study on the degradation of trace amounts of phenol contaminant in water under US, UV and (US + UV) irradiation in the presence of ZnO. Phenol is selected as the representative pollutant since it has been rated as one of the most toxic organic pollutants in wastewater. The comparative activity of TiO_2 and ZnO was evaluated based on which the latter is chosen for detailed investigations. The effect of various parameters such as catalyst loading, particle size, concentration of the contaminant, pH, reactant volume, presence of anions is investigated and optimum conditions for the degradation are identified. A mechanism is also proposed for the sonophotocatalytic degradation.

2. Materials and methods

ZnO and TiO_2 used in the study were supplied by Merck India Limited. In both cases the particles were approximately spherical and nonporous with over 99% purity. The surface areas of TiO_2 and ZnO, as determined by the BET method are 15 and 12 m^2/g respectively. Phenol AnalAR Grade (99.5% purity) from Qualigen (India) was used as such without further purification. Doubly distilled water was used in all the experiments. All other chemicals were of AnalAR Grade or equivalent. The average particle size of both ZnO and TiO_2 was approximately $10 \times 10^{-2} \mu\text{m}$, unless mentioned otherwise.

The experiments were performed using aqueous solutions of phenol of the desired concentration. Specified quantity of the catalyst is suspended in the solution and kept under agitation using a magnetic stirrer. In the case of US irradiation experiments, sonication was sufficient to ensure adequate mixing of the suspension. Additional mechanical mixing did not make any notable consistent difference in the US reaction rate. Hence mixing by sonication alone was chosen for all US and (US + UV) experiments. The reactor used in all experiments was a cylindrical Pyrex vessel of 250 mL capacity. In photocatalytic experiments, the reactor was placed in a glass vessel of 500 mL capacity through which water from a thermostat at the required temperature was circulated. A high intensity UV lamp (400 W medium pressure mercury vapour quartz lamp) mounted above is used as the UV irradiation source. In the case of sonocatalytic and sonophotocatalytic experiments, ultrasonic bath was used as the source of US. The ultrasonic bath operated at 40 kHz and power of 100 W. Water from the sonicator was continuously replaced by circulation from a thermostat maintained at the required temperature. Unless otherwise mentioned, the reaction temperature was maintained at $29 \pm 1^\circ\text{C}$. The position of the reactor in the ultrasonic bath was always kept the same. At periodic intervals samples were drawn, the suspended catalyst particles were removed by centrifugation and the concentration of phenol left behind was analyzed by Spectrophotometry at 500 nm, using similar reaction system kept in the dark under exactly identical conditions but without UV or US irradiation as the reference. The likely intermediates during phenol degradation such as catechol, hydroquinone and benzoquinone are not detected or detected only in negligible quantities by HPLC analysis, indicating that they undergo faster degradation compared to the parent compound. Hence they are not expected to interfere in the spectrophotometric analysis of phenol. H_2O_2 is determined by iodometry. Mineralization was

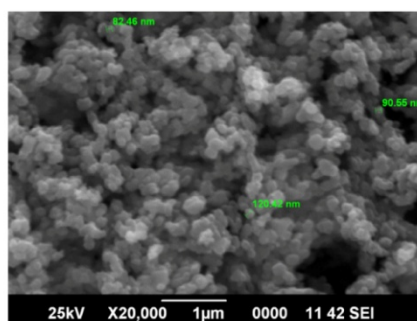


Fig. 1. Typical SEM image of ZnO of approx. $10 \times 10^{-2} \mu\text{m}$ size particles.

identified from the evolution of CO_2 which was detected by the precipitation of BaCO_3 when the gas phase above the reaction suspension was flushed with O_2 through $\text{Ba}(\text{OH})_2$ solution. Particles of various sizes were prepared by mechanical milling of ZnO. The average size of the particles is computed using Scanning Electron Microscopy (SEM). A typical SEM image of ZnO particles is shown in Fig. 1. Adsorption studies were performed as follows [24]:

A fixed amount (0.1 g) of the catalyst was added to 100 mL of phenol solution in a 250 mL beaker and the pH was adjusted as required. The suspension was agitated continuously at constant temperature of $29 \pm 1^\circ\text{C}$ for 2 h to achieve equilibrium. This was then centrifuged at 3000 rpm for 10 min. After centrifugation the concentration of phenol in the supernatant was determined colorimetrically.

The adsorbate uptake was calculated from the relation

$$q_e = \frac{(C_0 - C_e)V}{W}$$

where C_0 is the initial adsorbate concentration (mg/L), C_e is the equilibrium adsorbate concentration in solution (mg/L), V is the volume of the solution in Liter, W is the mass of the adsorbent in gram and q_e is the amount adsorbed in mg per gram of the adsorbent.

3. Results and discussion

Preliminary investigations on the sonocatalytic, photocatalytic and sonophotocatalytic degradation of phenol were made using ZnO and TiO_2 catalysts under identical conditions. The results are presented in Fig. 2.

Experiments conducted in the absence of various factors such as catalyst, light and ultrasound, individually as well as in combination showed that either catalyst and light or catalyst and sound are essential to effect the removal of phenol. Small quantity of phenol is degraded under US irradiation in presence of ZnO as well as TiO_2 . This is understandable since sonolysis of water is known to produce free radicals H^\bullet and OH^\bullet (via reaction (1)), which are capable of attacking the organic compounds in solution [25].



The process is facilitated in a heterogeneous environment [26] such as the presence of ZnO or TiO_2 . The presence of the particles help to break up the microbubbles created by US into smaller ones, thus increasing the number of regions of high temperature and pressure [19]. This leads to increase in the number of OH

Author's personal copy

86

S.G. Anju et al. / Chemical Engineering Journal 189–190 (2012) 84–93

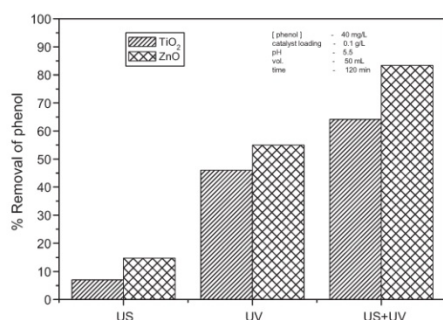


Fig. 2. Sono, photo and sonophotocatalytic removal of phenol in presence of ZnO and TiO₂.

radicals which will interact with the organic molecules present in water and oxidise them, resulting in eventual mineralization.

The results show that in the presence of ZnO as well as TiO₂, combination of light and sound (sonophotocatalysis) enhances the degradation of phenol significantly. In the case of sonocatalysis, the degradation is 13.7% and 7.0% after 2 h of exposure to US in presence of ZnO and TiO₂ respectively. In photocatalysis, the degradation is 55% (ZnO) and 46% (TiO₂) after 2 h of UV irradiation. However sonophotocatalysis resulted in approx. 85% degradation in the case of ZnO and 65% in the case of TiO₂ in 2 h.

Thus it is evident that the degradation of phenol under (UV + US) irradiation is more than the sum of degradation under individual UV and US irradiation, thereby showing a synergistic effect. The synergy index in the case of both catalysts is calculated from the rate of degradation using the following equation [27]:

$$\text{Synergy index} = \frac{R_{US+UV}}{R_{US} + R_{UV}}$$

where R_{US} , R_{UV} and R_{US+UV} are sono, photo and sonophotocatalytic degradation rates respectively. The synergy index thus calculated is 1.25 in the case of ZnO and 1.22 in the case of TiO₂ showing more or less the same degree of enhancement in both cases.

The results further showed that ZnO is more efficient for the sonophotocatalytic degradation of phenol compared to TiO₂ under identical conditions. It was shown earlier that ZnO is more efficient than TiO₂ for the visible light induced photocatalytic degradation of organic compounds because the former can absorb a relatively larger fraction of solar spectrum [28,29]. Since TiO₂ mediated photo and sonophotocatalytic degradation of phenol have been investigated extensively and the current study shows the superior efficiency of ZnO, further investigations were pursued using ZnO. No detailed investigation of the sonophotocatalytic degradation of phenol on ZnO has been reported, to the best of our knowledge.

3.1. Effect of ZnO dosage

The effect of mass of ZnO on the sonocatalytic, photocatalytic and sonophotocatalytic degradation of phenol is shown in Fig. 3. In all three cases the degradation increases with increase in catalyst loading and reaches an optimum range. Beyond this optimum, the degradation slows down and thereafter remains more or less steady or even decreases. The enhanced degradation efficiency is probably due to increased number of adsorption sites and more effective absorption of light which lead to higher number of reactive hydroxyl radicals and their interactions. Any further increase

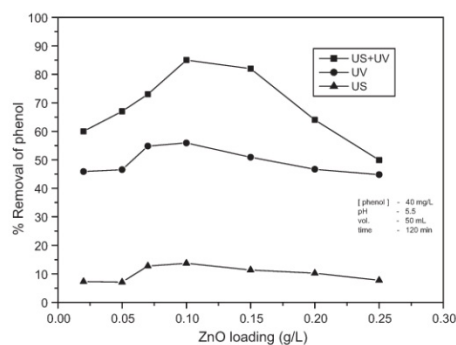


Fig. 3. Effect of catalyst loading on the sono, photo and sonophotocatalytic removal of phenol in presence of ZnO.

in catalyst concentration beyond the optimum will only result in light scattering and reduced passage of light through the sample. Another reason may be the aggregation of catalyst particles causing decrease in the number of available active surface sites. The particles cannot be fully and effectively suspended beyond a particular loading in a particular reactor which also leads to suboptimal penetration of light and reduced adsorption of the substrate on the surface. It is also possible that at higher loading, part of the originally activated zinc oxide is deactivated through collision with ground state catalyst according to the equation [30].



where MO is semiconductor oxide such as TiO₂ or ZnO, MO* has active species adsorbed on the surface and MO[#] is the deactivated form.

In sonophotocatalysis the maximum degradation attained is significantly higher than that in the case of photocatalysis for all catalyst loadings. This trend is seen both in the case of TiO₂ (not shown here) and ZnO thereby suggesting that it is dependent not only on the catalyst but also on the effect of UV and/or US. This is also evident from the identical synergy index value for both catalysts even though the actual degradation efficiency is more in the case of ZnO. In the case of sonophotocatalysis, the decrease in degradation with increase in catalyst loading beyond a particular maximum is more pronounced compared to photocatalysis. However, the optimum loading and the trend remain fairly the same suggesting that US induced increase in rate in photocatalysis is resulting at least partly from the increase in light absorbed by the reaction system. This leads to higher concentration of active species. At higher catalyst loading when filtering and/or scattering of light becomes important, the amount of photoproducted active species does not increase any more and the synergy between photocatalysis and sonocatalysis also remains almost constant or even decreases. This is corroborated from the observation that efficiency of photocatalysis which is determined by the process occurring at the semiconductor-water interface also starts decreasing at around the same catalyst dosage as in the case of sonophotocatalysis.

One of the reasons cited for the US induced enhancement in photocatalytic degradation is the deagglomeration of the aggregate catalyst particles. At higher ZnO concentrated suspension, the working volume of the slurry becomes low [31] and light cannot penetrate into the optically dense medium. Consequently, deagglomeration may not lead to any extra absorption of light as the

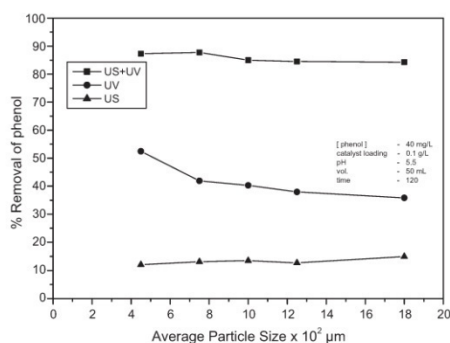


Fig. 4. Effect of particle size of ZnO on the removal of phenol.

zone of action of light can be different from the zone of action of US. Hence any further enhancement in degradation beyond the optimum catalyst loading is due to the production of hydroxyl radicals predominantly by the US only and not due to the combined sonophoto effect. Since US promoted OH radical generation is relatively less, the rate of degradation under sonophotocatalytic conditions at higher catalyst loadings will slow down, level off or even decrease slightly. Davydov et al. [17] also reported that once the optimum catalyst loading is reached in sonophotocatalytic systems, higher US power has to be used to achieve further enhancement in activity. In the current study also, enhancing the US power from 100 to 160 W at the optimized catalyst loading, under otherwise identical conditions, increased the removal of phenol from 13.7% to 16.2% under US and from 85% to 89.5% under (US + UV).

The optimum catalyst loading will also depend on the size, shape and geometry of the reaction assembly. Hence, for each reactor configuration the optimization has to be made separately. In the present case the optimum loading of ZnO for the sonophotocatalytic degradation of phenol is 100 mg/L. All further studies were carried out with this loading.

The effect of catalyst loading also points to the possible effect of particle size on the degradation. Hence the degradation experiments were conducted with ZnO of various particle sizes and the results are shown in Fig. 4. It is seen that particle size variation within limited range as in the current study does not have any significant effect in sonocatalysis. In sonophotocatalysis, the degradation decreases slightly with increase in particle size. The inverse relation between particle size of the catalyst and the degradation of phenol is more significant in photocatalysis. Decrease in particle size leads to increase in surface area, more surface sites for adsorption of the pollutant, better surface promoted interaction between the reactants and resulting higher conversion in photocatalysis. However in the case of sonophotocatalysis, the synergy as a result of the combination of UV and US is adequate to compensate for the decrease in photocatalysis due to increase in particle size. Further the US itself leads to decrease in particle size and enhanced surface area due to deaggregation. In the case of ZnO used in sonocatalysis for 2 h, the average particle size decreased, though slightly, from 10×10^{-2} to $8.5 \times 10^{-2} \mu\text{m}$ and the surface area increased from 12 to $14.5 \text{ m}^2/\text{g}$ approximately. The US also increases the mass transfer between the liquid phase and the catalyst surface [31], making the surface more readily available for reactants. Further, the US

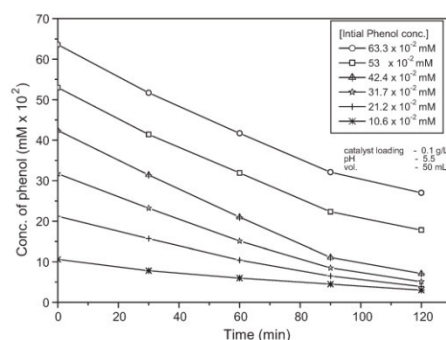
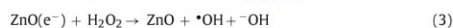


Fig. 5. Effect of initial concentration of phenol on its sonophotocatalytic removal in presence of ZnO.

reduces the charge recombination and promotes the production of additional $\bullet\text{OH}$ from the residual H_2O_2 [32].



Consequent to these US effects, the negative impact of increasing particle size of the catalyst on the rate of degradation of phenol is compensated in sono and sonophotocatalysis. In the case of photocatalysis also, the influence of particle size is minimal, at least in the range (4.5×10^{-2} to $18 \times 10^{-2} \mu\text{m}$) of our study.

3.2. Effect of initial concentration

The effect of initial concentration of phenol in the range of 10–60 mg/L on its sonophotocatalytic degradation is shown in Fig. 5. At higher initial concentration ($>40 \text{ mg/L}$) the $C-t$ plot gives a linear relationship in the initial stage implying that the reaction is of zero order. The optimum kinetic rate calculated from the slope of the $C-t$ plot is $3.9 \mu\text{mol}/\text{min}$. The initial degradation rate increased with increase in the initial concentration up to around 30 mg/L followed by almost constant degradation rate at higher concentration. The plot of $\ln[C/C_0]$ with time at low concentration range of 10–30 mg/L (Fig. 6) shows linear dependence indicating first order kinetics. The average first order rate constant is calculated as $1.4 \times 10^{-4} \text{ s}^{-1}$.

Decrease in the rate of photocatalytic degradation and hence in the order of the reaction at higher concentration of the reactant has been reported earlier [33–35]. Varying kinetics has been reported

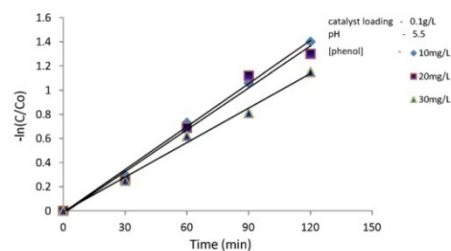


Fig. 6. Kinetics of ZnO mediated sonophotocatalytic degradation of phenol at lower concentrations.

Author's personal copy

88

S.G. Anju et al. / Chemical Engineering Journal 189–190 (2012) 84–93

Table 1
Effect of initial concentration of phenol on its removal. [ZnO]: 0.1 g/L; pH: 5.5; volume: 50 mL.

Initial concentration of phenol (mg/L)	Initial removal rate ($\text{mM} \times 10^3/\text{min}$)		
	US	UV	US + UV
10	0.17	0.72	0.93
20	0.34	1.48	1.83
30	0.50	2.25	2.83
40	0.67	2.12	3.75
50	0.70	2.04	3.87
60	0.65	2.20	3.90

in the case of sonocatalytic reactions also [36]. Davydov et al. [17] reported zero order kinetics in the sonophotocatalytic degradation of salicylic acid on TiO_2 . However the authors worked in the low conversion regime only. In the present case also the shift from zero to first order takes place only at higher conversion ranges.

The first order kinetics at lower concentrations and higher conversion ranges is understandable from both photocatalytic and sonocatalytic angles. In photocatalysis, with increase in concentration, more reactant molecules get adsorbed on to the catalyst site, get activated and interact with correspondingly more OH radicals (see Eqs. (7–14)). This will continue until all the surface sites are occupied. Thereafter, increase in concentration cannot result in increased surface occupation and the phenol removal becomes independent of concentration. The sonocatalytic degradation takes place in the bulk of the solution where the concentration of OH radicals is relatively smaller [37]. Hence increase in concentration of phenol can more effectively utilize the otherwise limited OH radicals leading to increased degradation. This will continue until the phenol concentration is sufficiently high to interact with optimum number of OH radicals.

It is also possible that some of the reaction products and intermediates may remain attached to the surface for relatively longer period resulting in nonavailability of the sites for fresh reactant molecules. Higher substrate concentration can also absorb more photons thereby decreasing the photons available for ZnO activation. In photocatalytic systems, complete domination of the surface by the reactant/intermediates/products can result in suppression of the generation of surface initiated OH radicals. However, in presence of US, the saturation of catalyst surface takes place at a relatively later stage due to deaggregation as discussed earlier. Further, the reaction can also take place at the cavitation bubble interface where the OH concentration can reach a higher limit. Consequently, the optimum concentration for degradation of phenol is higher in sono and sonophotocatalysis compared to photocatalysis. The results summarized in Table 1 confirm this observation.

It is seen that the optimum phenol concentration is 30 mg/L for photocatalysis while it is higher at above 40 mg/L for sono and sonophotocatalysis. This can also be explained based on the effects of microstreaming and increased mass transport associated with the interaction of US with solid matter. Microstreaming provides in situ regeneration of the catalyst surface as the cavitation near the solid surface causes a jet of fluid directed onto the particle [38]. Thus the blockage of active adsorption sites of ZnO can be partially cleared. US also increases the mass transfer on the solid–liquid interface [31,38,39] leading to enhanced adsorption and faster degradation.

3.3. Effect of pH

The extent of US or UV-induced degradation of organics is reported to be dependent on the pH value of the solution [40]. Hence the effect of pH on sonocatalytic, photocatalytic and sonophotocatalytic degradation of phenol is investigated in the

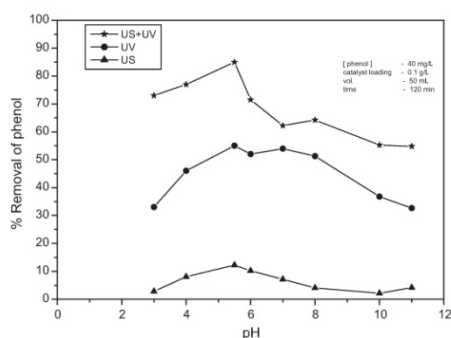


Fig. 7. Effect of pH on the catalytic removal of phenol in presence of ZnO.

range 3–11. The pH of the suspension was adjusted before irradiation and it was not controlled during the irradiation. The results are presented in Fig. 7.

The degradation is more efficient in the acidic region than in the alkaline region. In the case of sonophotocatalysis, in the acidic pH range of 4–5.5, over 85% conversion is effected in 2 h while it is around 60% in the alkaline range. In the photocatalytic system as well as in the sonocatalytic system also maximum degradation is seen in the acidic pH range. The optimum pH in all these cases is 5.5. This observation is similar to that of Wu et al. [40] who reported 98% of sonophotocatalytic degradation of phenol in presence of TiO_2 in the acidic range while it was only 60% under alkaline conditions. Higher degradation efficiency in the acidic range has been reported by other authors also [41–43] with different types of phenol using TiO_2 as the catalyst. In the present study, the relatively lower degradation rate below pH 4 is probably because ZnO is corroding more in this acidic range resulting in its decreased concentration and reduced catalytic activity.

The pH of the reaction medium has significant effect on the surface properties of semiconductor oxide particles (such as ZnO), including the surface charge, size of the aggregation and the band edge position. Hence pH can affect the adsorption–desorption characteristics of the surface of the catalyst. The adsorption of phenol from water solution on ZnO was studied at different pH values and the results are plotted in Fig. 8. Maximum adsorption is observed in the range 5.5–7 and it decreases thereafter in the alkaline range. The results further indicate that the pH dependence of sonophotocatalysed degradation of phenol cannot be fully attributed to the adsorption characteristics even though the trend shows some similarities. In addition to affecting the surface properties of the catalyst, pH also influences direct photolysis of phenol and the reactive $\cdot\text{OH}$ radical formation [44]. Alkaline range is expected to favour the formation of more OH radicals from the large quantity of OH ions present which could enhance the degradation significantly. However this is not reflected in the actual degradation rate possibly due to the poor adsorption.

The effect of pH can be explained at least partially based on the amphoteric behaviour and surface charge of ZnO. The acid–base property of metal oxides is known to have considerable influence on their photocatalytic activity [45]. The Point of Zero Charge (PZC) of ZnO is 9 ± 0.3 approximately [46]. This means that ZnO surface is positively charged when the pH is lower than this value and

Table 2
Formation of H₂O₂ under US, UV and (US + UV). [ZnO]: 0.1 g/L; pH: 5.5; Reaction volume: 50 mL; [Phenol]: 40 mg/L.

Reaction condition	H ₂ O ₂ in presence of phenol (mg/L)			H ₂ O ₂ in the absence of phenol (mg/L)		
	30 min	60 min	90 min	30 min	60 min	90 min
US	1.9	2.2	2.7	2.6	3.6	3.7
UV	5.7	8.5	10.1	2.9	4.1	4.6
US + UV	7.9	12.0	13.0	3.4	4.2	5.8

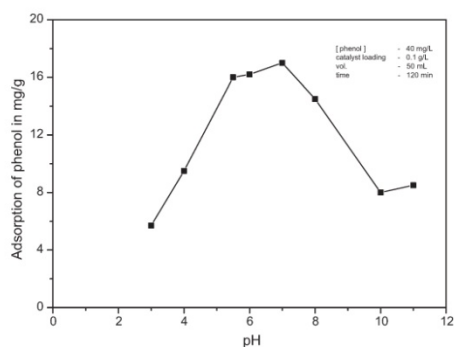


Fig. 8. Effect of pH on the adsorption of phenol from water on ZnO.

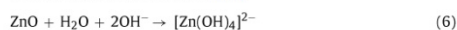
negatively charged when the pH is higher. Solution pH influences the ionisation state of ZnO surface according to the reaction:



In the alkaline pH range, where phenol is expected to be in the ionised form, the adsorption on ZnO will be weaker. Hence the surface mediated degradation will be less. However under acidic conditions, phenol which remains mainly in the neutral form can get adsorbed or come closer to the catalyst surface, resulting in its degradation via active surface species and/or bulk hydroxyl radicals produced in the aqueous media [47]. Further, the presence of more protons can facilitate the formation of reactive OH radicals from the available OH ions. Significant enhancement in the degradation under sonophotocatalysis can also be attributed to the effect of US in reducing the distance between the substrate molecule and the surface of the catalyst particles. This is not feasible in the alkaline range where repulsion between like charges of the substrate and the catalyst particles is much greater [48].

Two important factors responsible for the efficiency of degradation; i.e. adsorption of the substrate on the catalyst surface and the reactive OH radical formation, are effected conversely by the pH resulting in a balancing effect, though to a limited extent. Hence there is reasonably good degradation in both acidic and alkaline pH ranges. The rate of degradation starts decreasing from pH 5.5 onwards much earlier than the PZC of ZnO. Hence PZC

may not be the major factor that determines the adsorption or degradation. Lack of direct correlation between the PZC and the adsorption/degradation rate can also be due to the fact that the PZC itself depends on a number of factors including the size and nature of dispersion of the particles and the type of catalyst itself. ZnO is not stable even in the alkaline range due to the possibility of alkaline dissolution as follows [49]:



The complexity and lack of correlation of the pH or PZC with the rate of semiconductor catalysed photodegradation of phenol is reported by other authors [50] also.

The synergy in the sonophotocatalytic degradation is significantly higher in the acidic range compared to higher pH. In the region of pH 4–5.5, degradation of phenol under sonophotocatalytic conditions is approximately 75% more than that under photocatalysis. However, in the region of pH 7–11, this enhancement is only about 35%. This also points to the interplay of a number of factors that complicate the effect of pH on the sonophotocatalytic degradation of phenol on ZnO.

3.4. H₂O₂ formation and decomposition

Formation of H₂O₂ is observed in all three cases of degradation of phenol; sono, photo and sonophotocatalysis. Small amount of H₂O₂ is produced even in the absence of phenol indicating the formation of free radicals OH and HO₂ in liquid water by US/UV. The results are shown in Table 2. In the case of US, the concentration of H₂O₂ is less in the presence of phenol probably because some of the •OH radicals formed may be reacting with phenol before they could recombine to produce H₂O₂. Also in this case, thermal decomposition of H₂O₂ (which may occur in the vicinity of cavitation bubble where extreme local conditions exist) to water and oxygen rather than to reactive radical species may be occurring [51].

Under UV and (UV + US), where the degradation of phenol and the formation of H₂O₂ are higher, the concentration of H₂O₂ is increasing initially in the presence of phenol but not at the same rate at which phenol is degrading thereby showing that the H₂O₂ formed may be undergoing simultaneous decomposition. It is reported [52,53] that H₂O₂ decomposes and produces OH radicals during, sono, photo and sonophotocatalysis. These radicals can accelerate the degradation of phenol. This is tested by adding H₂O₂ in the beginning of the experiments. The results are shown in Table 3. H₂O₂ enhances the degradation of phenol significantly in the beginning. However this high rate of enhancement is not sustained later on. This can be explained as follows.

In the beginning, added H₂O₂ decomposes faster in presence of UV, US and US+UV, producing maximum OH radicals which can

Table 3
Effect of added H₂O₂ on the removal of phenol under US, UV and (US + UV). [ZnO]: 0.1 g/L; pH: 5.5; Reaction volume: 50 mL; [Phenol]: 40 mg/L.

Reaction condition	% removal of phenol without added H ₂ O ₂			% removal of phenol with added H ₂ O ₂			% enhancement by added H ₂ O ₂		
	30 min	60 min	90 min	30 min	60 min	90 min	30 min	60 min	90 min
US	1.1	6.0	9.5	3.0	7.1	11.2	172.7	18.3	17.9
UV	7.0	17.5	33.2	14.3	31.2	44.7	104.3	78.3	34.6
US + UV	26.1	52.5	73.8	46.4	63.3	85.4	77.7	20.5	15.7

Author's personal copy

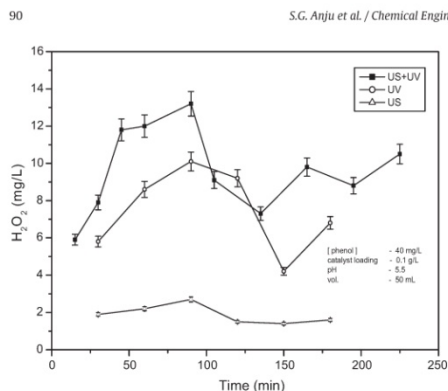


Fig. 9. Oscillation in the concentration of H_2O_2 formed during the degradation of phenol in presence of ZnO under US, UV and (US + UV) irradiation.

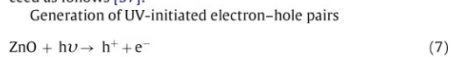
degrade phenol. However, the decomposition of H_2O_2 to water and oxygen also occurs in parallel which restricts the continued availability of the oxidizing species for phenol degradation. Further, even in those experiments without externally added H_2O_2 , the H_2O_2 formed in situ will be accelerating the reaction rate. Hence the effect of initially added H_2O_2 is not that prominent in the later stages of the reaction. The decrease in the enhancement of degradation with time is relatively less in the case of UV. Here the decomposition of H_2O_2 is occurring slowly thereby making the OH radicals available for degradation reaction for extended period. The thermal decomposition of H_2O_2 into inactive H_2O and O_2 also is lower in the case of UV irradiation compared to US or (US + UV).

Periodic measurement of H_2O_2 formed in the reaction during the UV, US and US + UV treatment shows that its concentration is fluctuating with time with periodic maxima and minima as shown in Fig. 9. At the same time, the degradation of phenol continues without break. This oscillatory behaviour [54] in the concentration of H_2O_2 and its influence on the sono photo and sonophotocatalytic degradation deserves detailed investigation. In the case of only US degradation of phenol on semiconductor oxides, H_2O_2 , whether formed in situ or externally added, is proven to be a major contributor towards the degradation irrespective of the catalyst [55].

3.5. Mechanism of the sonophotocatalytic degradation

Sonolysis of water is known to produce active radicals H^\bullet and OH^\bullet via cavitation which attack organic compounds in solution [25]. The presence of ZnO particles enhances this phenomenon as the microbubbles tend to break up into smaller ones thus increasing the total number of regions of high temperature and pressure [26]. Dissolved oxygen serves as a source for nucleus cavitation. The OH radicals attack and degrade phenol. Sonolysis can also result in the pyrolysis of vaporized molecules and eventual mineralization [19,56].

The photocatalytic degradation of phenol is established to proceed as follows [57]:



Recombination of electron-hole pairs



Formation of primary radicals by valence band holes



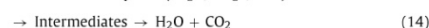
Scavenging of conduction band electrons



Formation of multiple peroxide species



Phenol + Reactivespecies($\bullet O_2^-$, HO_2^\bullet , OH^\bullet)



US is known to have the ability to disperse agglomerated particles and produce OH radical in aqueous phase. Deagglomeration of catalyst particles can increase the overall surface area, provide more active sites for adsorption of the reactant, enhance the absorption of US/UV and generate more reactive species. In order to verify this, as done by Chen and Smirniotis [19], the photocatalytic reaction was interrupted periodically (for 3 min each after 15, 45, 75 and 105 min of UV irradiation) by removing the reaction system from UV light and subjecting it to US during the interruption. The results are summarized in Table 4.

In the case of experiments with periodic short interruption of UV with US, there is enhancement in the degradation of phenol. Since the US was used only for a short period, the influence of sonolysis other than deagglomeration is expected to be minimal. Hence the enhancement can be attributed to deagglomeration and associated advantages. However, the extent of enhancement remains more or less the same (6–8%) in all cases, indicating that US has only limited influence when applied independently. Further, the enhancement is much less compared to that from simultaneous (UV + US) irradiation thereby confirming the synergistic role of US in presence of UV. Hence deagglomeration is not the only factor that contributes to the US induced synergy even though its contribution could be important.

Another major factor for the synergy may be the ability of US to prevent the deactivation of the catalyst by removing adsorbed moieties from the surface by microstreaming and microbubbles eruptions [19]. This kind of surface cleaning can contribute to enhanced reaction only by simultaneous use of US and UV because microstreaming and microbubbling can only occur in the solution during the instantaneous moment when US is applied. The current observation that the degradation is at best only additive when the UV is replaced for a short duration by US (interruption experiments as above) suggests that the synergy is operational only when US and UV are applied together.

Sonication of pure water leads to following chain reactions which is accelerated by the presence of suspended solid particles [32].



Further, the following reactions can occur in the presence of oxygen [58].



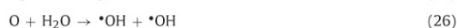
Table 4

Photocatalytic removal of phenol with and without interruption of UV irradiation. [ZnO]: 0.1 g/L; pH: 5.5; volume: 50 mL; [Phenol]: 40 mg/L

UV irradiation time (min)	Percentage removal of phenol	
	No interruption of UV	With interruption of UV
30	21.2	29.0 (3 min interruption of UV with US)
60	43.1	49.5 (6 min interruption of UV with US)
120	56.9	65.4 (12 min interruption of UV with US)

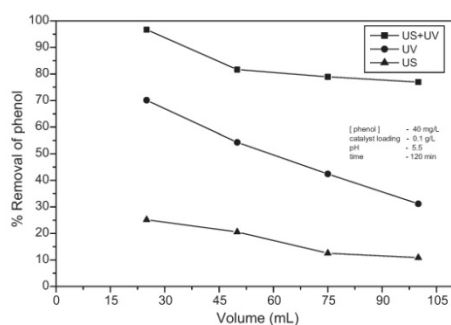


Various active species produced as above react with phenol in the bulk solution or at the interface between the bubbles and the liquid phase. The ozone produced as above can also promote the degradation of phenol in combination with UV via the direct and indirect production of hydroxyl radicals.



Naffrechoux et al. [59] explained that the synergy in sonophotocatalytic systems can be attributed to the US induced physical changes in the catalyst and consequent benefits coupled with concurrent action of three oxidation mechanisms – (i) photodegradation, (ii) sonodegradation and (iii) ozone oxidation.

Chen and Smirniotis [19] reported that in the case of TiO₂ catalyst, reducing the volume of the reaction solution results in dramatic increase in the synergistic effect of UV and US irradiation. We have examined this possibility using ZnO catalyst. The results are presented in Fig. 10. It is seen that the degradation under UV, US and UV + US increased with decreasing reaction volume. The synergistic effect is visible in all cases irrespective of the volume. The effect of volume change is less significant in the case of US irradiation alone while it is quite pronounced in the case of UV. In the case of (UV + US) the degradation decreases with increase in volume up to 45 mL and stabilizes thereafter. This improvement in the photocatalytic degradation is attributed to the decrease in the thickness of the irradiated region which minimises the attenuation of the UV intensity through the solution [58].

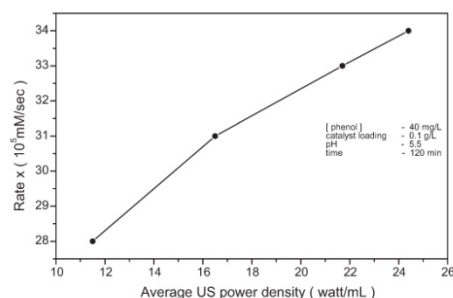
**Fig. 10.** Effect of reaction volume on the removal of phenol in presence of ZnO.

The relation between power density, i.e. applied ultrasonic power divided by the reaction volume [19] and the reaction rate is calculated and plotted in Fig. 11. The reaction rate increases with increase in the average US power density though the rate slows down eventually. The increase in degradation rate can be attributed to the increase in the number of active cavitation bubbles and consequent generation of more OH radicals. The slow down in the rate is caused possibly by eventual absorption of ultrasonic energy by the surrounding apparatus, i.e. the reactor wall and cooling water.

3.6. Effect of anions on the degradation

Anions are often present in natural water systems and hence the study of the effects of anions on the sonophotocatalytic degradation of pollutants is important, especially in the context of commercial application of the technique. In the present study we have investigated the effect of added NaCl and Na₂SO₄ on the degradation of phenol under the optimized conditions of other parameters. The anions inhibit photocatalytic, sonocatalytic and sonophotocatalytic degradation of phenol. The inhibition is more pronounced in the case of sonophotocatalysis. The results are presented in Fig. 12.

Previous studies have reported that sonocatalytic and photocatalytic reactions are sensitive to the presence of anions [34,60–63]. Seymour and Gupta [60] observed NaCl induced enhancement in sonocatalytic degradation of organics using 20 kHz US. It is also reported that the presence of massive amounts of Cl⁻ ions inhibit photocatalytic degradation [64]. The addition of salt increases the ionic strength of the aqueous phase. This is expected to drive the organic pollutants towards the bubble-bulk interface where the majority of the sonodegradation takes place [65]. The increase in surface tension can affect the nucleation process and the cavitation threshold. The presence of salt will also increase the partitioning of the organic species upon cavitation implosion. Thus it was expected that the interfacial concentration of the pollutants would increase which could enhance the overall degradation rate. However, the current observation is contrary to this. The current experiments were conducted at pH 5.5, which is below the PZC

**Fig. 11.** Effect of US power density on the sonophotocatalytic removal of phenol in presence of ZnO.

Author's personal copy

92

S.G. Anju et al. / Chemical Engineering Journal 189–190 (2012) 84–93

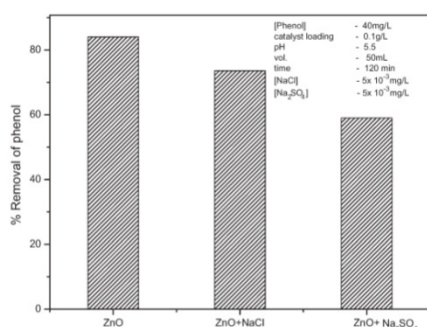


Fig. 12. Effect of chloride and sulphate ions on the sonophotocatalytic removal of phenol in presence of ZnO.

of ZnO. Hence the ZnO particles will be carrying positive charge. Consequently Cl^- and SO_4^{2-} ions can be strongly adsorbed onto these particles through ionic forces. The reaction of surface holes with these undesirable ions leads to decrease in the formation of hydroxyl radicals, resulting in low sonophotocatalytic efficiency.

The chloride ions scavenge the photoproducted holes and the hydroxyl radical more effectively as follows [63]:



The deactivation and decrease in the concentration of hydroxyl radicals caused by SO_4^{2-} can be explained as follows:



The sulphate radicals can react with water to produce more sulphate ions as follows:



$\text{SO}_4^{\bullet-}$ is also a strong oxidant which can contribute to the degradation of phenol as follows:



Of the two competing reactions (34) and (35), the former will be more facile resulting in regeneration of SO_4^{2-} which will again get adsorbed to the surface thereby denying access to the phenol molecule. This, together with reaction (33) which reduces the availability of active OH radicals will result in decreased degradation in the presence of sulphate ions. However, the influence of anions on the sonophotocatalytic degradation is complex and may depend on the interplay of a number of factors such as the catalyst and anion characteristics, pH, concentration, temperature which need to be investigated in detail.

4. Conclusion

ZnO mediated sonocatalytic, photocatalytic and sonophotocatalytic degradation of phenol in water is investigated. Of the two widely used semiconductor oxides, i.e. ZnO and TiO_2 , the former is more active. Combination of UV and US provides synergy for the degradation. Optimum parameters for the sonophotocatalytic

degradation are identified in terms of concentration of the substrate, catalyst loading, pH, reaction volume. The US power density has significant impact on the rate of degradation. The degradation follows variable kinetics, depending on the concentration of the substrate. Anions such as Cl^- and SO_4^{2-} inhibit the degradation. Acidic pH favours the degradation with maximum observed in the range 4–5.5. However, the activity of ZnO is less under extreme acidic conditions, possibly due to corrosion. H_2O_2 formed in the reaction undergoes simultaneous decomposition resulting in oscillation in its concentration. The size of catalyst particles has less impact on sonocatalytic and sonophotocatalytic degradation compared to photocatalysis. Possible reasons for the observations are discussed and a mechanism for the sonophotocatalytic degradation of phenol on ZnO is proposed.

Acknowledgement

Financial support from the Cochin University of Science and Technology by way of Junior Research Fellowship to one of us (S.G.A.) is gratefully acknowledged.

References

- [1] M.S.T. Gonsalves, A.M.F. Oliveira-Campos, E.M.M.S. Pinto, P.M.S. Plasencia, M.J.R.P. Queiroz, Photochemical treatment of solutions of azo dyes containing TiO_2 , *Chemosphere* 39 (1999) 781–786.
- [2] S. Devi Priya, S. Yesodharan, Photocatalytic degradation of pesticide contaminants in water, *Sol. Energy Mater. Sol. Cells* 86 (2005) 309–348.
- [3] Z.B. Guo, R. Ma, G.H. Li, Degradation of phenol by nanomaterial TiO_2 in wastewater, *Chem. Eng. J.* 119 (2006) 55–61.
- [4] A. Sobczyk, L. Duczmal, W. Zmudzinski, Phenol destruction by photocatalysis on TiO_2 ; an attempt to solve the reaction mechanism, *J. Mol. Catal. A* 213 (2004) 225–232.
- [5] P.A. Deshpande, G. Madras, Photocatalytic degradation of phenol by base metal-substituted orthovanadates, *Chem. Eng. J.* 161 (2010) 136–145.
- [6] M.J. Litter, Heterogeneous photocatalysis: transition metal ions in photocatalytic systems, *Appl. Catal. B* 23 (1999) 89–97.
- [7] R. Doong, W. Chang, Photodegradation of parathion in aqueous TiO_2 and zerovalent iron solutions in the presence of hydrogen peroxide, *J. Photochem. Photobiol. A* 116 (1998) 221–228.
- [8] T. Chen, R. Doong, W. Lei, Photocatalytic degradation of parathion in aqueous TiO_2 dispersion: the effect of hydrogen peroxide and light intensity, *Water Sci. Technol.* 37 (1998) 187–194.
- [9] M.G. Antoniou, P.A. Nicolaou, J.A. Shoemaker, A.A. de la Cruz, D.D. Dionysiou, Detoxification of water contaminated with cyanotoxin microcystin-LR by utilizing thin TiO_2 photocatalyst films, *Appl. Catal. B: Environ.* 91 (2009) 165–173.
- [10] L. Andronic, A. Enescu, C. Viaduta, A. Duta, Photocatalytic activity of cadmium doped TiO_2 films for photocatalytic degradation of dyes, *Chem. Eng. J.* 152 (2009) 64–71.
- [11] Y. Chen, D.D. Dionysiou, A comparative study of physicochemical properties and photocatalytic behavior of macroporous TiO_2 -P25 composite films and macroporous TiO_2 films coated on stainless steel substrates, *Appl. Catal. A: Gen.* 317 (2007) 129–137.
- [12] Z.D. Meng, W.C. Oh, Sonocatalytic degradation and catalytic activities for MB solution of Fe treated fullerene/ TiO_2 composite with different ultrasonic intensity, *Ultrason. Sonochem.* 18 (2011) 757–764.
- [13] S. Marouani, O. Hamdaoui, F. Saoudi, M. Chiha, Sonochemical degradation of Rhodamine B in aqueous phase: effect of additives, *Chem. Eng. J.* 158 (2010) 550–557.
- [14] L. Song, C. Chen, S. Zhang, Sonocatalytic performance of $\text{Tb}_2\text{O}_3/\text{TiO}_2$ under ultrasonic irradiation, *Ultrason. Sonochem.* 18 (2011) 713–717.
- [15] R.A. Torres-Palma, E. Combet, C. Petrier, C. Pulgarin, An innovative ultrasound, Fe^{2+} and TiO_2 photoassisted process for bisphenol A mineralization, *Water Res.* 44 (2010) 2245–2252.
- [16] P.R. Gogate, Treatment of wastewater streams containing phenolic compounds using hybrid techniques based on cavitation: a review of the current status and the way forward, *Ultrason. Sonochem.* 15 (2008) 1–15.
- [17] L. Davydov, E.P. Reddy, P. France, P.P. Smirniotis, Sonophotocatalytic destruction of organic contaminants in aqueous systems on TiO_2 powders, *Appl. Catal. B: Environ.* 32 (2001) 95–105.
- [18] C.G. Joseph, G.L. Puma, A. Bono, D. Krishniah, Sonophotocatalysis in advanced oxidation process: a short review, *Ultrason. Sonochem.* 16 (2009) 583–589.
- [19] Y.C. Chen, P. Smirniotis, Enhancement of photocatalytic degradation of phenol and chlorophenols by ultrasound, *Ind. Eng. Chem. Res.* 41 (2002) 5958–5965.
- [20] Y. He, F. Grieser, M. Ashokkumar, The mechanism of sonophotocatalytic degradation of methyl orange and its products in aqueous solutions, *Ultrason. Sonochem.* 18 (2011) 974–980.

- [21] M.T. Taghizadeh, R. Abdollahi, Sonolytic, sonocatalytic and sonophotocatalytic degradation of chitosan in the presence of TiO₂ nanoparticles, *Ultrason. Sonochem.* 18 (2011) 149–157.
- [22] K. Sekiguchi, C. Sesaki, K. Sakamoto, Synergistic effects of high frequency ultrasound on photocatalytic degradation of aldehydes and their intermediates using TiO₂ suspension in water, *Ultrason. Sonochem.* 18 (2011) 757–764.
- [23] E.A. Nepiras, Acoustic cavitation: an introduction, *Ultrasonics* 22 (1984) 25–40.
- [24] S. Jain, R. Yamgar, R.V. Jayram, Photolytic and photocatalytic degradation of atrazine in the presence of activated carbon, *Chem. Eng. J.* 148 (2009) 342–347.
- [25] A. Kottroutou, G. Mills, M.R. Hoffmann, Ultrasonic irradiation of p-nitrophenol in aqueous solution, *J. Phys. Chem.* 95 (1991) 3630–3638.
- [26] K.S. Suslick, L.A. Crum, in: M.J. Crocker (Ed.), *Encyclopedia of Acoustics*, vol. 1, Wiley Interscience, New York, 1997, pp. 271–282.
- [27] J. Madhavan, P.S. Sathish Kumar, S. Anandan, F. Grieser, M. Ashok Kumar, Sonophotocatalytic degradation of monocrotophos using TiO₂ and Fe³⁺, *J. Hazard. Mater.* 177 (2010) 944–949.
- [28] S. Sakthivel, H. Kish, Photocatalytic and photoelectrochemical properties of nitrogen doped TiO₂, *Chem. Phys. Chem.* 4 (2003) 487–490.
- [29] I. Poullos, A. Avranas, E. Rekliti, A. Zouboulis, Photocatalytic oxidation of Auramine O in the presence of semiconducting oxides, *J. Chem. Technol. Biotechnol.* 75 (2000) 205–212.
- [30] B. Neppolian, H.C. Choi, S. Sakthivel, B. Aurbindo, B. Murugesan, Solar/UV induced photocatalytic degradation of three commercial textile dyes, *J. Hazard. Mater.* 89 (2002) 303–317.
- [31] G. Heit, A.M. Braun, UV photolysis of aqueous systems: spatial differentiation between volumes of primary and secondary reactions, *Water Sci. Technol.* 35 (1997) 25–30.
- [32] N.H. Ince, G. Tezcanli-Guyer, R.K. Belen, I.G. Apikyan, Ultrasound as a catalyzer of aqueous reaction systems: the state of the art and environmental applications, *Appl. Catal. B: Environ.* 29 (2001) 167–176.
- [33] S. Rabindranathan, S. Devipriya, S. Yesodharan, Photocatalytic degradation of phosphamidon on semiconductor oxides, *J. Hazard. Mater.* 102 (2003) 217–229.
- [34] K.E. O'Shea, I. Garcia, M. Aguilar, Titanium dioxide photocatalytic degradation of dimethyl and diethyl methyl phosphonate: effect of catalyst and environmental factors, *Res. Chem. Intermed.* 23 (1997) 325–339.
- [35] S. Zhou, A.K. Ray, Kinetic studies for photocatalytic degradation of Eosin B on a thin film of titanium dioxide, *Ind. Eng. Chem. Res.* 42 (2003) 6020–6033.
- [36] S. Merouani, Q. Hamdaoui, F. Saoudi, M. Chih, Sonochemical degradation of Rhodamine B in aqueous phase: effects of additives, *Chem. Eng. J.* 158 (2010) 550–557.
- [37] M. Goel, H. Hongqiang, A.S. Majumdar, M.B. Ray, Sonochemical decomposition of volatile and nonvolatile organic compounds: a comparative study, *Water Res.* 38 (2004) 4247–4261.
- [38] Y.G. Adevuyi, Sonochemistry: environmental science and engineering applications, *Ind. Eng. Chem. Res.* 40 (2001) 4681–4715.
- [39] M. Mrowetz, C. Pirola, E. Selli, Degradation of organic water pollutants through sonophotocatalysis in the presence of TiO₂, *Ultrason. Sonochem.* 10 (2003) 247–254.
- [40] C. Wu, X. Liu, D. Wei, J. Fan, L. Wang, Photosonochemical degradation of phenol in water, *Water Res.* 35 (2001) 3927–3933.
- [41] T.J. Mason, J.L. Luche, *Chemistry Under Extreme or Nonclassical Conditions*, John Wiley & Sons, New York, 1997, p. 317.
- [42] P.N. Vijayalaxmi, P. Saritha, N. Rambabu, V. Himabindu, Y. Anjaneyulu, Sonochemical degradation of 2-chloro-5-methyl phenol assisted by TiO₂ and H₂O₂, *J. Hazard. Mater.* 174 (2010) 151–155.
- [43] A.K. Khodja, T. Sehlil, J.F. Pilichowski, P. Boule, Photocatalytic degradation of 2-phenyl phenol on TiO₂ and ZnO in aqueous suspensions, *J. Photochem. Photobiol.* 141 (2001) 231–239.
- [44] I.M. Khokhawala, P.R. Gogate, Degradation of phenol using a combination of ultrasonic and UV irradiations at pilot scale operation, *Ultrason. Sonochem.* 17 (2010) 833–838.
- [45] D.W. Bahnemann, D. Bockelmann, R. Goslich, Mechanistic studies of water detoxification in illuminated TiO₂ suspensions, *Sol. Energy Mater.* 24 (1991) 564–583.
- [46] S. Sakthivel, B. Neppolian, M.V. Shankar, B. Arabindoo, M. Palanichamy, V. Murugesan, Solar photocatalytic degradation of azodye: comparison of photocatalytic efficiency of ZnO and TiO₂, *Sol. Energy Mater. Sol. Cells* 77 (2003) 65–82.
- [47] J. Saïen, A.R. Soleymani, Degradation and mineralization of Direct blue 71 in a circulating up-flow reactor by UV/TiO₂ process and employing a new method in kinetic study, *J. Hazard. Mater.* 14 (2007) 507–512.
- [48] J. Saïen, H. Delavari, A.R. Soleymani, Sono-assisted photocatalytic degradation of styrene-acrylic acid copolymer in aqueous media with nano titania particles and kinetic studies, *J. Hazard. Mater.* 177 (2010) 1031–1038.
- [49] R. Comparelli, E. Fanizza, M.L. Curri, P.D. Cozzoli, G. Mascolo, A. Agostiano, UV induced photocatalytic degradation of azo dyes by organic capped ZnO nano crystals immobilized onto substrate, *Appl. Catal. B: Environ.* 60 (2005) 1–11.
- [50] C. Karunakaran, R. Dhanalakshmi, Semiconductor catalysed degradation of phenols by sunlight, *Sol. Energy Mater. Sol. Cells* 92 (2008) 1315–1321.
- [51] R. Chand, N.H. Ince, P.R. Gogate, D.H. Bremner, Phenol degradation using 20, 300 and 520 kHz ultrasonic reactors with hydrogen peroxide, ozone and zerovalent metals, *Sep. Purif. Technol.* 67 (2009) 103–109.
- [52] A.J. Hoffmann, E.R. Carraway, M.R. Hoffmann, Photoinduced catalytic production of H₂O₂ and Organic peroxides on quantum sized semiconductor colloids, *Environ. Sci. Technol.* 28 (1994) 776–785.
- [53] T. Wu, G. Liu, J. Zhao, H. Hidaka, N. Serpone, Evidence of H₂O₂ generation during the TiO₂ assisted photodegradation of dyes in aqueous dispersions under visible light illumination, *J. Phys. Chem. B* 103 (1999) 4862–4867.
- [54] J.C. Kuriacose, V. Ramakrishnan, E.P. Yesodharan, Photoinduced catalytic reactions of alcohols on ZnO suspensions in cyclohexane: oscillation in the concentration of H₂O₂ formed, *Indian J. Chem.* 19A (1978) 254–256.
- [55] S.G. Anju, K.P. Jyothis, S. Joseph, Y. Suguna, E.P. Yesodharan, Ultrasound assisted semiconductor mediated catalytic degradation of organic pollutants in water: comparative efficacy of ZnO, TiO₂ and ZnO-TiO₂, *Res. J. Rec. Sci.* (2012).
- [56] C. Petrier, M.F. Lamy, A. Francony, A. Benalccene, B. David, V. Renaudin, N. Condreson, Sonochemical degradation of phenol in dilute aqueous solutions: comparison of the reaction rates at 20 and 487 kHz, *J. Phys. Chem.* 98 (1994) 10514–10520.
- [57] L. Davydov, P.G. Smirniotis, Quantification of the primary processes in aqueous heterogeneous photocatalysis using single stage oxidation reactions, *J. Catal.* 191 (2000) 105–112.
- [58] M.A. Beckett, I. Hua, Elucidation of the 1,4-dioxane decomposition pathway at discrete ultrasonic frequencies, *Environ. Sci. Technol.* 34 (2000) 3053–3044.
- [59] E. Naffrechoux, S. Chanoux, C. Petrier, J. Suptil, Sonochemical and photochemical oxidation of organic matter, *Ultrason. Sonochem.* 7 (2000) 255–259.
- [60] J.D. Seymour, R.B. Gupta, Oxidation of aqueous pollutants using ultrasound: salt induced enhancement, *Ind. Eng. Chem. Res.* 36 (1997) 3453–3459.
- [61] E. Evgenidou, I. Konstantinou, K. Fyrtianos, I. Poullos, Oxidation of two organophosphorus insecticides by the photo-assisted Fenton reaction, *Water Res.* 41 (2007) 2015–2027.
- [62] P. Calza, E. Pelizzetti, Photocatalytic transformation of organic compounds in the presence of inorganic ions, *Pure Appl. Chem.* 73 (2001) 1829–1848.
- [63] M.A. Rauf, S.S. Ashraf, Fundamental principles and application of heterogeneous photocatalytic degradation of dyes in solution, *Chem. Eng. J.* 151 (2009) 10–18.
- [64] V. Augugliaro, L. Palmisano, A. Sclafani, C. Minero, E. Pelizzetti, Photocatalytic degradation of phenol in aqueous TiO₂ suspensions, *Toxicol. Environ. Chem.* 16 (1988) 89–95.
- [65] A. Henglein, C. Kormann, Scavenging of OH radicals produced in the sonolysis of water, *Int. J. Radiat. Biol.* 48 (1985) 251–258.



Ultrasound assisted semiconductor mediated catalytic degradation of organic pollutants in water: Comparative efficacy of ZnO, TiO₂ and ZnO-TiO₂

Anju S.G., Jyothi K.P., Sindhu Joseph, Suguna Y. and Yesodharan E.P.*

School of Environmental Studies, Cochin University of Science and Technology, Kochi-682022 INDIA

Available online at: www.isca.in

(Received 26th November 2011, revised 6th January 2012, accepted 25th January 2012)

Abstract

Sonocatalytic degradation of organic pollutants in water is investigated using ZnO, TiO₂ and combination of ZnO and TiO₂ (ZnO-TiO₂) as catalysts, with phenol as the test substrate. The efficacy of the catalysts is in the order ZnO-TiO₂ > ZnO > TiO₂. The degradation in presence of ZnO-TiO₂ is more than the sum of the degradation achieved in presence of the individual oxides under identical conditions, thereby demonstrating a synergistic effect. The ratio of the components in the mixed oxide is optimized. The kinetics of the degradation as well as the influence of various parameters such as catalyst loading, concentration of the pollutant and pH on the degradation efficiency is evaluated. Maximum degradation is observed in the acidic pH for all catalysts. H₂O₂ is formed in the reaction and it undergoes simultaneous decomposition resulting in periodic increase and decrease in its concentration. This observation of the phenomenon of oscillation in the concentration of H₂O₂ is the first of its kind in sonocatalytic systems. A mechanism for the degradation of phenol is proposed based on the observations as well as the concurrent formation and decomposition of H₂O₂.

Keywords: Zinc oxide, titanium dioxide, sonocatalysis, phenol, hydrogen peroxide.

Introduction

Advanced Oxidation Processes (AOP) involving Ultraviolet light, Fenton reagents, Ozone, Ultrasound etc have been tested individually as well as in combination, in the presence and absence of catalysts for the treatment of wastewater containing pesticides, phenols, chlorophenols, dyes and other pollutants¹⁻⁵. The mechanism in all these cases involves the formation of active ·OH radicals which mineralize the pollutants into carbon dioxide, phosphates, sulphates etc.

Recently, Ultrasonic (US) irradiation mediated by suitable catalysts (sonocatalysis) has been receiving special attention as an environment - friendly technique for the treatment of hazardous organic pollutants in wastewater⁶. However the degradation rate is slow compared to other established methods. Investigations aimed at enhancing the efficiency of US promoted decontamination of water are in progress in many laboratories. These include testing a variety of catalysts with different physico-chemical characteristics, modification of reactor design and reaction conditions, combining US with other AOP techniques etc⁶⁻⁹. Coupling US with Ultraviolet (UV) irradiation enhances the efficiency of semiconductor mediated degradation of aqueous pollutants synergistically^{6,7,10,11}.

In liquids US produces cavitation which consists of nucleation, growth and collapse of bubbles. The collapse of the bubbles results in localized supercritical condition such as high temperature, pressure, electrical discharges and

plasma effects¹⁰. The temperature of the gaseous contents of a collapsing cavity can reach approximately 5500°C and that of the liquid immediately surrounding the cavity reaches up to 2100°C. The localized pressure is estimated to be around 500 atmospheres resulting in the formation of transient supercritical water¹². The cavities are thus capable of functioning like high energy micro reactors. The consequence of these extreme conditions is the cleavage of dissolved oxygen molecules and water molecules into radicals such as H·, OH· and O· which will react with each other as well as with H₂O and O₂ during the rapid cooling phase giving HO₂· and H₂O₂. In this highly reactive nuclear environment, organic pollutants can be decomposed and inorganic pollutants can be oxidised or reduced. This phenomenon is being explored in the emerging field of sonocatalysis for the removal of water pollutants.

Most of the studies on the sonocatalytic degradation of water pollutants are made using TiO₂ catalyst, mainly due to its wide availability, stability, non-toxicity and reactivity. Another similar semiconductor oxide ZnO has received relatively less attention possibly due to its corrosive nature under extreme pH conditions. At the same time ZnO is reported to be more efficient than TiO₂ for the visible light induced photocatalytic degradation of organic pollutants because the former can absorb a larger fraction of solar spectrum compared to the latter^{13,14}. Earlier studies in our laboratory showed that ZnO is very efficient as a sono catalyst and sonophotocatalyst for the degradation of trace pollutants in water¹⁵. Comparative study of the catalytic

activity of nano-sized TiO₂, ZnO and composite TiO₂/ZnO powders for the sonocatalytic degradation of dyestuffs showed that the composite powder is more effective¹⁶. Similarly Tb₂O₃/TiO₂ composite was reported to perform better as sonocatalyst compared to the individual oxides for the degradation of amaranth¹⁷. In spite of the multitude of research papers on the sonocatalytic activity of TiO₂ and its modified forms, not many reports are available on the use of ZnO or coupled ZnO-TiO₂ as sonocatalysts for the removal of water pollutants. In this paper we report the comparative assessment of the sonocatalytic activity of ZnO, TiO₂ and ZnO-TiO₂ for the removal of trace amounts of phenol in water and the factors influencing their performance.

Material and Methods

ZnO and TiO₂ used in the study were supplied by Merck India Limited. In both cases the particles were approximately spherical and nonporous with over 99% purity. The surface areas of TiO₂ and ZnO, as determined by the BET method are 15 and 12 m²/g respectively. ZnO-TiO₂ catalysts were prepared by physically mixing respective components in required weight ratios and thoroughly mixing for 30 minutes using mechanical shaker. Phenol AnalaR Grade (99.5% purity) from Qualigen (India) was used as such without further purification. Doubly distilled water was used in all the experiments. All other chemicals were of AnalaR Grade or equivalent. The average particle size of both ZnO and TiO₂ was 10 μm, unless mentioned otherwise.

The experiments were performed using aqueous solutions of phenol of the desired concentration. Specified quantity of the catalyst is suspended in the solution. In the case of US irradiation experiments, sonication was sufficient to ensure adequate mixing of the suspension. Additional mechanical mixing did not make any notable consistent difference in the US reaction rate. The reactor was a cylindrical Pyrex vessel of 250 ml capacity. In the case of sonocatalytic experiments, ultrasonic bath was used as the source of US. The ultrasonic bath operated at 40 kHz and power of 100 W. Water from the sonicator was continuously replaced by circulation from a thermostat maintained at the required temperature. Unless otherwise mentioned, the reaction temperature was maintained at 27 ± 1°C. The position of the reactor in the ultrasonic bath was always kept the same. At periodic intervals samples were drawn, the suspended catalyst particles were removed by centrifugation and the concentration of phenol left behind was analyzed by Spectrophotometry at 500 nm. H₂O₂ is determined by standard iodometry. Degradation and mineralization were identified by the evolution of CO₂. Adsorption studies were performed as follows¹⁸:

A fixed amount (0.1 g) of the catalyst was introduced to 100 ml of phenol solution of required concentration in a 250 ml beaker and the pH was adjusted as required. The suspension

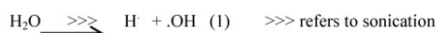
was agitated continuously at constant temperature of 27 ± 1°C for 2 hrs to achieve equilibrium. This was then centrifuged at 3000 rpm for 10 min. After centrifugation the concentration of phenol in the supernatant was determined colorimetrically. The adsorbate uptake was calculated from the relation: $q_e = (C_0 - C_e)V / W$

where C₀ is the initial adsorbate concentration (mg/L), C_e is the equilibrium adsorbate concentration in solution (mg/L), V is the volume of the solution in liter, W is the mass of the adsorbent in gram and q_e is the amount adsorbed in mg per gram of the adsorbent.

Results and Discussion

Preliminary investigations on the sonocatalytic degradation of phenol were made using ZnO and TiO₂ catalysts under identical conditions. The results show that ZnO with 14% degradation of phenol is more efficient as sonocatalyst than TiO₂ with 7% degradation in 2 hr time under otherwise identical conditions.

No significant degradation of phenol took place in the absence of US or the catalyst suggesting that both catalyst and sound are essential to effect degradation. Small quantity of phenol degraded under US irradiation even in the absence of the catalyst. This is understandable since sonolysis of water is known to produce free radicals H[•] and OH[•] (via reaction 1), which are capable of attacking the organic compounds in solution.



The process is facilitated in a heterogeneous environment such as the presence of ZnO or TiO₂. The presence of the particles helps to break up the microbubbles created by US into smaller ones, thus increasing the number of regions of high temperature and pressure¹⁰. This leads to increase in the number of OH radicals which will interact with the phenol present in water and oxidise it, resulting in eventual mineralization.

Coupling of ZnO and TiO₂ in the weight ratio 1:1 results in 13.5% phenol degradation which is same as in the case of ZnO of same mass. This is more than the sum of degradation achieved in the presence of individual ZnO and TiO₂ at loadings equivalent to their concentration in the combination, thereby showing synergistic effect. The % degradation varies with the composition of ZnO-TiO₂ with maximum degradation of 14% in presence of ZnO/TiO₂ at 4:6 as shown in figure 1. Hence further studies with the ZnO-TiO₂ combination were carried out using this ratio.

The synergy index can be calculated from the rate of degradation using the following equation: Synergy index = $R_{(Z-T)} / (R_Z + R_T)$

where R_z , R_T and $R_{(Z-T)}$ are sono catalytic degradation rates in presence of ZnO, TiO₂ and ZnO-TiO₂ respectively. The maximum synergy index thus calculated is approx. 1.30 for ZnO concentration of 10% (by mass) in the coupled ZnO-TiO₂. With increase in the concentration of ZnO in the couple, the synergy index drops slowly. Beyond 40% concentration of ZnO, the couple behaves more like pure ZnO as a sonocatalyst.

The effect of various parameters on the efficiency of the catalysts is investigated in detail in order to optimize the conditions of degradation of phenol in presence of each of them.

Effect of catalyst dosage: The effect of catalyst dosage on the sonocatalytic degradation of phenol is studied at different loadings of ZnO, TiO₂ and ZnO-TiO₂. The results are plotted in figure 2.

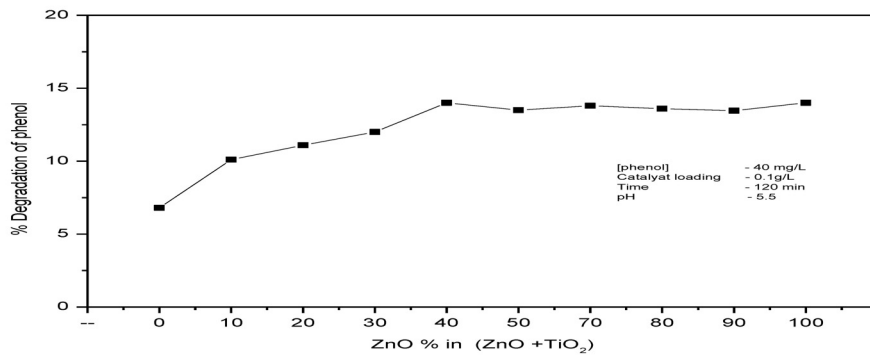


Figure-1
Effect of ZnO/TiO₂ ratio on the sonocatalytic activity

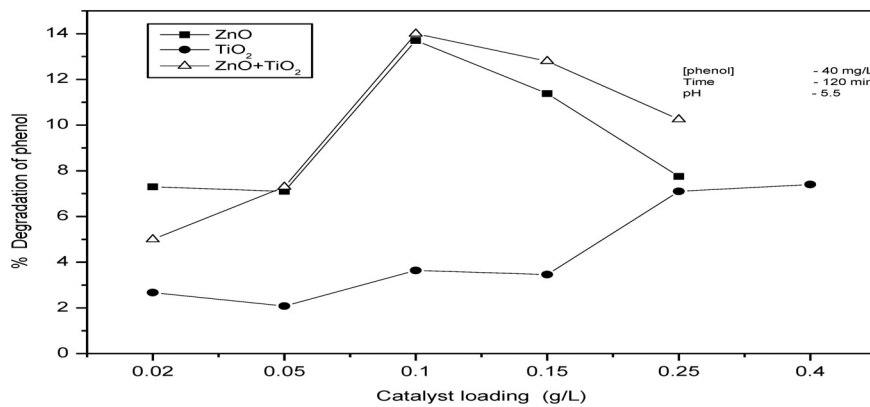


Figure-2
Effect of catalyst dosage on the sonocatalytic activity of ZnO, TiO₂ and ZnO+TiO₂

In all three cases the degradation increases with increase in catalyst loading and reaches an optimum range. Beyond this optimum, the degradation slows down and thereafter remains more or less steady or even decreases. The enhanced degradation efficiency with increase in the dosage is probably due to increased number of catalytic sites, higher production of OH radicals and more effective interaction with the substrate. It is known that the addition of particles of appropriate amount and size into the liquid system results in increase in the acoustic noise and a rise in temperature in the irradiated liquid¹⁹. Introduction of more catalyst particles in the solution provide more nucleation sites for cavitation bubbles at their surface. This will result in decrease in the cavitation thresholds responsible for the increase in the number of bubbles when the liquid is irradiated by US. The increase in the number of cavitation bubbles increases the pyrolysis of water and the sonocatalytic degradation of phenol. Any further increase in catalyst concentration beyond the optimum will only result in the particles coming too close to each other or aggregating thereby limiting the number of active sites on the surface. Higher concentration of the suspended particles may also disturb the transmission of ultrasound in water medium. Hence no further increase in the degradation of the pollutant is observed beyond the optimum dosage. However the number of particles alone or the effect of ultrasound on them is not the only factor leading to increased degradation with increase in catalyst dosage, as seen in the difference in the optimum amount of ZnO, TiO₂ or ZnO-TiO₂ with comparable particle size and surface area. Surface and bulk interactions of the reactant molecules play an important role in the sonocatalytic degradation of organics in suspended systems.

The increase in the degradation of phenol with increase in catalyst dosage as observed here is inconsistent with the report that adsorption of the pollutant molecules on the surface may protect them from ultrasonic degradation²⁰. The adsorption of phenol on the catalysts is determined at the optimum degradation dosages and the values are 24, 16 and 19 mg/g of the catalyst for TiO₂, ZnO and ZnO-TiO₂ respectively. TiO₂ is a better adsorber compared to the other two catalysts. However, the sonocatalytic activity is less compared to ZnO thereby confirming that adsorption is not the major factor in sonocatalysis. At the same time increase in the degradation rate with increase in catalyst loading, as observed in the current study shows that adsorption does not inhibit the degradation altogether. Adsorption helps the surface initiated degradation on the one hand and protects at least partly, the adsorbed species from cavitation effects. At the same time cavitation is known to alter the adsorption/desorption/degradation rates²¹.

The current study shows that ZnO is more efficient than TiO₂ for the degradation of phenol. Appropriate combination of ZnO-TiO₂ is having the same activity as ZnO. This also shows that the effect of particles is not limited to cavitation

or its consequences alone. Irradiation of aqueous solution by ultrasound is known to produce ultraviolet light by sonoluminescence²². Since ZnO is known to be a better harvester of light¹⁴, the higher sonocatalytic activity can be at least partly attributed to the photocatalysis occurring during US irradiation. The presence of suspended particles lead to better propagation of the ultrasonic wave in the suspended medium resulting in the production of cavitation bubbles and emission of light throughout the reactor. This light can activate ZnO leading to the production of OH radicals which can either react with phenol and degrade it or recombine to produce H₂O₂. Higher adsorption of the pollutant on the surface of the catalysts is known to retard the absorption of light resulting in lower degradation. At the same time lower adsorption can result in decreased reaction rate, prolonged degradation time and even incomplete degradation. Hence reasonable degree of adsorption combined with good absorption of light resulting from sonoluminescence lead to good sonocatalytic activity of semiconductor oxides. The higher activity of ZnO-TiO₂ indicates that the better adsorption capability of TiO₂ and the light absorption capability of ZnO can be suitably exploited to achieve maximum degradation of the pollutant in water by sonocatalysis.

H₂O₂ formation and decomposition: Formation of H₂O₂ is observed in the case of sonocatalytic and photocatalytic degradation of phenol in presence of ZnO, TiO₂ and ZnO-TiO₂. Hydrogen peroxide is produced even in the absence of phenol indicating the formation of free radicals OH and HO₂ in liquid water by US/UV. The results are shown in figures 3 and 4.

The results indicate that H₂O₂ formation is more in presence of UV than US in the case of ZnO and ZnO-TiO₂. In the case of TiO₂, the H₂O₂ formed is more in presence of US compared to UV, at least in the initial stages. In the case of US, the concentration of H₂O₂ is less in the presence of phenol probably because some of the ·OH radicals formed may be reacting with phenol before they could recombine to produce H₂O₂. Also in this case, thermal decomposition of H₂O₂ to water and oxygen rather than to reactive radical species may be occurring²³. In the case of TiO₂ the difference in H₂O₂ concentration in the reaction system, between in the presence and absence of phenol is not significant. In this case, the degradation of phenol is also less. The concentration of H₂O₂ is increasing and decreasing periodically showing that it is undergoing simultaneous formation and decomposition. At the same time, the degradation of phenol continues without break, though the rate of degradation slows down with time.

The decomposition and consequent decrease in the concentration of H₂O₂ is more evident even in the initial stages in the case of TiO₂. It is also pertinent to note that the maxima and minima attained in the case of respective

catalysts remain more or less in the same range, irrespective of the number of crests and valleys. This suggests that there is some kind of an equilibrium concentration for H_2O_2 in each system, at which the rate of decomposition and formation balances each other. The maximum concentration of H_2O_2 reached is different for different catalysts indicating that it is dependent on the catalyst. Similar oscillatory

behavior in the concentration of H_2O_2 during photocatalysis²⁴ and sonophotocatalysis¹⁵ has been reported earlier. It is known²⁵ that H_2O_2 decomposes and produces OH radicals during, sono, photo and sonophotocatalysis. These radicals can accelerate the degradation of phenol. This is tested by adding H_2O_2 in the beginning of the experiments. The results are shown in table 1.

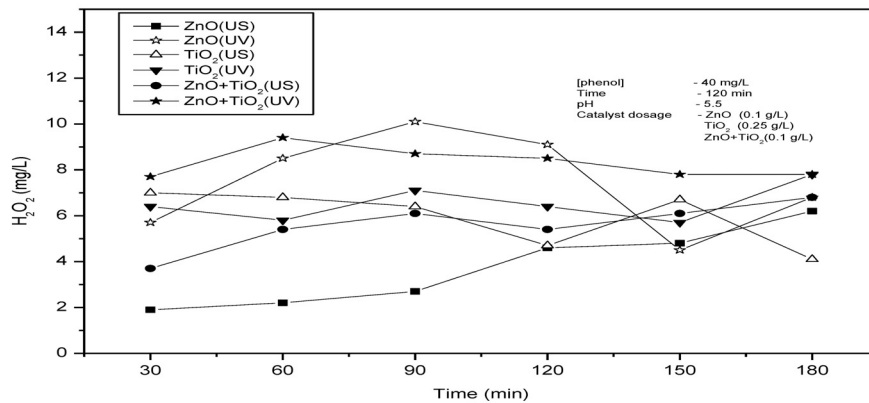


Figure-3
Oscillation in the concentration of H_2O_2 in the presence of phenol under sono and photo catalytic condition on various catalysts

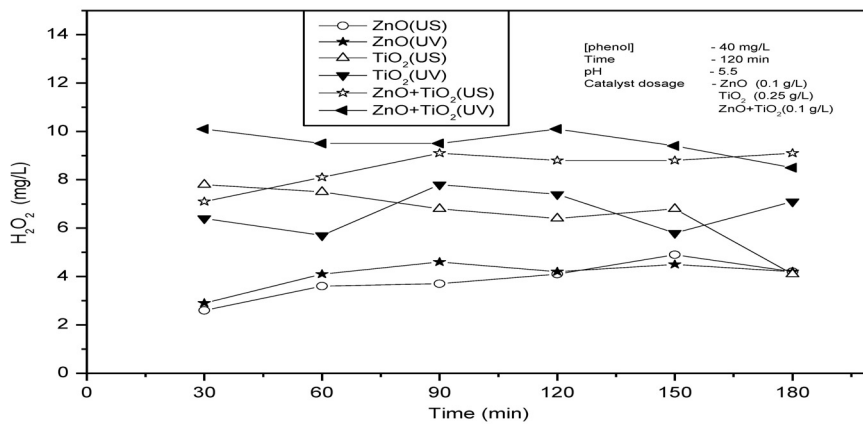


Figure-4
Oscillation in the concentration of H_2O_2 in the absence of phenol under sono and photo catalytic condition on various catalysts

Table 1
Effect of added H₂O₂ on the degradation of phenol under US, UV and (US + UV)
[Catalyst]: 0.1g/L pH: 5.5 Reaction Volume: 50 ml [Phenol]: 40 mg/L

Reaction Condition	% Degradation of phenol without added H ₂ O ₂			% Degradation of phenol with added H ₂ O ₂			% enhancement by added H ₂ O ₂		
	30 min	60 min	90 min	30 min	60 min	90 min	30 min	60 min	90 min
US (ZnO)	1.1	6.0	9.5	3.0	7.1	11.2	172.7	18.3	17.9
UV (ZnO)	7.0	17.5	33.2	14.3	31.2	44.7	104.3	78.3	34.6
US (TiO ₂)	0.8	3.7	5.2	1.8	4.7	5.8	125.0	27.0	11.5
UV (TiO ₂)	5.8	14.6	26.3	10.5	24.8	34.6	81.0	70.0	31.6
US (ZnO-TiO ₂)	1.1	6.2	10.1	2.7	7.4	11.4	145.5	19.4	12.9
UV (ZnO-TiO ₂)	9.2	18.3	36.6	16.1	29.5	45.8	75.0	61.2	25.1

H₂O₂ enhances the degradation of phenol significantly in the beginning. However this high rate of enhancement is not sustained later on. This can be explained as follows:

In the beginning, added H₂O₂ decomposes faster in presence of UV and US producing maximum OH radicals which can degrade phenol. However, the decomposition of H₂O₂ to water and oxygen also occurs in parallel which restricts the continued availability of the oxidizing species for phenol degradation. Further, even in those experiments without externally added H₂O₂, the H₂O₂ formed in situ will be accelerating the reaction rate. Hence the effect of initially added H₂O₂ is not that prominent in the later stages of the reaction. The decrease in the enhancement of degradation with time is relatively less in the case of UV. Here the decomposition of H₂O₂ is occurring slowly thereby making the OH radicals available for degradation reaction for extended period. The thermal decomposition of H₂O₂ into inactive H₂O and O₂ also is lower in the case of UV irradiation compared to US.

H₂O₂ accelerates the degradation in all cases following a fairly uniform pattern. The enhancement effect is comparable in the case of ZnO and ZnO-TiO₂. This shows that in the case of the coupled catalyst, the mechanism of degradation of phenol as well as the formation and decomposition of H₂O₂ is more or less dictated by ZnO since it has higher sono and photocatalytic activity compared to TiO₂.

Concentration Effect: The effect of concentration of phenol on the rate of degradation is investigated. The results are plotted in figure 5.

In the case of ZnO, TiO₂ as well as ZnO-TiO₂ the rate increases linearly with increase in concentration at lower concentration range of 10-40 mg/L. At higher concentrations, the rate slows down as the concentration increases. Thus the degradation follows first order kinetics at lower concentration which changes to lower order at higher concentration. Decrease in the rate of degradation and hence

in the order of the reaction at higher concentration of the reactant has been reported in the case of photocatalysis^{26,27}, sonocatalysis²⁸ as well as sonophotocatalysis¹⁵. In the present study the kinetics observed in the case of all three catalysts is similar indicating that the mechanism of degradation may be the same. However, the change of reaction order takes place at slightly lower concentration ranges in the case of TiO₂ showing the role of surface characteristics and adsorption on the rate of reaction.

Sonocatalytic reactions occur at the surface, in the bulk as well as at the interface of the cavitation bubble. At the surface of the collapsed bubble, the concentration of the OH radicals is relatively high. At low concentration, when the amount of phenol at the surface or in the bulk is low, a considerable part of the OH radicals will recombine yielding H₂O₂. Only about 10% of the OH radicals generated in the bubble can diffuse into the bulk solution²⁹. These factors result in lower degradation of phenol. With increase in concentration, the probability of interaction of OH radicals with phenol increases on the surface as well as in the bulk resulting in increased rate of degradation. The degradation rate slows down and reaches almost a constant level when the concentration of phenol on the catalyst surface as well as at the bubble surface reach a saturation limit during the persistence of the bubble. This is in agreement with earlier findings³⁰.

The general mechanism of sonocatalytic degradation in aqueous medium involves the formation of OH radicals and their attack on the organic substrate. This can also explain the decrease in the recombination of OH radicals resulting in lower concentration of H₂O₂ at higher concentration of phenol³¹. At higher concentration of the substrate, the surface is fully covered as a result of which it cannot effectively absorb the light produced by ultrasound, resulting in decreases photocatalytic effect and eventual stabilization. Also at higher concentrations, the phenol molecules can act as mutual screens thereby preventing effective interaction of all molecules with the ultrasound³².

Effect of pH: The pH of the reaction medium is known to have strong influence on US or UV-induced degradation of organic pollutants. In photolysis, the possibility of bond breakage and the site might be different at different pH due to difference in the distribution of molecular charges. In sonocatalytic reaction, pH can alter the distribution of the pollutants in the bulk region, on the surface and at the site of

the cavity collapse. The surface charge of semiconductors and the interfacial electron transfer and the photoredox processes occurring in their presence are also affected by pH. Hence the effect of pH on sonocatalytic degradation of phenol was investigated in the range 3-11. The pH of the suspension was adjusted initially and it was not controlled during the irradiation. The results are presented in figure 6.

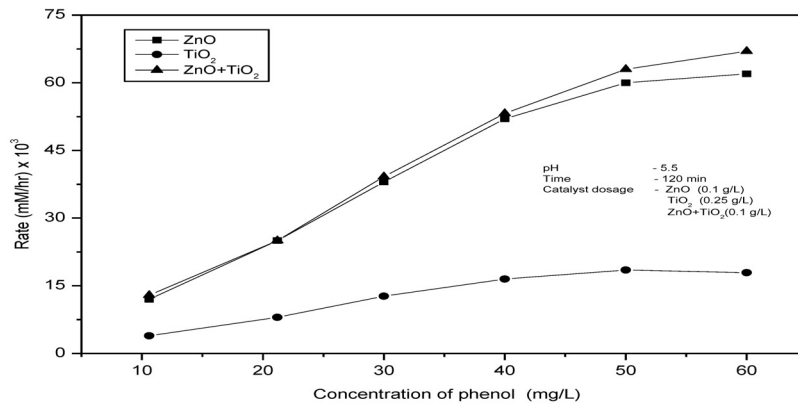


Figure-5
Effect of concentration of phenol on the initial rate of sonocatalytic degradation on various catalysts

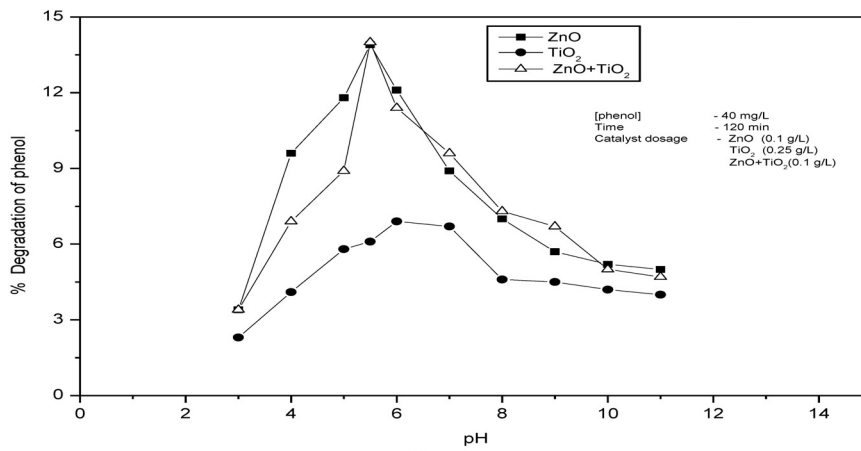
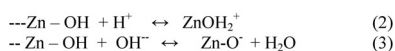


Figure-6
Effect of pH on the sonocatalytic degradation of phenol on various catalysts

The degradation is more efficient in the acidic region than in the alkaline region in the case of the three catalysts tested here. In the case of ZnO, maximum degradation is observed in the acidic pH range of 4-6, which peaks at pH 5.5. In the case of TiO₂ also similar trend follows with the maximum at pH 6. For ZnO-TiO₂, the pH effect is quite similar to that of ZnO as expected. The optimum pH in all these cases is 5.5-6. Higher degradation efficiency in the acidic range has been reported by other authors also³³⁻³⁵ with different types of phenol using TiO₂ as the catalyst. The steep fall in degradation rate below pH 4 in the case of ZnO and ZnO-TiO₂ can be attributed to the corrosion of ZnO under acidic conditions.

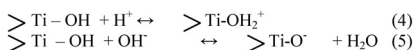
The pH of the reaction medium has significant effect on the surface properties of semiconductor oxide particles, including the surface charge, size of the aggregation and the band edge position³⁶. Hence pH can affect the adsorption – desorption characteristics of the surface of the catalyst. However, in the case of sonocatalysis, adsorption is not the only factor leading to the degradation for reasons explained earlier.

The acid-base property of metal oxides can influence their photocatalytic activity significantly. The Point of Zero Charge (PZC) of ZnO and TiO₂ are 9.3 and 6.8 approximately¹⁴. This means that the catalyst surface is positively charged when the pH is lower than respective PZC value and negatively charged when the pH is higher. Solution pH influences the ionization state of ZnO surface according to the reaction:



In the alkaline pH range, where phenol is expected to be in the ionized form, the adsorption on ZnO will be weaker. Hence the surface mediated degradation will be less. However under acidic conditions, phenol which remains mainly in the neutral form can get adsorbed or come closer to the catalyst surface, resulting in its degradation via active surface species or bulk hydroxyl radicals produced in the aqueous media. Further, the presence of more protons can facilitate the formation of reactive OH radicals from the available OH ions. Significant enhancement in the degradation can also be attributed to the effect of US in reducing the distance between the substrate molecule and the surface of the catalyst particles. This is not feasible in the alkaline range where repulsion between like charges of the substrate and the catalyst particles is much greater¹⁶.

Similarly in the case of TiO₂, solution pH influences the ionization state of TiO₂ surface according to the reaction¹¹

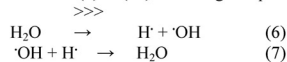


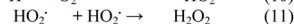
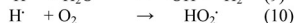
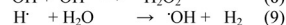
At pH less than ~7, when the TiO₂ surface is positively charged, phenol which is in neutral form can get closer to the surface or weakly adsorbed. At pH > 7, when the surface is negatively charged, phenol in neutral or ionized form will keep away from the surface. In the case of ZnO, weak adsorption or at least phenol coming closer to the surface is possible upto pH 9. Hence the surface promoted sonocatalytic degradation is more in the case of ZnO than TiO₂. As expected, the pH effect on the ZnO-TiO₂ is more or less similar to that on ZnO. The results clearly indicate that there is no well defined correlation between PZC of the semiconductor oxide catalyst and the sonocatalytic degradation rate.

Possible mechanism: Sonocatalytic degradation is generally explained based on sonoluminescence and hot spot theory. Ultrasonic irradiation results in the formation of light of a comparatively wide wavelength range of 200 -500 nm. Those lights with wavelength below 375 nm can excite the semiconductor catalyst and generate highly active OH radicals on the surface. Thus the basic mechanism is partly that of photocatalysis. At the same time the more complex phenomenon of formation of hotspots upon implosion of some bubbles on the catalyst surface also leads to the formation of electron-hole pairs and excess OH radicals¹⁴. Since the formation of electron-hole pairs is the first step in both photocatalysis and sonocatalysis, the efficiency of the process depends on the ability to prevent their recombination. This is achieved to some extent by combining the semiconductor oxides ZnO and TiO₂ which is one of the reasons for the observed synergy here. Under ultrasonic irradiation, a series of thermal and photochemical reactions take place on the surface of composite TiO₂/ZnO particles¹⁶. Because of the difference in adsorption capacity, the TiO₂ part is inclined to the hole oxidation and ZnO tends towards radical oxidation. The electron transport in the TiO₂/ZnO prevents the electron – hole recombination and increases the sonocatalytic activity. Because the TiO₂ and ZnO possesses similar energy band gap (3.2 eV) the electrons can transfer easily from TiO₂ to ZnO through the crystal interface between the two which results in complete separation of electrons and holes. Such electron transport through the crystal interface of composite oxides has been reported earlier also¹⁷.

The overall mechanism of H₂O₂ formation and the decomposition of phenol under sonocatalytic conditions can be explained as follows:

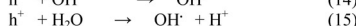
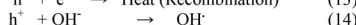
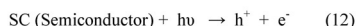
Acoustic cavitation produces highly reactive primary radicals such as OH and H as in reaction (6). Recombination and a number of other reactions occur within the bubble as in reactions (7) to (11) following this primary radical generation



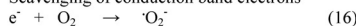


OH radical is a nonselective oxidant with a high redox potential (2.8 eV) which is able to oxidise most organic pollutants³⁷.

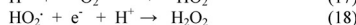
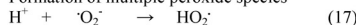
Similarly the photocatalytic reaction initiated by ultrasound can be represented as follows³⁸:



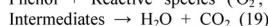
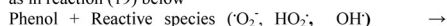
Scavenging of conduction band electrons



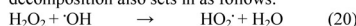
Formation of multiple peroxide species



Various reactive species produced as above react with phenol as in reaction (19) below



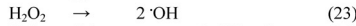
Once sufficient concentration of H₂O₂ is reached, its decomposition also sets in as follows:



H₂O₂ can also lead to reduction in charge recombination by taking up the electron



H₂O₂ can also produce OH radicals directly or reaction with superoxide anion



Conclusion

The sonocatalytic activity of ZnO, TiO₂ and ZnO-TiO₂ for the degradation of phenol pollutant in water is investigated. The efficacy of the catalysts for the degradation is in the order ZnO-TiO₂ > ZnO > TiO₂. At lower concentrations of ZnO, the percentage degradation in the presence of coupled ZnO-TiO₂ is more than the sum of the degradation achieved in the presence of individual oxides under identical conditions, implying a synergistic effect. The catalyst loading, irradiation time, initial pH and concentration of the substrate have profound effect on the rate of degradation. H₂O₂ formed during the degradation of phenol undergoes simultaneous decomposition as well. After initial accumulation upto certain concentration, decomposition of H₂O₂ also sets in resulting in oscillation in its concentration. Possible mechanism for the sonocatalytic degradation of phenol, formation and decomposition of H₂O₂ and the enhanced activity of coupled ZnO-TiO₂ is discussed.

Acknowledgement

ASG acknowledges the financial support from the Cochin University of S & T, Kochi, India. JKP and SJ acknowledge the financial support from the CSIR, New Delhi, India.

References

1. Ying-Shih M, Chi-Fanga S, Jih-Gaw L, Degradation of carbofuran in aqueous solution by ultrasound and Fenton processes: Effect of system parameters and kinetic study, *J Hazardous Mater.*, **178**, 320-325 (2010)
2. Zouaghi R, David B, Suptil J, Djebbar K, Boutiti A, Guittoneau S, Sonochemical and sonocatalytic degradation of monolinuron in water, *Ultrason.Sonochem.* **18**, 1107-1112 (2011)
3. Torres R.A, Abdelmalek F, Combet E, Petrier C, Pulgarin C, A comparative study of ultrasonic cavitation and Fenton's reagent for bisphenol A: Degradation in deionised and natural waters, *J Hazard. Mater* **146**, 546-555 (2007)
4. Devipriya S, Yesodharan S, Photocatalytic degradation of pesticide pollutants in water, *Solar Energy Mater and Solar Cells*, **86**, 309-348 (2005)
5. Malato S, Blanco J, Alarcon D.C, Maldonado M.I, Fernandez-Ibanez P, Gemjak W, Photocatalytic decontamination and disinfection of water with solar collectors, *Catalysis Today* **122**, 137-149 (2007)
6. Joseph C.G, Puma G.L, Bono A, Krishniah D, Sonophotocatalysis in advanced oxidation process: A short review, *Ultrason., Sonochem.* **16**, 583-589 (2009)
7. Gogate P.R, Treatment of wastewater streams containing phenolic compounds using hybrid techniques based on cavitation: a review of the current status and the way forward, *Ultrason. Sonochem.* **15**, 1-15 (2008)
8. Torres-Palma R.A, Nieto J.I, Combet E, Petrier C, Pulgarin C, An innovative ultrasound, Fe²⁺ and TiO₂ photo assisted process for bisphenol a mineralization, *Water Res.* **44**, 2245-2252 (2010)
9. Davydov L, Reddy E.P, France P, Smirniotis P, Sonophotocatalytic destruction of organic contaminants in aqueous systems on TiO₂ powders, *Appl. Catal.B: Environmental* **32**, 95-105 (2001)
10. Chen Y.C, Smirniotis P, Enhancement of photocatalytic degradation of phenol and chlorophenols by ultrasound, *Ind. Eng. Chem. Res.* **41**, 5958-5965 (2002)

11. Kritikos D.E, Xekoukoulotakis N.P, Psillakis E, Mantzavinou D, Photocatalytic degradation of reactive black 5 in aqueous solutions: Effect of operating conditions and coupling with ultrasound irradiation, *Water Res.* **41**, 2236-2246 (2007)
12. Nepiras E.A, Acoustic cavitation: An introduction, *Ultrasonics*, **22**, 25-40 (1984)
13. Poulivos I, Avranas A, Rekliti E, Zouboulis A, Photocatalytic oxidation of Auramine O in the presence of semiconducting oxides, *J Chem Technol. Biotechnol.* **75**, 205-212 (2000)
14. Sakthivel S, Neppolian B, Shankar M V, Arabindoo B, Palanichamy M, Murugesan V, Solar photocatalytic degradation of azodye: Comparison of photocatalytic efficiency of ZnO and TiO₂, *Solar Energy Mater. and Solar Cells*, **77**, 65-82 (2003)
15. Anju S.G, Yesodharan S, Yesodharan E.P, Semiconductor mediated sonophotocatalytic degradation of organic pollutants in water, Proc. 23rd Kerala Science Congress, Trivandrum 156-157 (2011)
16. Wang J, Jiang Z, Zhang L, Kang P, Xie Y, Lv Y, Xu R, Zhang X, Sonocatalytic degradation of some dyestuffs and comparison of catalytic activities of nanosized TiO₂, nano-sized ZnO and composite TiO₂/ZnO powders under ultrasonic irradiation, *Ultrasonics Sonochem.* **16**, 225-231 (2009)
17. Song L, Chen C, Zhang S, Sonocatalytic performance of Tb₂O₃/TiO₂ composite under ultrasonic irradiation, *Ultrason. Sonochem.* **18**, 713-717 (2011)
18. Jain S, Yamgar R, Jayram R.V, Photolytic and photocatalytic degradation of atrazine in the presence of activated carbon, *Chem. Eng. Journal*, **148**, 342-347 (2009)
19. Tuziuti T, Yasui K, Sivakumar M, Iida Y, Correlation between acoustic cavitation noise and yield enhancement of sonochemical reaction by particle addition, *J Phys Chem. A* **109**, 4869-4872 (2005)
20. Pandit A.B, Gogate P.R, Majumdar S, Ultrasonic degradation of 2,4,6 trichlorophenol in presence of TiO₂ catalyst, *Ultrason.Sonochem.* **8**, 227-231(2001)
21. Hamdaoui O, Naffrechoux E, Adsorption kinetics of 4-chlorophenol on granulated activated carbon in the presence of high frequency ultrasound, *Ultrason.Sonochem* **16**, 15-22 (2009)
22. Beckett M.A, Hua I, Impact of ultrasonic frequency on aqueous sonoluminescence and sonochemistry, *J.Phys.Chem A* **105**, 3796-3802 (2001)
23. Chand R, Ince N.H, Gogate P.R, Bremner D.H, Phenol degradation using 20,300 and 520 kHz ultrasonic reactors with hydrogen peroxide, ozone and zerovalent metals, *Separation and Purification Technology* **67**, 103-109 (2009)
24. Kuriacose J.C, Ramakrishnan V, Yesodharan E.P, Photoinduced catalytic reactions of alcohols on ZnO suspensions in cyclohexane: Oscillation in the concentration of H₂O₂ formed, *Indian J. Chem.* **19A**, 254-256 (1978)
25. Hoffmann A.J, Carraway E.R, Hoffmann M.R, Photocatalytic production of H₂O₂ and Organic peroxides on quantum sized semiconductor colloids, *Environ. Sci. Technol.* **28**, 776-785 (1994)
26. Rabindranathan S, Devipriya S, Yesodharan S, Photocatalytic degradation of phosphamidon on semiconductor oxides, *J Hazard. Mater.* **102**, 217-229 (2003)
27. Daneshvar N, Aber S, Dorraji M.S.S, Khataee A.R, Rasoulifard, Preparation and investigation of photocatalytic properties of ZnO nanocrystals: Effect of operational parameters and kinetic study, *World Acad of Sci. Eng. And Technol.* **29**, 267-272 (2007)
28. Zheng W, Maurin M, Tarr M A, Enhancement of sonochemical degradation of phenol using hydrogen atom scavengers, *Ultrason.Sonochem* **12**, 313-317 (2005)
29. Goel M, Hongqiang H, Majumdar A.S, Ray M.B, Sonochemical decomposition of volatile and nonvolatile organic compound: A comparative study, *Water Res.* **38**, 4247-4261 (2004)
30. Marouani S, Hamdaoui O, Saoudi F, Chiha M, Sonochemical degradation of Rhodamine B in aqueous phase: effect of additives, *Chem. Eng. J.* **158**, 550-557 (2010)
31. Madhavan J, Grieser F, Ashokkumar M, Combined advanced oxidation processes for the synergistic degradation of ibuprofen in aqueous environments, *J Hazardous Mater* **178**, 202-208 (2010)
32. Wang J, Jiang Y, Zhang Z, Zhao G, Zhang G, Ma T, Sun W, Investigations on the sonocatalytic degradation of Congo red catalysed by nanometer rutile powder and

- various influencing factors, *Desalination* **216**, 196-208 (2007)
33. Kaur S, Singh V, Visible light induced sonocatalytic degradation of Reactive Red dye 198 using dye sensitized TiO₂, *Ultrason. Sonochem.* **14**, 531-537 (2007)
34. Vijaya laxmi P.N, Saritha Rambabu P.N, Himabindu V, Anjaneyulu Y, Sonochemical degradation of 2 chloro-5methyl phenol assisted by TiO₂ and H₂O₂, *J Hazard Mater.* **174**, 151-155 (2010)
35. Ou X.H, Lo S.L, Wu C. H, Exploring the interparticular electron transfer process in the photocatalytic oxidation of 4-chlorophenol, *J Hazardous Mater.* **137**, 1362-1370 (2006)
36. Zhou S, Ray A.K, Kinetic studies for photocatalytic degradation of Eosin B on a thin film of Titanium dioxide; *Ind. Eng. Chem. Res.* **42**, 6020-6033(2003)
37. Neppolian B, Ciceri L, Bianchi C L, Grieser F, Ashok kumar M, Sonophotocatalytic degradation of 4-chlorophenol using Bi₂O₃/TiZrO₄ as a visible light responsive photocatalyst, *Ultrason. Sonochem* **18**, 135-139 (2011)
38. Davydov L, Smirniotis P.G, Quantification of the primary processes in aqueous heterogeneous photocatalysis using single stage oxidation reactions, *J Catal.* **191**, 105-112 (2000)



Sunlight induced removal of Rhodamine B from water through Semiconductor Photocatalysis: Effects of Adsorption, Reaction Conditions and Additives

Hariprasad N., Anju S.G., Yesodharan E.P. and Yesodharan Suguna
 School of Environmental Studies, Cochin University of Science and Technology, Kochi, INDIA

Available online at: www.isca.in

Received 31st July 2012, revised 18th January 2012, accepted 22nd January 2013

Abstract

Application of Advanced Oxidation Processes (AOP) for the removal of toxic pollutants from water has been receiving increasing attention in recent times. Photocatalysis using semiconductor oxides is one such AOP which is being investigated extensively for the degradation of dyes in effluent water. This paper reports our findings on the sunlight induced photocatalytic removal of the hazardous xanthene dye Rhodamine B from water, mediated by TiO₂ and 'platinum deposited TiO₂' (Pt/TiO₂). Unlike in the case of photocatalytic degradation of many organic pollutants which are driven by UV light, Rhodamine B can be removed in presence of TiO₂ even by visible light. Pt/TiO₂ is ~5 times more active than TiO₂ alone for the solar photocatalytic degradation of the dye, which is attributed to extension of the absorption of light to the visible range and retardation of the recombination of photogenerated electrons and holes. The dye itself can absorb visible light and act as a photo sensitizer to activate TiO₂. The effects of various parameters such as catalyst loading, concentration of the dye, pH, Pt concentration in Pt/TiO₂, externally added H₂O₂ etc on the adsorption and/or degradation of the dye are evaluated. The degradation of the dye proceeds through intermediates and complete removal of Total Organic Carbon (TOC) is achieved many hours after the decolorisation of the dye. The rate of degradation decreases beyond a critical concentration of the dye, possibly due to reduction in the path length of photons in deeply colored solution. The higher degradation in alkaline pH is explained in terms of the ionization state of the catalyst surface and the enhanced adsorption facilitated by the electrostatic attraction between the negatively charged catalyst surface and the zwitter ionic form of the dye. H₂O₂, upto a critical concentration, accelerates the degradation. The observations are critically analysed and suitable mechanism for the photocatalytic mineralisation of RhB is proposed.

Keywords: Photocatalysis, platinum, titanium dioxide, Rhodamine B, hydrogen peroxide, sunlight.

Introduction

Semiconductor mediated photocatalysis is fast becoming an efficient Advanced Oxidation Process (AOP) for the removal of chemical and bacterial pollutants from water¹⁻⁶. Generally, photocatalysis by semiconductors is the result of the interaction of photogenerated electrons and holes with the substrate. These electrons and holes can participate in reductive and oxidative reactions that lead to the decomposition of pollutants. The most widely studied catalyst in this respect is TiO₂ in view of its favorable physicochemical properties, low cost, easy availability, high stability and low toxicity. However, TiO₂ has a wide band gap (Anatase, E_{bg} = ca. 3.2 eV, rutile, E_{bg} = ca.3.0 eV) and can absorb light only below 400 nm, which is in the UV range that constitutes less than 5% of sunlight. In aqueous solution, the reactive OH radicals generated on the catalyst surface can promote the oxidation and eventual mineralization of organic compounds.

A number of studies have been reported on the modification of semiconductor oxides in order to extend the absorption of light to the visible range. These include dye sensitization, semiconductor coupling, impurity doping, use of coordination

metal complexes and metal deposition⁷⁻¹³. Composites such as TiO₂/carbon have also been reported¹⁴. Physical modification of TiO₂ with small amounts of transition metal cations such as V⁺ and Cr⁺ etc can extend the absorption upto 550 nm, making it efficient under UV as well as sunlight¹⁵. Deposition of noble metals such as Pt, Pd, Au, Ag etc on TiO₂ enhances the catalytic oxidation of organic pollutants¹⁶⁻²⁰. The enhancement is attributed to the increased light absorption and retarding of the photogenerated electron-hole recombination.

Water contaminated with dyes is a major threat to the environment. Even very low concentration of dyes in the effluents is highly visible and undesirable. It reduces the light penetration resulting in inhibition of photosynthesis and ultimate destruction of organisms living in water bodies. In the present paper the possibility of using TiO₂ and Pt deposited TiO₂ for the photocatalytic removal of Rhodamine B, a highly soluble basic dye of the xanthenes class is examined. The influence of various operational parameters such as concentration of the dye, pH, catalyst loading, added H₂O₂ etc. on the rate of removal of the dye is investigated and optimum reaction parameters are identified.

It is reported that nano particles of noble metals such as Au, Ag and Pt are capable of absorbing visible light due to the Surface Plasmon Resonance (SPR) in which their conducting electrons undergo a collective oscillation induced by the electric field of visible light^{16,21,22}. Ag and Au nanoparticles supported on insulators such as ZrO₂ and SiO₂ yield visible light active photocatalysts capable of promoting both oxidative and reductive reactions^{23,24}. Zheng et al¹⁶ has recently reported a facile insitu synthesis of visible light plasmonic photocatalysts M@TiO₂ (M= Au, Pt, Ag) and their evaluation for the oxidation of benzene to phenol in aqueous system. Other efficient and stable plasmonic catalysts such as Ag/AgCl and Ag/AgBr/WO₃.H₂O are also reported^{25,26}. In the case of such catalysts, visible light is absorbed by nanoparticles of the noble metal and the photogenerated electrons and holes are separated by the metal-semiconductor interface. Thus the electron-hole recombination is prevented and the photocatalytic process is accelerated. In the case of Au/TiO₂ plasmonic photocatalysts, the mechanism of visible-light induced photocatalytic oxidation involves the absorption of light by Au nanoparticles which causes electron transfer from them to the conduction band of TiO₂. Consequently, the oxidation of the organics will take place at the electron deficient Au nanoparticles¹⁶.

In the present study the comparative photocatalytic activity of TiO₂ and Pt/TiO₂ is evaluated for the removal of a typical pollutant dye, i.e. Rhodamine B, from water.

Material and Methods

Degussa P-25 TiO₂ (99% pure) consisting of approx. 70% anatase and 30% rutile is used as such without further purification. The average particle size was around 15-20 μm and the BET surface area was ~15 m²/g. Analytical grade chloroplatinic acid (H₂PtCl₆.6H₂O) and Rhodamine B (RhB, C.I. Basic violet, C.I number 45170, chemical class: xanthenes, molecular formula C₂₈H₃₁N₂O₃Cl, molecular weight: 479.01g/mole, IUPAC name: N-[9-(ortho-carboxyphenyl)-6-(diethylamino)-3H-xanthen-3-ylidene]diethylammonium chloride) were from Sigma Aldrich India. The molecular structure of RhB is shown in figure 1.

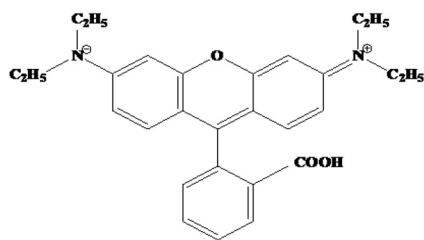


Figure-1
Structure of Rhodamine B

All other chemicals used were of AR grade. Doubly distilled water was used in all the experiments. The Pt/TiO₂ was prepared by standard techniques described earlier^{18,27}.

Aqueous suspension containing specific quantity of Degussa P-25 TiO₂ was taken in the photoreactor and purged with nitrogen to remove dissolved oxygen. Specified amounts of H₂PtCl₆.6H₂O dissolved in 20 ml methanol was then added to the aqueous suspension of TiO₂ and agitated with a magnetic stirrer. The suspension under nitrogen atmosphere is then irradiated with 400 W UV lamp for 8 hr. The milky white suspension turns grayish with the deposition of Pt. The suspension is then filtered and the residue, after repeated washings with doubly distilled water, is dried and powdered.

X-ray diffraction measurement was made by using Rigaku X-ray diffractometer with CuKα radiation. Scanning Electron Microscopy (SEM) measurements were performed with JEOL Model JSM-6390 LV. Diffuse Reflectance Spectra (DRS) were recorded with Varian Cary 5000 using BaSO₄ as the reference.

Photocatalytic experiments in presence of UV were performed in a jacketed pyrex reactor. The dye solution was taken in the inner compartment and cooling water from a thermostat (27± 1^oC) was circulated through the outer jacket. UV irradiation was done using a 400 W medium pressure mercury vapor lamp. Solar experiments were performed by placing the same system on the roof top of our laboratory at Kochi, Kerala, India (9^o 57' 51" N, 76^o 16' 59" E) during sunny days in February-May 2012. The suspension was stirred frequently to ensure uniform mixing. Samples were drawn periodically and analyzed for the dye concentration by Spectrophotometry (555nm). Suspension kept under identical conditions in the dark was used as the reference in each case to eliminate the contribution from adsorption towards the reduction in the dye concentration.

Results and Discussions

Surface characterization of the photocatalyst: The catalysts TiO₂ and Pt/TiO₂ were characterized by XRD analysis, Scanning Electron Microscopy (SEM) and Diffuse Reflectance Spectra. Photo deposition of platinum on the TiO₂ surface was indicated by color change of the particles from white to grey. However XRD analysis of the Pt deposited catalyst showed characteristic peaks of TiO₂ only with no indication of the presence of Pt (figure 2).

Since the deposition of Pt is confirmed by the visual color change, absence of Pt characteristics in the XRD may be because its concentration in the TiO₂ matrix is below detectable level.

Scanning Electron Microscopy (SEM) of the sample with 0.5 weight % of Pt on TiO₂ (figure 3) shows that the particles are approximately spherical in nature.

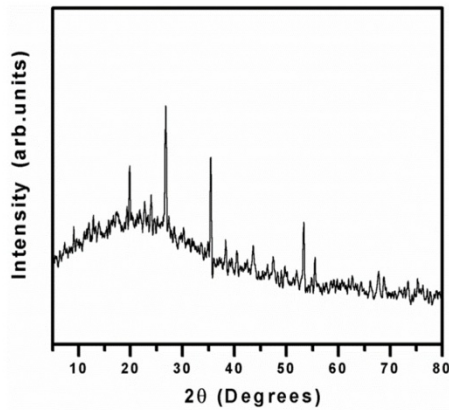


Figure-2
XRD pattern of Pt/TiO₂

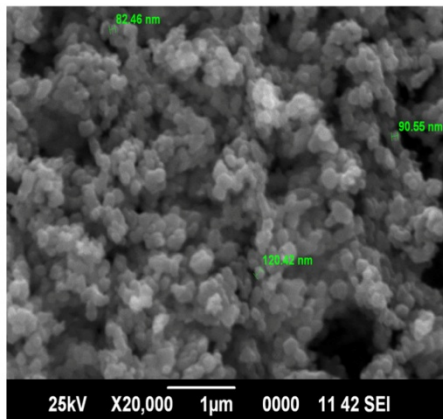


Figure-3
SEM image of Pt (0.5%) deposited on TiO₂

Diffuse Reflectance spectrum (figure-4) shows that in the Pt-deposited TiO₂ optical absorption of the material is enhanced significantly from 360 nm onwards.

This extension of absorption towards the visible region of the optical spectrum is consistent with the findings reported by earlier investigators^{19,20}. This is further illustrated by the enhanced activity of the prepared catalyst for the degradation of the dye in visible light.

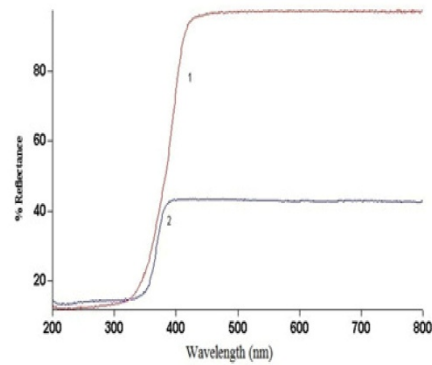


Figure-4
DRS spectra of (1) TiO₂ P-25 and (2) Pt-TiO₂

According to Li and Li¹⁸ and Chen et al¹⁹, deposition of Pt on TiO₂ results in the formation of Ti³⁺, possibly due to the interaction between Pt and TiO₂ during photo reduction. The presence of Ti³⁺ sites in the lattice may form a defect energy level in the band gap of TiO₂ thereby absorbing visible light more efficiently and resulting in enhanced photocatalytic activity. The dispersion of Pt nanoparticles in the TiO₂ matrix can also produce some energy levels in the band gap of the latter¹⁸. Sakthivel et al¹⁷ also concluded from similar studies that defect sites on the TiO₂ surface, identified as Ti³⁺ are necessary for adsorption and photoactivation of oxygen which are the primary steps in photocatalysis. In the present case, the deposition of Pt was made in the absence of air. Hence the in situ transformation of Ti³⁺ to Ti⁴⁺ by oxygen can be ruled out. However, in presence of the platinum salt, the photogenerated Ti³⁺ ions reduce the noble metal cations to neutral Pt atoms. These atoms can nucleate to grow into clusters, eventually forming nanoparticles of Pt on the TiO₂ surface. The Surface Plasmon Resonance (SPR) in Pt/TiO₂ under visible light irradiation enables the transfer of photogenerated electrons from the metal particles to TiO₂ conduction band by crossing the metal-semiconductor interface and surmounting the Schottky barrier²¹. This will reduce the recombination of the photogenerated electron-hole pair. The electrons are taken up by adsorbed oxygen forming reactive oxygen species which interact with the organic substrate, leading to eventual mineralisation. Presence of an organic substrate such as RhB in the present case compensates the depleted electron and the SPR is fully restored, thereby ensuring continued efficient photocatalytic activity.

Photocatalytic Degradation of Rhodamine B on TiO₂ and Pt/TiO₂: Photocatalytic degradation of Rhodamine B is evaluated using TiO₂ and Pt/TiO₂ insuspensions. Slow photodegradation of the dye takes place even in the absence of

catalyst. This may be due to the natural self-fading of the dye. The degradation is investigated in both UV light as well as in sunlight (SL). The pH of the system is maintained at 5.5 which is close to the natural pH of the dye solution under the reaction conditions used in the study. The results are plotted in figure 5.

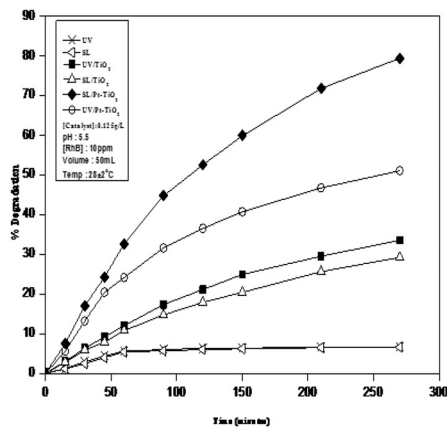


Figure-5
Degradation of Rhodamine B in UV and sunlight in presence of TiO₂ and Pt/TiO₂

As expected, Pt/TiO₂ is more active in the visible sunlight. In the UV region also, it is more active compared to TiO₂. Approximately 80% decolorisation of the dye is achieved in 4 hr time in presence of Pt/TiO₂ catalyst in sunlight.

The degradation in presence of SL/Pt/TiO₂ is about 60% more compared to UV/TiO₂. However SL/Pt/TiO₂ is approximately 2.5 times more reactive than Sunlight/TiO₂. The comparative enhancement in this case increases as the irradiation progresses. This is due to the inability of pure TiO₂ to get activated significantly in sunlight while Pt/TiO₂ continues to absorb visible light resulting in the formation of electron-hole pairs and subsequent activation of adsorbed oxygen. The comparative advantage of Pt/TiO₂ is not that significant in UV irradiation because TiO₂ itself is very active in this region. The photogenerated superoxide/hydroperoxide (O₂⁻/HO₂[•]) radicals initiate degradation of the dye. Repeated attacks by the O₂⁻ / HO₂[•] radicals on the pollutant nuclei can lead to the mineralization producing mainly CO₂ and water.

The effect of catalyst loading on the photocatalytic degradation of the dye is tested using pure TiO₂ and Pt/TiO₂ keeping all other reaction parameters constant (figure-6). The optimum loading is 0.100 and 0.125 g/L in the case of TiO₂ and Pt/TiO₂ respectively.

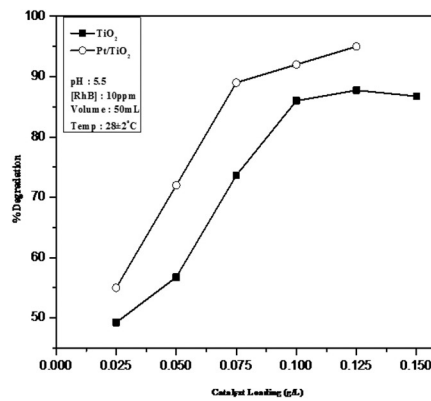


Figure-6
Effect of catalyst loading on the photodegradation of Rhodamine B

The effect of concentration of Pt in Pt/TiO₂ on the rate of degradation of the dye is tested by varying the loading of the former in TiO₂ from 0.2 to 1.0%. The initial rate constant of degradation in sunlight at various Pt concentrations is plotted in Figure 7. The rate increases with Pt loading initially. However, it levels off or even decreases slightly beyond the optimum level of 0.6%.

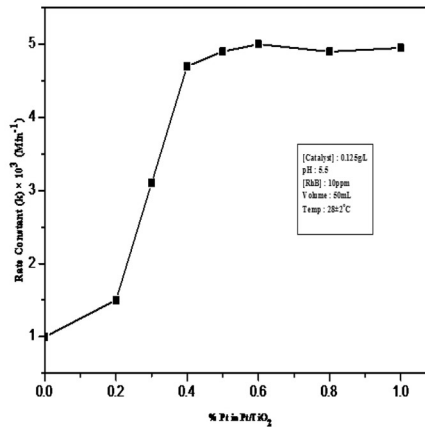


Figure-7
Effect of Pt concentration in Pt/TiO₂ on the photocatalytic degradation of Rhodamine B

All further studies were made using 0.1 g/L of TiO₂ or 0.125 g/L of Pt (0.6%)–TiO₂ unless mentioned otherwise. The detrimental effect of higher content of Pt in the Pt-semiconductor oxide catalyst on photocatalytic degradation has been reported earlier also¹⁹. During irradiation, photogenerated electrons are transferred from Pt metal to the TiO₂ conduction band. The metal-semiconductor interface separate the electron-hole pairs which prevents their recombination. However, at higher concentrations of Pt, the average distance of separation between the electrons and holes decreases and the Pt clusters themselves can act as recombination centers. Choi et al²⁸ also observed that there is an optimal metal dopant concentration above which the photocatalytic activity decreases.

Studies on the effect of concentration of Rhodamine in the range of 3-40 mg/L on the rate of photocatalytic degradation in presence of TiO₂ as well as Pt/TiO₂ in sunlight showed that the degradation remains steady or decreases with increasing initial concentration. The results are plotted in figure 8.

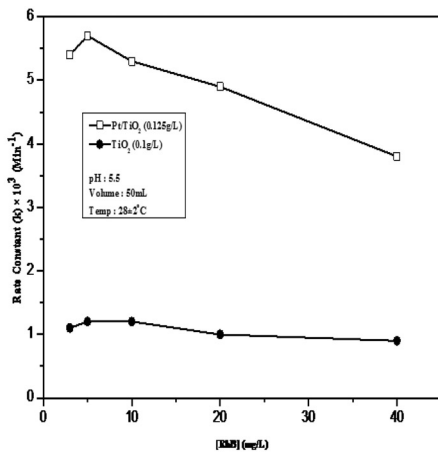


Figure-8'
Effect of initial concentration of Rhodamine B on its photocatalytic degradation

Since the degradation is accelerated by both catalyst and light, the negative effect of increasing concentration implies that at higher concentration, the dye is inhibiting the action of catalyst and/or light. At higher concentration there will be better adsorption of the dye on the surface of the catalyst. This will inhibit the direct absorption of light by the catalyst thereby affecting its ability to generate free radicals and reactive oxygen species. In the absence of continued significant degradation, the adsorbed dye will not leave the surface sites. This prevents the

adsorption of new molecules and continued degradation. Thus it is clear that light absorption and number of adsorption sites are the two factors affected by higher concentration of the dye. It is also known that the dye itself will be absorbing more solar light at higher concentration. The path length of light entering the system also decreases with increase in concentration²⁹.

The pH is an important factor in the case of wastewater and hence its effect on the photocatalytic degradation of the dye is investigated. The degradation increases with increase in pH, the rate of increase being more in the alkaline range. The results are shown in figure 9.

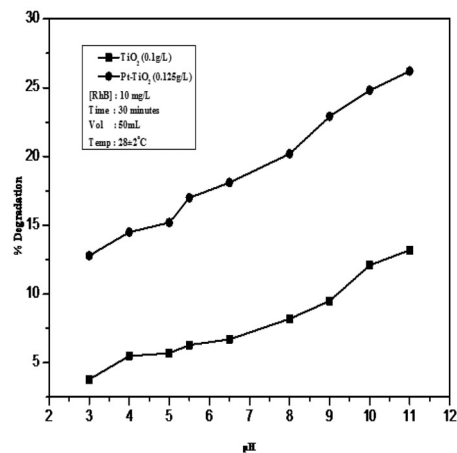
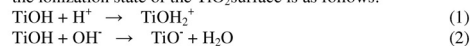


Figure-9
Effect of pH on the photocatalytic degradation of Rhodamine B

The variation is not due to any change in the absorption of light as the λ_{max} for the dye changes very little (551-553 nm) in the pH range of 1-13 even though rhodamine exists in two principal forms in water, i.e. cationic (RhB⁺) or zwitter ionic (RhB[±])²⁹. At pH value less than the Point of Zero Charge (PZC) of TiO₂ (6.5), the surface will be positively charged. The effect of pH on the ionization state of the TiO₂ surface is as follows:



In the acidic range the dye will be in cationic form (RhB⁺). Hence due to electrostatic repulsive forces, the adsorption of the dye on the catalyst is less. Thus the surface promoted degradation is less and the observed degradation is primarily taking place in the solution. At higher pH value, the RhB[±] gets deprotonated and its zwitter ion is formed (figure 10).

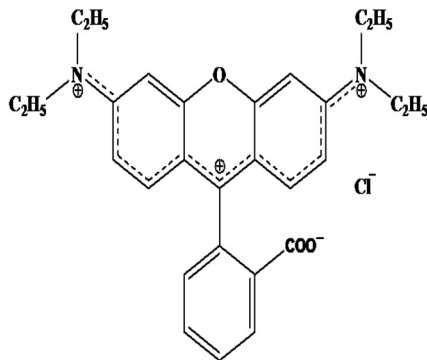


Figure-10
Zwitterion Structure of Rhodamine B

This can get adsorbed onto the negatively charged catalyst surface resulting in increased degradation of the dye. Further, under alkaline conditions, more OH radical formation is possible from the abundant hydroxide ions, which also enhances the degradation²⁹.

Adsorption vs Degradation: Since RhB is known to get adsorbed onto various solid surfaces, the comparative adsorption on some of the commonly used catalysts/adsorbents is measured and is shown in figure-11.

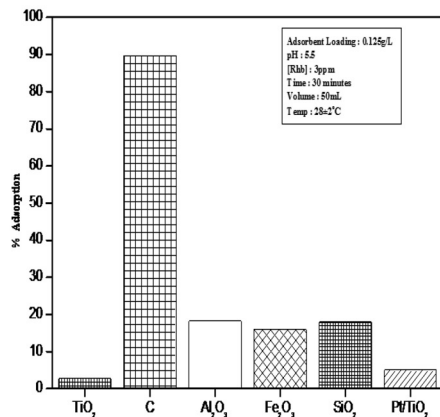


Figure-11
Adsorption of Rhodamine B on various surfaces

Activated carbon is a good adsorbent. But it does not degrade the dye. The adsorption is less on both TiO₂(3%) and Pt/TiO₂(3.5%). However, both these can act as good photocatalysts for the removal of the dye in sunlight. Thus it is clear that the photocatalytic color removal is not due to simple adsorption. It happens by the degradation of the adsorbed molecule followed by liberation of the catalyst site, further adsorption of new dye molecules and reaction. Effective photocatalytic degradation is necessary to ensure continued adsorption of fresh molecules and their degradation. The more the degradation, the better will be the adsorption of new molecules. However, the net adsorption capability at any point of time is more or less the same.

Further, the color removal does not guarantee that the RhB is completely mineralized. As seen in figure 5 almost 80% of RhB is disappearing in two hr time. No other product detectable by UV-Vis spectroscopy is left in the reaction mixture. However, the TOC remained substantially higher after the first one hr showing that RhB is not fully mineralized and it is transformed to other organic compounds. In order to confirm the complete elimination of the pollutant the TOC concentration was determined. The results are plotted in figure-12.

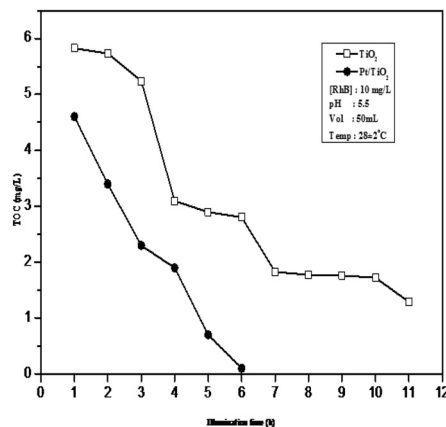


Figure-12
Decrease in TOC during the photocatalytic degradation of Rhodamine in presence of TiO₂ & Pt/TiO₂

As can be seen, the TOC remains high even when the dye is fully decolorized. In the case of Pt/TiO₂, the TOC is 3.4 mg/L after 2 hr. Continuation of the irradiation reduces the TOC and eventually brings it close to zero after about 11 hr and 6 hr in the case of TiO₂ and Pt/TiO₂ respectively. NMR studies of the products of photoelectrocatalytic degradation of RhB by Li et al³⁰ showed the presence of intermediates formed by deethylation and chromogen destruction. However, these

intermediates also get eventually mineralized resulting in CO₂ and H₂O.

Effect of added H₂O₂: One of the products of photocatalytic degradation of organic pollutants in water is H₂O₂ which itself can act as a source of active free radicals. In order to investigate the effect of H₂O₂, the photocatalytic degradation of RhB (10ppm) was performed with initially added H₂O₂ (3ppm). The results are shown in figure 13.

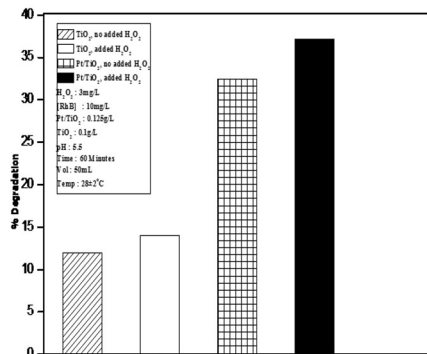


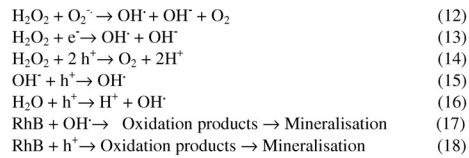
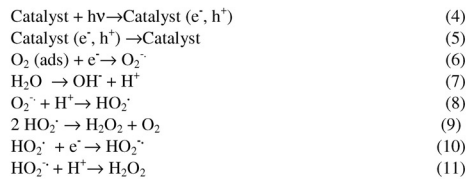
Figure-13
Effect of initially added H₂O₂ on the photocatalytic degradation of [RhB] in presence of TiO₂ and Pt/TiO₂

Control experiments with only H₂O₂ or H₂O₂ and catalyst, with no irradiation showed very little change in concentration of RhB. Irradiation after addition of H₂O₂ in the absence of the catalyst also showed very little degradation. Addition of H₂O₂ and irradiation by sunlight resulted in slight enhancement in the degradation of RhB in the case of TiO₂ as well as Pt/TiO₂.

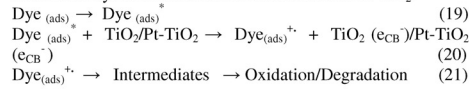
The enhancement is due to additional free radical generation³¹. However, the enhancement is not significantly high which may be due to ·OH radical scavenging by H₂O₂ as follows:

$$H_2O_2 + \cdot OH \rightarrow H_2O + HO_2 \cdot \quad (3)$$

The overall mechanism of the photocatalytic degradation of RhB in presence of TiO₂ or Pt/TiO₂ can be proposed as follows:



In the case of pure TiO₂ also, the degradation of the dye is significant in sunlight unlike in the case of substrates like phenol, alcohol, cresol etc where the degradation is much slower³². This may be because Rhodamine B can absorb visible light and act as a sensitizer thereby transferring electrons from the excited dye molecule to the conduction band of TiO₂.



The electrons are scavenged by the oxygen adsorbed on the surface of TiO₂ as in (6) above. The dye behaves like an electron donor at the excited state and injects electrons directly to the conduction band upon irradiation. Anandan et al³³ also suggested similar pathway for the degradation of dyes on Ag/TiO₂ catalysts.

The extent of degradation effected by dye sensitized TiO₂ is much less compared to that by Pt/TiO₂. Deposition of Pt enhances the photocatalytic activity in two ways, ie by the prevention of electron hole recombination and the extension of the light absorption range. Pt particles in the TiO₂ matrix produce extra defect energy levels in the band gap of TiO₂. This will reduce the effective band gap thus making visible light adequate to promote electrons from the defect energy level to CB¹⁹. Modification of the surface of TiO₂ by Pt can also result in enhancement of the number of active sites for the dye-catalyst interaction which in turn can increase the photodegradation rate. On the other hand, dye sensitization leads to only visible light absorption which is highly concentration dependent. At lower concentration, when there is only monolayer coverage of the dye, light absorption may not be adequate to acquire sufficient energy to be transferred to the semiconductor. At the same time multilayer adsorption of the dye does not enhance the light absorption or photocatalytic efficiency significantly because the inner layers will tend to act as insulators with respect to outer layers⁴.

Conclusion

TiO₂ and Pt deposited TiO₂ are good photocatalysts capable of mineralizing the dye Rhodamine B in presence of UV as well as direct sunlight. Pt incorporated in the TiO₂ matrix extends the light absorption of TiO₂ from UV to the visible range which makes the composite a good photocatalyst for solar decontamination of polluted water. Pt/TiO₂ is more effective than TiO₂ alone for the removal of the pollutant. Higher pH

favours the removal of Rhodamine B while increase in concentration of the dye decreases the rate of removal. There is an optimum for the catalyst loading as well as concentration of Pt beyond which the rate of degradation stabilizes or decreases. H₂O₂ enhances the degradation slightly. Simple decolorisation of the dye solution does not result in mineralisation as seen by the measurement of TOC which takes longer time to disappear. The degradation is proceeding through many stable intermediates which also get degraded further and mineralized, though slowly. A tentative mechanism for the photocatalytic degradation of the dye is proposed and discussed.

Acknowledgement

Financial support from the Cochin University of Science and Technology to one of the authors (ASG) by way of Senior Research Fellowship is gratefully acknowledged.


References

1. Matthews R.W., Photocatalytic oxidation of organic contaminants in water: An aid to environmental preservation, *Pure and Appl. Chem.*, **64**, 1285-1290 (1992)
2. Devipriya S. and Suguna Yesodharan, Photocatalytic degradation of pesticide contaminants in water, *Solar Energy Materials and Solar Cells*, **86**, 309-348 (2005)
3. Chong M.N, Jin B., Chow C.W.K and Saint C., Recent developments in photocatalytic water treatment technology: A review, *Wat. Res.* **44**, 2997-3027(2010)
4. Anju S.G., Jyothi K.P., Sindhu Joseph, Suguna Yesodharan and Yesodharan E.P., Ultrasound assisted semiconductor mediated catalytic degradation of organic pollutants in water: Comparative efficacy of ZnO, TiO₂ and ZnO-TiO₂, *Res. J. Recent Sci.* **1**, 191-201 (2012)
5. Deshpande P.A. and Madras G., Photochemical degradation of phenol by base metal-substituted orthovanadates *Chem. Eng. J.* **161**, 136-145 (2010)
6. Takeuchi J.P., Cuong M., Zhang T-M, Matsuoka M. and Anpo M., Recent advances in visible light-responsive titanium oxide-based photocatalysis, *Res. Chem. Intermed.* **36**, 327-347 (2010)
7. Ollis D., Pichat P. and Serpone N., TiO₂ photocatalysis – 25 years, *Applied Catal B: Environmental*, **99** (3-4), 377-387 (2010)
8. Moon J., Yun C.Y., Chung K.W., Kang M. and Yi J., Photocatalytic activation of TiO₂ under visible light using Acid red, *Catal. Today*, **87**(1-4), 77-86 (2003)
9. Pei D. and Luan J., Development of visible light-responsive sensitized photocatalysts, *Int. J. Photoenergy*, article id. 262831, 13 pages, (2012)
10. Chen H., Li W., Liu H. and Zhu I., Performance enhancement of CdS sensitized TiO₂ mesoporous electrode with two different sizes of nanoparticles”, *Microporous and Mesoporous Materials*, **138**(1-3) 235-238 (2011)
11. Wu C.G., Chao C.C. and Kuo F.T., Enhancement of the photocatalytic performance of TiO₂ catalysts via transition metal modification, *Catal.Today*, **97**(23), 103-112 (2004)
12. Bae E and Choi W, Highly enhanced photoreductive degradation of perchlorinated compounds on dye sensitized metal/TiO₂ under visible light, *Environ. Sc. Technol.*, **37**(1), 147-152 (2003)
13. Pellegrin Y., Le Pleux L., Blart E, Renaud A., Chavillon B., Szuwarski N. Boujitta M., Cario L., Jobic S., Jacquemin D. and Odobel F., Ruthenium polypyridine complexes as sensitizers in NiO based p-type dye-sensitized solar cells: Effects of the anchoring groups, *J Photochem. Photobiol. A-Chem.*, **219**(2), 235-242 (2011)
14. Li Y., Sun S., Ma M., Ouyang Y. and Yan W., Kinetic study and model of the photocatalytic degradation of rhodamine B (RhB) by a TiO₂-coated activated carbon catalyst: Effects of initial RhB content, light intensity and TiO₂ content in the catalyst, *Chem. Eng. J.*, **142**, 147-155 (2008)
15. Anpo M. and Takeuchi M., Design and development of highly reactive titanium dioxide photocatalyst, *J. Catal.*, **216**(1-2), 505-5146 (2003)
16. Zheng Z., Huang B., Qin X., Zhang X., Dai Y and Whangbo M.H., Facile in situ synthesis of visible-light plasmonic photocatalysts M@TiO₂(M = Au, Pt, Ag) and evaluation of their photocatalytic oxidation of benzene to phenol” *J. Mater. Chem.*, **21**, 9079-9087 (2011)
17. Sakthivel S., Shankar M.V., Palanichamy M., Arabindoo A., Bahnemann D.M. and Murugesan B.V., Enhancement of photocatalytic activity by metal deposition: characterization and photonic efficiency of Pt, Au, and Pd deposited on TiO₂ catalyst, *Wat. Res.*, **38**(130), 3001-3008 (2004)
18. Li F.B. and Li X.Z., Enhancement of photodegradation efficiency using Pt/TiO₂ catalyst, *Chemosphere*, **48**(10) 1103-1111 (2002)
19. Chen H-W, Ku Y. and Kuo Y-L, Effect of Pt/TiO₂ characteristics on temporal behavior of o-cresol decomposition by visible light induced photocatalysis, *Water Res.*, **41**, 2069-2078 (2007)
20. Herrmann J.M., Disdier J. and Pichat P., Photo assisted platinum deposition on TiO₂ powder using various platinum complexes, *J Phys Chem.*, **90**, 6028-6033 (1986)
21. Kamat P.V., Photophysical, photochemical and photocatalytic aspects of metal nanoparticles, *J. Phys Chem. B*, **106**, 7729-7744 (2002)
22. Eustis S. and El-Sayed M.A., Why gold nanoparticles are more precious than pretty gold: Noble metal surface plasmon resonance and its enhancement of the radiative

- and nonradiative property of nanocrystals of different shapes, *Chem Soc. Rev.*, **35**, 209-217 (2006)
23. Zhu H.Y., Chen X., Zheng Z.F., Ke X.B., Jaatinen E., Zhao J.C., Guo C., Xie T.F. and Wang D.J., Mechanism of supported gold nanoparticles as photocatalysts under ultraviolet and visible light irradiation *Chem Commun.*, 7524-7526 (2009)
24. Chen X., Zheng Z.F., Ke X.B., Jaatinen E., Xie T.F., Wang D.J., Guo C., Zhao J.C. and Zhu H.Y., Supported silver nanoparticles as photocatalysts under ultraviolet and visible light irradiation, *Green Chem.*, **12**, 414-419 (2010)
25. Wang P., Huang B., Qin X., Zhang X., Dai Y., Wei J. and Whangbo M.H., Ag@AgCl: A highly efficient and stable photocatalyst active under visible light, *Angew. Chem.Int.Ed.*, **47**, 7931-7933 (2008)
26. Wang P., Huang B., Qin X., Zhang X., Dai Y. and Whangbo M.H., Ag/AgBr/WO₃.H₂O: Visible-light photocatalyst for bacteria destruction, *Inorg.Chem.*, **48**, 10697-10702 (2009)
27. Devipriya S.P., Suguna Yesodharan and Yesodharan E.P., Solar photocatalytic removal of chemical and bacterial pollutants from water using Pt/TiO₂- coated ceramic tiles; *Int. J Photoenergy*, Article ID 970474, 8 (2012)
28. Choi W.Y., Termin A. and Hoffmann M.R., The role of metal ion dopants in quantum sized TiO₂: Correlation between photo reactivity and charge carrier recombination dynamics, *J Phys Chem*, **98(51)**, 13669-13679 (1994)
29. You-ji L. and Wei C., Photocatalytic degradation of Rhodamine B using nanocrystalline TiO₂-zeolite surface composite catalysts: effects of photocatalytic condition on degradation efficiency, *Catal. Sci. Technol.*, **1**, 802-809 (2011)
30. Li X.Z., Liu H.L., Li F.B. and Mak C.L., Photocatalytic oxidation of Rhodamine B in aqueous solution using Ti/TiO₂ mesh electrodes, *J Env Sci and Health A*, **37(1)**, 55-69 (2002)
31. Merouani S., Hamdaoui O., Saoudi F. and Chiha M., Sonochemical degradation of rhodamine B in aqueous phase: Effects of additives, *Chem. Eng. J.*, **158**, 550-557, (2010)
32. Anju S.G., Suguna Yesodharan and Yesodharan E.P., Sonophotocatalytic degradation of phenol over semiconductor oxides, *Chem Eng J*, **189-190**, 84-93 (2012)
33. Anandan S., Sathish kumar P., Pugazhenthiran N., Madhavan J. and Maruthamuthu P., Effect of loaded silver nanoparticles on TiO₂ for photocatalytic degradation of Acid Red 88, *Solar Energy Mater and Solar Cells*, **92**, 929-937 (2008)

TDWT 908417
29 March 2014

Initial

CE: VK QA: KM
Coll: QC:


Desalination and Water Treatment
www.deswater.com
doi: 10.1080/19443994.2014.908417

XX (2014) XX-XX
XXXX

Investigations on semiconductor sonocatalysis for the removal of pathological micro-organisms in water

S.G. Anju, I.S. Bright Singh, E.P. Yesodharan, Suguna Yesodharan*

School of Environmental Studies, Cochin University of Science and Technology, Kochi 682022, India, Tel. +91 484 2862557;
Fax: +91 484 2577311; email: epyesodharan@gmail.com

AQF

Received 11 December 2013; Accepted 17 March 2014

ABSTRACT

Contamination of drinking water by bacterial pollutants is a major environmental problem. In the current study, the possibility of using zinc oxide-mediated sonocatalysis, as a potential advanced oxidation process for the removal of a major pollutant, i.e. *Escherichia coli*, is investigated. Critical parameters for optimum efficiency are identified. The organism deactivation is fully irreversible in the case of ZnO-mediated sonocatalysis. Scanning electron microscopy images show that morphological changes and cell-wall disruption of organisms are more in sonocatalysis compared to sonication alone. The deactivation is practically unaffected by initial pH in the range 5–9. Reactive oxygen species including *in situ*-formed free radicals play significant role in the deactivation. Sonoluminescence-induced photocatalysis is a major contributor in the disinfection process. A probable mechanism involving physical effects and semiconductor activation by ultrasound followed by the events leading to the deactivation of the bacteria is proposed.

Keywords: Zinc oxide; Sonocatalysis; Micro-organisms; Disinfection; Water; Hydrogen peroxide

1. Introduction

Semiconductor-mediated photocatalysis has been investigated extensively as a viable technique for the removal of organic and inorganic pollutants from water [1–4]. Photocatalytic deactivation of bacterial pollutants [5–7] from aqueous streams has also been reported extensively in recent years. Another advanced oxidation process under investigation in this context is sonolysis as well as sonocatalysis in which ultrasound (US) is used as the energy source in place of conventional heat or light [7–10]. Major observations in this respect up to 2003 were summarized by Piyasena [10]. US is able to inactivate bacteria and

de-agglomerate bacterial clusters or flocs through a number of physical, mechanical and chemical effects arising from cavitation [11–13]. The mechanism underlying ultrasonic inactivation of bacteria involves both chemical and physical effects [12]. The chemical effects in liquid include cavitation which consists of nucleation, growth, and collapse of bubbles which result in localized supercritical condition such as high temperature, pressure, electrical discharges, and plasma effects. The gaseous contents of a collapsing cavity reach temperatures of ~5,500°C and that of the liquid's immediately surrounding the cavity reach up to 2,100°C. The localized pressure is estimated to be around 500 atmospheres resulting in the formation of transient supercritical water. The cavities thus serve the purpose of high-energy micro reactors. The

*Corresponding author.

2

S.G. Anju et al. / Desalination and Water Treatment XX (2014) XXX–XXX

5 consequence of these extreme conditions is the cleavage of dissolved oxygen and water molecules resulting in reactive oxygen species (ROS) such as H[•], OH[•], HO₂[•] and O[•] radicals and H₂O₂. These ROS can disrupt or damage various cellular functions or structures of micro-organisms and play a significant role in the cell deactivation process through DNA damage [7].

10 Mediation by semiconductor oxides has been proven to be effective in enhancing the rate of chemical and bacterial decontamination of water under sono and photochemical conditions [9,14–16]. However, most of these studies used titanium dioxide (TiO₂) as the catalyst. Earlier studies from our laboratories revealed that zinc oxide (ZnO) is an efficient sono and photocatalyst for the removal of chemical and bacterial pollutants from water [9,16]. In this paper, the application of ZnO as a sonocatalyst for the removal of a common bacterial pollutant, i.e. *Escherichia coli* (*E. coli*), a Gram negative organism, from water is investigated with special reference to the influence of various reaction parameters on the sonobactericidal effect.

25

2. Experimental and methods

E. coli is one of the main species of bacteria that live in the lower intestines of warm-blooded animals (including birds and mammals) and are necessary for the proper digestion of food. It is a subgroup of fecal coliform bacteria that belongs to the family of *Enterobacteriaceae* and is non-spore forming, Gram negative, straight rod-shaped, and facultative anaerobes arranged singly or in pairs. There are numerous different strains within the species, some of which can be harmful. Generally, release of these naturally occurring organisms into the environment is not a cause for alarm. However other disease-causing bacteria, which can include some pathogenic strains of *E. coli* or viruses, may also be present in these wastes and can cause clinical syndromes like diarrhea, urinary tract infection, pyrogenic infection and septicemia.

40 ZnO (99.5%) from Merck India Limited used in the studies was characterized by surface area, pore size distribution, particle size analysis, adsorption and scanning electron microscopy (SEM). The particles are approximately spherical in shape and porous as seen in the SEM image in Fig. 1.

50 The average size of the particles as computed from the image is $10 \times 10^{-2} \mu\text{m}$. The Brunauer–Emmett–Teller surface area was $\sim 12 \text{ m}^2/\text{g}$. All reagents used were AnalaR Grade or equivalent. The cell-culture medium and the irradiating solutions were prepared by standard techniques. For stock culture of *E. coli* the nutrient broth contained 5 g/L yeast extract, 5 g/L peptone (CAS No. 91076-46-8), and 5 g/L NaCl (CAS

55

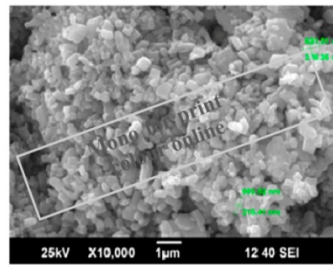


Fig. 1. Typical SEM image of ZnO.

No. 7647-14-5) in distilled water at pH 7.5. The bacterial cells were inoculated and subcultured under sterile conditions for 24 h at 37°C in 100 mL of the nutrient broth under aerobic conditions and constant agitation in a shake incubator at 140 rpm. The cells were then sedimented by centrifugation at 8,000 rpm for 15 min at 4°C. The bacterial pellet obtained was washed with sterile distilled water. It was then resuspended in sterile distilled water and the absorbance was measured at 600 nm using UV–Visible spectrophotometer. The cell suspensions were diluted with sterile distilled water in Pyrex glass beakers to the required cell density of $\sim 10^7$ colony forming units/mL (CFU/mL). This suspension in required volume was taken in bottles containing weighed amounts of the catalyst and irradiated using US in the dark in an ultrasonic bath operating at 40 kHz and power of 100 W. The samples were covered with aluminum foil before and after irradiation to eliminate the effects of diffused light illumination, if any. The temperature was kept at 37°C during US irradiation by circulating cooling water maintained at appropriate temperature. Sampling was done at predetermined time intervals by pipetting out 1 mL of the experimental solution into 9 mL sterile saline and was serially diluted. After mixing, 0.1 mL aliquots of each dilution were spread onto MacConkey agar plates. The cell inactivation was monitored by counting the CFU/mL after 24 h incubation at 37°C. All experiments were repeated at least thrice and the average value was taken.

60

65

70

75

80

85

3. Results and discussion

Disinfection of *E. coli* was examined in the presence of ZnO and US individually and in combination. As expected, no deactivation of the organisms was

90

5 observed in the absence of US irradiation, with or
without catalyst. The deactivation by US alone in the
absence of the catalyst is 20% while it is over 65% in
presence of ZnO. The enhancing effect is not due to
10 the aggregation or adsorption of the cells as no such
reduction was observed during the incubation of the
organisms in the presence of catalyst, in the absence
of irradiation. The enhancement in presence of the catal-
15 yst can be attributed to the increased production of
OH radicals on the surface of the ZnO particles. When
US energy is supplied to the ZnO particles, excited
electrons move from the valence band to the conduc-
tion band and positive holes are generated in the
20 valence band. In the vicinity of the surface of ZnO
particles, the holes react with water to produce more
hydroxyl radicals [17] which provide additional disin-
fection effect. An ultrasonic wave is propagated
throughout the vessel via the solvent so that all the
particles in the vessel are expected to contribute to
generating radical species. The microscale bubbles
formed during the US irradiation get collapsed gener-
ating local high-temperature fields where water mole-

25 cules are pyrolytically decomposed to generate more
hydroxyl radicals. These radical species are moving
into the intracellular portion of bacteria and destroy-
ing the metabolic pathway. Strong shear forces that
rupture the cell membranes of bacteria are also gener-
ated during the collapse of the bubble [13]. SEM
images of the organisms (Fig. 2(a)–(c)) before and after
30 US irradiation show that irradiation causes morpho-
logical changes and possibly cell-wall disruption.
Before illumination, the cells had cylindrical shape.
After illumination many of the cells were completely
damaged and the cells lost their viability, as observed
35 from the number of CFU/mL. The damage caused by
the US in presence of catalyst is significantly more
than that in the absence of the catalyst under other-
wise identical conditions.

3.1. Effect of catalyst loading

40 The effect of catalyst concentration on the ultra-
sonic disinfection of *E. coli* was tested by keeping all

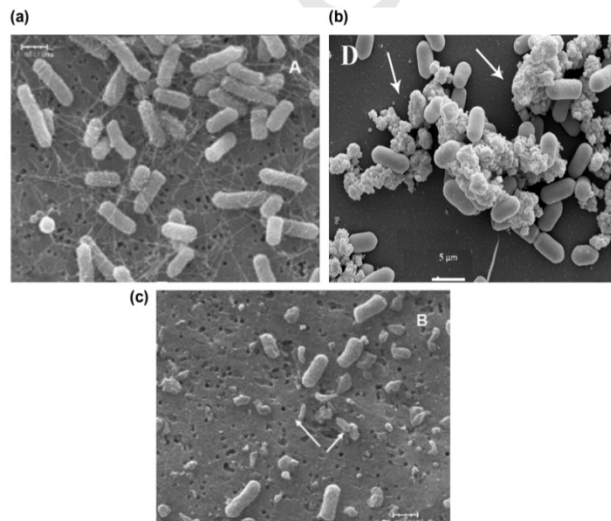


Fig. 2. SEM image of *E. coli*: (a) before US irradiation, (b) after US irradiation, and (c) after US irradiation in presence of ZnO.

4

S.G. Anju et al. / Desalination and Water Treatment XX (2014) XXX-XXX

other parameters constant. The results are shown in Fig. 3. The deactivation increased with increase in catalyst loading especially in the lower range 0.02–0.1 g/L. However, above 0.1 g/L, the increase was less pronounced as seen by comparing the results of 0.1 and 0.15 g/L. The optimum catalyst loading may depend on the initial cell count present in the system. The disinfection was significant in the initial stage. However, the rate decreased as time progressed. For example, at 0.1 g/L loading of ZnO the concentration of *E. coli* decreased by 65% in 2 h, while in the next 2 h the reduction effected was only an additional 20%. Increased deactivation with increase in catalyst loading may be due to increased number of active sites for interaction between the semiconductor particles and the bacterial cells in suspension together with the increased ROS production from the enhanced surface area. However, at higher loadings there is rapid saturation of the surface micro-organism encounters which result in stabilized or even decreased rate of deactivation. This saturation by the organisms or their damaged remnants on the catalyst surface also can cause the decreased rate (number of organisms deactivated per unit time, say h) of deactivation with time. The screening effect seen in photocatalysis which spatially limits the photoactive region is not seen in sonocatalysis as the ultrasonic energy is propagated throughout the entire region in the vessel. Hence, the optimum dosage is much higher in sonocatalysis compared to photocatalysis under identical conditions in reaction vessels of same size and geometry. In any case there is an optimum beyond which the activity is lower which may be due, at least partially, to the shielding effect of these overcrowded particles from the energy source. The optimum dosage of ZnO, as determined experimentally, is 0.1 g/L. Hence, all further studies on the organisms were carried out at this loading.

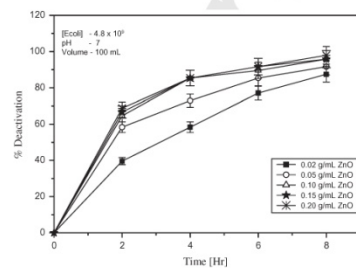


Fig. 3. Effect of ZnO loading on the disinfection of *E. coli*.

Time taken for complete deactivation of the organisms depends on their population density as well as the catalyst loading. At cell concentrations of approximately below 1.9×10^3 CFU, complete deactivation is achieved in 7–8 h while it takes more time, often >16 h (not shown here) when the initial concentration was higher. Complete deactivation can be accelerated for a particular concentration by enhancing the catalyst dosage.

3.2. Effect of concentration of the organism

The effect of changing concentration of the organisms on the rate of deactivation is shown in Fig. 4. The rate increased with increase in concentration and is eventually tending towards stabilization. This showed that the rate is dependent on the concentration of the organisms and the catalyst sites' availability. As the reaction progressed the effective concentration of organism decreased and the concentration-dependent deactivation rate also decreased correspondingly.

Further it is seen that at higher concentrations of the organisms ($>3 \times 10^6$ CFU/mL) and at higher catalyst loadings (>0.1 g/L) the rate is almost stabilized. The final relative cell (FRC) concentration N/N_0 calculated after 4 h, where N_0 and N are the concentrations of viable cells before and after irradiation, respectively, also shows that at higher concentrations of the cells at lower catalyst loadings, the FRC concentration is more or less the same. Similarly, in the lower cell concentration range and higher catalyst loadings the FRC concentration does not change much. Hence, variation in the concentrations of the cells within these respective ranges does not make any significant changes in the rate of the disinfection under otherwise

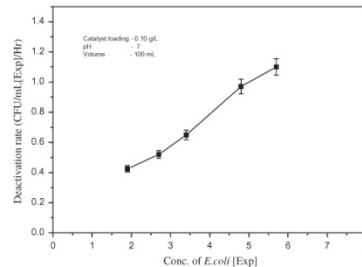


Fig. 4. Effect of concentration of *E. coli* on the disinfection rate.

TDWT 908417 29 March 2014	Initial	CE: VK QA: KM Coll: QC:
------------------------------	---------	----------------------------

identical conditions. Typical calculations are shown in Table 1. The results are in agreement with the findings of Dadjour et al. [18] who reported that in the case of TiO₂-catalyzed ultrasonic disinfection of *E. coli*, initial concentration of the organism has no significant effect on the process over a wide range, i.e. 1.6 × 10³–1.1 × 10⁷ CFU/mL.

3.3. Effect of pH

The effect of initial pH of the reaction system on the sonocatalytic deactivation of *E. coli* is investigated and the results are shown in Fig. 5. In the absence of catalyst, ~20% decrease in the bacterial population was observed under US irradiation at neutral pH which increased in both highly acidic

(pH 3) and alkaline pH (pH 11). The disinfection is negligible in the absence of US irradiation either in the presence or absence of the catalyst at all pHs indicating the tolerance of the organisms to acidic and alkaline conditions. Even in the presence of catalyst and US irradiation, the inactivation was independent of the initial pH value in the range 4–9. However, as irradiation progressed the deactivation became fully independent of pH. Earlier studies on the photocatalytic deactivation of *E. coli* in presence of TiO₂ showed that the deactivation is followed by a decrease in the pH of the system. In the current study also decrease in pH is observed, though to a much lesser extent, from 7 to 6.5. The relative stability of the bacteria in the otherwise lethal acidic pH in the absence of US irradiation is due to the presence of acid-induced proteins that protect the cells from an acid shock and the tolerance of acid-adapted cells towards osmotic stress [19]. However, in presence of the high-energy US radiation, such protection will be ineffective making the influence of pH less visible in the wider of range.

The sonocatalytic disinfection, as explained earlier, is caused by the direct action of US as well as attack by the reactive oxidative species generated on ZnO during the US irradiation.

Table 1
Effect of concentration of *E. coli* vs. catalyst loadings on the FRC concentration

Concentration (CFU/mL)	Catalyst loading (g/L)	FRC (N/N ₀)
1.9 × 10 ³ (L)	0.1 (H)	0.26*
1.9 × 10 ³ (L)	0.02 (L)	0.50
2.7 × 10 ⁵ (L)	0.1 (H)	0.23*
2.7 × 10 ⁵ (L)	0.02 (L)	0.54
3.4 × 10 ⁷ (H)	0.10 (H)	0.14
3.4 × 10 ⁷ (H)	0.02 (L)	0.35**
4.8 × 10 ⁹ (H)	0.10 (H)	0.11
4.8 × 10 ⁹ (H)	0.02 (L)	0.37**

Notes: H: High; L: Low.
*Indicate comparable rates of disinfection.
**Indicate comparable rates of disinfection.

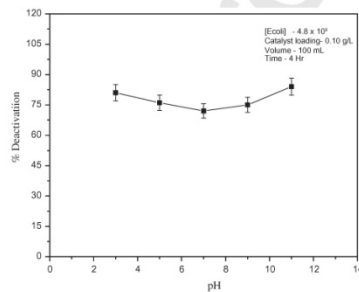
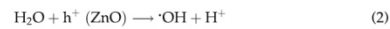
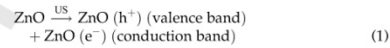
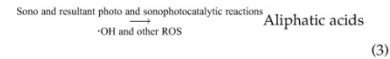


Fig. 5. Effect of pH on the disinfection of *E. coli*.



Bacterial organisms in water



where ROS are the oxygenated species generated during the sonocatalytic- and the sonoluminescence-induced photo and sonophotocatalytic process [20].

3.4. Effect of H₂O₂

H₂O₂ is an important intermediate as well as end product in the sono and photocatalytic degradation of organic pollutants in water. Though H₂O₂ by itself induces the disinfection, it did not show any extra enhancing effect in presence of ZnO and US irradiation. In fact the disinfection in presence of H₂O₂, catalyst, and US irradiation together was less than the sum of infection achieved individually by (i) H₂O₂ and (ii) US + ZnO. Hence, added H₂O₂ does not

- contribute to any extra effect or synergy as in the case of sonophotocatalytic deactivation of chemical contaminants [9]. Though H_2O_2 is a metastable molecule of high redox potential (1.77 V), its disinfecting properties are derived mostly from the free radicals formed in presence of catalysts. H_2O_2 enhances the sensitivity of bacteria to heat, light, or sound. However, the benefits of added H_2O_2 are not reflected in the sonocatalytic system possibly because H_2O_2 formed *in situ* in the sonocatalytic system is already enhancing the rate of decontamination making the added H_2O_2 superfluous. We have earlier reported that both the formation and decomposition of H_2O_2 takes place concurrently in sonocatalytic systems leading to oscillation in its concentration [9,16]. Hence, the concentration of H_2O_2 either formed *in situ* or externally added cannot increase beyond a critical limit, thereby restricting the enhanced detrimental effect on bacterial organisms.
- 4. Re-emergence**
- One of the major problems associated with environment-friendly deactivation of bacterial agents by solar energy is its re-emergence, once the source of energy is discontinued. The possibility of such re-emergence of *E. coli* deactivated by sonication and sonocatalysis is examined by measuring the bacterial concentration after the sonication has been put off. The deactivation continued for some more time after the US is put off, possibly because the free radicals generated in the process continue to be active for some more time until they are totally consumed by various processes taking place. In the case of sonocatalysis no re-emergence is noticed even after 16 h. Hence, the destruction can be considered complete and irreversible in this case. This is in contrast with the bacterial deactivation by sunlight or other softer techniques where a sizeable population of the bacteria re-emerge once the source of irradiation is off. The regrowth occurs as not all of the bacteria have been deactivated by the "soft" process. In such cases the bacteria may have entered a viable but non-culturable stage and then recovered their culturability after a period of more favorable conditions.
- 5. Mechanisms of disinfection**
- During sonocatalysis, the disinfection can occur both in the bulk phase and at the catalyst surface. In the bulk phase, the bacterial cells were inactivated by the micro jet shear stress and the OH radicals generated under US irradiation. At the surface, the *E. coli* were deactivated by the OH radicals generated by sonocatalytic excitation of the semiconductor. The amount of OH radicals produced in the presence of semiconductor was significantly greater than the amount generated by US alone [21].
- In aqueous phase sonolysis, there are four potential sites for sonochemical activity [22]:
- The gaseous region of the cavitation bubble where volatile and hydrophobic species are easily degraded through pyrolytic reactions as well as reactions involving the participation of hydroxyl radicals with the latter being formed through water sonolysis:

$$H_2O \longrightarrow H\cdot + \cdot OH \quad (4)$$
 - The bubble–liquid interface where hydroxyl radicals are localized and therefore radical reactions predominate although pyrolytic reactions also may occur to a lesser extent.
 - The liquid bulk where secondary sonochemical activity may take place mainly by free radicals that escaped from the interface and migrated to the liquid bulk.
 - Catalyst–liquid interface where OH radicals initiate reaction.
- OH radicals can recombine to produce H_2O_2 which may in turn interact with hydrogen to generate OH radicals:
- $$\cdot OH + \cdot OH \longrightarrow H_2O_2 \quad (5)$$
- $$H_2O_2 + H\cdot \longrightarrow H_2O + \cdot OH \quad (6)$$
- Reactions initiated by $\cdot OH$ radicals primarily in the liquid bulk as well as the bubble interface and the catalyst surface may be the dominant deactivation pathway.
- The catalyst particles, in addition to promoting the OH radicals, may also stabilize the reactive species resulting in more intensive disinfection. Further, sonocatalysis leads to the formation of H_2O_2 which also acts as a ROS. The photocatalytic characteristics of ZnO induced by the US-initiated sonoluminescence caused by the implosion of bubbles, also will result in disinfection. It is known that flashes of single bubble sonoluminescence (SBSL) involve intense UV light which can activate ZnO photocatalytically [18]. The semiconductor particles can also lead to strong jet streams and physical stresses in the ultrasonic system which can affect the cell structure as well as the cell

membrane of the organisms [7,21]. US can also increase catalyst surface area producing more active sites for reactions with target species. Further, smaller catalyst particles may enter the bacterial cells which may have already damaged cell membranes and cause additional damage to intracellular components. Sonication itself can also cause greater intracellular damage in damaged bacterial cells. Other factors leading to disinfections include pressure and pressure gradients resulting from bubble collapse causing cell damage due to mechanical fatigue and shear forces induced by microstreaming. Intrinsic oxygen vacancies on the catalyst surface can also lead to more cavitation [23].

The photocatalytic disinfection of *E. coli* in water has been modeled with kinetic equations based on a simplified reaction mechanism which consists of three different stages; i.e. (i) initial delay or smooth decay at the beginning of the reaction, usually called “shoulder,” (ii) a log-linear disinfection region that covers most part of the reaction, and (iii) a deceleration of the process at the end of the reaction, usually called “tail” [24]. Kinetic constant, pseudo-adsorption constant, and inhibition coefficient were the three key parameters used in the model. It was seen that the inhibition coefficient is not influenced by the experimental conditions while the other two are most sensitive. The presence of different inorganic anions and cations in water strongly influences the efficiency of the disinfection process as has been observed in our laboratory as well. The effect is also dependent on the concentration of the ions. This indicates the possibility of different mechanisms for the disinfection and thus different values of kinetic and pseudo-adsorption constants depending on the water characteristics. However, the model cannot be applied as such in the current instance of sonocatalytic deactivation because the “shoulder” is not observed here. The log-linear inactivation region that covers over 50% of the reaction and the “tail” are observed here as well. Hence in sonocatalysis, the physical and chemical effects of sonolysis may be the dominant driving forces of disinfection initially. As the reaction proceeds, the SBSL sets in making the disinfection a complex process involving a combination of sonolysis, sonocatalysis, photocatalysis, and possibly sonophotocatalysis.

6. Future outlook

The advantage of sonocatalysis in wastewater treatment compared with conventional techniques lies in processing safety, reduction in the amount of secondary waste, and irreversibility in the bacterial decontamination. However, appropriate reactor design

and relatively high operating costs of the sonoreactor are impediments in the large-scale commercial application of the process at present [25]. Fundamental research on the origin of extreme conditions created by acoustic cavitation in complex fluids is required to optimize the sonochemical-processing applications. The effect of frequency of US and the presence of suspended solid particles, dissolved solids and gases, ionic species, etc in water on the efficiency of the process should be studied at different operating scales. The economy of the process, compared to other processes can be ascertained only after identifying all relevant parameters including engineering data required to improve sonoreactor design and scale-up. Large-scale commercial application of the technique may have to wait until some of these issues are resolved.

7. Conclusions

Sonocatalysis as a means of bacterial decontamination of water is investigated using ZnO as the catalyst. The influence of various parameters on the rate of sono-deactivation of *E. coli*, is evaluated. The rate of deactivation increases with increase in catalyst loading and with increase in concentration of the organism. Externally added H₂O₂ does not accelerate the deactivation as expected probably because the *in situ*-formed H₂O₂ may have already played the role. The deactivation is independent of the initial pH, though at higher acidic and alkaline range, slight enhancement in the deactivation is observed. The ZnO-induced sono-deactivation is irreversible. The study reveals conclusively that ZnO-mediated sonocatalysis has the potential to be used an effective tool for the irreversible decontamination of bacterial organisms in water.

Acknowledgment

The authors acknowledge the financial support to one of us (ASG) from the Cochin University of Science and Technology by way of Senior Research Fellowship.

References

- [1] M.N. Chong, B. Jin, C.W.K. Chow, C. Saint, Recent developments in photocatalytic water treatment technology: A review, *Water Res.* 44 (2010) 2997–3027.
- [2] S. Devipriya, Y. Suguna, Photocatalytic degradation of pesticide contaminants in water, *Sol. Energy Mater. Sol. Cells* 86 (2005) 309–348.
- [3] D. Ollis, P. Pichat, N. Serpone, TiO₂ photocatalysis – 25 years, *Appl. Catal., B: Environ.* 99 (2010) 377–387.

Semiconductor Mediated Photocatalytic Degradation of Plastics and Recalcitrant Organic Pollutants in Water: Effect of Additives and Fate of Insitu Formed H₂O₂

Phonsy P. D., Anju S. G., Jyothi K. P., Suguna Yesodharan, Yesodharan E. P.*

School of Environmental studies, Cochin University of Science and Technology, Kochi 682022, India

Abstract:

Contamination of water by chemical and bacterial pollutants as well as 'white pollution' caused by carelessly discarded waste plastics are major environmental problems. In the current study, the possibility of using semiconductor photocatalysis for the removal of last traces of organic water pollutants of different types is investigated. Semiconductors ZnO and TiO₂ were characterized by standard techniques and evaluated as photocatalysts. The pollutants tested include low density polyethylene plastics (PEP), phenol, catechol and organophosphorous pesticides such as phosphamidon, monocrotophos and dichlorvos. Hydrogen peroxide (H₂O₂) and peroxydisulphate (PDS) enhance the TiO₂ catalysed photomineralization rate. More than 10% of PEP could be irreversibly degraded in presence of UV-TiO₂-PDS in 300 hr time. The degradation is pH dependent in all cases though no thumb rule can be applied. H₂O₂ formed insitu during the degradation undergoes parallel decomposition resulting in stabilization or oscillation in its concentration depending on the equilibration or domination of the formation/ decomposition process. Anions naturally present in water such as NO₃⁻, Cl⁻ and CO₃²⁻ inhibit the degradation while SO₄²⁻ enhances the same. However, this effect depends on a number of factors and no generalized conclusions are possible. The results and the probable mechanism for the degradation of the pollutants are discussed.

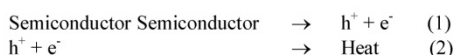
Keywords: Photocatalysis, Semiconductor, Monocrotophos, Phosphamidon, Dichlorvos, Phenol, Plastics

Introduction

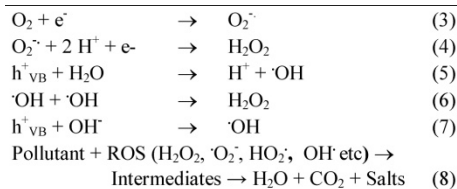
Advanced Oxidation Processes (AOP) such as photocatalysis, sonolysis, fenton and photo-fenton, ozonation, radiolysis, UV/H₂O₂ etc are emerging as viable tools for the removal of chemical and bacterial pollutants from water. Photocatalysis is one of the most promising AOPs in view of its potential to harness solar energy as alternative natural resource under appropriate conditions (1-10). Semiconductor oxides such as TiO₂, ZnO, CdS, GaP etc have been extensively investigated as potential photocatalysts for the removal of toxic chemical and bacterial pollutants from water. Of these, ZnO and TiO₂ are the two most widely investigated photocatalysts for the purification of chemical- contaminated water. The advantages of TiO₂ include abundance, non toxic nature, stability and relatively lower cost. However, it absorbs mostly the UV region of solar spectrum, making it a poor candidate for harnessing solar energy. On the other hand, ZnO has been proven to have absorption over a wider range (8-10) though it suffers from the disadvantages of photocorrosion in acidic

aqueous suspensions and incongruous dissolution to yield Zn(OH)₂ on ZnO particles leading to catalyst inactivation over time. Earlier studies have shown that by suitably modifying the reaction conditions, in particular the pH of the medium, this problem of corrosion/dissolution can be overcome to a great extent and optimum reaction parameters to take advantage of the wider solar absorption spectrum of ZnO can be identified (11, 12).

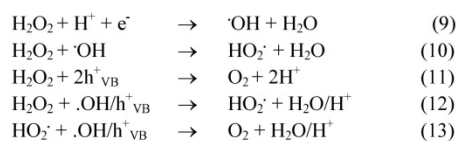
When a semiconductor is irradiated with photons of energy equal or greater than its band gap energy (3.2 eV in the case of TiO₂ as well as ZnO) the photons are absorbed and electron-hole pairs are created. These electrons and holes can either recombine or migrate towards the surface participating in several redox reactions eventually leading to the formation of Reactive Oxygen Species (ROS) such as OH radicals and H₂O₂ (1, 7). These transitory ROS can initiate and promote a number of reactions which end up in complete mineralisation of the pollutants into harmless products such as CO₂, water and salts as follows (2):



*Corresponding author; E-mail: epyesodharan@gmail.com



The H_2O_2 formed does not increase corresponding to its formation since it is concurrently decomposing by a series of reactions taking place on the surface and in the bulk (11) resulting in the formation of more free radicals as follows:



This simultaneous formation and decomposition of H_2O_2 leads to oscillation in its concentration as established in the case of sono, photo and sonophotocatalytic degradation of organic pollutants in water (12). The fundamental mechanism of semiconductor photocatalysis (TiO_2 in this case) can be represented as in Figure 1 (6).

In the present paper we are reporting some of our findings on the ZnO and TiO_2 mediated photocatalytic degradation of a variety of environmental/water pollutants i.e. phenol and catechol (petrochemical pollutants), monocrotophos, phosphamidon and dichlorvos (organophosphorous pesticides) and polyethylene (PE) plastics. Some of these molecules were investigated earlier for their degradation under photocatalysis in presence of TiO_2 (13-18). However, to the best of our knowledge, there has been no systematic study on the photocatalytic degradation of these diverse water contaminants under identical conditions which is important in the design of multi-purpose photocatalytic reaction systems. Further, the fate of concurrently formed H_2O_2 also has not been investigated in detail as the focus was always on improving the efficiency of degradation of the pollutants. This study is intended to fill the gap, to a limited extent.

Experimental

Commercial ZnO and TiO_2 from Merck India Limited were used in the study. In both cases the particles were spherical and nonporous with >99% purity. The BET surface area of ZnO and TiO_2 were 12 and 15 m^2/g respectively. The average particle size in

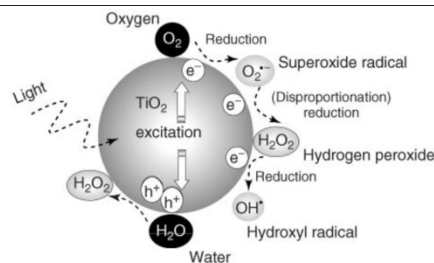


Figure 1. Mechanism of TiO_2 photocatalysis showing formation of OH free radicals and H_2O_2 . (Ref. 6).

both cases was $10 \times 10^{-2} \mu\text{m}$. Typical Scanning Electron Microscopy (SEM) images of ZnO and TiO_2 are shown in Figure 2a, b. TiO_2 consisted of approximately 70% anatase and 30% rutile. All reagents used were of AnalaR Grade or equivalent unless indicated otherwise. Dichlorvos, Phosphamidon and Monocrotophos (Technical grade) samples were from HIL, India. Phenol and catechol were from Qualigen India. All substrates were used as such without any extra purification. The solutions were prepared in doubly distilled water.

Photocatalytic experiments were conducted as explained earlier (12) using a high intensity UV lamp (400 W medium pressure mercury vapor quartz lamp). The reactor was a cylindrical pyrex vessel of 250 ml capacity. This was placed in a glass vessel of 1 litre capacity through which water from a thermostat at the required temperature was circulated. Unless mentioned otherwise, the reaction temperature was maintained at $29 \pm 1^\circ\text{C}$. The irradiation was done from above. The pH of the reaction system was kept at the natural value for each pollutant suspension i.e. 5.5-6. The pollutant concentration at various intervals of irradiation was determined by drawing samples at desired intervals, centrifugation to remove suspended particles and analysis using UV-VIS spectroscopy (Phenol, 500 nm), Gas Chromatography (GC) with Flame Ionization Detector (Phosphamidon, Catechol), GC with Electron Capture Detector (Dichlorvos) and High Performance Liquid Chromatography with UV detector (Monocrotophos). Mineralisation was confirmed by verifying that the total organic carbon (TOC) content (measured using TOC analyzer model Elementar analysensysteme GmbH.) and Chemical Oxygen Demand (measured by standard methods) are 'nil' and by qualitatively measuring CO_2 evolution during the irradiation. H_2O_2 was determined iodometrically.

For experiments with plastics, widely used PE plastic bags of approximately 30 μm size abandoned

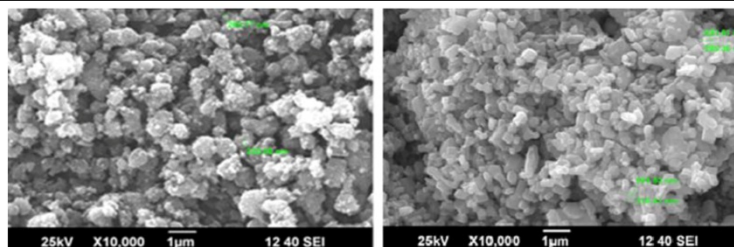


Figure 2. Typical SEM image of (a) TiO₂ (b) ZnO.

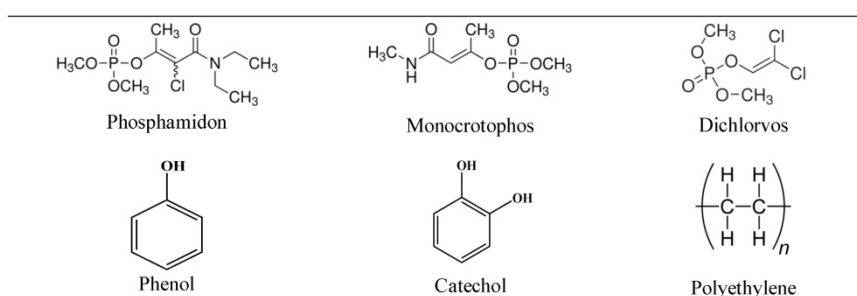


Figure 3. Chemical structures of various water pollutants subjected to the study.

in the open were collected, washed, dried, sorted and cut into small thin strips of approximately 6 cm length and 1 cm width. They were immersed in catalyst suspension in water and irradiated by UV light as done in the case of regular photocatalytic experiments. The degradation was monitored by weight loss at regular intervals, SEM, decrease in tensile strength and physical appearance. The chemical structures of the molecules are given in Figure 3.

Results and Discussion

Control experiments showed that both light and catalyst are essential for the degradation of all pollutants. The degradation was negligible in all cases in the absence of UV light in presence of catalyst or in the presence of catalyst in the absence of light. The decrease in concentration of the substrate in these cases is from 0.5 to 2% which may be due to adsorption on the catalyst. This is treated as insignificant when compared with the degradation under photocatalytic conditions.

As expected, UV light is more efficient than visible light to effect the degradation. The degradation in presence of TiO₂ and ZnO is fairly comparable in presence of UV light in the case of all pollutants

tested here (Figure 4). In the case of phenol (PH) and catechol (CC), the degradation is slightly more in presence of ZnO. In the case of the three organophosphorous pesticides, i.e. phosphamidon (PPM), monocrotophos (MCP) and dichlorvos (DC), TiO₂ is more efficient. Similarity in the extent of degradation of structurally similar phenol and catechol as well as monocrotophos and phosphamidon shows that, in addition to the characteristics of the catalyst and the irradiation source, the substrate structure and hence the substrate-surface interaction are also important in the degradation process. In fact catechol is formed as an intermediate in the photocatalytic degradation of phenol along with many other products (19, 20). The intermediate is equally vulnerable to photocatalytic oxidation as the original compound. Adsorption studies of the two compounds independently and in combination also showed that these two get adsorbed on ZnO and TiO₂ at comparable rates and quantities (20). Hence the concentration of catechol detected as an intermediate during the photocatalytic degradation of phenol is often negligible.

Of the two catalysts, TiO₂ is often rated as superior from the commercial application angle because of its higher chemical stability over wide pH range,

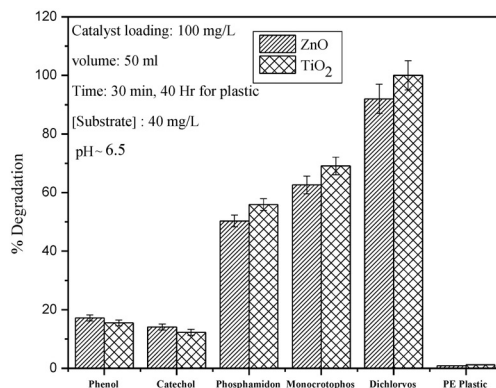


Figure 4. Comparison of ZnO and TiO₂ as photocatalysts for the degradation of various pollutants.

availability and economy. Hence further studies were carried out using TiO₂ as the catalyst.

Effect of Catalyst Loading

The effect of catalyst loading on the degradation of each of the pollutant (excluding the plastic, which is dealt with separately in the later part of this paper) is shown in Figure 5. Since it is more reliable to compare the effect of loading in the early stages of reaction before the influence of intermediates or reaction products set in, the results after 30 minutes of irradiation are considered here. The optimum loading is more or less the same, i.e. 0.1 g/L for all pollutants except in the case of the relatively more complex-structured phosphamidon for which the value is 0.15 g/L. This indicates that the major factors influencing the optimum catalyst loading are the catalyst itself and to a limited extent the structure of the reactant as long as the irradiation source and reactor geometry are kept constant. Increase in the number of effective surface sites with increase in concentration of the catalyst result in enhanced production of reactive free radicals. The number of pollutant molecules adsorbed on the surface also increases due to increased availability of catalyst particles. Stabilization or decrease in the rate of degradation beyond the optimum catalyst loading may be due to the screening effect of excess catalyst particles in the solution. Agglomeration and sedimentation of the particles also occur at higher loading leading to ineffective absorption of light and light scattering resulting in decreased catalyst activation.

Kinetics

The kinetics of degradation of each of the pollutant is determined by varying the concentration keeping all

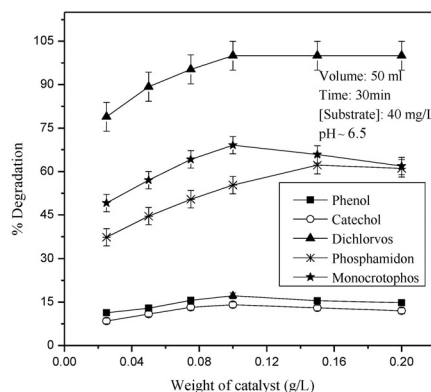


Figure 5. Effect of catalyst concentration on the degradation of various pollutants.

other parameters constant. In most cases, the photocatalytic degradation of organic compounds in water is known to follow pseudo-first order kinetics which is rationalized in terms of the Langmuir-Hinshelwood model modified to accommodate reactions occurring at solid-liquid interface (21-24). Assuming that there is no competition with reaction intermediates/byproducts, the simplest representation for the rate of degradation of the pollutant is as follows (25):

$$-dC/dt = r_0 = k_r K C_0 / (1 + K C_0) \quad (14)$$

where r_0 is the initial rate of disappearance ($\text{mgL}^{-1} \text{min}^{-1}$) of the pollutant, C_0 (mgL^{-1}) its initial concentration, K the equilibrium adsorption constant and k_r ,

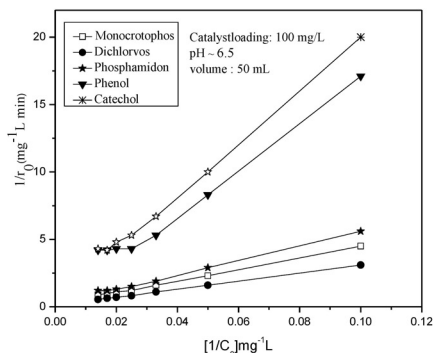


Figure 6. Reciprocal kinetic plot for the photocatalytic degradation of various pollutants.

the limiting reaction rate constant at maximum coverage for the experimental conditions. Equation 14 can be rewritten as

$$1/r_0 = 1/k_r + 1/k_r K * 1/C_0 \quad (15)$$

A plot of $1/r_0$ vs $1/C_0$ will yield a straight line if the degradation follows apparent first order kinetics. Figure 6 shows that in the case of the pollutants investigated here, this relation holds good, especially in the lower concentration range. However in the case of phenol and catechol, and to limited extent in the case of monocrotophos and phosphamidon, the rate of degradation slows down at higher substrate concentration and stabilises eventually thereby decreasing the order of the reaction and reaching zero order. In the concentration range studied here the degradation of dichlorvos was always higher and the reaction followed apparent first order kinetics throughout. At higher concentration of the substrates at least a part of the UV light may be absorbed by them blocking the availability of light to the catalyst (26). Another reason for the decrease in degradation at higher concentration of the substrate may be that the intensity of radiation may not be reaching all the molecules, especially those on the other side of the reactor, away from the reaction zone due to retardation of the penetration of light (27). At low substrate concentrations, the number of catalytically active sites will not be a limiting factor and the rate of degradation is proportional to the substrate concentration in accordance with apparent first order kinetics. At high substrate concentration, the adsorbed reactant molecules and/or the respective intermediates may occupy all or most of the catalytically active sites and this leads to zero order kinetics. But the intensity of light, illumination time and catalyst

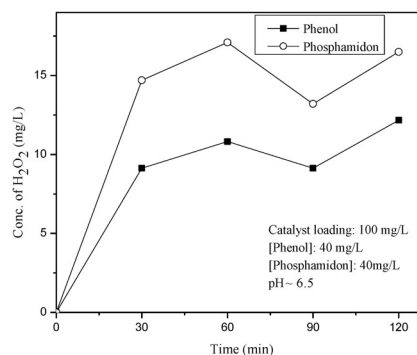


Figure 7. Fate of H_2O_2 formed during the photocatalytic degradation of phenol and Phosphamidon.

concentration are constant. The concentration of active electron-hole pair generated and the reactive species formed i.e. $\cdot OH$, HO_2 , H_2O_2 , O_2^- etc. also are at the maximum. Thus at higher concentrations of the substrate, the relative ratio of the reactive species available for interacting with the pollutant molecules is less. Similarity in the kinetics of degradation of different pollutants on the same catalyst indicates that the mechanism of surface-initiated processes also may be similar.

Fate of H_2O_2

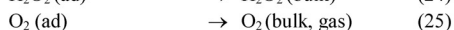
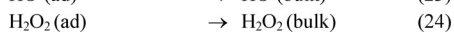
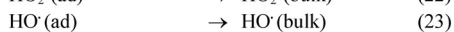
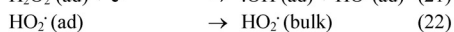
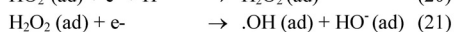
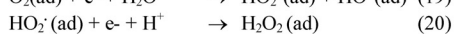
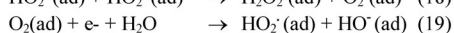
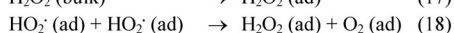
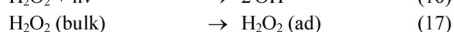
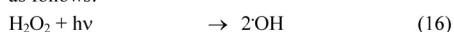
One of the major products of photocatalytic degradation of organic pollutants in water is H_2O_2 which functions as a reactant, intermediate and end product. However, the concentration of H_2O_2 does not increase corresponding to the degradation and often stabilises or undergoes oscillation with periodic increase and decrease (12). Similar results have been reported in the case of sonocatalytic degradation of organic pollutants in water (28). In the present study also formation of H_2O_2 is detected during the photocatalytic degradation of all five substrates. The fate of H_2O_2 is followed in the case of two typical substrates i.e. phenol and phosphamidon under optimized reaction conditions. The results are plotted in Figure 7. As seen from the figure, the concentration of H_2O_2 is smaller than expected from the decomposition of phenol or phosphamidon indicating that H_2O_2 formed may itself be decomposing or participating in other reactions. H_2O_2 is known to decompose under photocatalytic conditions to $\cdot OH$ and HO_2 radicals as in reactions 9 and 10. Further H_2O_2 itself is a good electron acceptor capable of preventing the recombination of photo-generated electrons and holes on the surface. This

Table 1. Effect of anions on the photocatalytic degradation of water pollutants
 [Pollutant]: 40 mgL⁻¹, [TiO₂]: 100 mgL⁻¹, pH: ~5.5-6, Time: 30 min, [Anion]: 4x10⁻¹ mg L⁻¹

Anion	DC	% Degradation of the pollutant			
		MCP	PPM	PH	CC
None	90.5	61.7	50.0	16.5	12.0
Cl ⁻	78.0 (-13.8)	42.5 (-31.1)	42.2 (-15.6)	11.2 (-26.1)	9.8 (-22.4)
SO ₄ ²⁻	85.9 (-5.1)	64.3 (+4.2)	53.6 (+7.2)	16.9 (+2.4)	14.1 (+17.5)
CO ₃ ²⁻	81.2 (-10.3)	56.5 (-8.4)	44.8 (-10.4)	14.0 (-15.2)	9.9 (-17.5)
NO ₃ ⁻	84.5 (-6.6)	55.4 (-10.2)	48.5 (-3.0)	14.9 (-9.7)	11.5 (-4.2)

(% change within brackets)

concurrent formation and decomposition of H₂O₂ result in oscillation. In the beginning of the pollutant degradation, when the concentration of H₂O₂ is smaller, the formation process dominates. Once a critical maximum is reached, the free radicals generated in the system interacts with H₂O₂ more frequently resulting in its decomposition. This continues until the critical minimum is reached when the formation process picks up again. The reactive free radicals generated insitu in the system, including those formed by the decomposition of H₂O₂, participate in a series of reactions which result in further formation as well as decomposition of H₂O₂. Hence it will be difficult to correlate the amount of H₂O₂ at any point in time during the photocatalytic reaction with the substrate degradation or other surface initiated processes. Yi et al (29) showed using Cavity Ring Down Spectroscopy (CRDS) that even the HO₂[·] radicals formed by decomposition of H₂O₂ cannot be correlated with the latter. This illustrates the complex nature of free radicals and their interactions in photocatalytic systems, which influences the role and fate of H₂O₂. The surface initiated free radical interactions eventually continue in the bulk as well until the degradation of the pollutant is completed, various active free radicals are deactivated by interactions and/or the system is stabilized. Various steps involved in the formation and decomposition of H₂O₂ and related interactions, in addition those listed in steps 9-13 may be summarized as follows:



Yi et al (29) demonstrated that photocatalytic decomposition of H₂O₂ proceeds in a unique way as it plays simultaneously the role of electron and hole scavenger. The initial electron or hole transfer to H₂O₂ generate HO₂[·] or [·]OH which may further react on the surface or desorb into the bulk. The desorption of OH radicals from the surface of TiO₂ to the bulk has been proven by single molecule imaging using fluorescence spectroscopy (30).

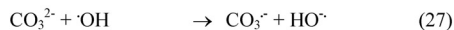
Effect of Anions

Wastewater contains different salts which are either naturally present or introduced from industrial and other human activities. The salts will normally remain in ionized form in water and can influence the photocatalytic degradation of trace organic pollutants. Accordingly we have investigated the effects of four typical anions commonly found in water, i.e. chloride, sulphate, carbonate and nitrate. Preliminary results are shown in Table 1.

Chloride ion shows maximum inhibition in all cases followed by Carbonate ion except in the case of monocrotophos where inhibition by Nitrate is slightly more than that by Carbonate. Sulphate ion enhances the degradation in all cases except in the case of dichlorvos where the degradation as such in the absence of any additive is very high (>90%). In the case of chloride ions, the inhibition is expected as it can get better adsorbed on the TiO₂ surface under the reaction conditions, thereby depriving the substrate molecules from interacting with the surface and getting activated. Cl⁻ ions also act as a scavenger of the photoproduced OH radical (31) as follows:

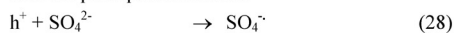


Though the Cl[·] radicals are also capable of oxidizing the pollutants, the rate will be lower than that of [·]OH radicals due to the lower oxidation power of the former (32). The inhibition caused by carbonate ion also may be explained by their reaction with the reactive OH radicals (33).

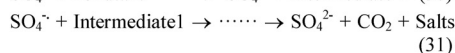
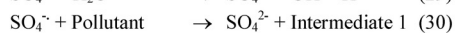
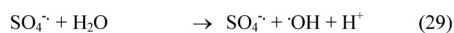


The effect of NO_3^- ions on the degradation seems to depend more on the substrates. In the case of phosphamidon and catechol, the effect, though slightly negative, can be treated as negligible. In the case of other substrates, the degradation is inhibited probably due to the competitive adsorption by NO_3^- and reduction in the number of sites available for the substrate and consequent depletion of reactive species. The lower inhibition compared to other anions tested here can be explained based on the weak adsorption of NO_3^- ions on TiO_2 (34). The enhancement of photocatalysed degradation by SO_4^{2-} ions has been observed by many authors and the most consistent explanation offered is as follows (31, 35, 36):

SO_4^{2-} gets adsorbed on the surface and interacts with the photoproduced holes



Since S is a strong oxidizing agent, the sulphate radical can accelerate the degradation process according to the reaction (36):



Intermediate 1 represents first reaction intermediate, which may go through many reactions before eventual mineralization. As seen in reaction 29, presence of SO_4^{2-} can lead to the formation of extra $\cdot\text{OH}$ radicals which can enhance the degradation. Further $\text{SO}_4^{\cdot-}$ radicals are also strong oxidizing agents. The two highly reactive free radical species together can more than compensate for the inhibition caused by the depletion of surface sites taken up by the sulphate ions. However, this need not be true for all substrates as seen in the inhibition caused by SO_4^{2-} in the case of dichlorvos. In this case, since the conversion of dichlorvos is quite facile, the net concentration of the substrate will be relatively less in the early stage of the reaction itself. Hence the adsorption by SO_4^{2-} can dominate resulting in decreased adsorption and degradation of dichlorvos at later stages. Our ongoing studies show that in the case of certain anions, the initial trend gets reversed at later stages of reaction and this is being investigated in detail. Hence the effect of anions on the photocatalytic degradation of organic pollutants on any particular catalyst cannot be generalized. This is evident from the contradicting results on this aspect from different research groups. The structure of the substrate, characteristics of the catalyst, concentration of the anion, pH of the medium,

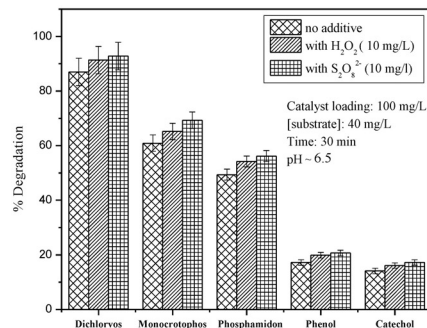


Figure 8. Effect of H_2O_2 and $\text{S}_2\text{O}_8^{2-}$ on the photocatalytic degradation of various pollutants.

reaction time etc can influence the behavior of the anion which needs to be investigated in detail in each case.

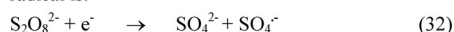
Effect of Oxidizing Agents

H_2O_2 and peroxydisulphate (PDS) are two oxidants known to enhance the photocatalytic degradation of organic pollutants in water (25, 37-40). In order to confirm this in the present context, the effect of these two oxidants on the degradation of the pollutants being investigated here is examined and the results are shown in Figure 8. The oxidants alone at concentrations of < 20 mg/L, in the absence of any catalyst, do not cause any significant degradation (1-2.5% only) under standardized experimental conditions. In typical photocatalytic experiments the degradation increases moderately with the addition of 10 mg/L of H_2O_2 or PDS. The effect is dependent on the H_2O_2 /substrate ratio (25, 39, 41) and hence study of the concentration effect of H_2O_2 is important which is underway currently. The results will be reported later. H_2O_2 is known to function as an electron acceptor which can prevent the recombination of electrons and holes thus enhancing the degradation (24, 27, 39). H_2O_2 can also produce $\cdot\text{OH}$ radicals by insitu decomposition. The Concurrent formation and decomposition of H_2O_2 in photocatalytic systems leading to its oscillation is reported in many cases (11, 12, 20) as well as earlier in this paper. The reaction between the hydroxyl radicals generated in the system and the substrate is expected to occur at or near the surface of the semiconductor as no OH radicals are produced by direct photolysis without the catalyst. However, once the surface initiated reaction has begun the OH radicals generated can propagate the decomposition of H_2O_2 in liquid phase as well as on

the catalyst surface. This will result in the formation of more reactive OH radicals for interaction with the pollutant. However at higher concentration of H₂O₂, the OH radicals will interact more with the former than with the pollutant molecule and hence the effect may be negative. Since the precise concentration of H₂O₂ is unpredictable at any point of time due to these competing reactions, generalized conclusions or predictions on the exact effect of added H₂O₂ on the degradation of different pollutants may not be desirable. For each pollutant, the concentration of H₂O₂ to be added to achieve maximum degradation/mineralisation needs to be optimized. Various reactions in this respect leading to the formation of reactive free radicals from H₂O₂ and subsequent rinteractions are listed in equations 9-13 and 16-25.

Hydroxyl radical has 2.05 times more oxidation power than chlorine, 1.58 times the oxidation power of H₂O₂ and 1.35 times the oxidation power of ozone (42). This implies that H₂O₂ formed insitu should also enhance the degradation, though the efficiency is much lower compared to its decomposition product ·OH. Since the effect is similar in all cases, irrespective of the characteristics of the substrate, it may be inferred that the catalyst and the surface-initiated free radical processes are more important determinants of the H₂O₂ effect.

The enhancement is slightly more in presence of PDS than H₂O₂ under identical conditions, as seen in the figure. This may be because, the persulphate in addition to trapping the electrons and preventing their recombination with the holes also produces sulphate radical which itself is a very strong oxidizing agent whose reduction potential E₀ is 2.6V (25). The reactions leading to the formation of reactive sulphate radical is:



Further reactions which result in enhanced degradation of the pollutant is shown earlier in reactions 28-31.

The inhibition caused by SO₄²⁻ in the degradation of dichlorvos is not seen in the presence of PDS. Hence, it may be presumed that the inhibition contributed by the occupation of active surface sites by the former is more than compensated by the trapping of photogenerated electrons by the latter which prevent the recombination of electrons and holes. This, in turn facilitates the formation of various ROS that is responsible for the enhancing effect by PDS.

pH Effect

Solution pH has profound influence on the oxidation potential and surface charge of semi-

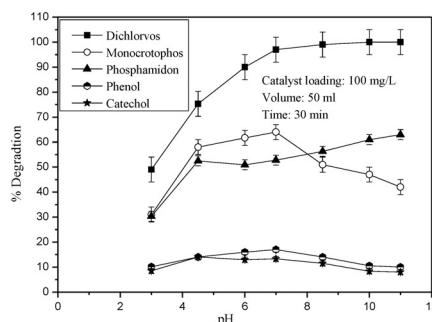
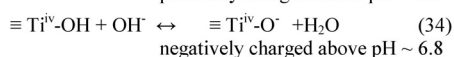
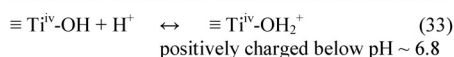


Figure 9. Effect of pH on the photocatalytic degradation of various pollutants.

conductor oxides. Consequently adsorption and degradation of the pollutant also may be affected (26). In the current study, the effect of pH on the degradation of the pollutants is studied in the range 3-11. The results are presented in Figure 9. The results show that there is no clear pattern or predictability in the effect of pH on the photocatalytic degradation of pollutants. As the figure shows, in all cases except in the case of dichlorvos and phosphamidon, the degradation increases with increase in pH, reaches a maximum around the neutral range of 6-7 and decreases again. The effect of pH is usually attributed to the surface charge of the semiconductor and its relation with the ionic form of the organic compound (25). Electrostatic attraction or repulsion between the catalyst surface and the organic molecule takes place which in turn can enhance or reduce the photocatalytic degradation rate. In the case of TiO₂ its point of zero charge (pzc) is ~ 6.8 below which the surface is positively charged. In the alkaline condition, the surface is negatively charged. The ionization state of the surface of TiO₂ under acidic and alkaline conditions is as shown below.



In the case of monocrotophos, it is observed that the degradation is maximum at around the pzc of TiO₂. The pKa value of monocrotophos is 4.4. The protonated form predominates in the extreme acidic pH while it exists in the anionic form at higher pH. Hence monocrotophos will not get adsorbed on the catalyst surface in the acidic range, especially below pH 4.5 which explains the lower degradation. Above pH 4.5, monocrotophos gets deprotonated. Hence the

repulsion is not there and the monocrotophos molecules may get adsorbed or come closer to the surface at least upto pH 6.8. This is consistent with the optimum degradation in the pH range of 6-7. However, there is still good amount of degradation in the alkaline range where the adsorption is expected to be minimal. Hence more than the adsorption, other factors favor the degradation of monocrotophos in alkaline pH. Similar results are reported by Sankar et al (43).

In the case of dichlorvos, the degradation increases steadily and reached 100% above pH 8.5, i.e. the degradation doubled as the pH varied from 3 to ~ 9. Dichlorvos is known to hydrolyze in alkaline media which also may have contributed to the higher degradation at least marginally in the presence of the faster photocatalytic process. Since dichlorvos is an unionizable compound, the increase in degradation in the alkaline range can be attributed to the high hydroxylation of the catalysts surface due to the presence of large quantity of OH⁻ ions. Consequently more OH radicals are formed and the overall rate is increased. The degradation of phosphamidon also follows similar trend as dichlorvos and the degradation is more in the alkaline pH (23). In the case of phenol the degradation increases as the pH is increased from 3 to 7. The degradation remained fairly stable in the neutral pH range and decreased again. In the case of catechol, maximum degradation is seen in the pH range of 4.5-7, remains fairly steady in this range and decreases thereafter. Higher degradation of phenol and catechol in the acidic range is understandable since they remain mainly in the neutral form and can get adsorbed onto the positively charged surface. In the alkaline region, the surface is negatively charged and the phenolate anions get repelled resulting in lower degradation. However Yang et al (44) reports that the photoelectrocatalytic degradation of 4-chlorophenol at TiO₂ electrode is higher at pH 10 contrary to what might be expected from the repulsive forces between the phenolate anions and the surface. This is explained based on the enhanced formation of OH radicals at the alkaline pH (45).

The results thus clearly show that the point of zero charge of the semiconductor catalyst and consequent adsorption of the substrate are important factors that determine the pH effect on photocatalysis. At the same time, these are not the only critical factors as is evidenced by the fair amount of degradation in the alkaline range. There cannot be any thumb rule for predicting or interpreting the effect of pH on the photocatalytic degradation of organic pollutants on semiconductor oxides. For e.g. the three organophosphorous pesticides considered here behave

differently with respect to the optimum degradation and corresponding pH irrespective of structural similarities. In the case of phenol and catechol the trend remains fairly similar even though the pH at which maximum degradation occurred varies. Multiple factors such as variation in the surface characteristics of the semiconductor oxide, electrostatic interactions between the substrates, intermediates, solvent molecules, charged radicals, reactive oxygen species etc. may be influencing the pH effect. Similar inferences were made by other researchers also (46).

In general, the change of surface charge of the catalyst with pH can be exploited to favor adsorption of the active species. Adsorption of anionic substrates on TiO₂ and hence their degradation is favored in the lower pH range where the surface is positively charged. Similarly the degradation of some phenols decreases with increasing pH because they can dissociate and can be repelled by a negatively charged surface (47). From the observations it may be inferred that the total photocatalytic degradation is not just a surface phenomenon. At the same time the activated surface is essential for the generation of various reactive species and free radicals. Once this initiating step is executed, close neighborhood of the surface as well as the bulk of the system can also host the subsequent degradation reaction steps. When the structural orientation of the molecules favor, respective reactive species under acidic or alkaline conditions may interact with the surface and result in degradation and eventual mineralisation. The results points to the need for conducting experiments at different pH values for each substrate on each catalyst in order to identify the most efficient degradation conditions.

Photocatalytic Degradation of Plastics

Since TiO₂ mediated photocatalysis has been found to be an efficient method for the degradation of a variety of water pollutants the technique was explored for the mineralisation of extremely recalcitrant environment pollutant of the day, i.e. low density PE plastics (PEP). Comparative degradation of samples of carelessly thrown away plastics in presence of UV irradiation mediated by ZnO and TiO₂ is shown in figure 4. Accordingly TiO₂ is found to be a better catalyst and is hence chosen for detailed studies. Total Organic Carbon determination in water in which the plastic strip was suspended and irradiated in presence of TiO₂ reveal that there is no carbon left behind in solution thus confirming that the degradation does not lead to the formation of any stable intermediate and it results in complete mineralisation. The intermediates may be getting degraded faster than the plastic itself.

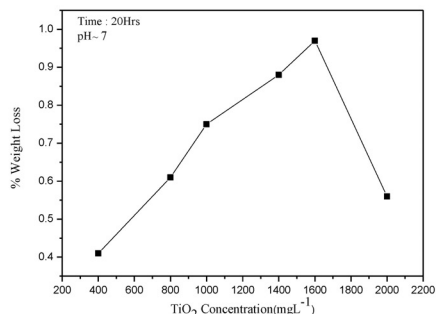


Figure 10. Effect of catalyst loading on the photocatalytic degradation of PE plastics.

The effect of catalyst loading on the degradation of the plastic is shown in Figure 10. As in the case of other substrates, in this case also there is an optimum catalyst dosage. Accordingly ~1400 mg/L is the optimum catalyst weight under the reaction conditions and this quantity is chosen for further studies. The effect of pH on the TiO₂ photocatalysed degradation of plastic is determined and the result is shown in Figure 11. Acidic pH favours slight degradation of plastic even in the absence of catalyst or light. However from pH 6 onwards, it does not have any effect on the degradation of the plastic in the presence of light in the absence of TiO₂ or in the presence of TiO₂ in the dark. Extreme acidic conditions may not be feasible from the environmental or economical angle in view of the need for subsequent neutralization and other processes. Hence all further investigations are made in TiO₂-natural water suspension whose pH is 6.5-7.

As in the case of photocatalytic degradation of organic pollutants, H₂O₂ is detected in the case of PEP degradation also. However, its concentration is much smaller (< 2 mg/L) and is hence not followed up. The effect of added H₂O₂ and PDS on the photocatalytic degradation of PEP in presence of TiO₂ is investigated and the results are plotted in Figure 12. The degradation is enhanced significantly by both oxidants. The effect is concentration-dependent and has an optimum in both cases (Figure 13). H₂O₂ enhances the degradation up to 1500 mg/L concentration. Above this concentration the degradation of plastics is stabilised or slightly decreased. This may be because at higher concentration of H₂O₂ the reactive free radicals as well as the electrons and holes interact more with it and less with the pollutant. H₂O₂ may also be acting as a hole or ·OH scavenger as stated earlier. The

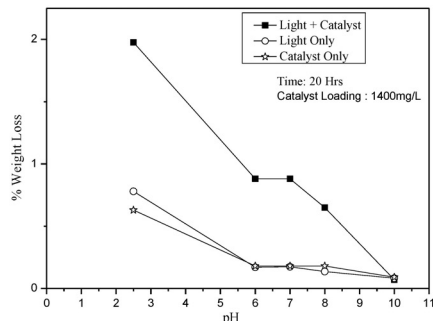


Figure 11. Effect of pH on the photocatalytic degradation of PE plastics on TiO₂.

observation by Malato et al (39) and Evgenidou et al (25) that the effect of H₂O₂ depends on the H₂O₂/Contaminant molar ratio is not relevant in the context since the pollutant is not dissolved in water.

Many reports including the current study suggest that PDS is a much better accelerator of photocatalysed degradation of organic pollutants in water (24, 25, 48, 49). Relatively faster mineralization of the pollutants and lower consumption of the oxidant make the process commercially attractive. The degradation is accelerated by the addition of sulphate anion also (Figure 12). This confirms the mechanism proposed earlier suggesting that the sulphate anions and the sulphate radical formed from the persulphate are at least partially responsible for the enhanced degradation. The TiO₂ catalysed photodegradation of PPE is almost doubled in the presence of even smaller concentration of PDS (5% of TiO₂) as in figure 12. At the optimized concentrations (Figure 13) of the oxidants, PDS is at least three times more efficient than H₂O₂ in enhancing the TiO₂ catalysed photodegradation of PPE plastic. In addition to preventing the electron-hole recombination, the oxidants accelerate the degradation by acting as sensitizers through the production of ·OH and SO₄· radicals. The general mechanism of the acceleration is shown in equations 32 and 28-31.

SEM images of typical plastic strips before and after photocatalytic treatment shown in Figure 14 clearly illustrate that the surface morphology of plastic is severely changed and the technique is effective for the degradation of recalcitrant plastics. As irradiation progresses, the plastic sheet becomes thinner, crumbles and breaks. It is logical to assume that the cavities inside the plastic film also expand with irradiation and the photocatalytic degradation happens both on the surface and inside the film simultaneously.

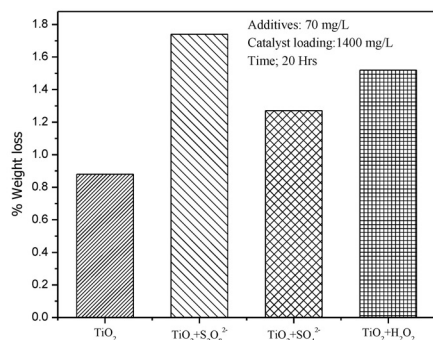
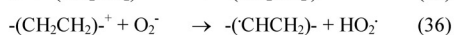
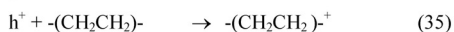


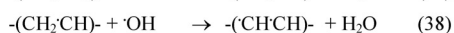
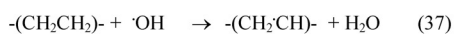
Figure 12. Effect of additives on the photocatalytic degradation of PE plastics on TiO₂.

The holes generated and the O₂⁻ participate in the degradation directly as well as through various radicals generated as follows:



HO₂[·] radicals combine to form H₂O₂ as in reaction 18 which in turn can photodecompose as in reaction 16 to yield ·OH radicals.

The degradation is faster in the beginning and it slows down with time. This is similar to the observations by Shang et al (50) who demonstrated that photocatalytic degradation of polystyrene plastic and evolution of CO₂ and volatile organic compounds under fluorescent light deteriorate gradually. The initial faster rate can be ascribed to the interaction of reactive oxygen species with adjacent polymer chains. These molecules have to be etched away so that the catalyst surface is available for interaction with more molecules and generation of reactive free radicals. It is also possible that the degradation is initiated by photons attacking the polymer to create excited state followed by chain scission, branching, cross linking and oxidation (51). During the irradiation, the OH radicals can attack the polymer as follows:



The carbon centered radicals thus formed react with more O₂ leading to chain cleavage and production of new reactive radicals (50, 53).

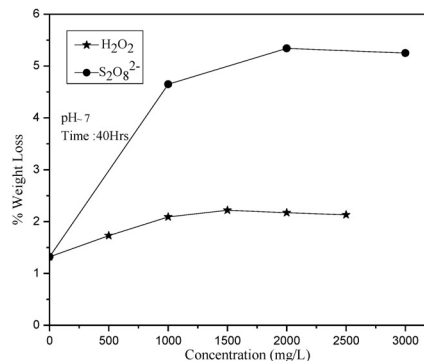
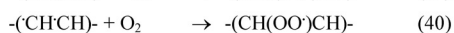
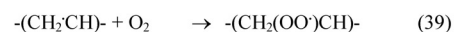
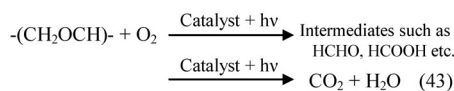
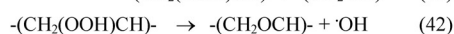
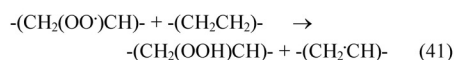


Figure 13. Effect of concentration of H₂O₂ and S₂O₈²⁻ on the photocatalytic degradation of PE plastics on TiO₂.



The intermediates are not detected in water indicating that they are getting degraded faster than the plastic. Absence of any TOC in water in which the plastic strip was suspended also confirms this.

Conclusion

Semiconductor photocatalysis mediated by TiO₂ is found to be an efficient method for the removal of trace organic pollutants from water. Organophosphorous pesticides such as phosphamidon, monocrotophos and dichlorvos, phenol, catechol and even recalcitrant polyethylene plastic can be mineralized into harmless end products by this method. The degradation follows first order kinetics in most cases, even though variable kinetics with reaction order of <1 is observed at higher concentration of certain slow-degrading substrates. The influence of pH on the degradation is complex and no generalized mechanism can explain the process. The point of zero charge of the semiconductor and substrate-surface interaction are major factors that determine the pH effect. H₂O₂ and peroxydisulphate enhance the pollutant mineralization. H₂O₂ formed insitu during the degradation undergoes parallel decomposition resulting in stabilization or oscillation in its concentration depending on the equilibration or domination of the formation/

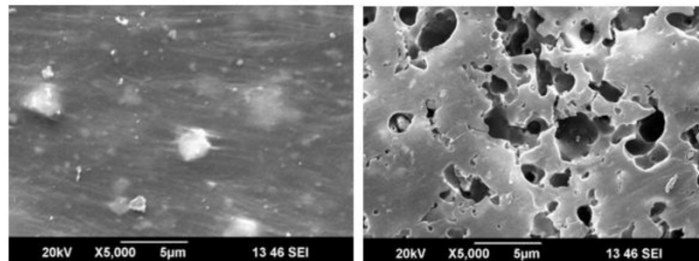


Figure 14. SEM images of polyethylene plastic (a) before and (b) after photocatalytic treatment using TiO_2 (1400mg/L) and $\text{S}_2\text{O}_8^{2-}$ (2000mg/L). Time: 300 hours.

decomposition process taking place at respective critical concentrations. Anions such as Cl^- , CO_3^{2-} and NO_3^- inhibit the degradation while SO_4^{2-} enhances the same. Critical parameters for optimum efficiency for the removal of each of the pollutant are identified and optimized.

Acknowledgement

Financial support to KPJ (Junior Research Fellowship from UGC, India) and to SGA (Senior Research Fellowship from Cochin University of Science and Technology) is gratefully acknowledged.

References

- (1) Fujishima, A; Zhang, X; Tryk, D.A. *Surf. Sci. Rep.* **2008**, *63*, 515-582.
- (2) Chong, M.N; Jin, B; Chow, C.W.K; Saint, C. *Water Res.* **2010**, *44*, 2997-3027.
- (3) Chen, C.C; Ma, W.H.; Zhao, J.C. *Chem. Soc. Rev.* **2010**, *39*, 4206-4219.
- (4) Pelaez, M.; Nolan, N.T.; Pillai, S.C.; Seery, M.K.; Falaras, P.; Kontos, A.G.; Dunlop, P.S.M.; Hamilton, J.W.J.; Byrne, J.A.; O'Shea, K.; Entezari, M.H.; Dionysiou, D.D. *Appl. Catal. B: Environ.* **2012**, *125*, 331-349.
- (5) Ollis, D.F; Pichat, P; Serpone, N. *Applied Catal. B: Environ.* **2010**, *99*, 377-387.
- (6) Nosaka, Y; Nosaka, A. In *Photocatalysis and Water Purification*; First Edition, Pichat, P. Ed., Wiley-VCH Verlag GmbH and Co.: 2013, pp 1-24.
- (7) Herrmann, J. M. *Catal. Today* **1999**, *53*, 115-129.
- (8) Hoffmann, M.; Martin, S.; Choi, W.; Bahnemann, D. *Chem. Rev.* **1995**, *95*, 69-96.
- (9) Ollis, D.F; Pelizzetti, E.; Serpone, N. In *Photocatalysis: Fundamentals and Applications*; Serpone, N; Pelizzetti E, Eds., John Wiley and Sons Inc.: New York, 1989, p 603.
- (10) Ollis, D.F; Al-Ekabi, H. *Photocatalytic purification and treatment of water and air*; Elsevier Amsterdam, 1993.
- (11) Jyothi, K.P; Joseph, S.; Yesodharan, S.; Yesodharan, E.P. *Res. J. Recent. Sci.* **2013**, *2*, 136-149.
- (12) Anju, S.G; Yesodharan, S.; Yesodharan, E.P. *Chem. Eng. J.* **2012**, *189-190*, 84-93.
- (13) Devipriya, S.P; Yesodharan, S. *Solar Energy Mater. and Solar Cells* **2005**, *86*, 309-348.
- (14) Madhavan, J.; Sathish kumar, P.S; Anandan, S.; Grieser, F.; Ashok kumar, M. *J. Hazard. Mater.* **2010**, *177*, 944-949.
- (15) Konstantinou, I.K; Albanis, T.A. *Appl. Catal. B: Environ.* **2003**, *42*, 319-335.
- (16) Wang, K.H.; Hsieh, Y.H.; Chou, M.Y.; Chang C.Y. *Appl. Catal. B: Environ.* **1999**, *21*, 1-8.
- (17) Burrows, H.D; Caule, L.M; Santaballa, J.A; Steenken, S. *J. Photochem. Photobiol.* **2002**, *67*, 71-108.
- (18) Lu, M-C; Roam, G-D; Chen, J-N; Huang, C.P., *J. Photochem. Photobiol. Chem.* **1993**, *76*, 103-110.
- (19) Okamoto, K.; Yamamoto, Y.; Tanaka, H.; Tanaka, M.; Itaya, A. *Bull. Chem. Soc. Japan* **1985**, *58*, 2015-2022.
- (20) Joseph, S.; Jyothi, K.P.; Devipriya, S.P.; Yesodharan, S.; Yesodharan, E.P. *Res. J. Recent. Sci.* **2013**, *2*, 82-89.
- (21) Turchi, C.S; Ollis, D.F. *J. Catal.* **1990**, *122*, 178-192.
- (22) Poullos, I.; Avranas, A.; Rekliti, E.; Zouboulis, A. *J. Chem. Technol. Biotechnol.* **2000**, *75*, 205-212.
- (23) Rabindranathan, S.; Devipriya, S.P.; Suguna Yesodharan. *J. Hazard. Mater.* **2003**, *B102*, 217-229.
- (24) Al-Ekabi, H.; Serpone, N. *J. Phys. Chem.* **1988**, *92*, 5726-5731.
- (25) Ewegenidou, E.; Fytianos, K.; Poullos, I. *Appl. Catal. B: Environ.* **2005**, *59*, 81-89.
- (26) Anandan, S.; Vinu, A.; Venkatachalam, N.; Arabindoo, B.; Murugesan V. *J. Mol. Catal. A. Chem.* **2006**, *256*, 313-320.
- (27) Yatmaz, H.C; Akyol, A.; Bayramoglu, M. *Ind. Eng. Chem. Res.* **2004**, *43*, 6035-6042.

- (28) Jyothi, K.P.; Yesodharan, S.; Yesodharan, E.P. *Ultrason. Sonochem.* **2014**, *21*, 1787-1796.
- (29) Yi, J.; Bahrini, C.; Shoemaeker, C.; Fittschen, C.; Choi, W. *J. Phys. Chem.* **2012**, *116*, 10090-10097.
- (30) Tachikawa, T.; Majima, T. *Langmuir* **2009**, *25*, 76791-7802.
- (31) Barka, N.; Quorzal, S.; Assabane, A.; Nounah, A.; Ait-Ichou, Y. *J. Photochem. Photobiol. A: Chem.* **2008**, *195*, 346-351.
- (32) Kiwi, J.; Lopez A.; Nadrochenko V. *Environ Sci Technol.* **2000**, *34*, 2162-2168.
- (33) Haarstrick, A.; Kut, O.M.; Heinzle, E. *Environ Sci Technol.* **1996**, *30*, 817-824.
- (34) Guillard, C.; Puzenat, E.; Lachheb, H.; Houas, A.; Herrmann, J.M. *Int. J. Photoenergy* **2005**, *7*, 1-9.
- (35) Low, G.K.C.; McEvoy, S.R.; Matthews, R.W. *Environ Sci. Technol.* **1991**, *25*, 460-467.
- (36) Kositz, M.; Antoniadis, A.; Poulis, I.; Kiridis, I.; Malato, S. *Solar Energy* **2004**, *77*, 591-600.
- (37) Evgenidou, E.; Fytianos, K.; Poulis, I. *J. Photochem. Photobiol. A: Chem.* **2005**, *175*, 29-38.
- (38) Muneer, M.; Bahnemann, D. *Appl. Catal B: Environ.* **2002**, *36*, 95-111.
- (39) Malato, S.; Blanco, J.; Maldonado, M.I.; Fernandez-Ibanez, P.; Campos, A. *Appl. Catal B: Environ.* **2000**, *28*, 163-174.
- (40) Poulis, I.; Kositz, M.; Kouras, A. *J. Photochem. Photobiol. A: Chem.* **1998**, *115*, 175-183.
- (41) Hua, Z.; Manping, Z.; Zongfeng X.; Low, G. K.-C. *Water Res.* **1995**, *29*, 2681-2688.
- (42) Fujihira, M.; Satoh, Y.; Osa, T. *Bull. Chem. Soc. Japan* **1982**, *55*, 666-673.
- (43) Shankar, M.V.; Anandan, S.; Venkatachalam, N.; Arabindoo, B.; Murugesan, V. *J. Chem. Technol. Biotechnol.* **2004**, *79*, 1279-1285.
- (44) Yang, J.; Dai, J.; Chen, C.; Zhao, J. *J. Photochem. Photobiol. A: Chem.* **2009**, *208*, 66-77.
- (45) Sakthivel, S.; Neppolian, B.; Shankar, M.V.; Arabindoo, B.; Palanichamy, B.; Murugesan, V. *Solar Energy Mater. Solar Cells* **2003**, *77*, 65-82.
- (46) Umar, K.; Haque, M.M.; Mir, N.A.; Muneer, M.; Farooqi, I.H. *J. Adv. Oxid. Technol.* **2013**, *16*, 252-260.
- (47) Brugnera, M.F.; Rajeshwar, K.; Cardoso, J.C.; Boldrin Zanoni, M.V. *Chemosphere* **2010**, *78*, 569-575.
- (48) Al-Ekabi, H.; Butters, B.; Delany, D.; Ireland, J.; Lewis, N.; Powell, T.; Story, J. In *Proceedings of the first international conference on TiO₂ photocatalytic purification and treatment of water and air*; London, Canada, Ollis, D.F.; Al-Ekabi, H. (Eds.), Elsevier: Amsterdam 1993, p 321.
- (49) Pelizzetti, E.; Carlin, V.; Minero, C.; Gratzel, M. *New J. Chem.* **1991**, *15*, 351-357.
- (50) Shang, J.; Chai, M.; Zhu, Y. *Environ Sci. Technol.* **2003**, *37*, 4494-4499.
- (51) Crawford, K.D.; Hughes, K.D. *J. Phys. Chem.* **1997**, *B 101*, 864-869.
- (52) Wells, R.K.; Royston, A.; Badyal, J.P.S., *Macromolecules* **1994**, *27*, 7465-7468.

Received for review November 9, 2013. Revised manuscript received August 21, 2014. Accepted November 15, 2014.

